Codenitrification under ruminant urine patch conditions: microbial contributions, substrates and nitrogen flux kinetics

---

A thesis

submitted in partial fulfilment

of the requirements for the Degree of

Doctor of Philosophy

at

Lincoln University

by

David Rex

Lincoln University

2018

Lincoln University
Te Whare Wānaka o Aoraki

DECLARATION

This dissertation/thesis (please circle one) is submitted in partial fulfilment of the requirements for the Lincoln University Degree of PhD

The regulations for the degree are set out in the Lincoln University Calendar and are elaborated in a practice manual known as House Rules for the Study of Doctor of Philosophy or Masters Degrees at Lincoln University.

Supervisor's Declaration

I confirm that, to the best of my knowledge:

- the research was carried out and the dissertation was prepared under my direct supervision;
- except where otherwise approved by the Academic Administration Committee of Lincoln University, the research was conducted in accordance with the degree regulations and house rules;
- the dissertation/thesis (please circle one)represents the original research work of the candidate;
- the contribution made to the research by me, by other members of the supervisory team, by other members of staff of the University and by others was consistent with normal supervisory practice.
- external contributions to the research (as defined in the House Rules) are acknowledged. (Delete if not applicable)

Supervisor T. S. CLOUGH Date 23/10/18

Candidate's Declaration

I confirm that:

- this dissertation/thesis (please circle one) represents my own work;
- the contribution of any supervisors and others to the research and to the dissertation/thesis (please circle one) was consistent with normal supervisory practice.
- external contributions to the research (as defined in the House Rules) are acknowledged. (Delete if not applicable)

Candidate David M. Date 23.10.2018

Pre-Publication of Parts of this dissertation/thesis (please circle one)

Either:

1 We confirm that no part of this dissertation has been submitted for publication in advance of submission of the dissertation/thesis (please circle one) for examination.

Candidate _____ Date _____

Supervisor _____ Date _____

Or:

2 Parts of this dissertation/thesis (please circle one) have been submitted and/or accepted for publication in advance of submission of the dissertation/thesis (please circle one) for examination.

In this case, please set out on a separate page information on:

- which sections have been submitted, which have been accepted and which have appeared;
- which journals they have been submitted to;
- who are the co-authors.

Candidate David M. Date 23.10.2018

Supervisor T S Clough Date 23/10/18

“The Lord is my Shepherd, I shall not lack.”

-- Psalm 23:1 --

Pre-Publication of Parts of this Thesis

Chapter 4 - a manuscript from this section has been published as follows:

Rex D, Clough TJ, Richards KG, de Klein C, Morales SE, Samad Md S, Grant J, Lanigan GJ 2018. Fungal and bacterial contributions to codenitrification emissions of N_2O and N_2 following urea deposition to soil. *Nutrient Cycling in Agroecosystems* 110: 135-149.

Chapter 5 - a manuscript from this section has been submitted for publication as follows:

Rex D, Clough TJ, Richards KG, Condron LM, de Klein CAM, Morales SE, Lanigan GJ 2018. Impact of nitrogen compounds on fungal and bacterial contributions to codenitrification in a pasture soil. *Scientific Reports*.

Abstract of a thesis submitted in partial fulfilment of the
requirements for the Degree of Doctor of Philosophy

Codenitrification under ruminant urine patch conditions: microbial contributions, substrates and nitrogen flux kinetics

by
David Rex

A large fraction of anthropogenic nitrous oxide (N_2O) emissions can be traced back to grazed grasslands, where N_2O is mainly emitted from livestock-urine affected soils (so called 'urine patches'). Since N_2O is a potent greenhouse gas and an ozone-depleting substance, research has focused on its formation pathways inside agricultural soils in order to mitigate agricultural N_2O emissions. In recent years, evidence was found for the significance of N_2O-formation pathways, creating so called "hybrid N_2O" where a soil derived nitrogen (N) source is co-metabolised with an applied N source (e.g. urine-urea or mineral N fertilizers). This reaction(s) is referred to as 'codenitrification' and may, besides denitrification and nitrification, be responsible for up to 95% of the emitted gaseous N-compounds. First reports of the potential for microorganisms to produce hybrid N_2O and/or hybrid dinitrogen (N_2) were almost last 100 years ago, however, the current state of knowledge about codenitrification remains sparse. For example, it still remains unclear what the relative contributions of different microbial groups are, within a pasture soil context, or what the co-metabolites might be dominant in such a process as codenitrification. The number of studies relating to codenitrification performed *in vitro* by far outnumber the studies dealing with soils. Thus soil mesocosm experiments are required in order to gain more insight into codenitrification reactions responsible for N_2O emissions from urine patches. Filling this important knowledge gap is an essential step for furthering N_2O emission mitigation strategies.

Two experiments were carried out in 2015-2016 (year one) and 2017 (year two) using freshly collected soil from the nearby Lincoln University Research Dairy Farm. The first experiment focused on the fungal and bacterial contributions to hybrid N_2O emissions following a simulated bovine urine event. Fungal and bacterial inhibitors were used in order to inhibit the different microbial groups individually or collectively, and while utilizing applied ^{15}N-labelled urea at a rate of 1000 kg N ha^{-1}. The stable isotope approach allowed N transformations to be traced, as performed over time by the microbial groups. It was demonstrated that under elevated soil pH conditions, codenitrification generated hybrid N_2O and N_2, with codenitrified N_2O accounting for > 30% of the total N_2O flux. The

inhibition of fungi lead to a reduction of ≥ 42% of the codenitrification derived N_2O flux while the bacterial inhibition did not cause a significant reduction in codenitrification. Despite there being mainly bacterial driven ammonia (NH_4^+) oxidation, the results demonstrated that soil fungi were the main organisms undertaking codenitrification.

The second experiment was designed to identify some of the co-metabolized compound(s) utilized for hybrid N_2O formation. Soil mesocosms were prepared and (non ^{15}N-labelled) urea applied (equalling 500 kg N ha^{-1}). Eight days afterwards, when codenitrification was theoretically able to occur, four different potential ^{15}N-labelled co-metabolites (so called 'nucleophiles') were applied to the soil mesocosms to measure their relative contribution to hybrid N_2O formation. Glycine and phenylalanine were studied, as they are two amino acids occurring within the soil organic matter (SOM) matrix, and these were complemented with NH_4^+ and hydroxylamine (NH_2OH), each applied at a rate of 20 µg N g^{-1} soil. The same inhibitors as used in the first experiment were used to identify the microbial groups using the nucleophiles. This time, only codenitrified N_2O was measured. All applied nucleophiles were observed to contribute to hybrid N_2O formation, indicating that soil microbes are capable of using a wide range of possible N compounds for codenitrification. The most reactive nucleophile, in biotically and abiotically mediated reactions, was NH_2OH.

Finally, a modelling approach was used to investigate the underlying N transformations rates and N pool developments in pasture soil subsequent to a simulated urine event. Data from a previous experiment with known codenitrification fluxes were used to run a model, suitable for modelling the gross N transformation rates, prior to the N_2O formation. The modelled output matched well with the measured data and revealed significant changes in the labile and recalcitrant fraction of soil organic matter and their related transformation rates subsequent to the urea application. Evidence was found for the NH_4^+, NO_3^-, labile and recalcitrant N pool to be involved in codenitrification reactions. Especially the labile N pool was assumed to provide possible nucleophiles, consisting not only of easy degradable N compounds but also of N loosely bound to organic carbon components due to reactions of NH_3 with dissolved organic carbon. Furthermore, an increasing enrichment of SOM with ^{15}N of up to 23 atm% ^{15}N after 1519 h (63 d) and at the same time, 43% and 29% (wet and dry soil, respectively) of the applied N were still stored in clay minerals. This clearly affects the following N transformations further and, compared with the previously detected codenitrification fluxes, indicates that in addition with free NO_3^-, a high soil moisture content and increased SOM are favouring codenitrification.

This body of work shows that codenitrification is closely linked with the activity of fungi and that a wide range of organic and mineral N compounds can be utilized as nucleophiles.

Keywords: nitrous oxide, codenitrification, urine patch, stable isotopes (^{15}N), selective inhibition, ^{15}N–trace model

Acknowledgements

Firstly, I would like to thank my main supervisor, Professor Timothy Clough, for his guidance throughout this process. His rapid feedback to all requests and his detailed comments were of great value and are much appreciated. I am grateful for all the time he spent editing manuscripts and chapter drafts and mentoring me as I progressed through this PhD project.

I would also like to thank my co-supervisors, Dr Karl Richards and Dr Gary Lanigan for their input, comments, support and overall organization which made this PhD project possible. The cooperation between Teagasc Institute, Johnstown Castle, and Lincoln University, Lincoln, is highly appreciated since it provided a solid base to conduct this international PhD project.

I greatly appreciate the funding for this PhD from the New Zealand Government through the New Zealand Fund for Global Partnerships in Livestock Emissions Research to support the objectives of the Livestock Research Group of the Global Research Alliance on Agricultural Greenhouse Gases (Agreement number: 16084). Also I gratefully acknowledge the funding received from the Teagasc Walsh Fellowship Scheme.

I also would like to thank all of the technical and analytical staff at Lincoln University who helped make all of this work possible. Specially, I like to thank Roger Cresswell for his great help with all the many issues during the laboratory work this project was based on. He often solved unsolvable problems.

I am thankful for the love and support from my family back in Germany. Staying in contact, even while being on the opposite side of the planet has meant much to me over these years.

Finally, I'd like to thank all my friends here in New Zealand. The staff and students from the department, my flatmates and friend's flatmates who were there in times of need helped so much with the overall progress. A special thanks to my officemates, Tihana Vujinović and Camilla Gardiner, together, we turned a blank 3rd floor office into a nice, welcoming, flowering pot oasis that was noticed and appreciated throughout the department, not least because of the continuous fresh coffee supply that lead to so many good memories.

I also want to thank my friends from the Christian fellowship at Lincoln University and Arise Church in Christchurch, their support and prayers helped to endure even hardest times.

Table of Contents

List of Tables

List of Figures

List of Abbreviations

AM	Arbuscular mycorrhiza
AOA	Ammonia oxidising archaea
AOB	Ammonia oxidising bacteria
C	Carbon
CO_2	Carbon dioxide
CO_2-eq.	Carbon dioxide equivalents
DNRA	Dissimilatory NO_3^- reduction
DOC	Dissolved organic carbon
EF	Emission factor
GC	Gas chromatograph
GHG	Greenhouse gas
HCO_3^-	Bicarbonate
KCl	Potassium chloride
MC	Monte Carlo
MCMC	Markow chain Monte Carlo
N	Nitrogen
N_2	Dinitrogen
N_{2co}	Codenitrified dinitrogen
NO	Nitric oxide
NO^+	Nitrosyl
N_2O	Nitrous oxide
N_2O_{co}	Codenitrified nitrous oxide
NH_2OH	Hydroxylamine
NH_3	Ammonia
NH_4^+	Ammonium
NO_2^-	Nitrite
NO_3^-	Nitrate
O_2	Oxygen
OH^-	Hydroxide ion
SD	Standard deviation of mean
SEM	Standard error of the mean
SOM	Soil organic matter
WFPS	Water-filled pore space
WHC	Water holding capacity

N trace model specific

N fluxes

A_{NH4}	Mineral sorbtion of NH_4^+
D_{NO3}	Dissimilatory NO_3^- reduction
H_u	Urea hydrolysis
$I_{NH4Nlab}$	Immobilisation of NH_4^+ in N_{lab}
$I_{NH4Nrec}$	Immobilisation of NH_4^+ in N_{rec}
I_{NO3}	Immobilisation of NO_3^- in N_{rec}
M_{Nlab}	Mineralisation of N_{lab} to NH_4^+
M_{Nrec}	Mineralisation of N_{rec} to NH_4^+
O_{Nrec}	Oxidation of N_{rec}
O_{NH4}	Oxidation of NH_4^+
R_{NH4}	Release of sorbed NH_4^+
V_{NH3}	Volatilization of NH_3

N pools

urea	Urea
NH_3	Ammonia
NH_4^+	Ammonium
$NH_4^+{}_{ads}$	Clay Mineral sorbed Ammonium
N_{lab}	Labile soil nitrogen
N_{rec}	Recalcitrant soil nitrogen
NO_3^-	Nitrate
$NO_3^-{}_{sto}$	Stored nitrate in organic matter

Chapter 1
Introduction

1.1 Background

Nitrous oxide (N_2O) is a greenhouse gas and an ozone-depleting substance (Ravishankara et al. 2009). A major source of anthropogenic N_2O emissions are urine patches within grazed grasslands where the applied urea N, resulting from fertiliser-N or urinary-N inputs is emitted as N_2O before its complete reduction to environmentally benign N_2 (Flessa et al. 1996; Oenema et al. 1997). The development of management techniques to mitigate N_2O emissions is therefore of particular importance in countries where their economies are dependent on pasture grazing. For example, Ireland and New Zealand, where 3.3 million ha and 2.1 million ha, respectively, are covered with pastures (Eurostat 2012; Statistics New Zealand 2013). Thus, urine patches are a major source of N_2O emissions in Ireland (Eurostat 2012) and New Zealand (Ministry for the Environment 2016) and new mitigation strategies need to be found in order to reduce these N_2O emissions. In order for relevant mitigation strategies to be developed for urine-affected pasture soils, it is vital that N_2O emission processes are understood. Recently, (Selbie et al. 2015b) found the formation of "hybrid N_2O" was highly significant in pasture soils. This hybrid N_2O and N_2 was formed via biotic nitrogen-nitrosation that co-metabolised organic or mineral N compounds. Because of its simultaneous occurrence with conventional denitrification this process has been termed 'codenitrification' (Spott et al. 2011).

However, relatively little is known about codenitrification's role in N_2O formation, the microbial groups contributing to the process, or the relative contributions of various potentially co-metabolized substances within a soil matrix.

This PhD aimed to fill the knowledge gap with respect to codenitrification within a soil matrix by characterising aspects of codenitrification within urine patches.

Potentially new knowledge about codenitrification will enable researchers to better understand N_2O generating processes and assist in understanding how mitigation tools and management practices can be designed to reduce N_2O emissions.

1.2 Research Objectives

The objectives of this PhD research programme were to:

- Identify the microbial groups involved in and performing the process of codenitrification in soil
- Determine possible nucleophiles, used as co-metabolites by these microbial groups within the soil
- Model the N transformations and N pool dynamics occurring under urea-affected soil under contrasting soil moisture conditions, which potentially favour or reduce the potential for (co)denitrification fluxes.

1.3 Thesis Structure

This thesis is divided into 7 chapters. The first and second chapters provide an overview of the thesis topic and a review of the relevant literature, respectively. Then chapter three contains a short introduction into the materials and methods used for this project. The following chapters, four, five, and six, present and discuss the results of the experiments conducted, while the final chapter seven summarises the overall findings of this thesis and provides directions for future research.

Chapter 1 This chapter gives a general overview of the thesis topics, the research objectives, and an outline of the thesis structure.

Chapter 2 This chapter summarises the background knowledge in a literature review, identifies the gaps in our knowledge and provides the reasoning and justification for the research conducted in this PhD thesis.

Chapter 3 This chapter was set up in order to describe the commonly used materials and methods and the set up procedures for the main experiments.

Chapter 4 The first laboratory experiment is presented in this chapter. This experiment was performed in order to determine the role of codenitrification in urine-affected pasture soil and to identify the related microbial groups.

Chapter 5 The second laboratory experiment is presented here. This time the aim was to identify N compounds potentially used as nucleophiles by the different microbial groups.

Chapter 6 This chapter presents the outcome of the N trace model run. Here the aim was to investigate the N transformations which are related/required to create the circumstances resulting in codenitrification.

Chapter 7 This chapter summarises the results from Chapters 4-6 and provides recommendations for future research on this topic.

Chapter 2
Literature Review

2.1 Introduction

Nitrous oxide (N_2O) is both a greenhouse gas (GHG), with a global warming potential 265-298 times that of carbon dioxide (CO_2) over a 100 year time period (WMO 2013; IPCC AR5 2014), and a precursor to reactions involved in the depletion of stratospheric ozone (Ravishankara et al. 2009). A major source of anthropogenic N_2O emissions is the ruminant urine deposition that occurs during the intensive grazing of grasslands (Flessa et al. 1996; Oenema et al. 1997). Recently, studies have shown that > 90% of the N_2O and/or dinitrogen (N_2) emitted from pasture soils may derive from a reaction called codenitrification (Laughlin and Stevens 2002; Selbie et al. 2015b). Thus, a better understanding of this process may enable it to be manipulated to assist in the mitigation of N_2O emissions from grazed pasture soils. The aim of this review is therefore:

- to summarize the current knowledge about codenitrification in pasture soil as it relates to ruminant urine deposition,
- to analyse microbial N-turnover activities within the soil N-cycle, especially as they relate to N_2O emissions, in order to identify the contribution of different microbial groups to codenitrification, and
- outline possible methods for the analysis of microbial activities in soils with respect to codenitrification.

2.2 Pastures of temperate climates

The use of temperate climate meadows as pastures for grazing livestock, such as cattle or sheep, has a long history and occurs in many countries. Pastures are of special interest in countries where large agricultural sectors are based on producing pasture generated livestock products, and hence where pasture management variations can affect economic returns and the environment. In this context, Ireland and New Zealand are two examples of such countries.

2.2.1 Ireland

Pastures and meadows cover around 3.3 million ha of Ireland (2010), ~ 50% of its total surface area (Eurostat 2012). Predominately, ruminant livestock are grazed on these pastures, with dairy and beef

cattle numbers equalling > 4.7 million in 2010, supplemented with another 0.5 million sheep (Eurostat 2012). With most of the produced milk being exported (85% in 2014), dairy farming is currently both, the biggest agricultural sector and the agricultural field with the highest growing expectations, with the aim to increase exports by 50% by 2020 (Rodens 2014). Thus, it is likely that an increase in total livestock and an intensification of farm land use will occur within the next decade. Presently, agricultural emissions make up to 40% of Ireland's non-emission trading sectors and without adjusted management practices, they are likely to increase. As a signatory to the Kyoto Protocol Ireland needs to reduce its GHG emissions from the agricultural sector by 20% compared to 2005.

2.2.2 New Zealand

New Zealand's economy is largely based on agriculture, contributing more than 65% to national exports (Statistics New Zealand (2013)). Besides horticultural products, it is mainly milk, meat and wool that is produced for export, from a total pasture area of 2.1 million hectares. These pastures are predominantly grazed by 30 million sheep, 6.7 million dairy cattle and 3.7 million beef cattle (Statistics New Zealand (2013)), with dairy farming the fastest growing sector, with an 88.4% increase in dairy cow number compared to 1990 (Ministry for the Environment (2015)). Like Ireland, New Zealand has signed the Kyoto Protocol and thus is obliged to reduce the GHG emissions to 50% below the 1990 levels by 2050. Since 1990 agriculture has intensified, resulting in a 23% increase in N_2O emissions (Ministry for the Environment (2015)). Currently, 93.4% of all New Zealand's emitted N_2O can be traced back to agricultural soils and thus pasture management methods that mitigate N_2O emissions are required.

2.3 Nitrogen transformations in pasture soil

2.3.1 Mineralization, nitrification and immobilization

Most pasture soils contain between 0.1 - 0.6% N, corresponding to 2-12 t N ha^{-1} (Cameron et al. 2013). Depending on the soil type and recent climatic and management events this N pool consists of mineral and organic components. Usually, the major fraction of N is present in organic forms (plant residues, humic compounds, as well as dead and living microbial biomass), while mineral forms (ammonium, NH_4^+; nitrite, NO_2^-; and nitrate, NO_3^-) represent a minor pool but with a more rapid turnover. A complex network of inputs and outputs (fluxes) connects the different pools, influencing the amount of both plant and microbially available N, and the amount of reactive N that can leave the soil via leaching or volatilization processes (Cameron et al. 2013).

Since 1828, with the discovery of the minimum law by C. Sprengel (and the subsequent extension and popularization by J. Liebig), the N content of agricultural soils has become a key subject of

agricultural chemistry. Subsequently, over time, the findings concerning the different N pools and N fluxes have been reviewed in great detail by several authors, including Löhnis (1926), Czygan (1971), Knowles (1982), Ehrlich et al. (2000), Cameron et al. (2013), Müller (2016) and Van Groenigen et al. (2016).

In brief, the main fluxes for agricultural soils can be depicted with a simple graphic:

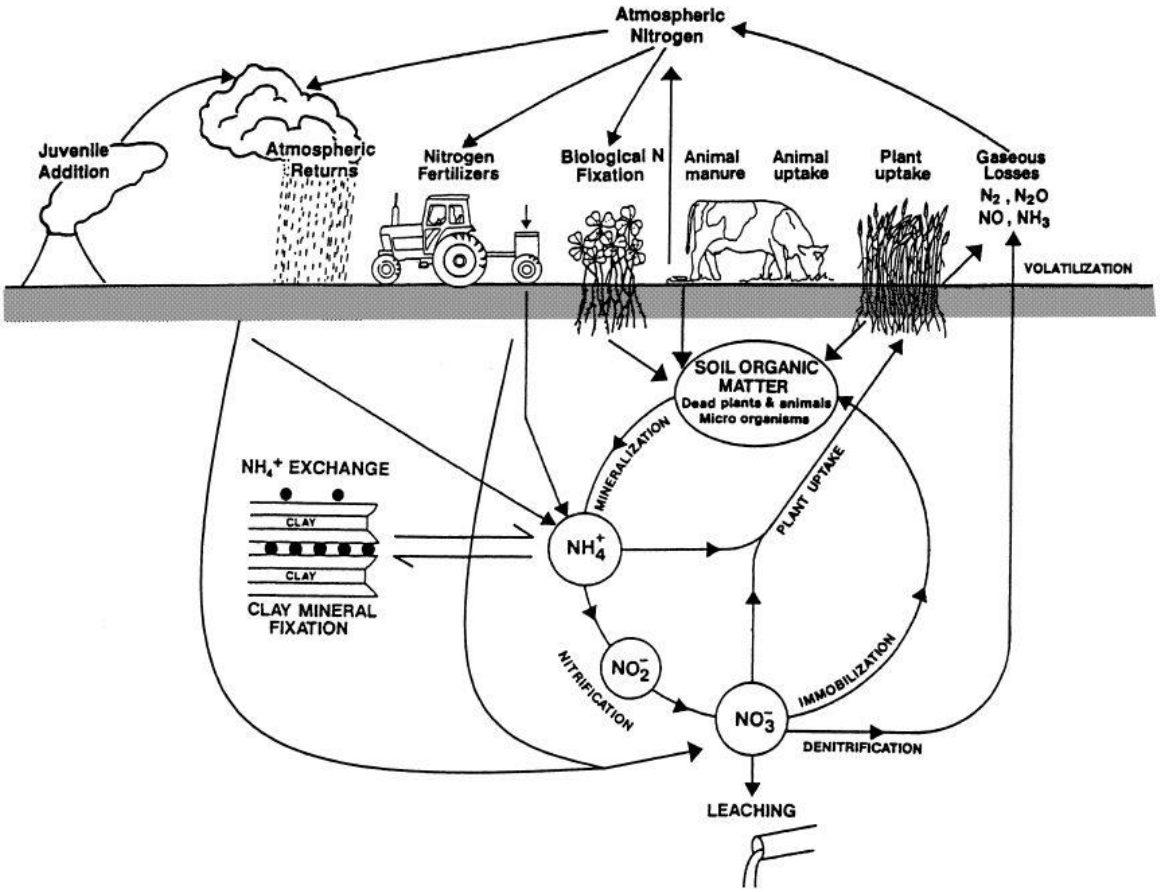

Figure 1. The Nitrogen cycle in grazed grasslands (Di and Cameron 2002)

Within grazed grassland ecosystems, livestock urine deposition is of special importance due to the fact that ruminants excrete 70-90% of the dietary N ingested (Jarvis et al. 1995). Each urine deposition event causes a sudden, and high increase in available N compounds within the topsoil, usually exceeding the utilization capacities of plants (Haynes and Williams 1993). This leads to an imbalance of the system represented in Fig. 1 and subsequently causes large and varied N fluxes until the background parameters are re-established, as discussed below.

2.3.2 Urine patches

The concentration of urinary N in ruminant animals is highly variable, ranging between 1 – 20 g N L^{-1} (Dijkstra et al. 2013). This concentration varies due to ruminant species, reproductive status, time of the day, season, and water intake (Selbie et al. 2015a). However, the diet is likely to be the most important factor, since N intake directly influences N excretion (Yan et al. 2007). This leads to similar urine compositions across different ruminant species and also influences the water intake of livestock (Spek et al. 2013; van Vuuren and Smits 1997). Hence, the N concentration of urine varies within a species more than between different species (Haynes and Williams 1993; Hoogendoorn et al. 2010). In case of a grass based diet, an average urinary N concentration of 6.9 - 12 g N L^{-1} might be assumed for dairy cattle and around 8.7 g N L^{-1} for sheep (Dijkstra et al. 2013; Selbie et al. 2015a; Whitehead 1995).

Table 1. N compounds of cattle urine (adapted from reviews by Dijkstra et al. (2013) and Selbie et al. (2015a)

Urinary Constituent	Average Concentration (g N L^{-1})	Concentration Range (g N L^{-1})	Average % of total N
Urea	6.0	2.1 – 19.2	73
Allantoin	0.86	0.27 – 1.5	10
Hippuric acid	0.51	0.37 – 1.5	6
Creatinine	0.26	0.08 – 0.65	3
Creatine	0.26	0.12 – 0.51	3
Ammonia	0.2	0.03 – 1.0	2.5
Amino acids	0.15	0.03 – 0.3	2
Uric acid	0.08	0.03 – 0.18	1
(Hypo)xanthine	0.05	0.03 – 0.09	0.6

More than 70% of urinary-N is present as urea with other urinary-N compounds consisting of allantoin, hippuric acid, creatine, creatinine and ammonia (Table 1). However, while these compounds could contribute up to 26% of urinary N, more than 70% is typically excreted as urea. In the case of a high N-containing grass diet urea might even represent 90% of the excreted N (Jarvis et al. 1995), making it by far the most important component with respect to the chemical reactions in the soil that occur post urine deposition.

Grazing livestock like cattle and sheep excrete urine many times per day. On a permanent grassland, 9 – 14 urinations per day have been reported for cattle and 18 – 20 for sheep (Haynes and Williams 1993; Lantinga et al. 1987). The average volume of the urine is estimated to be 1.6 – 2.2 L and 0.10 – 0.18 L, for cattle and sheep, respectively (Haynes and Williams 1993). However, this may strongly vary depending on factors like time of the day, diet or water intake (Betteridge et al. 1986; Eriksson and Rustas 2014). A single bovine urine event covers an area averaging 0.16 – 0.49 m^2, while the respective area for sheep is 0.03 – 0.05 m^2 for sheep (Haynes and Williams 1993), and over a year these deposition events may cover up to 30% of a pasture's surface (Moir et al. 2011). The so called 'urine patch' that results from a single urine deposition event, consists not only the wetted top-soil, but also the surrounding soil and deeper soil layers as urine soaks in (Williams and Haynes 1994). The exact spatial distribution of the urine is influenced by many factors like urinary volume, wind and soil surface slope (Luo et al. 2013). Consideration also needs to be given to the factors that affect infiltration (like soil moisture and texture) when predicting the average shape and volume of the urine-affected soil. However, for most pastures with no slope, typical urine patch dimensions, as demonstrated by Williams and Haynes (1994) (Fig 2), might be assumed. Typically, up to 46% of the urine infiltrates to a depth below 150 mm (Williams et al. 1990), but >70% of the urinary N remains in the top 100 mm (Monaghan et al. 1999), 50% might even stay in the top 50 mm (Williams and Haynes 1994). This enriches the topsoil with N loading rates between 200 - 2000 kg N ha^{-1} for cattle (Di and Cameron 2002; Jarvis et al. 1995; Lantinga et al. 1987; Oenema et al. 1997; Williams and Haynes 1993), and also sheep (Haynes and Williams 1993).

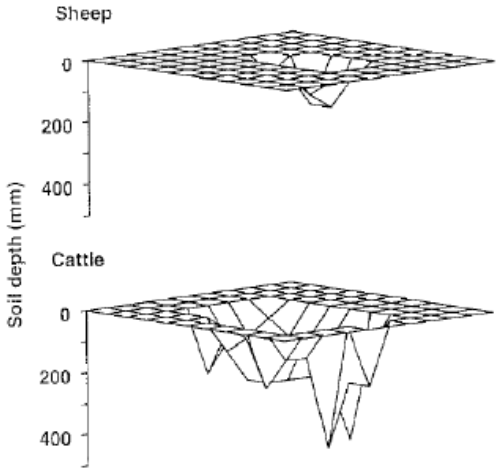

Figure 2. Distribution of urine through the soil profile under sheep (200 mL) and cattle (2000 mL) urine patches (Williams and Haynes 1994)

2.3.3 Ammonia volatilization

Following urine deposition, urea ($CO(NH_2)_2$) has by far the biggest influence on the following N transformations (Table 1). Within 48 h of deposition the urease enzyme hydrolyses 80 – 90% of the applied urea [Eq. 1], to form ammonium, bicarbonate ($HCOH_3^-$) and hydroxide ions (OH^-), (Jarvis and Pain 1990). Thus urine patches become localised areas of high pH:

$$(CO(NH_2)_2) + 2H_2O \xrightarrow{urease} 2NH_4^+ + HCO_3^{2-} + OH^- \quad [1]$$

The elevated soil pH shifts the chemical equilibrium, that exists between NH_3 and NH_4^+ [Eq. 2] towards NH_3.

$$NH_4^+ + OH^- \leftrightarrow NH_3 + H_2O \quad [2]$$

This results in an increased potential for NH_3 volatilization (Ernst and Massey 1960; Overrein and Moe 1967; Vermoesen et al. 1996). Elevated NH_3 concentrations in soil solution can also lead to inhibition of nitrifiers (Breuillin-Sessoms et al. 2017; Monaghan and Barraclough 1992). Typical volatilization rates are in the range of 1 – 38% of the applied urea N (Laubach et al. 2013). Solution phase NH_3 concentrations and subsequent NH_3 volatilization is influenced by the soil moisture, the soil NH_4^+ adsorption capacity and the initial N loading rate (Venterea et al. 2015). According to Sherlock et al. (2009), on average, around 10% of the urinary-N deposited may be assumed volatilized for most New Zealand pastures. However, the remaining NH_4^+-N is most likely to undergo plant uptake or nitrification, primarily driven by ammonia oxidizing bacteria (AOB) (Di et al. 2009; Samad et al. 2017). Soil mineral adsorption, plant uptake, but predominantly bacterial nitrification (Inselsbacher et al. 2010), lead to a rapid depletion of the NH_4^+-N pool. The nitrification process, and the release of H^+ ions as a consequence of volatilisation, result in the soil returning to the initial pH, or lower usually within a two week time period (Haynes and Williams 1992), which in turn prevents remaining NH_4^+ forming NH_3.

2.3.4 Nitrification and NO_3^- leaching

Under aerobic or partially aerobic soil conditions, NH_4^+-N is oxidized, via hydroxylamine (NH_2OH) to nitric oxide (NO), NO_2^- and subsequently to NO_3^- (Fig. 3). During this process, a fraction (0.24-1.92% of the utilized substrate N) of the N may be lost due to microbial cells leaking NH_2OH (Liu et al. 2017b).

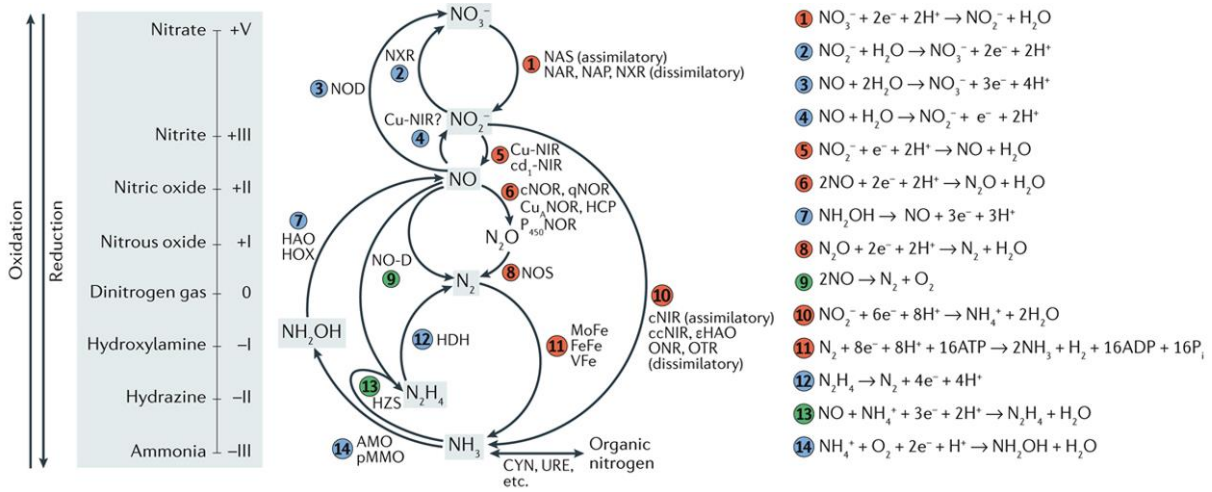

Figure 3. Nitrogen transformations in terrestrial ecosystems (Kuypers et al. 2018); Microorganisms carry enzymes that perform 14 redox reactions involving 8 key inorganic nitrogen species of different oxidation states (enzyme-bound intermediates and their redox states are not shown). The interconversion of ammonia and organic nitrogen does not involve a change in the redox state of the nitrogen atom. The reactions involve reduction (red), oxidation (blue) and disproportionation and comproportionation (green). The following enzymes perform the nitrogen transformations: assimilatory nitrate reductase (NAS, *nasA* and *nirA*); membrane-bound (NAR, *narGH*) and periplasmic (NAP, *napA*) dissimilatory nitrate reductases; nitrite oxidoreductase (NXR, *nxrAB*); nitric oxide oxidase (NOD, *hmp*); haem-containing (cd_1-NIR, *nirS*) and copper-containing (Cu-NIR, *nirK*) nitrite reductases; cytochrome *c*-dependent (cNOR, *cnorB*), quinol-dependent (qNOR, *norZ*) and copper-containing quinol-dependent nitric oxide reductases (Cu_ANOR); NADH-dependent cytochrome P_{450} nitric oxide reductase (P_{450}NOR, *p450nor*); flavo-diiron nitric oxide reductase (NORvw, *norVW*); hybrid cluster protein (HCP, *hcp*); hydroxylamine oxidoreductase (HAO, *hao*); hydroxylamine oxidase (HOX; *hox*); nitrous oxide reductase (NOS, *nosZ*); nitric oxide dismutase (NO-D, *norZ*); assimilatory nitrite reductase (cNIR; *nasB* and *nirB*); dissimilatory periplasmic cytochrome *c* nitrite reductase (ccNIR, *nrfAH*); ε-hydroxylamine oxidoreductase (εHAO; *haoA*); octahaem nitrite reductase (ONR); octahaem tetrathionate reductase (OTR); molybdenum-iron (MoFe, *nifHDK*), iron-iron (FeFe, *anfHGDK*) and vanadium-iron (VFe, *vnfHGDK*) nitrogenases; hydrazine dehydrogenase (HDH, *hdh*); hydrazine synthase (HZS, *hzsCBA*); ammonia monooxygenase (AMO, *amoCAB*); particulate methane monooxygenase (pMMO, *pmoCAB*); cyanase (CYN, *cynS*); and urease (URE, *ureABC*).

This NH_2OH may react with either NO or NO_2^-, present in the soil, to form N_2O. However, most of the oxidized NH_4^+-N accumulates in the NO_3^- pool (Fig. 3). Nitrification reactions are mainly microbial driven, with bacteria being predominantly active at this stage as discussed below. The duration of these nitrification reactions within the soil varies strongly (Chen et al. 2010), but is generally favoured by a low clay content in addition to constant moisture, or a high clay content with multiple drying and rewetting cycles (Sahrawat 2008). Nitrification usually happens within a range of pH 5.5 – 10.0, with an optimum at 8.5 (Sahrawat 2008) and an optimal temperature between 25 - 35°C, depending on the microbial adaption to certain climatic conditions (Focht and Verstraete 1977; Justice and Smith 1962; Myers 1975; Sabey et al. 1956). Since plants are able to take up NH_4^+ and

NO_3^- ions through their root systems, plant mineral N uptake is one of the major soil N pool reduction factors. The total pasture N uptake for grazed grasslands is in the range of 300 – 700 kg N ha^{-1} a^{-1} (Moir et al. 2007) averaging 41% of the total urine N (Selbie et al. 2015a). Most of this N uptake under permanent grassland conditions is assumed to be NO_3^--N, while plants are unable to outcompete the well adapted microbial community in these grasslands for NH_4^+ (Inselsbacher et al. 2010). In general, plant N uptake increases with increasing NH_4^+ and/or NO_3^- ion concentrations in the rhizosphere (Richards and Wolton 1975), however, low temperatures, seasons of inactive plant metabolism or a soil pH out of the optimum range for plant growth can periodically reduce this uptake capacity (Goh and Haynes 1986). Nitrogen loading rates exceeding plant uptake capacities, as often caused by ruminant urine depositions, may cause high mineral soil N concentrations to be prolonged. Thus, depending on soil porosity and rainfall (or irrigation), excess amounts of the mobile NO_3^- ions are likely leached or diffuse below the root zone (Cameron et al. 2013; Cameron and Haynes 1986; Hillel 1998). The leaching rate is positively correlated to the N loading rate (Stout 2003). Cameron et al. (2013) found an average of 60 kg N ha^{-1} was leached from N application rates of up to 750 kg N ha^{-1}, based on a comparison of 22 field studies carried out in the United Kingdom and New Zealand, averaging 21% loss of the applied N via NO_3^- leaching. However, under high soil moisture conditions, NO_3^- not taken up by plants or leached may also be microbially utilized.

2.3.5 Denitrification and N_2O emissions

Once the N has been transferred to NO_3^- it has reached its highest oxidative state (Fig. 3) and is stable under aerobic conditions. However, the accumulated NO_3^- can be microbially metabolized if oxygen becomes limiting. The microbial denitrification process can produce emissions of nitric oxide (NO), N_2O or N_2 from soil. The contribution of different microbial groups, as well as possible abiotic denitrification reactions, are discussed below. Denitrification can generally be seen as a microbial response to low oxygen availability at times of available NO_3^- (Luo et al. 2000; Luo et al. 1998; Wrage-Mönnig et al. 2018; Zhu et al. 2013a). This typically happens following precipitation, irrigation or when urine patches overlap (Turner et al. 2008) due to the percentage of water-filled pore space (WFPS) increasing, and blocking the supply of atmospheric oxygen to soil microorganisms. According to Rabot et al. (2015), a WFPS above 60% usually favours denitrification with most NO_3^- being denitrified between 70 – 90% WFPS.

However, according to the findings of Ball (2013), Hamonts et al. (2013) and Balaine et al. (2016), WFPS must be considered in addition to soil bulk density and soil matric potential. It was observed that soil N_2O emissions increased exponentially as soil relative gas diffusivity (D_p/D_o, where D_p is the soil-gas diffusion coefficient (cm^3 soil air cm^{-1} soil sec^{-1}) and D_o is the gas diffusion coefficient in free air (cm^2 air sec^{-1})) decreased until reaching a value of 0.005, where upon N_2O fluxes decreased

rapidly due to complete denitrification, such that N_2 fluxes reached a maximum of 60% of N applied at a D_p/D_o of < 0.005 (Fig. 4, note the log scale). Thus N_2O is more likely to be further transformed to N_2 with increasing D_p/D_o (Balaine et al. 2016).

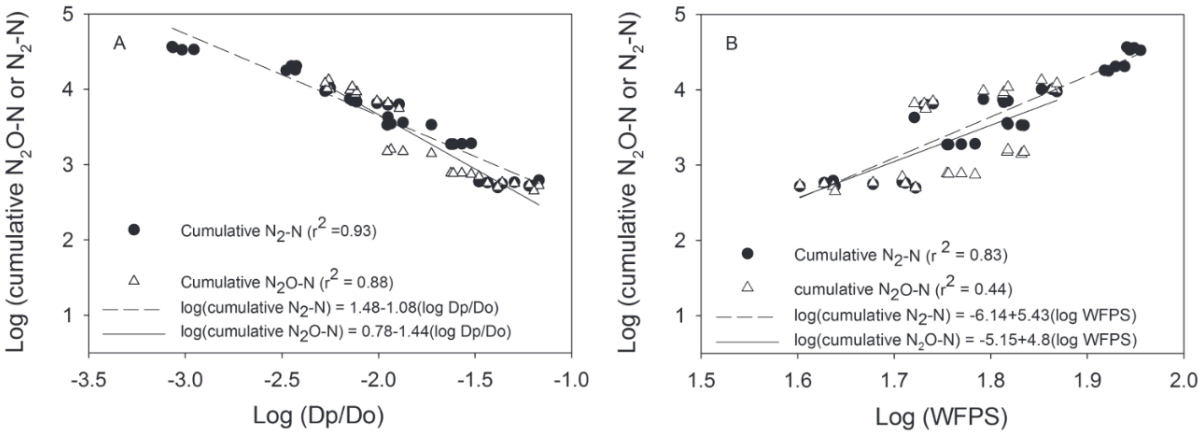

Figure 4. Regression of cumulative N_2O-N and cumulative N_2-N fluxes, expressed as their respective log values, vs. the log of relative gas diffusivity (D_p/D_o). Cumulative N_2O-N fluxes are plotted for D_p/D_o values of 0.005 while cumulative N_2-N fluxes are plotted for D_p/D_o values of > 0.0. Data points are individual replicates (Balaine et al. 2016).

Under such conditions, microorganisms start to metabolically reduce NO_3^- in the stepwise process of denitrification:

$$NO_3^- \rightarrow NO_2^- \rightarrow NO \rightarrow N_2O \rightarrow N_2 \quad [3]$$

Soils with a high clay content or a high bulk density are more likely to be found with conditions favouring denitrification, although it can occur in any soil with aggregates big enough to create low oxygen conditions inside (McLaren and Cameron 1996; Saggar et al. 2004). Although this process has the potential to end in environmental benign N_2, a fraction of the denitrified N usually leaves the soil as N_2O (Balaine et al. 2016; Weier et al. 1993). Due to its dilution with atmospheric N_2, emissions of N_2 are more difficult to detect and, given that, reported less often. Still, Monaghan and Barraclough (1993) measured 30 – 65% and Selbie et al. (2015b) 56.9% of the initially applied N being finally emitted as N_2. Clough et al. (1996) observed 3% of the applied N being finally lost as N_2O and approximately 0.3 – 2.5% of the initially applied N over a 4 month duration might be a representative N_2O emission factor (EF) for undisturbed grasslands (de Klein et al. 2003), depending on the above mentioned soil conditions.

2.3.6 Codenitrification

Besides denitrification, N_2O and N_2 emissions have been reported to result from biotic or abiotic N nitrosation. Based on early observations of N-gas production, exceeding the amount of added N substrates *in vitro*, an additional reaction besides denitrification was assumed. Over the last 40 years and with the introduction of stable isotope (^{15}N) labelled N substrates, a number of ^{15}N tracer experiments were able to show that this additional gas production is the result of N_2O and N_2 with one ^{15}N atom (from the applied substrate) and one ^{14}N atom (from another interacting N pool), as depicted in Figure 5. So far, it is well recognized that nitrosation reactions may form what is termed 'hybrid' N_2O or N_2, due to the merging of N from two different sources into one molecule. Grimbert (1899), Renner and Becker (1970) and Kumon et al. (2002) for example, all reported this effect *in vitro* following NO_3^- addition, a number of other studies have also reported codenitrification following NO_2^- addition (e.g. Garber and Hollocher (1982), Iwasaki et al. (1956), Shoun et al. (1992)) while others have identified the process following NO addition (e.g. Aerssens et al. (1986) Okada et al. (2005), Su et al. (2004)). In most of these studies, this process was found co-occurring with 'conventional' denitrification (resulting in N_2O and N_2 which solely derives from one N source). Thus, the reaction(s) was (were) termed 'codenitrification'. However, besides the often reported gaseous products, relatively little is known about the exact reaction pathways. It was not until relatively recently that evidence was found for codenitrification occurring in pasture soils (Laughlin and Stevens 2002) and in some cases it has been reported to be the dominant N_2 forming process in pasture soil (Selbie et al. 2015b). Clough et al. (2017) found that, like for denitrification, a high soil moisture content favours codenitrification and Long et al. (2013) found further evidence for the role of fungi in this process, confirming the previous findings of Laughlin and Stevens (2002). Spott et al. (2011) previously reviewed a number of potential fungal, bacterial and abiotically mediated reaction pathways for codenitrification, indicating that in pasture soils it is a process likely to be microbially driven as discussed below. However, experiments measuring codenitrification in the context of a soil matrix remain rare, and thus little is known about the exact chemical pathways of codenitrification, the microbial groups operating 'codenitrification' and the substrates utilized within urine patches. This underlines the basic need for experiments to further improve knowledge and to better understand how the characterization of codenitrification, based on *in vitro* studies, can be applied to the codenitrification reaction(s) in pasture soil urine patches.

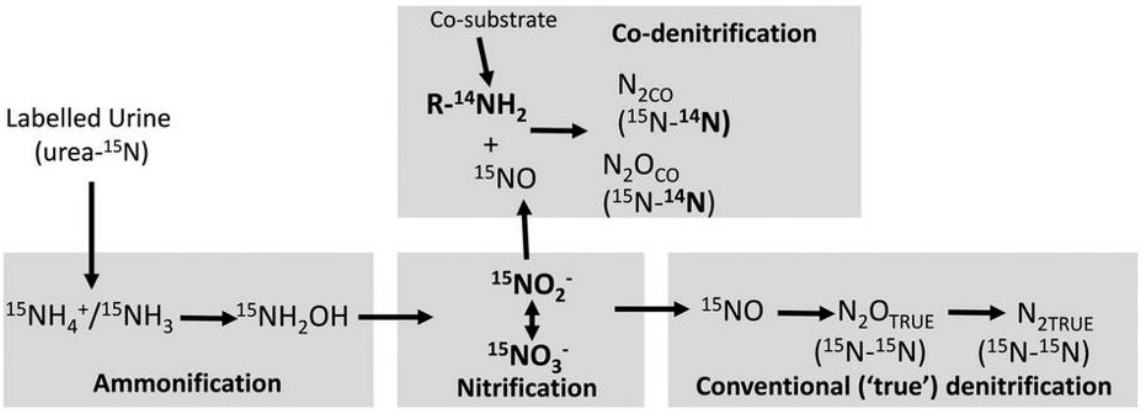

Figure 5. Conceptual model of codenitrification under urine patches in grassland soils, commencing with urea (Selbie et al. 2015b)

In conclusion, the term 'codenitrification' concludes a number of different chemical reactions, based on highly reactive N compounds, reacting biotically or abiotically with N compounds from the soil organic matter pool in order to create N_2O or N_2 from two different sources. Based on the above mentioned findings, it is proposed that a predominant codenitrification reaction in urine patches happens, when, under denitrifying conditions, NO_3^- is reduced to NO_2^- which co-metabolically reacts with components from the soil organic matter pool (Fig. 6).

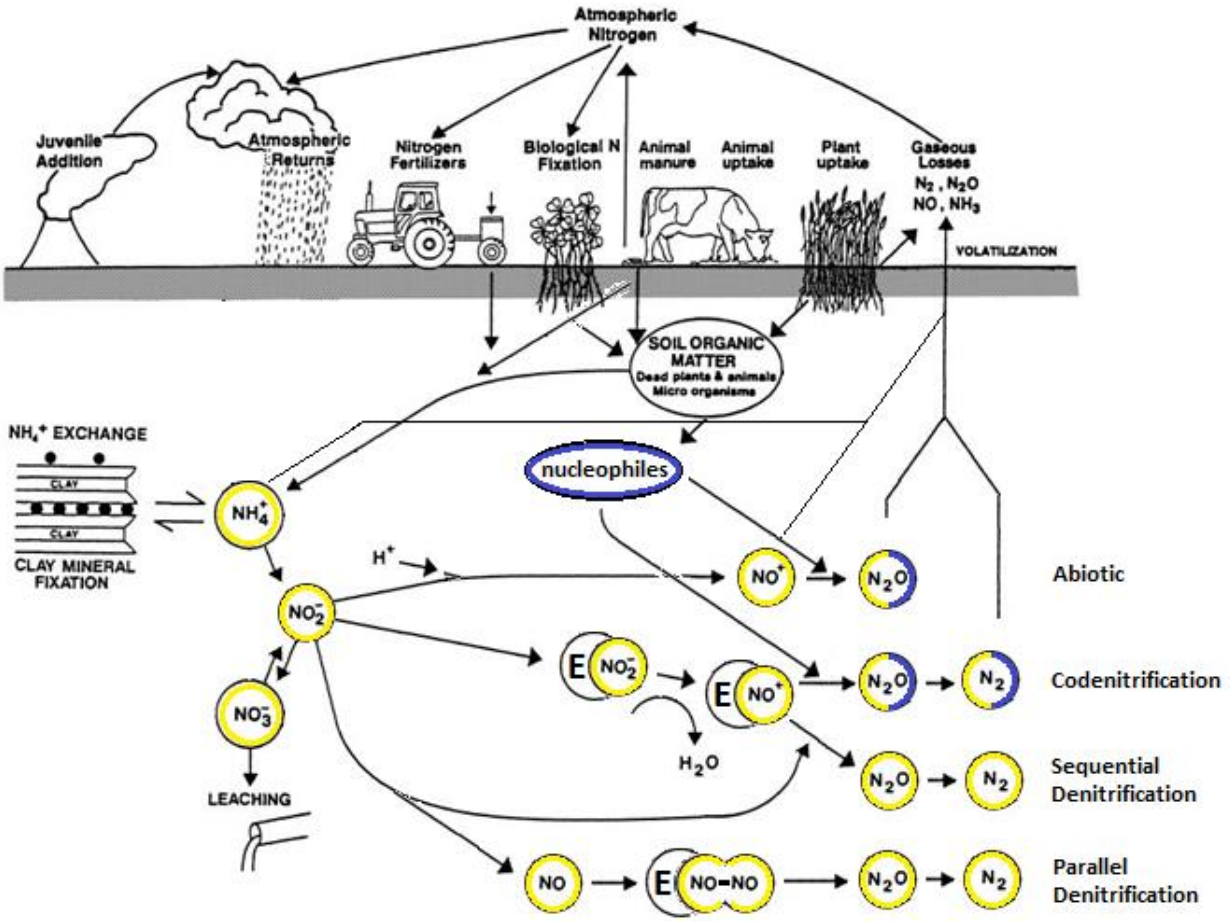

Figure 6. Proposed process of N_2O and N_2 formation in pasture soils, including codenitrification, within the general N cycle, E = enzyme, (adapted from Di and Cameron (2002) and Clough et al. (2017)).

2.4 Microbial contributions to codenitrification and other N transformations

Abiotic reactions alone can not explain the hybrid N_2O/N_2 formation under urine patch conditions. Abiotic N_2O and N_2 formation are often observed (Spott et al. 2011), and are discussed in greater detail below, however, the reported reactions require usually specific conditions (e.g., acidic soils pH < 5.0 (Römpp 1999)) which generally do not prevail within intensively managed pasture soils. In some instances the substrates involved in an abiotic reaction may be the product of microbial activity and thus the reaction may not be seen as a pure abiotic reaction pathway (Liu et al. 2017b). Thus, the (direct and indirect) contribution of different microbial groups to codenitrification has been debated, especially after codenitrification fluxes have been shown to decrease with microbial inhibition (Laughlin and Stevens 2002). In order to participate in codenitrification possible microbial protagonists must be common in pasture soils and have at least one enzyme with a known denitrifying function. In this chapter, a number of microbial groups, potentially capable of codenitrification as well as abiotic reactions are discussed with their respect to their potential contribution to N_2O and N_2 fluxes following urine deposition.

2.4.1 Mycorrhizal fungi

Fungal cells may represent up to 21% of the organic matter in grassland soils (Frostegård and Bååth 1996) and, due to the cell biomass superiority of mycorrhizal fungi to saprophytic fungi (Olsson et al. 1998), they may represent most of the fungal biomass in permanent grasslands. Among the different types of mycorrhiza, the arbuscular mycorrhiza (AM) dominate plant-fungal interactions in pasture soils in association with *Glomerales* species of AM (Munkvold et al. 2004). The analysis of specific phospholipid fatty acids (PLFA, (Olsson et al. 1995)) permits estimations of AM's abundance and distribution (Olsson 1999), and using glomalin analysis (Treseder and Turner 2007) in conjunction with ^{15}N and ^{13}C isotope tracing, it is possible to link AM's abundance to net primary productivity of plants. For example, an AM mediated N supply for plants, from a non-root-accessible N source, accounted for 3% of the plant's total N and 31% of AM N over a duration of 120 days (Hodge and Fitter 2010; Rillig et al. 2001). A review by Van Groenigen (2016) found that, although AM utilize less organic N compounds compared with ectomycorrhiza, their contributions to soil N-transformations and gaseous emissions might still be significant due to their potential to take up high amounts of N in case of sudden high N application rates (Thomas et al. 2010; Treseder et al. 2018), a consequence of their high fungal biomass. For most grasslands, it might be assumed that 0 – 20% of plant N uptake reaches the plant via AM (Van der Heijden et al. 2015) which in general means that the presence of AM is likely to reduce N_2O emissions (Bender et al. 2014). However, the role of AM in contributing to N_2O and N_2 emissions is unknown (Van der Heijden et al. 2015).

2.4.2 Saprophytic fungi

The term 'saprophytic fungi' refers to fungal species, solely living off heterotrophically utilized organic material without mutualistic plant interactions (Clegg and Mackean 2006; Setälä and McLean 2004). Depending on the amount of available organic material and microbial competition for it, saprophytic fungi potentially represent one of the largest fractions of the soil microbial biomass. Furthermore, their heterotrophic metabolism and ability to utilize N substrates from different sources predestines them to be likely candidates involved in the formation of hybrid N_2O (and N_2). In contrast to the mycorrhizal fungi, saprophytic fungi solely consume different kinds of organic material (mostly dead) and minerals, which simplifies the process of laboratory cultivation. Almost all studies dealing with fungal contributions to N_2O emissions (and N_2 emissions (Shoun et al. 1992)) have been performed with saprophytic fungi.

It was first discovered that *Fusarium oxysporum*, a cosmopolitan soil fungus, was able to convert NO_3^- and NO_2^- to N_2O (Shoun and Tanimoto 1991). Shoun et al. (1991) further demonstrated the importance of a cytochrome P-450 enzyme (P-450_{dNIR}) for this process and proved its presence in 7 different fungal species, including *Fusarium solani* which was later on observed to produce N_2 emissions, although the mechanism is unknown (Sameshima-Saito et al. 2004; Shoun et al. 1992). Shoun et al. (2012) later specified an enzymatic system in the fungal mitochondria of *F. oxysporum* and *Cylindrocarpon tonkinense* for (co)denitrifying activities, based on a nitrate reductase, a copper-containing nitrite reductase (encoded by the *nirK* gene) and the P450nor enzyme for the final conversion of NO_2^- to N_2O. It was further stated that this end-product could also be N_2, via a hybrid production pathway, with the product N_2O or N_2, depending on the redox state of the N donor: amine groups result in N_2 whereas imines and azides form N_2O (Spott et al. 2011). This fits well with the findings of Shoun et al. (1992) and Tanimoto et al. (1992). Since this work, further experiments have proved that at least 52 (saprophytic) fungal species are capable of producing N_2O (Maeda et al. 2015; Shoun et al. 1992), mainly belonging to the Ascomycota (Mothapo et al. 2015), with *F. oxysporum* and *F. solani* contributing to codenitrification via this reaction (Sameshima-Saito et al. 2004; Shoun et al. 1992; Su et al. 2004; Tanimoto et al. 1992). Finally, Higgins et al. (2016) tested 214 fungal isolates including 15 different morphological groups and found 151 of them capable of forming N_2O via Cytochrome P450nor and that there were two different *nirK* gene versions. Thus, it might be assumed that there is a great number of different fungal species that are potentially capable of codenitrification and the formation of N_2O from grassland soil (Laughlin and Stevens 2002) and soil in general (Wankel et al. 2017). Fungi have been shown to respond to variations in pasture management, for example increasing in biomass after rainfall events or in phylotypes after phosphorus fertilization (Wakelin et al. 2009). Also N fertilization and biochar amendments have been shown to increase fungal biomass (Kamble and Bååth 2016; Rex et al. 2015), although the most

important factor for fungal biomass increase might be the lack of cultivation in pasture soils (de Vries et al. 2007).

2.4.3 Bacteria (Nitrifier)

Among the bacteria, nitrifiers are typically the most active subsequent to urine deposition. According to Winogradsky et al. (1890) this includes ammonia-oxidizing bacteria (AOB, genus *Nitrosomonas*, *Nitrosococcus* and *Nitrosospira*) as well as NO_2^- oxidizing bacteria (genus *Nitrobacter*, *Nitrolancetus*, *Nitrospina*, *Nitrospira* and *Nitrococcus*). Due to its high energy yield, nitrification reactions are performed by many bacteria who gain 235 kJ mol^{-1} out of NH_3 oxidation alone, and following the further oxidation of NO_2^- to NO_3^- another 76 kJ mol^{-1}. However, these substrates are in abundance for only a relatively short period of time. For over 100 years it was assumed that the best way for a microbial species to compete with other species was for it to specialize in one step of the nitrification process, due to a trade-off between maximizing the rate or product gain which favours short reaction pathways in case of limited time (Costa et al. 2006), a theory that linked well with the 'hole in the pipe' model (Firestone and Davidson 1989; Zhang et al. 2015a). But more recent research calls this into question, identifying *Nitrospira* species as being able to perform the complete oxidation of NH_4^+ (Daims et al. 2015; Kuypers 2015; Van Kessel et al. 2015).

It seems that the exact chemical pathways transforming most of the applied N are more dependent on environmental factors like the soil moisture content, soil bulk density, oxygen availability and temperature than on the present microbial species (Chen et al. 2010; Giguere et al. 2017; Santoro 2016).

The main contribution of nitrifiers to the N-cycle may be seen in the transformation of NH_4^+ to NO_3^-, however, under low oxygen conditions in soils with low carbon content, nitrifiers may also denitrify which directly leads to N_2O emissions, accounting for 30% or more of the total N_2O emissions (Kool et al. 2011; Meinhardt et al. 2018; Wrage-Mönnig et al. 2018; Wrage et al. 2001). In addition to autotrophic nitrifiers, heterotrophic nitrifiers may also produce a considerable amount of N_2O (Zhang et al. 2015a). Under most pasture soil conditions, they oxidize N and with that provide a substrate for subsequent (co)denitrification, which is therefore assumed to be their main (indirect) contribution to N_2O and N_2 emissions (Anderson and Levine 1986).

2.4.4 Bacteria (Denitrifier)

Many bacterial species have been reported to act as denitrifiers (e.g. genus *Paracoccus*, *Pseudomonas* and *Thiobacillus*). When oxygen becomes limited, they are able to use NO_3^- as an electron acceptor for further oxidative reactions (Schreiber et al. 2012). Within this stepwise reaction, highly reactive intermediates like NO_2^- and NO are produced. Initially, NO_3^- is reduced to NO_2^- via an enzymatic reaction with nitrate reductase and subsequently, NO_2^- is further reduced by nitrite reductase to NO (Fig. 7). According to Goretski and Hollocher (1991) and Ye et al. (1991) this NO also acts as a nitrosyl (NO^+) donor in prokaryotic cells for an enzymatic reaction with NO_2^- potentially forming hybrid N_2O, according to (Averill 1996); simplified:

$$R_2Fe^{2+} - NO^+ + NO_2^- + H_2 \rightarrow R_2Fe^{2+} - N_2O_2 + H_2O \quad [4]$$

$$R_2Fe^{2+} - N_2O_2 + H_2 \rightarrow R_2Fe^{2+} - N_2O + H_2O \quad [5]$$

$$R_2Fe^{2+} - N_2O \rightarrow R_2Fe^{2+} + N_2O \quad [6]$$

For the final N-N linkage reaction a heme cd1-containing NIR enzyme (Wang and Averill 1996) or a copper containing NIR (Averill 1996) is assumed.

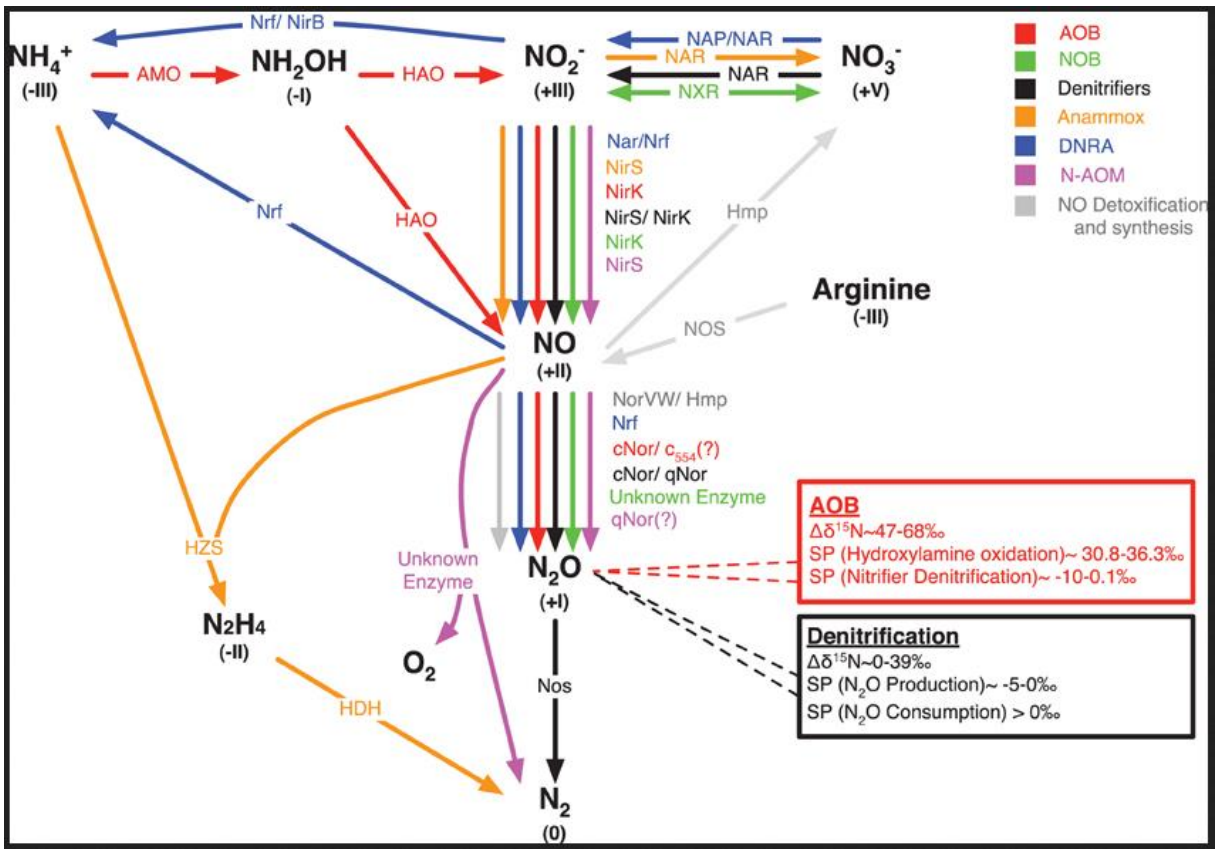

Figure 7. Biological pathways for NO and N_2O turnover in the catabolic branch of the N-cycle plus NO synthesis and detoxification. Different colours are allocated to different microbial guilds or turnover pathways: AOB (red), ammonia oxidizing bacteria; NOB (green), nitrite oxidizing bacteria; anammox (orange), anaerobic oxidation of ammonia; DNRA (blue), dissimilatory nitrate/nitrite reduction to ammonia; N-AOM (purple), oxygenic nitrite-dependent anaerobic oxidation of methane. Key enzymes of each microbial guild are depicted that are known to mediate the conversion from one chemical N-species into another: AMO, ammonia monooxygenase; HAO, hydroxylamine oxidoreductase; NXR, nitrite oxidoreductase; Nar, membrane-bound nitrate reductase; Nap, periplasmic nitrate reductase; NirK, copper-containing nitrite reductase; NirS, cytochrome *cd*$_1$ nitrite reductase; Nrf, cytochrome *c* nitrite reductase; NirB, cytoplasmic nitrite reductase; cNor, nitric oxide reductase that accepts electrons from c-type cytochromes; qNor, nitric oxide reductase that accepts electrons from quinols; c554, cytochrome c_{554}; NorVW, flavorubredoxin, Hmp, flavohemoglobins; HZS, hydrazine synthase; HDH, hydrazine dehydrogenase; Nos, nitrous oxide reductase; NOS, nitric oxide synthase; unknown enzymes, nitric oxide dismutation to N_2 and O_2 during N-AOM and nitrous oxide producing enzyme in NOB. Roman numbers in brackets denote the oxidation state of the chemical N-species. The red and the black box denote the isotopic composition ($\delta^{15}N$) and the site preference (SP) in isotopomers of N_2O produced by AOB and denitrifiers, respectively (Schreiber et al. 2012).

However, many of those species are capable of performing a wide range of enzymatic reactions, dependent on substrates present, soil pH and oxygen availability (Zhang et al. 2015a; Zhang et al. 2015b). Some species, for example, possess an electron acceptor system that works for both, NO_3^- and O_2 which allows heterotrophic nitrification and aerobic denitrification (Castignetti and Hollocher 1984; Robertson et al. 1989). Others, like *Pseudomonas* sp. are not only known for their

(co)denitrifying activities (Spott et al. 2011), but also to play an important role within the rhizospheric metabolism in general (Lebinay et al. 2012; Tarnawski et al. 2006). In order to gain energy, bacterial species are likely to adapt their metabolism to current circumstances, including the consumption of any suitable substrate, so that "we should know by now that if a reaction is thermodynamically possible, microbes will find a way." (Santoro 2016). Hence, if N from different sources can be found in bacterial cells, it might also lead to hybrid N_2O/N_2 formation.

2.4.5 Archaea

Since different archaea species are known to play an important role in C and N turnover (He et al. 2012b; Munroe et al. 2016), a possible contribution to soil hybrid N_2O production might be assumed (Immoos et al. 2004). Archaeal species can also act as NH_4^+ oxidizers (He et al. 2012a; He et al. 2012b) and even as hybrid N_2O producers (Immoos et al. 2004; Renner and Becker 1970). However, it appears that their contribution to nitrification within urine-urea affected soil is low (Di et al. 2014; Samad et al. 2017). Thus, it might be assumed that their total contribution to hybrid N_2O formation as consequence of a bovine urine event is negligible, despite their wide distribution in pasture soils and contributions to the N turnover under low N input conditions (Hink et al. 2017; Leininger et al. 2006; Prosser and Nicol 2008).

2.4.6 Abiotic formation of hybrid N_2O and N_2

A number of abiotic reactions are known to result in the formation of hybrid N_2O or hybrid N_2 (Bothner-By and Friedman 1952; Bottomley 1978; Clough et al. 2001b; Williams 2004). According to Spott et al. (2011), the type of N gas is largely dependent on the nucleophilic substrate.
Hybrid N_2 gas formation mostly occurs due to N-nitrosation reactions with primary amines or amides via a diazo ($R_2C{=}N_2$) and/or diazonium compound ($R_2C{—}N_2^+$) as the intermediate species (= diazonium). The subsequent dediazoniation of this N_2-group can proceed by various pathways (Fig. 8) depending on the reaction conditions (e.g. temperature, nucleophilic substrate etc.) (Hart 1989; Römpp 1999; Williams 2004; Zollinger 1995). Hybrid N_2O has been mainly reported to occur following N-nitrosation reactions with oxime compounds (C=N—OH) or NH_2OH (Freeman 1973; Zollinger 1995) (Fig. 9).

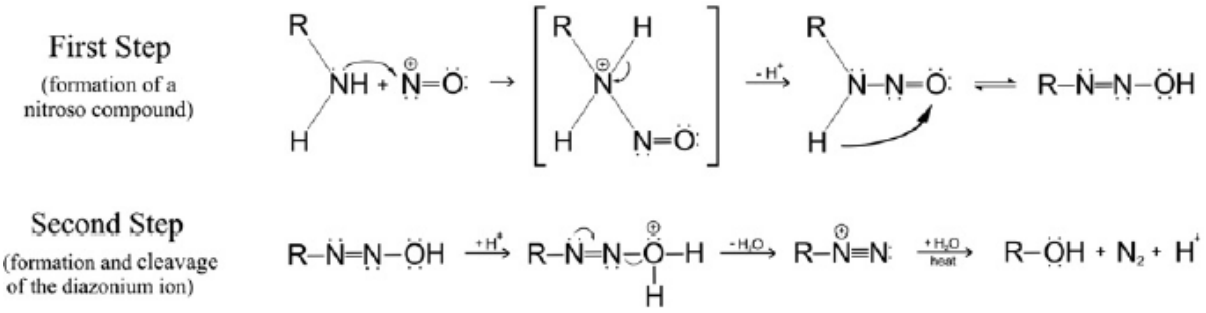

Figure 8. Abiotic formation of hybrid N_2 gas due to an N-nitrosation of a nucleophilic primary amine by the electrophile NO^+ (Spott et al. (2011), after Hart (1989))

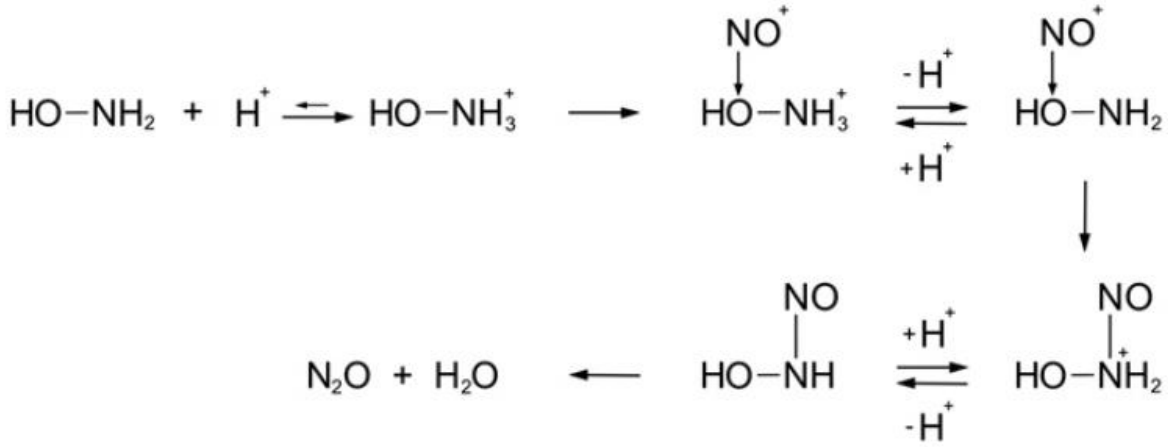

Figure 9. Abiotic formation of hybrid N_2O gas due to an N-nitrosation of NH_2OH by the electrophile NO^+ (Spott et al. (2011), after Zollinger (1988))

Spott et al. (2011) concluded therefore that (i) N_2 is formed, if the formal oxidation state of the nucleophilic N is -3 (e.g., R-NH_2, NH_3), (ii) N_2O is formed if the formal oxidation state of the nucleophilic N is -1 (e.g., NH_2OH), and (iii) N_2O and N_2 are formed, if the formal oxidation state of the nucleophilic N is -2 (e.g., hydrazine).

Recently it was discovered that AOB 'leak' NH_2OH (Ermel et al. 2018) and thus may form gaseous N compounds as a result of abiotic reactions with soil NO_2^- (Heil et al. 2015; Liu et al. 2017b), however, since hydroxylamine itself requires microbial formation it may not be seen as a purely abiotic pathway for hybrid N gasses. Similarly, the findings of Phillips et al. (2016) who observed hybrid N_2O and N_2 formation in the presence of dead fungal biomass ('fungal necromass'), might be seen as indirect microbial contributions to gaseous emissions.

2.5 Methods for studying N cycling

2.5.1 Selective inhibition

In contrast to total microbial inhibition using sterilization methods for soils or growth media (e.g. autoclaving), selective inhibition aims to inhibit just a fraction of the present microbial community. For the separation of a single microbial species or the measurement of contributions to a microbial community's biomass or metabolic response, several chemicals have already been used in the reported literature based on their inhibitory potential with respect to specific microbial groups (Kreutzer 1963). Since many of these substances can be used for microbial communities *in vitro* (Tsao 1970), problems may occur with their use in soils due to unknown non-target effects (e.g. fungal inhibitors also inhibiting some archaeal species (Vajrala et al. 2014)). However, within a series of many experiments, Anderson and Domsch developed a method for selective inhibition of fungi and bacteria in soil samples (Anderson and Domsch 1973; Anderson and Domsch 1974; Anderson and Domsch 1978). Within this method, cycloheximide ($C_{15}H_{23}NO_4$) is used as fungal inhibitor to inhibit the peptidyl transferase activity of the eukaryotic 60 S ribosomal subunit (Schneider-Poetsch et al. 2010) and streptomycin ($C_{21}H_{39}N_7O_{12}$) is used to inhibit the bacterial protein synthesis (Luzzatto et al. 1968). These chemicals are simply applied as a dry powder to the soil and distributed via subsequent mixing of the sample (Anderson and Domsch 1973). Later evaluations of this method revealed a few problems caused by the rapid decomposition of the inhibitory substances in soils and the non-inhibition of a few bacterial groups (Badalucco et al. 1994), however, these chemicals can be assumed to inhibit most fungi (cycloheximide) or bacteria (streptomycin) within 24 – 48 h after application. Other chemicals have also been used for soil microbial selective inhibition, e.g. ethyne (C_2H_2), Captan ($C_9H_8Cl_3NO_2S$) or oxytetracycline hydrochloride ($C_{22}H_{24}N_2O_9$*HCl) (Bailey et al. 2002; Klemedtsson et al. 1988). However, limited inhibition time and non-target effects are common problems among almost all selective inhibitory substances (Oremland and Capone 1988), and the refined method of Anderson and Domsch (1978) is still regarded as one of the most precise and simplest methods for selective inhibition of bacteria and fungi in soil samples and therefore it is frequently used (e.g., Lin and Brookes (1999), Rex et al. (2015) and Koijman et al. (2016)).

2.5.2 ^{15}N-tracer techniques

The discovery of ^{15}N as a naturally occurring stable isotope of N (Naudé 1929) provided a simple yet effective way to mark N within a chemical compound in order to trace back its transformation and distribution over the duration of an experiment (or rather a chemical reaction pathway). The natural abundance of ^{15}N in atmospheric N_2 is only 0.3663% (and so it is in the biosphere), and thus the distribution of the initial N from an applied N source can be traced back by measuring the ^{15}N

percentage within the subsequent reaction products. First techniques were already developed in the 1940s (Rittenberg 1948) and since then ^{15}N has been used as tracer element for further investigation of the N cycle (Chen et al. 1995; Hauck et al. 1958; Hüser et al. 1960; Jansson 1955; Peterson 1999; Peterson and Fry 1987; Turtschin et al. 1960). Usually the N samples require a certain procedure for purification and transformation into an N gas (e.g., distillation and titration (Bremner and Edwards 1965) or a diffusion method (Brooks et al. 1989; Sorensen and Fresquez 1991)) to be finally analysed using a mass spectrometer. In more recent years, this approach was used for the characterization of chemical reactions forming N_2O and N_2 (Garber and Hollocher 1981; St John and Hollocher 1977) where subsequent calculation procedures allow the identification of N pool of origin and (indirectly) the generating pathway (Arah 1997; Boast et al. 1988). Such an approach is used in almost all recent studies focusing on (co)denitrification (Clough et al. 2017; Heil et al. 2015; Laughlin and Stevens 2002; Phillips et al. 2016; Selbie et al. 2015b; Spott et al. 2011).

2.5.3 ^{15}N-modelling

Another tool for the estimation of N fluxes/transformations between the different N pools in soil are models which are used to predict gaseous N emissions or to estimate the N turnover in soil. Although recent techniques allow the constant measurement of N fluxes and leaching (e.g. NH_3 (Demmers et al. 1999; Rhoades et al. 2010)), most measured N flux data refer to few points in time and naturally lack information for the intervals in between. Another issue, given limitation of resources, is the lack of simultaneous measurements for all N-pools at the same time.

However, using a ^{15}N tracing model data can be acquired for modelling such information. This approach started with the pioneering work of Kirkham and Bartholomew (1954), firstly experimenting with an analytical model based on two N pools. In their first paper they made the assumptions that there would be (i) no preferential use of ^{15}N or ^{14}N, (ii) immobilized N would not be re-mineralized, and (iii) N transformation rates would follow zero-order kinetics (constant rates). The latter two assumptions were rejected in a following paper (Kirkham and Bartholomew 1955) and as the N transformation rates changed into first-order kinetics. Still, there was no distinction between the NH_4^+ and NO_3^- pools, and no distinction was made as to the availability of N within the organic pool, along with no consideration of possible N losses due to volatilization. So, further work was performed in consideration of these gaps. Subsequently studies have modelled N turnover of the NH_4^+ and NO_3^- pools using an analytical approach (Ambus and Christensen 1995; Barraclough 1991; Davidson et al. 1990; Nishio et al. 1985; Schimel et al. 1989; Tietema and Wessel 1992), while other studies have tried to find a numerical solution (Bjarnason 1988; Myrold and Tiedje 1986; Smith et al. 1994; Wessel and Tietema 1992). However, to find an analytical solution for 3 or more possible N pools is challenging. Most of the analytical models are based on an 'isotopic dilution' approach,

meaning that one N pool is initially enriched with ^{15}N and becomes 'diluted' over time with ^{14}N from a less enriched source. In order to determine the dynamics of NH_4^+ and NO_3^- for example, a paired experiment would be necessary with one treatment including $^{15}NH_4^+$ enrichment and one for $^{15}NO_3^-$. Numerical models on the other hand include a description of the modelled system, a numerical resolution of the differential equations and a non-linear optimization procedure (Mary et al. 1998). Thus, the 'isotopic exchange' principle, which is able to consider inward- and outward N fluxes from N pools, provides a good model fit to the measured data from an unpaired experiment. Conclusively, with the cost of a minimal loss in precision the numerical approach enables the design of more complex models.

Despite Nishio et al. (1994) using an analytical approach, all following descriptions of the N transformations were based on numerical solutions. Mary et al. (1998) proposed a model named FLUAZ, which included 5 different N pools, 10 possible N transformations (Fig 10) and was based on the Runge-Kutta algorithm (4^{th} order, variable time steps) and a non-linear fitting program (based on Marquardt's algorithm). The Runge-Kutta and Marquard algorithms were further used for the '^{15}N tracing' model as presented in Müller et al. (2004), this time in combination with the Markow Chain Monte-Carlo (MCMC) method and the Metropolis algorithm (Metropolis et al. 1953) to avoid the optimization procedure being trapped in a local minimum of the misfit function.

This basic version includes 4 mineral and 2 organic soil N pools and 9 possible N transformations ((Müller et al. 2004), model B, (Müller et al. 2007)). This model was later on modified (Inselsbacher et al. 2013; Müller et al. 2014), depending on the raw data provided in the experiment. Another useful novelty was the possible inclusion of a separated NO_2^--N pool (Müller et al. 2014; Rütting and Müller 2008), which allows the estimation of NO_2^- and N_2O formation via different chemical pathways (Fig. 11). Thus, the ^{15}N tracing model group is a highly valuable tool that can be used when methods of direct measurement reach their limits.

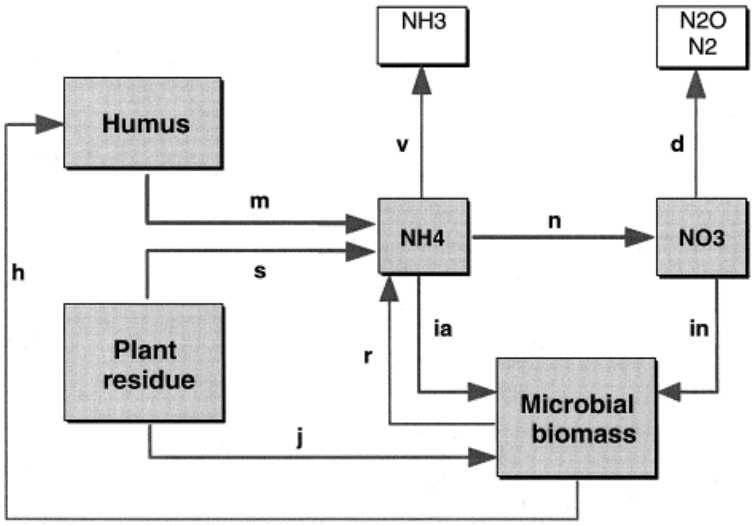

Figure 10. Compartmental model of N rates considered in FLUAZ (Mary et al. 1998)

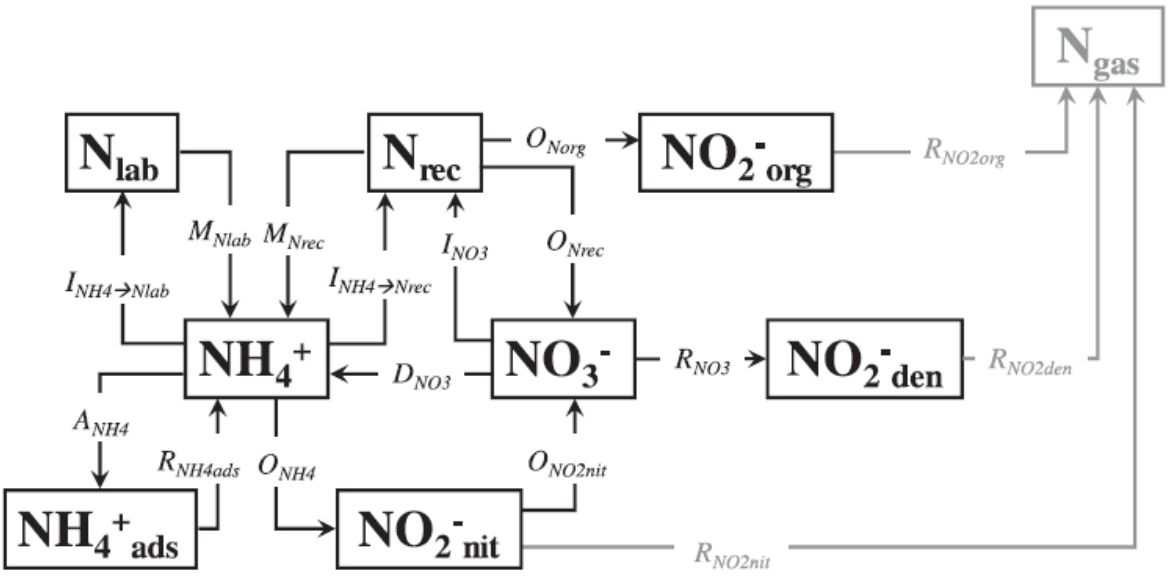

Figure 11. ^{15}N tracing model to identify pathway specific NO_2^- dynamics (Müller et al. 2014). The different N-pools are; N_{lab} = labile soil organic N, N_{rec} = recalcitrant soil organic N, NH_4^+ = ammonium, $NH_4^+{}_{ads}$ = adsorbed NH_4^+, NO_3^- = nitrate, NO_2^-nit = nitrite of autotrophic nitrification, NO_2^-org = nitrite of heterotrophic nitrification, NO_2^-den = nitrite of denitrification, N_{gas} = volatilized NO, N_2O and N_2. The transformation rates are; A = adsorption, D = dissimilatory nitrate reduction, H = hydrolyzation, I = immobilization, M = mineralization, R = release, O = oxidation, V = volatilization.

2.6 Summary

Dairy farming in Ireland and New Zealand is continuously intensifying, leading to more mineral N circulating in the pasture N cycle. Ruminant urine deposition may cause local N loading rates of up to 1000 kg N ha^{-1}, exceeding the plants N uptake capacity and, combined with a high soil moisture content, promote NO_3^- leaching and NO_3^- reduction via (co)denitrification. While complete denitrification reduces NO_3^- to environmentally benign N_2, the soil conditions may allow the emission of N_2O before its complete reduction. Since evidence was found for a significant codenitrification contribution to N_2O and N_2 emissions following ruminant urine deposition (Selbie et al. 2015b), the related chemical processes must be characterized in more detail in order find mitigation strategies for N_2O emissions.

Codenitrification forms hybrid N_2O and hybrid N_2 via biotic nitrogen-nitrosation, co-metabolizing organic and/or mineral N compounds to form N_2O and N_2. Although a number of abiotic reactions resulting in hybrid N gases are known (Spott et al. 2011), there is no evidence for a significant contribution within urine affected grassland soil. It is more likely that the identified microorganisms, performing biotic N-nitrosation (= codenitrification) are mainly responsible for the formation of hybrid N gasses in urine patches. Although many bacterial and two archaeal species are also known for their ability to form hybrid N gasses (Spott et al. 2011), most of the total microbial biomass in long-term undisturbed grasslands is allocated to soil fungi and thus, it seems that fungi are likely to be an important microbial group in this context (Laughlin and Stevens 2002; Spott et al. 2011).

Still, there is a clear gap in knowledge about the exact contribution of different microbial groups to codenitrification since most previous experiments were performed *in vitro*, based on only one or a few microbial species. The few recent experiments on the other hand, based on soil mesocosm or field experiments, rarely focus on the underlying chemical reaction pathways codenitrification is based on. Thus, to better understand and characterize N_2O forming processes in grassland soils, experiments are needed which investigate the contribution of different microbial groups to codenitrification and the related N compounds and transformations within a soil matrix. With methods for selective inhibition, the ^{15}N tracer approach and newly developed N trace models, a range of suitable tools is already in place for these further investigations.

2.7 Objective and hypothesis

This literature review identifies three key knowledge gaps, where there is a lack of understanding;

i. What are the codenitrification performing microbial groups in pasture soils, forming hybrid N_2O and N_2 subsequent to ruminant urine deposition and what is their range of contribution?
ii. Besides the applied N source, what are the co-metabolized N compound(s) from within the soil?
iii. What are the related soil N dynamics favouring N transformations or creating conditions favouring hybrid N_2O and hybrid N_2 formation?

The following research chapters will address these questions.

Chapter 3
General materials and methods

3.1 Introduction

Laboratory experiments were conducted from November 2015 – January 2016 (1st experiment, first year) and from August – September 2017 (2nd experiment, year two). Each experiment was carried out in the laboratory facilities of Lincoln University, Lincoln, New Zealand with freshly collected soil from the nearby Lincoln University Research Dairy Farm. The experiments were based on soil mesocosms and set up to trace back the reaction pathways of ^{15}N labelled N compounds as manipulated with selective microbial inhibitors. This chapter gives a detailed description of the conditions, soil properties and techniques used for the experiments and the related laboratory tests ('pilot studies') that were performed to finalise the experimental set ups.

3.2 Soil mesocosms

3.2.1 Side and soil properties

Lincoln University is located on the East of New Zealand's South Island, south of Christchurch and relatively central within the Canterbury Plains, at an altitude of 11-12 m above the sea level (Fig. 12). The average climate (1971 – 2000) of this region is temperate-dry, with 500 – 750 mm of precipitation annually, and an annual average air temperature of 10.1 - 12^{o}C (Fig. 13). The agricultural land here is mainly used for cropping and perennial pasture. Lincoln University Research Dairy Farm is located north of the university campus with a perennial pasture cover, predominantly consisting of rye-grass (*Lolium perenne* L.) and white clover (*Trifolium repens* L.).

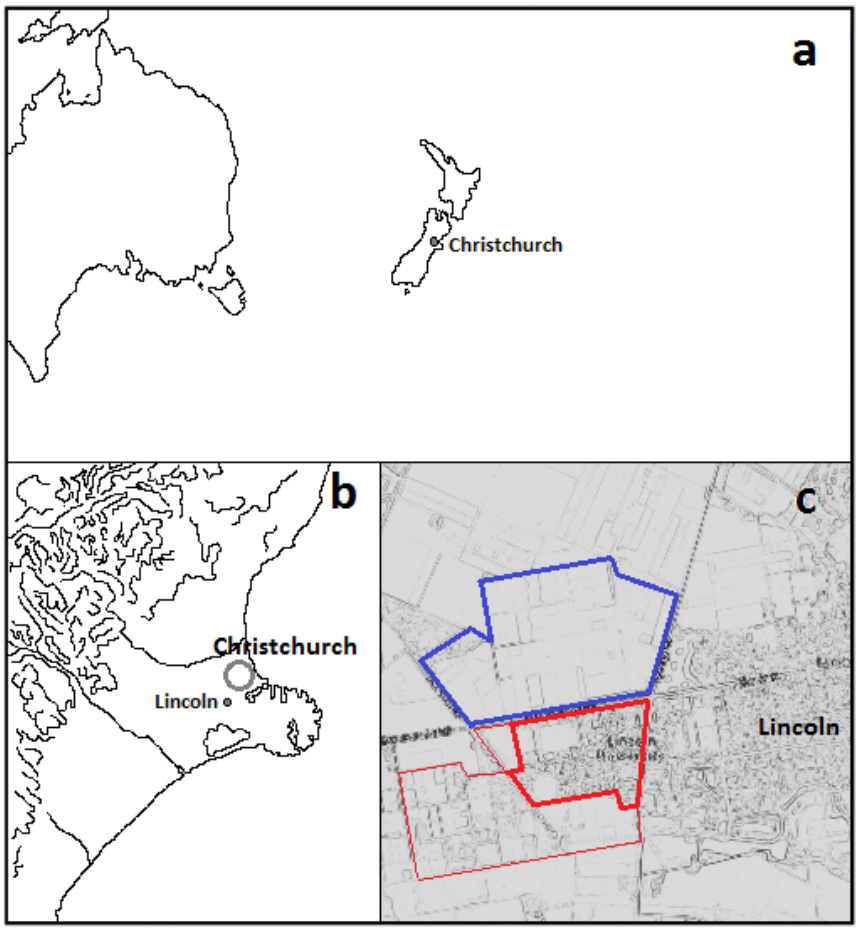

Figure 12. Location of Lincoln University (red) and the Research Dairy Farm (blue) at Lincoln (c) near Christchurch (b) on the South Island of New Zealand (a).

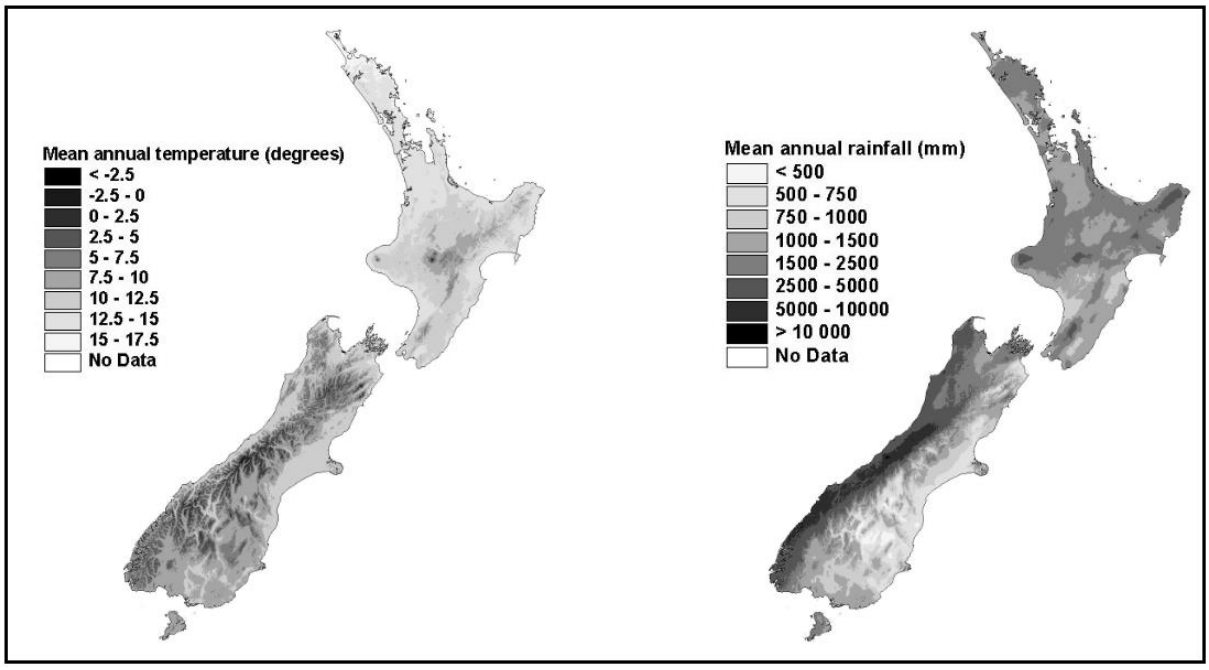

Figure 13. Average rainfall and temperature of New Zealand (Leathwick and Stephens 1998)

Figure 14. The Research Dairy Farm (blue marked) of Lincoln University, orange marked are the soil sampling areas of the 1st experiment (1.) and the 2nd (2.).

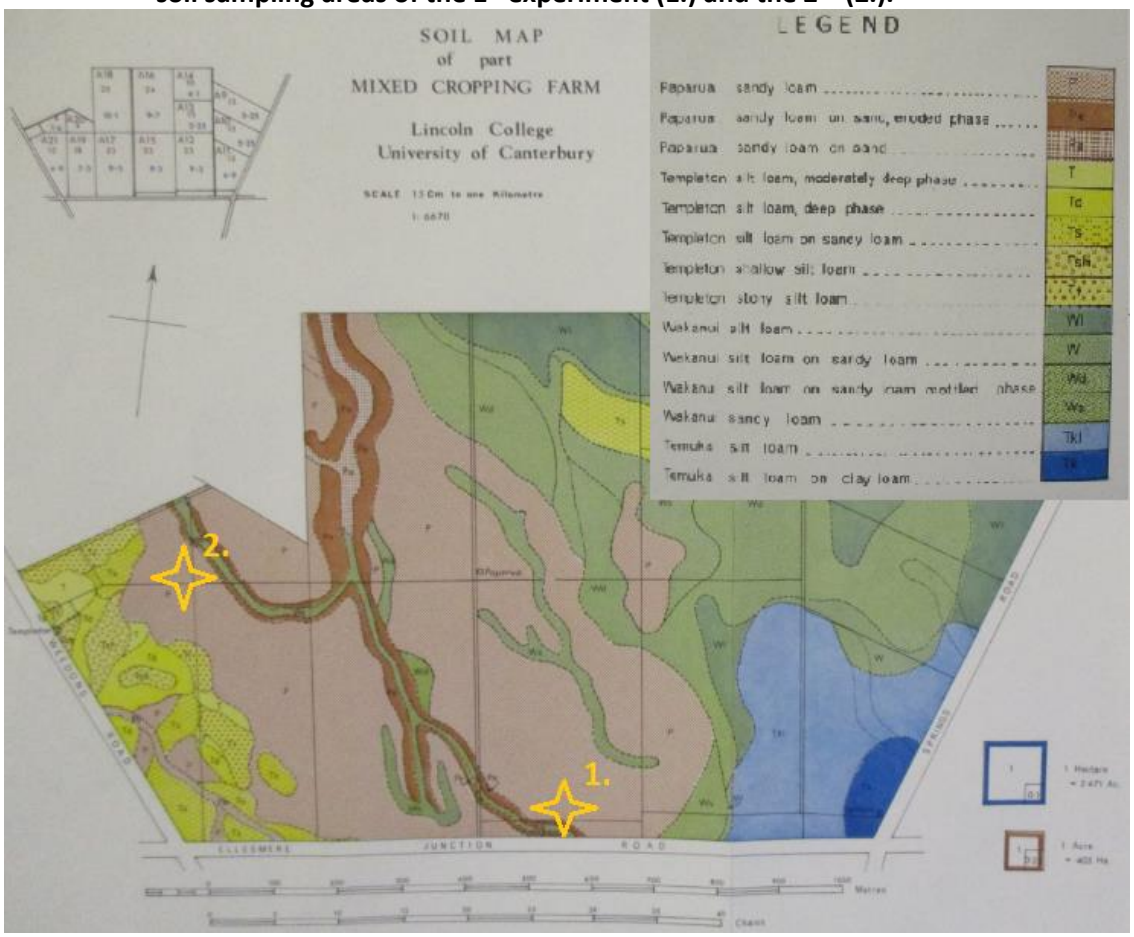

Figure 15. Lincoln University Research Dairy Farm, soil types by E. J. B. Cutler (Lincoln College 1971), Shown in yellow are the locations for the soil sampling for the 1st (1.) and the 2nd (2.) experiment (both times a 'Paparua sandy loam').

Figure 16. Soil sampling site (1st experiment)

For both experiments, 1st and 2nd (Fig. 14), the top 10 cm of pasture soil was collected (at 43°38'33.73"S, 172° 27'40.38"E for the first experiment and at 43°38'25.23"S, 172°27'24.71"E for the second one, Fig. 15, 16) and soil parameters were subsequently analysed. For both experiments the sampled soil was classified as a 'Paparua sandy loam' (Fig. 16) which is classified as a Typic Immature Pallic Soil (New Zealand Soil Classification (Landcare Research Soils Portal; https://soils.landcareresearch.co.nz)). After sampling, the soils were sieved (4 mm) and stored in a plastic bag at 4°C for no longer than 2 months prior to the experiment. A full report of the soil properties can be found in the appendix (p. 171-176), but are described briefly in Table 2 below.

Table 2. Soil properties, sampled Paparua sandy loam

Soil variable:	Typic immature pallic soil	(Paparua sandy loam)
	Level found	**Unit**
Clay content(< 2 µm)	10.07	%
Silt content (2 – 63 µm)	49.12	%
Sand content (> 63 µm)	40.81	%
pH	5.9	
Olsen Phosphorus	11	mg L^{-1}
Organic matter	3.9	%
Total C	2.3	%
Total N	0.24	%
C/N Ratio	9.5	

In addition to these soil characteristics, the soil's water holding capacity (WHC) was also determined. First the gravimetric water content of the field moist soil was determined. Tarred tins were filled with 10 g of field moist soil and dried at 105°C for 24 hours. Then the oven dry weight was recorded. The WHC was determined according to the following equation:

$$\left(\frac{Soil_{fresh} - Soil_{dry}}{Soil_{dry}}\right) + \left(\frac{Soil_{wet} - Soil_{fresh}}{Soil_{fresh} * \left(\frac{Soil_{dry}}{Soil_{fresh}}\right)}\right) = WHC \quad [7]$$

$Soil_{fresh}$ = weight of freshly collected field moist soil (g)

$Soil_{dry}$ = weight of the same mass overnight oven dried soil (g)

$Soil_{wet}$ = weight of an identical mass of fresh soil after soaking in water (g)

WHC = water holding capacity (g water g^{-1} $soil_{dry}$)

The high oven temperature may have altered organic matter compounds and may therefore have altered the soil water storage potential. So, small PVC tubes (length 4 cm, Ø 3 cm) were covered at the bottom with a water permeable mesh and a small disk of filter paper was then placed inside the tube on the mesh (to avoid soil particle loss through the mesh). These prepared tubes were then tarred before filling with field moist soil to a depth of 2 cm. The mass of the soil-filled tubes was determined and the tubes were subsequently placed in deionised water, covering the soil surface by 1 cm. After 24 h of soaking, all tubes were placed on a rack in a closed box to allow gravity induced water loss. After another 24 h, the mass of each soil-filled tube was determined (Noggle and Wynd 1941).

All WHC determinations were performed in triplicate. The calculations for dry and wet soil were performed individually for each soil subsample. The final calculation (Eq. 7) was performed with values based on the calculated averages, corresponding to the same mass of dry soil.

Following this procedure, a soil WHC of 0.62 g H_2O g^{-1} soil was determined for the soil from both of the sample sites (2015 and 2017, Fig. 15).

3.2.2 Soil mesocosm set up

Both experiments were based on soil mesocosms, treated with ^{15}N labelled substances, separately or in combination with inhibitory substances. A soil mesocosm in this context means a defined mass of soil, corresponding to 50 or 100 g of dry soil mass (1st and 2nd experiment, respectively), which was placed in a 250 mL glass jar (Fig. 17). Subsequently, the soil was moistened to 50% of the predetermined WHC with daily readjustments in order to compensate for water loss through evaporation. The soil-filled jars were placed in an incubator at 23°C, in the dark and brought out for surface pH measurement and/or gas sampling Fig. 18).

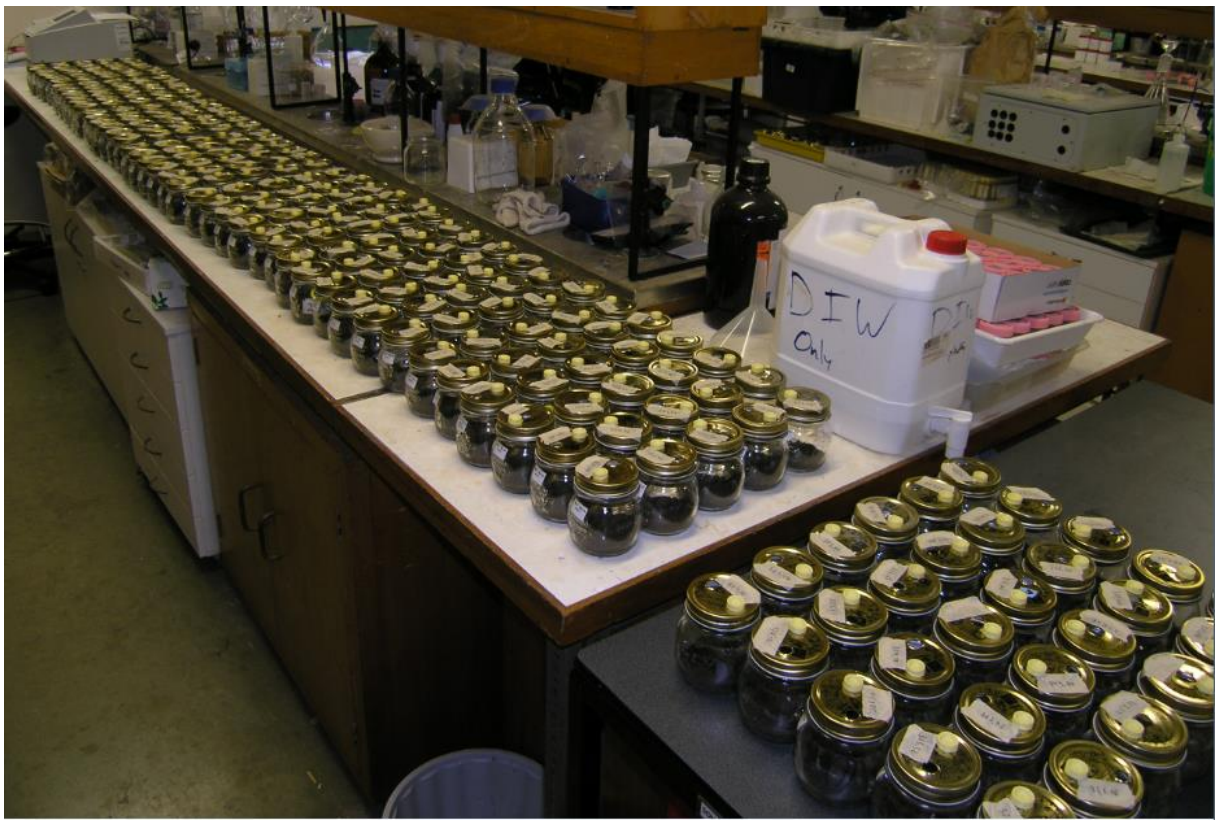

Figure 17. The 240 soil-filled jars at the start of the 1st experiment prior to headspace gas sampling (Nov. 2015)

Figure 18. The 240 jars, 1st experiment, in the incubator (Nov. 2015), note the water-filled trays at the bottom to slow down soil water loss through the incubator's ventilation system.

3.2.3 Inhibition treatments

Selective microbial inhibition was performed using cycloheximide as fungal inhibitor and streptomycin as bacterial inhibitor, according to Anderson and Domsch (1974). These two antibiotics inhibit the synthesis of new proteins, resulting in almost complete inhibition of population growth and microbial cell metabolism. Microbial activities can not be completely inhibited, due to proteins in fungal and bacterial cells already present, which leads to the occurrence of some metabolic end products (e.g., CO_2 or N_2O) that can not be clearly traced back to their origin. Although different soils may respond in slightly different ways to this selective inhibition method (Anderson and Domsch 1974), a similar pattern was observed across different soil types (Fig. 19).

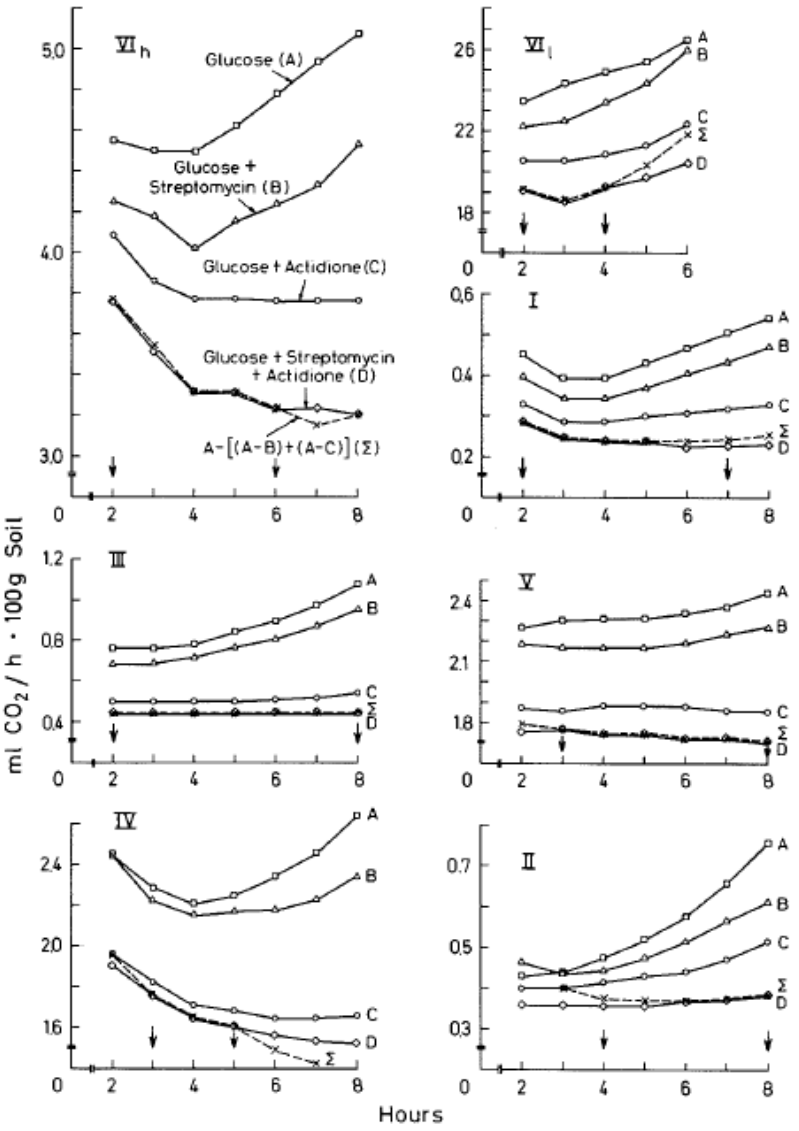

Figure 19. CO_2 production in soils supplemented with glucose, or glucose plus inhibitor(s) in six different soils (I, II, III, IV, V, VI_h) and the litter of soil VI (VI_l) (Anderson and Domsch 1974).

To determine the best rate of cycloheximide and streptomycin on the microbial community within the soil mesocosms, a small pilot study was carried out, based on substrate induced respiration (SIR). Soil mesocosms were prepared, as discussed above, with 100 g dry soil. The soils were adjusted to 50% WHC and stored in the incubator at 23°C in the dark. After five days, to allow time for microbial adjustment, headspace CO_2 concentrations were measured to determine the soil CO_2 flux prior to the application of a glucose substrate. The measurement was performed using the "Licor-820" measurement unit. This unit was connected to an air pump to generate a flux from the Licor back to the jar, the gas from the mesocosm headspace entered the Licor-820 via a filter and flow meter (to adjust for optimal air flow). A thick rubber bung ensured a tight fitting on the jar, ensuring a closed circulating headspace system. The corresponding software on a laptop connected to the Licor-820 allowed real-time CO_2 measurement within the mesocosm headspace (Fig. 20). Measuring intervals were usually 90 – 120 s for each jar. Thus, the plot of CO_2 concentration in the headspace versus time allowed a CO_2 flux to be calculated (µg CO_2-C jar^{-1} h^{-1}) (Fig 21).

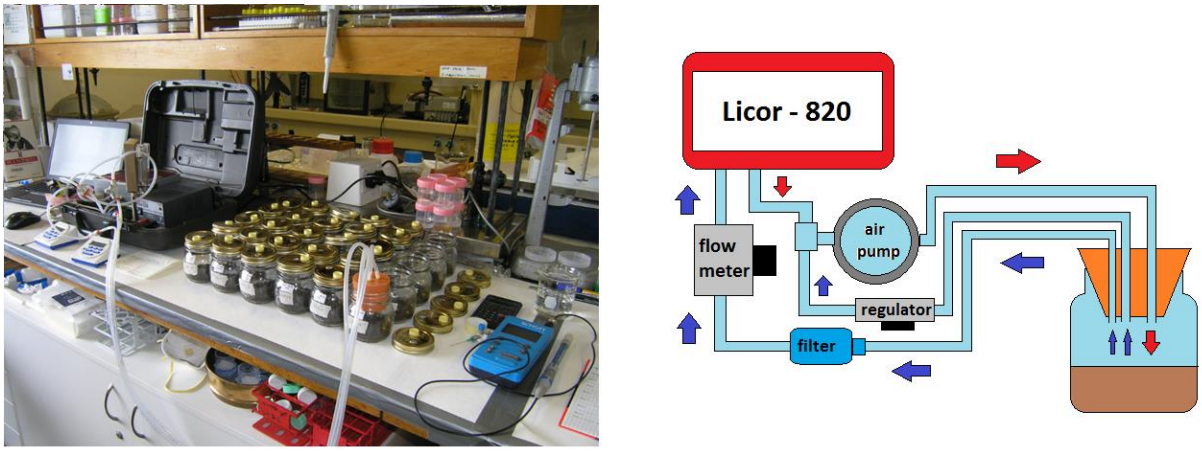

Figure 20. Experimental set up for CO_2 flux measurement, photo of the measurement and drafted equipment set up

At a rate of 8 mg cycloheximide g^{-1} dry soil or 5 mg streptomycin g^{-1} dry soil, similar inhibition rates were attained as observed by Anderson and Domsch (1973) and (1974), and were thus used for both experiments, 1st and 2nd.

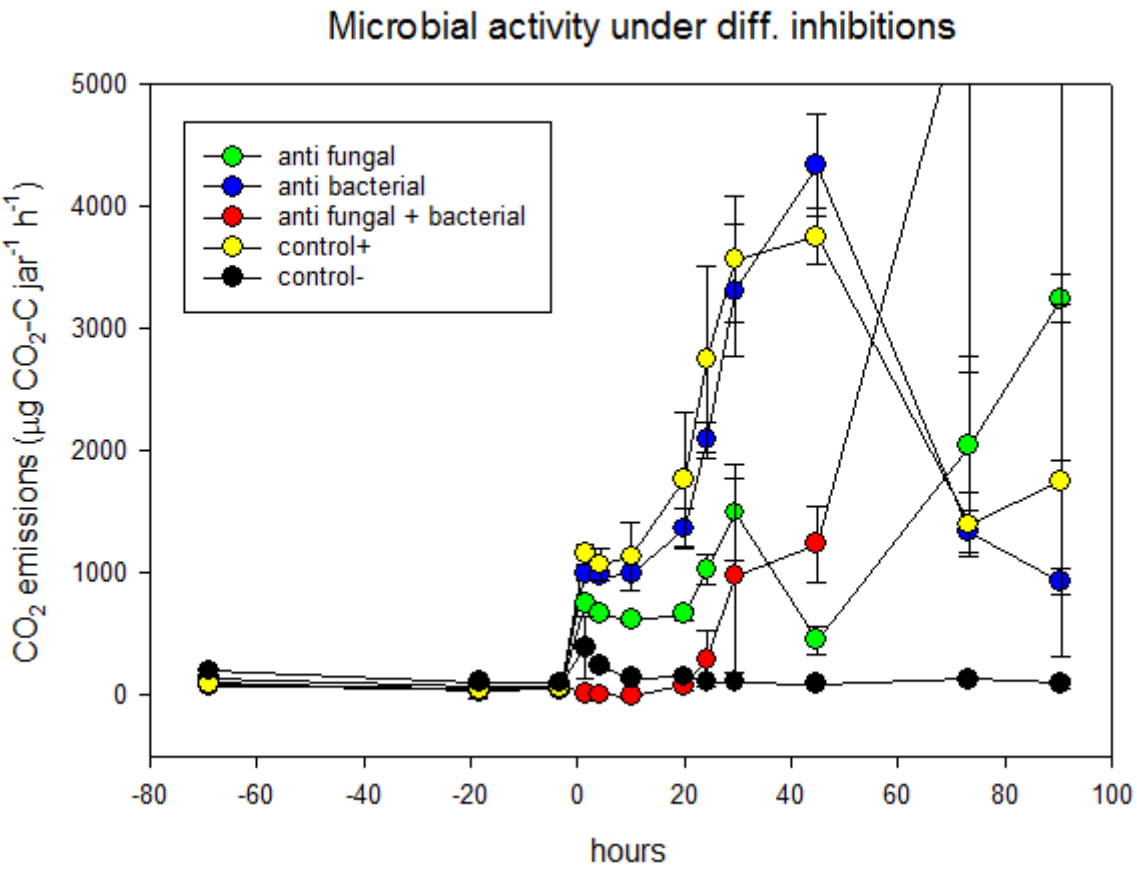

Figure 21. Selective inhibition effect on bacteria and fungi; pilot study for the experimental set for this project. Control+ = glucose, anti fungal = + glucose + cycloheximide, anti bacterial = + glucose + streptomycin, anti fungal + anti bacterial = + glucose + heat sterilization, control- = no glucose or inhibitor addition.

3.3 Mineral N and DOC measurements

3.3.1 NH_4^+ and NO_3^- extraction and analysis

For the measurement of soil mineral NH_4^+ and NO_3^-, a potassium chloride (KCl) extraction method was used according to Blakemore et al. (1987) and Clough et al. (2001b). On the day of destructive soil mesocosm sampling, 10 g of the moist soil was subsampled and transferred to a 400 mL plastic vial. Then 100 mL of a 2 M KCl solution was added to each vial (a 1:10 ratio was used due to the expected high mineral N concentrations). Then the vials were tightly closed and placed in an end-over-end shaker for 1 h. The slurry was then transferred to 200 mL plastic bottles and centrifuged for 10 min at 2,000 rotations per minute (rpm). Funnels with filter paper (Whatman 41) were also prepared and rinsed with 2 M KCl solution to leach any inorganic-N in the filter paper. Finally, the liquid phase was filtered with the filtrate placed in 30 mL vials and stored at -20°C until analysis. Soil inorganic-N concentrations were determined on a Flow Injection Analyser (FIA, Alpekem FS3000 twin channel analyser).

With the NH_4^+ and NO_3^- ion concentrations in the 2M KCl solution known, and the known initial soil moisture content (50% WHC) the concentration of NH_4^+-N or NO_3^--N in the soil was calculated (in µg N g^{-1} dry soil) as follows:

$$\left(\frac{C_{FIA}}{1000}\right) * \left(V + \left(M - M_{dry}\right)\right) = mineral\ content \quad [8]$$

$$\left(\frac{mineral\ content}{V_{dry}}\right) * 1000 * N_{mineral} = C_N \quad [9]$$

C_{FIA} = N mineral concentration (NH_4^+ or NO_3^-) within the KCl extract as given by the FIA (mg L^{-1})

V = volume of KCl extraction volume (mL)

M = mass of extracted soil subsample (g)

M_{dry} = mass of corresponding dry soil mass (g)

mineral content = total amount of N mineral within the extracted solution

$N_{mineral}$ = N content of the N mineral (%)

C_N = concentration of the mineral N in the soil (µg N g^{-1} $soil_{dry}$)

3.3.1.1 NH_4^+-^{15}N determination

The NH_4^+-^{15}N diffusion method was used to determine the ^{15}N content of soil 2M KCl extracts, based on the procedure described by Brookes et al. (1989), Kelley et al. (1991) and Liu and Mulvaney (1992). The method is readily adjusted for relatively large sample extract volumes (10 – 50 mL), containing 25 – 120 µg of enriched inorganic-N at < 30 atm%.

The required chemical solutions, 2 M KCl and 2.5 M $KHSO_4$, were prepared, carefully avoiding N contamination. Glass fibre filter paper disks (Whatman GF/F) were washed three times with 100 mL of the 2 M KCl solution, followed by three washings with deionized water (both washings with the vacuum filtration unit) before being oven dried overnight at 55—80°C. Subsequently, small disks (Ø 5 mm) were prepared (with a cleaned hole punch) and stored in a clean 30 mL vial. Glass beads (Ø 4 mm) were acid washed (24 h in 1 M HCl solution) and then washed, 9 times, with deionized water before they were stored in a plastic container. Magnesium oxide (MgO) was placed in a crucible (50—100 g) and dried in a furnace for 2 h at 600°C. The dried MgO was stored in a dry and clean glass bottle. Finally, stainless steel (SS) wires (5 cm long) were washed (detergent solution) and rinsed (deionized water).

With all chemicals and equipment in place, ^{15}N standards were prepared (50, 25 and 0 atom% excess) using a ^{15}N enriched NH_4^+ standard (98 atm% ^{15}N, Cambridge Isotope Laboratories, Inc.). The volume of each KCl sample was determined so that the mass of NH_4^+-N corresponded to a range of 25 – 120 µg NH_4^+-N. A new 120 mL plastic specimen jar was used for each sample. A stainless steel wire with a small filter disk was suspended in the jar lid and two glass beads were put in each jar. Firstly, KCl solution, with a volume calculated so that the final volume was 50 mL after sample addition, was added to each jar. Then, for each sample extract, the calculated amount of extract solution was transferred into the 120 mL jar, then 10 µL of the $KHSO_4$ solution was added to the filter paper disk on the wire in the lid. Finally, 0.2 g of dry MgO were put into the jar and the lid was closed within the following few seconds (Fig 22, a). The jar was gently swirled, avoiding contact of the KCl solution with the filter paper disk suspended in the lid, and placed aside. The same procedure was repeated for each sample extract. The jars were placed on the bench. The acid trap inside the headspace captured the volatilized NH_3 (Fig. 22, b).

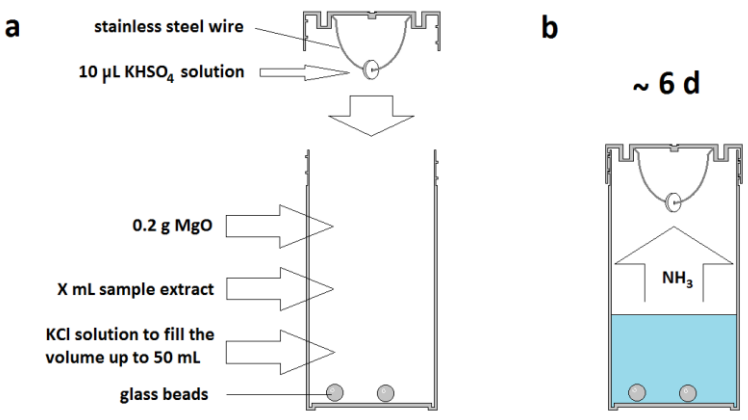

Figure 22. Set up for the NH_4^+-N diffusion via NH_3 conversion and acid trap (Brooks et al. 1989; Liu and Mulvaney 1992).

After the 6 days, the lids were carefully opened and the filter disks removed (still on the wire). The SS wire was fixed into a polystyrene tray and the filter disks were dried in an oven at 50°C overnight. Finally, the filter disks were removed from the wire, avoiding cross contamination, and wrapped in small tin capsules for subsequent analysis via heat combustion on a continuous flow isotope ration mass spectrometer (CFIRMS, Sercon 20-20 Stable Isotope Analyser) connected with gas, solid, liquid module (GSL unit).

3.3.1.2 NO_3^--^{15}N determinations

For the determination of NO_3^--^{15}N, the method used was based on Stevens and Laughlin (1994) and Keeney and Nelson (1982). The method produces N_2O from NO_3^- for ^{15}N atm% determination by CFIRMS, based on the following cadmium (Cd) / copper (Cu) catalysed reactions:

$$NO_3^- + 2H^+ \rightarrow NO_2^- + H_2O \quad \text{(pH 4.7)} \qquad [9]$$

$$HNO_2 + HN_2OH \rightarrow N_2O + 2H_2O \qquad [10]$$

It is applicable for KCl extracts with a minimum amount of 0.5 µmole NO_3^-, with an optimum range between 5 and 25 µ mole/test (1-2 µ mole/test in case of high enrichments, > 30 atm%).
First the Cd was prepared by placing Cd pieces (25 mm x Ø 8 mm) in a beaker were they were rinsed with deionized water. Subsequently, the Cd was washed with 6 M HCl solution for 1 min and then again rinsed with deionized water (2 x), before being immersed with a 0.04 M $CuSO_4$ (*$5H_2O$) solution for 1 min, and the rinsed once more with deionised water. Glass medicine bottles (200 mL) were used as the incubation vessel with each bottle, lid and rubber septum carefully cleaned (bottles - acid washed, lids and rubber septae – detergent washed), prior to use.
The medicine bottles were then filled with the precalculated volume of the KCl extract, corresponding to 2 µmol NO_3^-, with the volume topped up to 50 mL with 2 M KCl. To remove any antecedent NO_2^- sulfamic acid solution (0.2 M, 2.5 mL) was added and then the bottles were closed and shaken for 5 s before re-opening to allow N_2 gas to diffuse. Sulfamic acid dropped the pH to < 2, which caused antecedent NO_2^- to be converted to N_2 gas. Then following the addition of 5 mL of a buffer solution (1 M sodium acetate and 1 M acetic acid, mixed at a 1:1 ratio) the pH of the KCl solution was buffered at 4.7. Then one piece of the prepared Cd was placed inside and the bottle closed. This procedure was performed individually for each sample extract, before the bottles were placed on an orbital shaker for 2 h at 120 rpm. After this, a gas sample was taken from the bottle's headspace through the rubber septum, with a 30 mL one-way syringe, equipped with a three-way

stop cock and a 25G hypodermic needle. This gas sample was injected into a previously evacuated and helium (He) rinsed 12 mL Labco Exetainer®, and then analysed on the CFIRMS.

3.3.2 NO_2^- extraction

Although the NO_2^- extraction is similar in nature to the NH_4^+ and NO_3^- extraction procedure there are some differences, requiring different equipment (Keeney and Nelson 1982; Stevens and Laughlin 1995). First, a 2 M KCl solution was prepared and, using potassium hydroxide (KOH; 2 M), for the pH adjustment to a pH > 8. Then, a small amount of moist soil was sampled (3 – 20 g) and placed into a 50 mL Falcon tube. After the addition of 2M KCL + KOH solution (1:3 ratio), the slurry was blended with a mechanical blender for 1 min (Fig. 23). The resulting slurry was centrifuged at 3300 rpm and filtered with a vacuum filtration unit (Fig. 24).

Figure 23. Stirrer set up for the blending procedure of a NO_2^- sample. An additional wire sling was adjusted to the original rotating disk at the bottom of the stirring rod. A small hole in the falcon tub's lid allowed both; access of the wire sling to the soil slurry and a tight fit closing of the tube to avoid spilling.

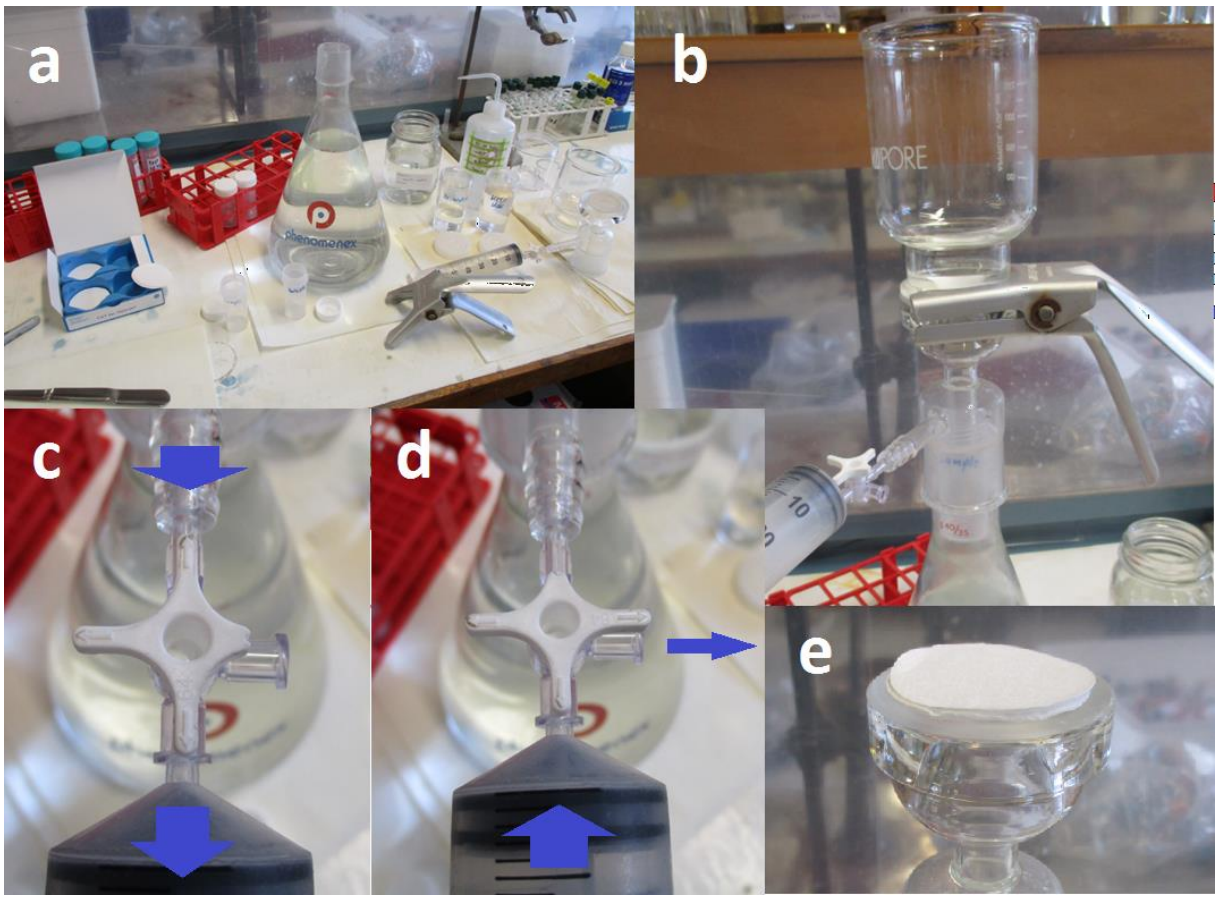

Figure 24. Vacuum filtration of a centrifuged soil slurry sample. First all equipment was cleaned and the Erlenmeyer flask was filled with deionised water to reduce the volume (a). A 30 mL vial was placed on the top opening of the Erlenmeyer flask and covered with the vacuum filtration unit and the glass funnel, having two glass fibre (GF) filter disks between them (b), GF/D (41 µm pores, on top), GF/F (bottom, to avoid GF/D fibres being sucked into the glass pores). Finally a 60 mL plastic syringe was connected to the suction port via a 3-way stop cock. The liquid phase of the centrifuged soil slurry samples as placed in the glass funnel (b) and the air removed with the syringe, due to repeated air removal from the filtration unit into the syringe (c) and from the syringe to the ambient air (d). Once all liquid of a sample passed the filter disk between filtration unit and glass funnel (e) into the 30 mL vial, the stop cock is opened to allow re-establishing of atmospheric pressure in the filtration unit. The 30 mL vial with the filtered sample is then removed and closed, the glass funnel removed and rinsed with deionised water from a squeezing bottle and the used filter paper removed and disposed. Finally a 30 mL waste vial was placed on the Erlenmeyer flask and the filtration unit (without GF filter) placed on top for a washing run with first deionised water and a subsequent rinse with the same KCl + KOH solution used for the sample preparation. This procedure was repeated for every sample individually.

The NO_2^- concentration was measured on a spectrophotometer. A standard reagent solution based on NED (N-1(1-napthyl)ethylenediamine dihydrochloride) and sulphanilamide was made and 4 mL of it added to a subsample of 2 mL of each sample solution (Fig. 25). The colour development was measured after 15 min using a photo spectrometer with a UV light of 540 nm wave length. The absorption referring to a certain concentration was determined with a set of standard solutions of

known NO_2^--N concentrations, with the measured values used to the calculate the NO_2^--N per g dry soil mass in the initial soil sample as follows:

$$\left(\frac{C_{spec}}{1000}\right) * \left(V + \left(M - M_{dry}\right)\right) = NO_2^- \ content \quad [11]$$

$$\left(\frac{NO_2^- \ content}{V_{dry}}\right) * 1000 * N_{mineral} = C_N \quad [12]$$

C_{spec} = NO_2^--N concentration of the KCl extract, according to the photo spectrometric reading (µg L^{-1})

V = volume of KCl extraction solution

M = mass of extracted soil subsample (g)

M_{dry} = mass of corresponding dry soil mass (g)

NO_2^- content = total amount of N mineral within the extracted solution

$N_{mineral}$ = N content of NO_2^- (%)

C_N = concentration of the mineral N in the soil (µg N g^{-1} $soil_{dry}$)

Figure 25. NO_2^- sample preparation for the photo spectrometric reading.

3.3.2.1 ^{15}N diffusion – NO_2^-

Determination of NO_2^--^{15}N was performed according to Stevens and Laughlin (1994). This method is used to produce N_2O from NO_2^- [Eq. 9] for ^{15}N atm% determination. It is applicable for KCl extracts with a minimum of 0.05 µmol NO_2^-. It aimed to get 2 µmol for each sample tested, since high NO_2^- concentrations were previously measured and a greater mass reduces the error.

Glass medicine bottles (200 mL), closed with a tin lid containing a rubber septum, were used as the reagent container and each bottle, lid and rubber septum was carefully cleaned (bottles - acid washed, lids and rubber septae – detergent washed), prior to usage. The medicine bottles were then filled with a volume of the sample extract, corresponding to 2 µmol NO_2^- and filled up to 50 mL with a 2 M KCl solution, followed by the addition of 1 mL HCl solution (1 M) and 0.5 mL NH_2OH solution (0.04 M). This procedure was performed individually for each sample extract, before the bottles were placed on an orbital shaker for 16 h at 120 rpm. Finally, a gas sample taken from the bottle's headspace through the rubber septum, with a 30 mL one-way syringe, equipped with a three-way stop cock and a 25G hypodermic needle. This gas sample was injected into a previously evacuated and He rinsed 12 mL Labco Exetainer®, and then analysed by CFIRMS. For the final calculation of initial NO_2^- ^{15}N atm% values the measured value must be multiplied by 2, due to one N atom of the final N_2O coming from the initial NO_2^- and the other one from the applied NH_2OH at natural abundance [Eq. 9].

3.3.3 Dissolved organic carbon (DOC)

For the measurement of dissolved organic carbon (DOC), 10 g of moist soil was taken from each jar at the time of destructive soil sampling and placed into 400 mL plastic jars. Based on Lundquist et al. (1999), deionised water at room temperature was added, 100 mL according to a 1:10 ratio, and the closed jars were placed on an orbital shaker at 20 rpm for 30 min. Here after, a part of the liquid phase was placed into a 50 mL Falcon tube before being centrifuged at 3300 rpm for 10 min. Finally, 25 mL of the liquid phase was collected with a 30 mL plastic syringe with screw fitting (without needle) and subsequently a syringe filter, equipped with a glass fibre filter (Whatman GF/C, 41 µm pore size) was screwed onto the syringe. The sample was then injected through the filter into a labelled 30 mL sample vial.
After this procedure was performed individually for each soil mesocosm, the collected water leachates were analyses using a Shimadzu Total Organic Carbon Analyser (TOC-5000A) fitted with a Shimadzu ASI-5000A auto sampler.

3.4 N_2O and N_2 emission measurements

3.4.1 N_2O and N_2 emissions

3.4.1.1 Gas sampling and N_2O concentration analysis

Headspace gas samples were taken in order to determine the ^{15}N enrichment of the N_2 and N_2O fluxes and the total flux rates. Considering the soil mass was only 50 g dry weight (100 g in the second experiment), a relatively long jar closure time was elected (jars were sealed for 3 – 5.5 h) in order to increase N_2O and N_2 flux detection. Samples were taken using a 30 mL syringe, fitted with a three-way-stopcock and 25G hypodermic needle, and injected into previously evacuated 6 mL (N_2O determinations on a gas chromatograph (GC)) or 12 mL (helium flushed for ^{15}N enrichment determinations of N_2 and N_2O) Exetainer® vials (Labco Ltd., High Wycombe, UK), creating a positive pressure.

Immediately prior to N_2O analyses the samples were brought to ambient pressure. Then they were analysed on a GC (SRI-8610, SRI Instruments, Torrance, CA) coupled to an auto sampler (Gilson 222XL; Gilson, Middleton, WI) equipped with a ^{63}Ni electron capture detector (Fig. 27), as described by Clough et al. (2006a). PeakSimple 4.44 software (SRI Instruments, Torrance, CA), in conjunction with calibrated N_2O standards (0 to 100 μL L^{-1}; BOC, ISO Guide 34 Reference Material Certificate), were used to construct standard curves in order to determine the sample N_2O concentration. Prior testing had shown N_2O fluxes were linear over the sampling period. Fluxes of N_2O (μg N_2O-N m^2 h^{-1}) were determined as follows:

$$N_2O\ flux = \left(\frac{V \times \Delta N_2O \times P}{R \times T}\right) \times m_N \times t^{-1} \times A^{-1} \quad [10]$$

V = headspace in L

ΔN_2O = change in headspace N_2O concentration during sampling (μL L^{-1})

P = pressure (atmospheres)

R = gas constant = 0.08206 L atm K^{-1} mol^{-1}

T = temperature (K)

m_N = mass of N per mole of N_2O (g mol^{-1})

t = time (h)

A = soil surface area in (m^2)

Figure 26. Gas sampling, 2nd experiment. At this time, the first gas sampling is just performed and the syringes filled with sampled gas.

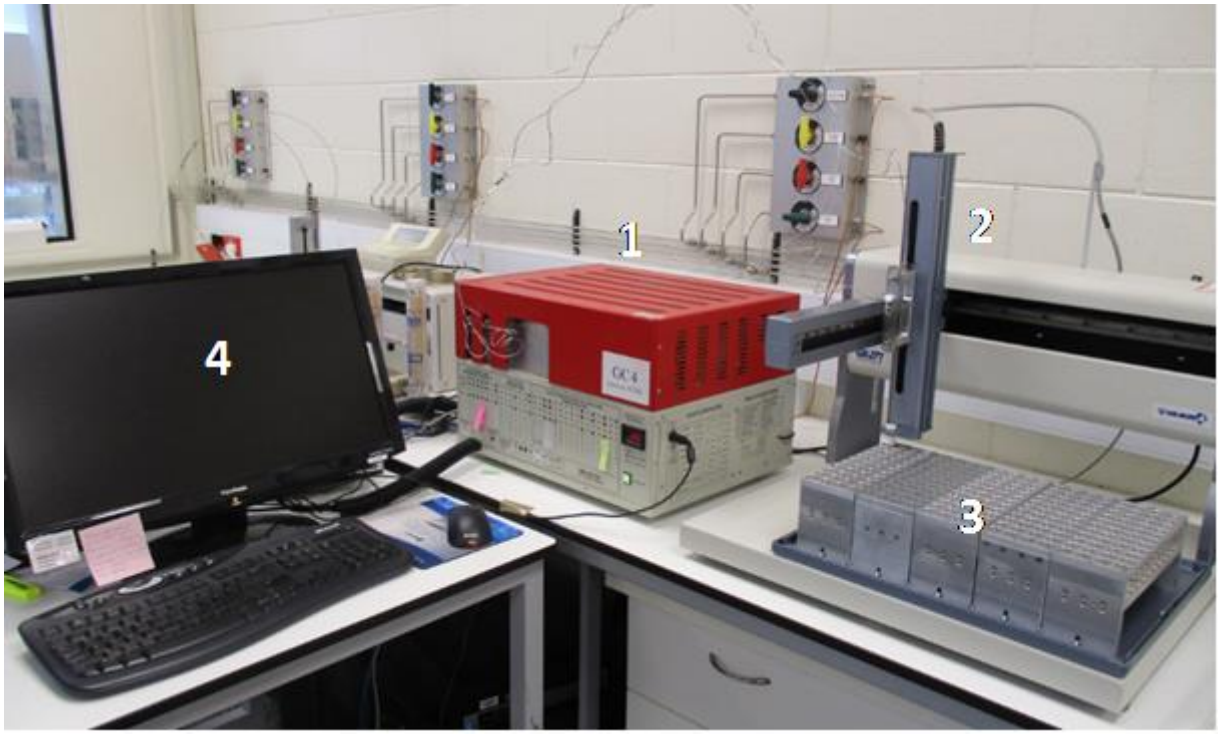

Figure 27. An automated gas analysis station set up in the laboratory. A gas chromatograph (1) is connected with an auto sampler (2), sampling from the racks (3). The gas chromatograph is operated by a 'Peak Simple' software on the nearby computer (4).

3.4.1.2 N_2O and N_2 – ^{15}N atm% determination

The ^{15}N enrichments of both N_2O and N_2 were determined using CFIRMS (Sercon 20/20; Sercon, Chesire, UK) inter-faced with a TGII cryofocusing unit (Sercon, Chesire, UK) (Fig. 28). If required, dilutions of the ^{15}N gas samples were performed by taking 2 or 6 mL of sample gas, from the original Exetainer®, and injecting this into a pre-evacuated vial and then diluting the sample by bringing the vial to atmospheric pressure with helium.

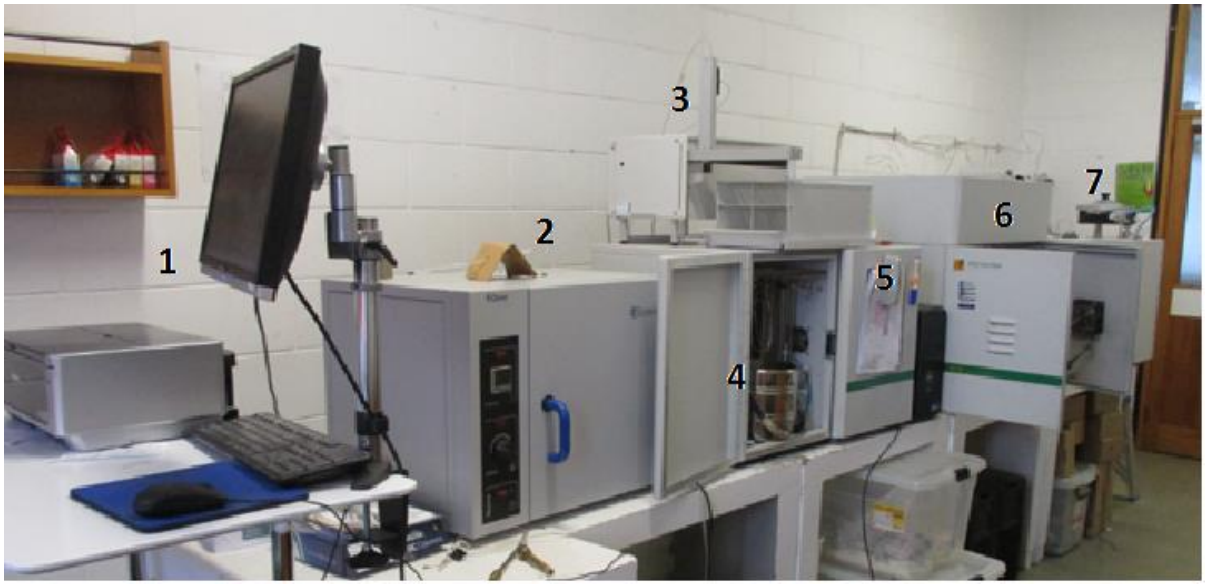

Figure 28. Mass spectrometer for CFIRMS procedure. 1 = operating PC, 2 = GC oven, 3 = Gilson Auto sampler, 4 = TG II Cryo trapping, based on liquid N_2, 5 = Trace Gas Preparation Module, 6 = 20-22 Stable Isotope Analyser with Sercon electric unit, 7 = GSL unit (Gas, Solid, Liquid) for combustion

3.4.2 Codenitrification calculations

To identify the contribution of codenitrification to N_2O and N_2 emissions, a method was set up using the ^{15}N enrichment of N_2O and N_2 for the calculation of the codenitrified fraction. It was assumed that N_2O and N_2 were generated from one ^{15}N enriched pool-fraction and a fraction derived from a pool or pools at natural abundance (^{15}N atom fraction q'_N). This method then distributes the fractions of 'conventional denitrified' and 'hybrid' gaseous emissions, involving one or both N pools, respectively. Analysing the N_2O and N_2 gas as described above, using continuous-flow-isotope ratio mass spectrometry (CFIRMS) lead to the detection of three different values for the ion mass currents, 44, 45 and 46 for N_2O and 28, 29 and 30 for N_2 . These ion mass currents correspond to the molecular fractions of 44, 45 and 46 g mol^{-1} (N_2O) and 28, 29 and 30 g mol^{-1} (N_2). Hypothetically, a 47 or 48

fraction for the N_2O is possible, depending on the oxygen isotope, however these fractions are too small to have a significant impact on the total data and are therefore neglected.

The ratios r'_1 and r'_2, were determined from the N_2O m/z ion currents at m/z 44, 45 and 46 (Arah 1997):

$$r'_1 = {}^{45}i/{}^{44}i \quad [11]$$

$$r'_2 = {}^{46}i/{}^{44}i \quad [12]$$

where, ${}^{44}i$, ${}^{45}i$ and ${}^{46}i$ represent the ion-currents of the N_2O mass fractions 44, 45 and 46.

Then, following Arah (1997); equations 22 and 23, the values of the ^{15}N atom fraction of the sample (a'_s) and the $^{30}N_2$ component of the molecular fraction, of the N_2O molecule, in the sample (x'_s) were calculated using r'_1 and r'_2, while allowing for the presence of oxygen isotopes.

Defining the molecular fractions v', w' and x' of N_2O molecules containing zero, one and two ^{15}N atoms, respectively, and assuming that the oxygen atoms are randomly distributed, Arah (1997) defines *A* and *B* as correction factors, according to equations (3) and (4):

$$A = (w'/v') = r'1 - (\beta/\alpha) \quad [13]$$

$$B = (x'/v') = r'2 - (\beta/\alpha)A + (\gamma/\alpha) \quad [14]$$

were α, β and γ represent the isotopic fractions of oxygen ^{16}O, ^{17}O and ^{18}O, respectively.

In Arah (1997) a'_s and x'_s are defined as follows:

$$a'_s = (1-d'_D-d'_N)*a'_A + d'_D*a'_D + d'_N*a'_N \quad [15]$$

$$x'_s = (1-d'_D-d'_N)*a^{2\prime}_A + d'_D*a^{2\prime}_D + d'_N*a^{2\prime}_N \quad [16]$$

When letting d'_N equal $(1-d'_D)$ and a'_A equal the ^{15}N enrichment at natural abundance (0.003663) equations 3 and 4, when set to equal zero, become:

$$0 = d'_D*a'_D + (1-d'_D)*0.003663 - a'_s \quad [17]$$

$$0 = d'_D*a^{2\prime}_D + (1-d'_D)*0.003663^2 - x'_s \quad [18]$$

Since a'_s and x'_s are known the values of d'_D and a'_D could be determined using the Solver function in Microsoft Excel™ while setting the target value at zero, with the result accepted when the target value was $< 1 \times 10^{-5}$.

Then the codenitrification flux was calculated according to Clough et al. (2001) as:

$$d_{CD} = -\Delta^{45}R p_1^2 / (-\Delta^{45}R p_1^2 + \Delta^{45}R p_1 p_2 + q_1 p_2 - q_2 p_1) \quad [19]$$

where d_{CD} is the fraction of N_2O within the headspace derived from codenitrification and $\Delta^{45}R$ is the $^{45}N_2O/^{44}N_2O$ ratio, while p_1 (0.9963) and q_1 (0.0037) are fractions of ^{14}N and ^{15}N in the natural abundance pool, and where q_2 equals $\alpha' D$, derived above, with p_2 equal to 1-q_2.
Finally the codenitrification flux was determined as:

$$N_2O_{CD} = d_{CD} \times (\text{total } N_2O \text{ flux}) \quad [20]$$

The calculated fraction of codenitrification derived N_2O was expressed in µg N_2O-N m^{-2} h^{-1}.

Subsequently, a similar calculation procedure was used to determine the amount of emitted N_2 caused by codenitrification. Here, the mass fractions of $^{44}N_2O$, $^{45}N_2O$ and $^{46}N_2O$ were replaced with the mass fractions of $^{28}N_2$, $^{29}N_2$ and $^{30}N_2$, respectively. Again, the raw data (detection values for three different molecular masses of $^{28}N_2$, $^{29}N_2$ and $^{30}N_2$) were used for the calculation of the ratios of $^{29}N_2/^{28}N_2$ and $^{30}N_2/^{28}N_2$, following equations [11] and [12]. Considering the great amount of N_2 within the ambient air, the $^{29/28}N_2$ ratio of ambient air is subtracted from the same ratio of the sample. The same procedure applies for the $^{30/28}N_2$ ratio. Since no oxygen is included in the N_2 molecule, the calculation of correction factors *A* and *B* is not necessary. However, it is assumed for N_2 to be generated solely by the reduction of (codenitrification and denitrification caused) N_2O, meaning that the same values for $d'D$ and $\alpha' D$ that have been determined for N_2O are valid for the formation of N_2. Given that, the $^{29/28}N_2$ ratio ($\Delta^{29}R$) was used for equation [19], providing the value for d_{CD}. The codenitrification flux rate was then subsequently calculated using this d_{CD} value and the total flux of N_2 (total N_2 flux) instead of the total N_2O flux [Eq. 20].

3.4.3 Pilot studies

Before each of the two experiments, pilot studies were performed to test different possibilities of possible experimental set up adjustments. The main tests and findings are summarized here:

1st experiment

Pilot study I **Soil microbial activities at different moisture contents at 23°C**
Freshly collected soil was sieved (4 mm) and jars filled with an equivalent of 50 g dry soil mass. The jars were split into 3 WHC-treatments (25%, 50% and 75%) and microbial activities induced with glucose addition. The CO_2 emissions were measured over the following 3 days with the Licor - 820.
Results: at 23°C, a soil moisture content of 50% resulted in the highest gas fluxes

Pilot study II **Concentration increase of headspace N_2O over time**
Jars were filled with the sampled soil (50 g dry soil mass) and moistened to 50% WHC. The jars were split into 4 treatments for different gas sampling patterns (gas sampling every; 15 min, 15 min with reinjection of sampled volume, 1.5 h and 4 h). Microbial activities were induced via urea solution application and the jars stored at 23°C. The gas sampling performed 25 days afterwards at one day for 8 h.
Results: the headspace N_2O concentration increase is linear over 8 h. Best measurement results over durations ≥ 3 h were achieved with one sample every 4 h.

2nd experiment

Pilot study I **Soil N_2O response on glycine, NH_4^+ and NH_2OH application to NO_3^- enriched soil**

Freshly collected soil was sieved (4 mm) and jars were filled with an equivalent of 100 g dry soil mass and moistened to 50% WHC. The jars were split into different treatments for the different N substrates (glycine + NO_3^-, NH_4^+ + NO_3^-, and NH_2OH + NO_3^- and only NO_3^-, at different N loading rates). Microbial activities were induced via NO_3^- solution application and the jars stored at 23°C. The gas sampling was performed over the following 11 days. On Day 7 after the NO_3^- application, the second N substrate was applied according to treatment (substrate x N loading rate).
Results: At a loading rate of 100 µg NO_3^--N g^{-1} soil and 30 µg N g^{-1} soil for the added substance, NH_4^+ and glycine lead to a N_2O flux increase of ca. 20 µg N m^{-2} h^{-1} on Day 8 and 9, NH_2OH to an increase of 1000 µg N m^{-2} h^{-1}.

Pilot study II **Effect of different microbial inhibition methods on N_2O fluxes following NH_2OH application to soil**

Jars were filled (100 g dry soil mass) with the collected soil and NH_2OH was added (30 µg N g^{-1} soil) in addition with different microbial inhibition methods (heat sterilization, cycloheximide, streptomycin and no inhibition). Headspace gas samples were taken for a duration of 3 days.
Results: Fungal and bacterial inhibition reduced the N_2O fluxes by ca. 10%, heat sterilization almost completely.

Pilot study III **Application of microbial inhibitory substances as dry powder vs. aqueous solution**

Jars were filled (100 g dry soil mass) with the collected soil and glucose (500 mg jar-1) added to the soil in addition with; dry streptomycin powder and subsequent soil mixing, streptomycin aqueous solution, or without inhibitor. Emitted CO_2 fluxes were measured over 2 days (Licor – 820).
Results: Dry streptomycin reduced the fluxes by ca. 30%, streptomycin solution by ca. 20%.

Pilot study IV **Soil mesocosm pH adjustment via KH_2PO_4:$KH_2PO_4^-$ buffer solution**

Jars were filled (100 g dry soil mass) with the collected soil and NO_3^- solution (100 µg N g^{-1} soil) added to the soil in addition with 30 mL of water or buffer solution (to adjust the soil to pH 7 or 8). Emitted N_2O and soil NO_2^- concentrations were measured over 3 days.
Results: The addition of buffer solution inhibited N_2O and NO_2^- formation.

Pilot study V **Soil N_2O response of different urea-N loading rates to nucleophile N addition**

Jars were filled (100 g dry soil mass) with the collected soil and urea solutions were applied (200 - 1000 µg N g^{-1} soil). Soil N_2O emissions were measured over the following 12 days. The nucleophile solution was applied 4 days after the urea solution.
Results: urea-N loading rates of 500 and 1000 µg N g^{-1} soil resulted in best N_2O response.

Applications to the experimental design:

1. **experiment**

- the soil mesocosms were incubated at 23°C and 50% WHC
- the closed incubation time for each gas sampling was kept between 3 and 5 h
- one gas sample was taken at the start of the incubation time, one at the end

2. **experiment**

- soil mesocosms were again incubated at 23°C and 50% WHC and 3 h for the gas sampling
- urea-N was applied at a rate of 500 µg N g^{-1} soil and the nucleophile at 20 µg N g^{-1} (to ensure a timely N_2O response with > 10 µg N m^{-2} h^{-1} being nucleophile caused), no other chemicals were added
- the same inhibitory substances were applied, again as dry powder, and mixed into the soils

Chapter 4
Fungal and bacterial contributions to codenitrification emissions of N_2O and N_2 following urea deposition to soil

A manuscript from this study has been published in Nutrient Cycling in Agroecosystems: Rex D, Clough TJ, Richards KG, de Klein C, Morales SE, Samad Md S, Grant J, Lanigan GJ 2018. Fungal and bacterial contributions to codenitrification emissions of N_2O and N_2 following urea deposition to soil. Nutrient Cycling in Agroecosystems 110: 135-149.

4.1 Introduction

Ruminant urine deposition is the dominant source of nitrous oxide (N_2O) emissions from grazed grasslands (Flessa et al. 1996; Oenema et al. 1997). Emissions of N_2O are of concern since N_2O is a greenhouse gas with a stratospheric ozone depletion potential (Ravishankara et al. 2009). Consequently, strategies to mitigate N_2O emissions from pastures are of global interest. Soil microbial biomass is a key factor in regulating nitrogen (N) turnover in soil (Viebrock and Zumft 1988; Yang et al. 2015), and it is recognized that N_2O emissions can be reduced by manipulating the N substrate supply to microbes and by inhibiting microbial pathways such as nitrification (Cameron et al. 2014; Duan et al. 2016; Shi et al. 2016). However, the development of effective management options to minimise N_2O emissions from soil affected by ruminant urine deposition requires a more detailed knowledge of the microbial pathways responsible for these emissions.

Initially, when ruminant urine is deposited onto soil the N composition of this urine is dominated by urea, with >70% of urine N commonly in this form, and it is the precursor to the urine-induced N cascade that occurs in grazed pasture soils. Commencing with the hydrolysis of urea, ammonium (NH_4^+) and carbonate ions are formed, with the hydrolysis of the latter resulting in an elevated soil pH of ca. 8.0 or higher (Avnimelech and Laher 1977). This results in a pH driven equilibrium between NH_4^+ and ammonia (NH_3). Ammonium not volatilized as NH_3 may undergo fixation, plant uptake, immobilization or nitrification (Sebilo et al. 2013). During nitrification, N_2O may be produced as nitrate (NO_3^-) is formed. Under anaerobic conditions NO_3^- may be used as a microbial energy source in a process termed 'denitrification' which, if complete, forms dinitrogen (N_2) or if incomplete N_2O (Butterbach-Bahl et al. 2013; Cameron et al. 2013; Spott et al. 2011). Nitrifer-denitrification may also occur as soil O_2 becomes limiting (<5%), a process whereby nitrifiers may convert nitrite (NO_2^-) to N_2O and N_2 (Wrage et al. 2001; Zhu et al. 2013b).

However, emissions of N_2O and N_2 are not only driven by classical denitrification, nitrification and nitrifer-denitrification. Other soil processes (both, microbial and abiotic) can produce N_2 and/or N_2O

(Spott et al. 2011). For example, abiotic reactions of NO_2^- with reduced iron (Fe_2^+) can occur at the interface between an aerobic zone overlying an anaerobic zone where NO_2^- diffusing downwards meets Fe_2^+ diffusing upwards (Cleemput and Baert 1983; Sørensen and Thorling 1991). However, concentrations of Fe_2^+ ions in most soil are considered too small to promote NO_2^- decomposition (Cleemput and Samater 1996; Nelson and Bremner 1970). Abiotic-nitrosation, sometimes referred to as chemodenitrification, results in a nitroso group forming following the reaction with nitrous acid under acidic conditions (pH < 5.0), with the labile nitroso group able to undergo further reactions to form N_2O. This is due to NO_2^- and hydrogen ions forming nitrous acid, which can react with either amino compounds, hydroxylamine, ammonium or other forms of organic matter to form N_2O (Chalk and Smith 1983; Heil et al. 2016). However, under urine patch conditions biologically mediated nitrosation may occur via codenitrification (Selbie et al. 2015b; Spott et al. 2011) as oxygen concentrations decline. In addition, under aerobic conditions ammonium oxidizing bacteria (AOB) and/or ammonium oxidizing archaea (AOA) may generate intermediate compounds capable of generating N_2O via N-nitrosation reactions (Stieglmeier et al. 2014; Terada et al. 2017). Studies indicate that these processes may be based on metal-containing enzymes (Garber and Hollocher 1982). Such enzymes have been reported for bacteria (cytochrome cd1 NIR, *Pseudomonas aeruginosa*) and fungi (cytochrome P450 NOR, e.g. *Fusarium oxysporum*), where they bind to a nitrosating agent and form hybrid N_2 and/or N_2O molecules (Averill 1996). Codenitrification results in the formation of N_2O with one N atom originating from the original inorganic-N compound (e.g. NO_2^-) and one N atom from a co-metabolised organic compound (e.g. amino acid, hydroxylamine).
While the potential for codenitrification (Spott et al. 2011), to occur has been recognized for many decades (Iwasaki et al. 1956) the significance of codenitrification in grasslands has only recently been recognized for N_2O and N_2 (Laughlin and Stevens 2002; Selbie et al. 2015b). However, the number of studies on codenitrification remains extremely limited, especially with respect to the relative roles of bacteria and fungi. Combining a substrate-induced respiration method with the ^{15}N gas-flux method, Laughlin and Stevens (2002) demonstrated that fungi produced N_2O and N_2 solely via the reduction of NO_3^-, with fungi dominating N_2O production. Using a ^{15}N isotope tracer technique, Laughlin and Stevens (2002) were able to demonstrate that up to 92% of the N_2 emitted was the result of codenitrification. The codenitrification process was also observed to be responsible for 95% of N emissions (principally N_2) under a high rate of urinary-N deposition (Selbie et al. 2015b). While Clough et al. (2017) found codenitrification from a pasture soil to be favoured under wet soil conditions when NO_2^- concentrations were elevated. Thus, under conditions that are tending, or that are anaerobic, codenitrification may potentially play a major role in soil N turnover where there is a well-established archaeal, fungal and/or bacterial community (Müller et al. 2006). However, in an *in vitro* study with fungal necromass, Philips et al. (2016) presented evidence for abiotic nitrosation reactions occurring at pH 6.2-6.9, with N_2 production occurring following the hybridisation of

inorganic and organic N sources under aerobic and anaerobic conditions. Thus the importance, and the relative roles of fungi and bacteria in codenitrification processes remains unclear.
Hence, the aim of this study was to examine the contributions of archaea, fungi and bacteria to codenitrification under a simulated ruminant urine event. Given that fungi and archaea are both susceptible to cycloheximide it was hypothesised that in the presence of cycloheximide, codenitrification fluxes of N_2O and N_2 would be reduced.

4.2 Materials and Methods

4.2.1 Experimental design

The top 10 cm of a sandy loam soil was sampled from a representative area of a pasture on the Lincoln University dairy farm, New Zealand (43°38'33.73"S, 172°27'40.38"E, Typic Immature Pallic Soil, Table 1) and sieved (4 mm). This area had received no fertiliser and had not been grazed for 12 months. Pasture consisted of perennial rye grass (*Lolium perenne* L.) and white clover (*Trifolium repens L.*).

Field moist soil, 50 g dry weight, was placed into jars (250 mL) and moistened to 50% of water-holding-capacity (Rex et al. 2015). A total of 200 jars were prepared in this way. These jars were divided into 5 treatments, with 5 independent replicates and 8 different destructive sample times: Day 3, 9, 15, 21, 27, 33, 42, and 51.

The five treatments were:

1. a negative control (application of 2 mL deionised water);
2. a positive control (application of 2 mL urea solution containing 0.238 g urea, 0.55 mg mL^{-1});
3. an antibacterial treatment (2 mL of the urea solution + 250 mg streptomycin + 1.88 mg penicillin in total);
4. an antifungal treatment (2 mL urea solution + 400 mg cycloheximide in total);
5. an antifungal + antibacterial treatment (2 mL urea solution + 250 mg streptomycin + 1.88 mg penicillin + 400 mg cycloheximide).

The urea was ^{15}N enriched (50 atm%) with the rate of urea-N corresponding to 1000 kg N ha^{-1} in order to simulate a high bovine urine deposition event (Haynes and Williams 1993). At the beginning of the experiment all jars (except the negative control) received the urea solution (experiment Day 0). During the experiment the jars were stored in an incubator under dark conditions at 23°C and 55% relative air humidity. To reduce soil drying, the jars were partially closed and the gravimetric soil water content measured frequently and adjusted to maintain a continuous moisture content of 50% water-holding-capacity, ± 5%. Lids had rubber septum for gas sampling and a 1 cm diameter hole that

could be sealed during gas sampling periods, but allow gas exchange with the ambient air during non-gas sampling periods.

4.2.2 Gas sampling and analysis

Daily headspace gas samples were taken in order to determine the ^{15}N enrichment of the N_2 and N_2O fluxes. Considering the soil mass was only 50 g dry weight, a relatively long jar closure time was elected (jars were sealed for 3 – 5.5 h) in order to increase N_2 flux detection. Samples were taken using a 50 mL syringe, fitted with a three-way-stopcock and 25G hypodermic needle, and injected into previously evacuated 6 mL (N_2O determinations on a gas chromatograph (GC)) or 12 mL (helium flushed for ^{15}N enrichment determinations of N_2 and N_2O) Exetainer® vials (Labco Ltd., High Wycombe, UK), creating a positive pressure. Immediately prior to N_2O analyses the samples were brought to ambient pressure. Then they were analysed on a GC (SRI-8610, SRI Instruments, Torrance, CA) coupled to an auto sampler (Gilson 222XL; Gilson, Middleton, WI) equipped with a ^{63}Ni electron capture detector as described by Clough et al. (2006a). PeakSimple 4.44 software (SRI Instruments, Torrance, CA), in conjunction with calibrated N_2O standards (0 to 100 $\mu L\ L^{-1}$; BOC, ISO Guide 34 Reference Material Certificate), was used to construct standard curves in order to determine the sample N_2O concentration. Prior testing had shown N_2O fluxes were linear over the sampling period. Fluxes of N_2O ($\mu g\ N_2O\text{-}N\ m^2\ h^{-1}$) were determined according to equation (10).
The ^{15}N enrichments of both N_2O and N_2 were determined using continuous-flow-isotope ratio mass spectrometry CFIRMS (Sercon 20/20; Sercon, Chesire, UK) inter-faced with a TGII cryofocusing unit (Sercon, Chesire, UK). If required, dilutions of the ^{15}N gas samples were performed by taking 2 or 6 mL of sample gas, from the original Exetainer®, and injecting this into a pre-evacuated vial and then diluting the sample by bringing the vial to atmospheric pressure with helium. Soil surface pH was measured, 10 – 12 times over the 51 days depending on the destructive sampling time, by adding two drops of deionised water to the soil surface and then placing a flat surface pH probe onto the soil surface (Broadley James Corp., Irvine, California). The codenitrification fluxes of N_2O and N_2 were calculated as described in chapter 3.

4.2.3 Destructive soil sampling

On each sampling occasion treatment-determined inhibitors were added to jars 48 h before destructive soil sampling on days 3, 9, 15, 21, 27, 33, 42, or 51, a total of 25 jars (5 treatments by 5 replicates). Streptomycin and cycloheximide were both applied as a dry powder and mixed with the soil for 90 seconds using a spatula (Rex et al. 2015). Penicillin was dissolved in deionised water (2 mL) and applied as a solution before mixing. Control soils were mixed simultaneously, without substance

addition. After 48 h, soil in the jars was remixed and then subsampled. To determine the NO_2^--N concentrations 20 g of wet soil was extracted with 20 mL of 2M KCl solution adjusted to pH 8 with KOH (Stevens and Laughlin 1995). A further 10 g of wet soil was extracted with 100 mL of 2M KCl solution, pH 7, to determine soil NH_4^+-N and NO_3^--N concentrations (Blakemore et al. 1987; Clough et al. 2001b). Inorganic-N concentrations in the extracts were determined using Flow Injection Analysis (Blakemore et al. 1987). The concentration of NH_3 was calculated, using the soil's NH_4^+ concentration, temperature and pH (Barnabe 1990). Dissolved organic carbon (DOC) was extracted from a 10 g subsample following the procedure of (Lundquist et al. 1999). Soil gravimetric water content was determined after drying a 10 g soil subsample for 24 h at 105°C. The ^{15}N atm% was determined as described in chapter 3.

4.3 Results

4.3.1 Soil pH, DOC and inorganic-N

Within 10 h of applying the urea solution, the soil surface pH increased from a value of 6.5 in the negative control, to peak at 8.9 on Day 5 (Fig. 1). After the initial increase the soil pH of the urea-affected soil remained relatively stable until Day 33, but higher than in the negative control (p < 0.05), where after it declined to be 6.8 and 6.6 on Days 42 and 51, respectively (Fig. 29 a, b).

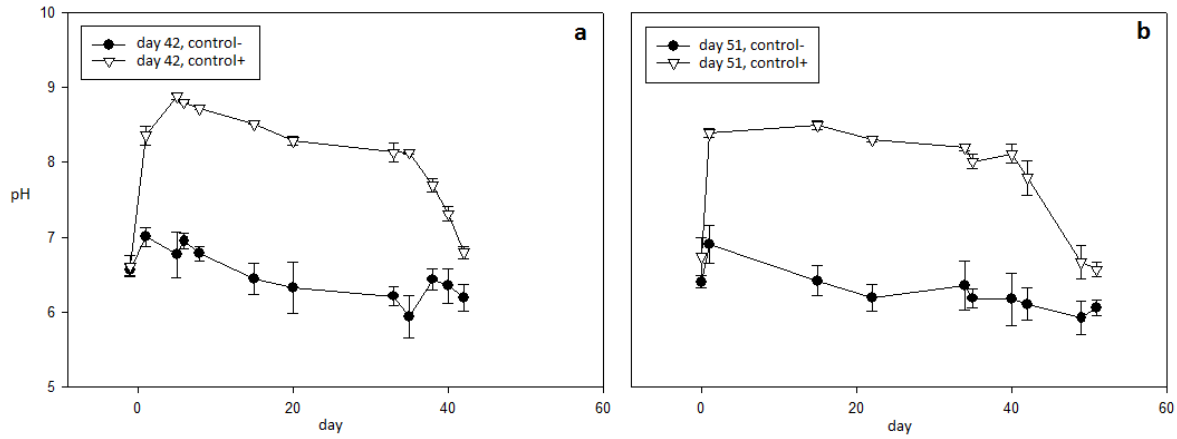

Figure 29. Soil surface pH values under the negative (control-) and positive (control+) control treatments are shown for jars destructively sampled on day 42 (a) and day 51 (b), error bars are ± standard deviation, n= 4.

In the negative control the DOC concentration declined (p < 0.001) over time from 1.02 ± 0.09 mg g^{-1} soil to equal 0.15 ± 0.01 µg DOC g^{-1} soil on Day 51. In the positive control the DOC concentration deceased (p < 0.05) from 1.1 ± 0.19 µg DOC g^{-1} soil to equal 0.45 ± 0.03 µg DOC g^{-1} soil on Day 51, which was higher than the concentration in the negative control at this time (p < 0.001).

The fluxes of both N_2O and N_2 only became significant after Day 33, therefore the inorganic-N results presented focus on results for Days 42 and 51. Destructive soil sampling on Day 3 showed that in the negative control NH_4^+ concentrations were below detection on Day 3 and they remained at < 4 µg NH_4^+-N g^{-1} soil until Day 51. However, on Day 3, soil NH_4^+ concentrations under urea-treated soil ranged from 920 – 1300 µg NH_4^+-N g^{-1} soil (Fig. 30 a) with no difference in NH_4^+-N concentrations, when compared with the positive control, as a result of inhibitors having been applied 48 hours prior to destructive soil analysis. In the urea-treated soil NH_4^+-N concentrations decreased linearly (r^2 = 0.81; $p < 0.05$) from Day 3 to range from 580 – 700 µg NH_4^+-N g^{-1} soil on Day 51 (Fig. 30 a). Calculated values of free NH_3 were 300 µg NH_3-N g^{-1} soil during the first 33 days. On Day 42 the NH_4^+-N concentrations in the antibacterial and antifungal treated soils were > 80 µg NH_4^+-N g^{-1} soil higher ($p < 0.05$) when compared with the positive control. But antibacterial/antifungal treated soils did not differ significantly from the positive control on Day 51 (Table 3).

Soil NO_2^--N concentrations were low (< 2.5 µg NO_2^--N g^{-1} soil) in all treatments until Day 33 when they began to increase in urea-treated soils (Fig. 30 a). On Day 42, the positive control had significantly higher soil NO_2^--N concentrations than the negative control. The 'antifungal + antibacterial' treatment had NO_2^--N concentrations almost 50% lower than in the positive control (Table 3). On Day 51 NO_2^--N concentrations were of a similar magnitude to those on Day 42 but there were no significant differences between the positive control and inhibited treatments.

In the negative control soil NO_3^--N concentrations ranged from 23 – 30 µg NO_3^--N g^{-1} soil throughout the experiment. Differences, due to urea addition, were detected at Day 42, when NO_3^--N concentrations reached 69 µg NO_3^--N g^{-1} soil in the positive control, but they remained significantly lower (42 to 53 µg NO_3^--N g^{-1} soil) in the inhibited treatments (Table 3). On Day 51 the positive control had soil NO_3^--N concentrations of 73 µg NO_3^--N g^{-1} soil but there was no difference compared to the inhibited treatments (Table 3).

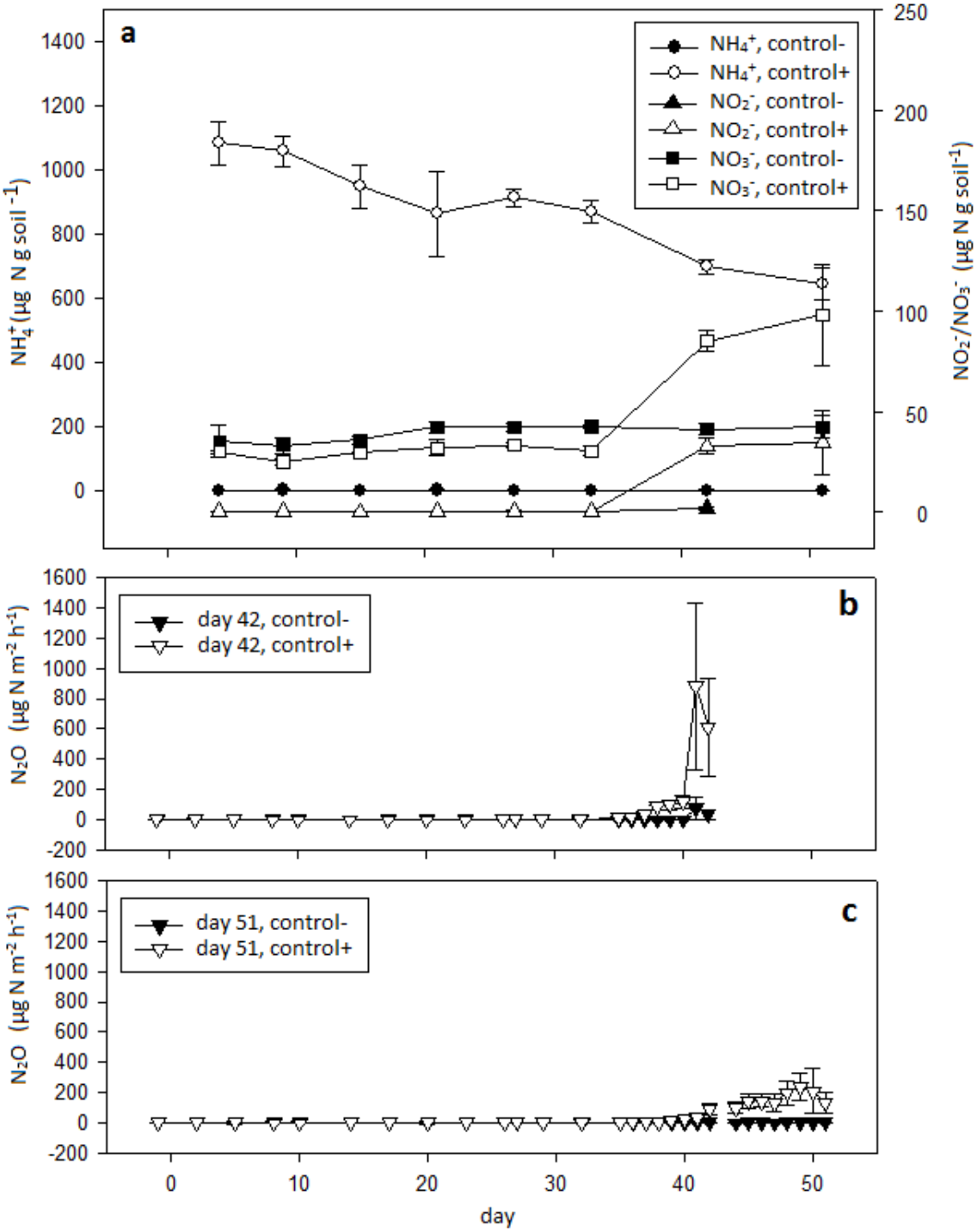

Figure 30. (a) Soil inorganic-N concentrations over time, after inhibitors had been present for 48 h. Error bars are ± standard deviation, n = 4; (b and c) N2O fluxes of soils destructively sampled on day 42 (b) and 51 (c), error bars are ± standard deviation, n = 4

The ^{15}N enrichment of the NH_4^+ in the positive control on Day 42 equalled 41.0 atm% ^{15}N, but the combined 'antifungal + antibacterial' treatment had a significantly lower NH_4^+ ^{15}N enrichment, equal to 36.5 atm% ^{15}N (Table 4). At Day 51, NH_4^+ ^{15}N enrichment in both treatments containing fungal inhibitors were ca. 4 atm% ^{15}N lower compared with the positive control and antibacterial treatment (Table 4). For the NO_2^- pool the ^{15}N enrichment was 48 atm% ^{15}N in the positive control on both Days

42 and 51 and there were no significant treatment effects observed. Similarly, the ^{15}N enrichment of NO_3^- pool on Days 42 and 51 ranged from 19.5 – 24.2% with no treatment effects on either Day (Table 4).

Table 3. Mean (n = 4) soil inorganic-N concentrations (± standard deviation) 48 h after microbial inhibition treatments were applied.

Treatment	Day 42			Day 51		
	NH_4^+ [μg N g_{soil}^{-1}]	NO_2^- [μg N g_{soil}^{-1}]	NO_3^- [μg N g_{soil}^{-1}]	NH_4^+ [μg N g_{soil}^{-1}]	NO_2^- [μg N g_{soil}^{-1}]	NO_3^- [μg N g_{soil}^{-1}]
Control-	1.88 ± 0.8^{c}	1.8 ± 0.7^{c}	20.3 ± 3.1^{c}	0.7 ± 0.3^{b}	<1.8^{c}	26.3 ± 3.1^{b}
Control+	698.4 ± 22.5^{b}	32.7 ± 3.9^{a}	68.6 ± 5.5^{a}	645.4 ± 50.8^{a}	34.6 ± 15.9^{a}	72.7 ± 5.6^{a}
Antibacterial	798.5 ± 39.1^{a}	21.8 ± 9.3^{ab}	42.5 ± 11.8^{b}	630.9 ± 42.5^{a}	24.7 ± 7.1^{a}	71.7 ± 4.8^{a}
Antifungal	769.5 ± 25.5^{a}	24.4 ± 5.4^{ab}	46.4 ± 9.8^{b}	621.4 ± 10.2^{a}	33.5 ± 5.2^{a}	71.1 ± 5.2^{a}
Antibacterial + Antifungal	802.3 ± 28.1^{a}	18.9 ± 6.6^{b}	53.0 ± 9.5^{b}	638.8 ± 15.1^{a}	39.1 ± 4.6^{a}	67.3 ± 11.5^{a}
Level of significance	*	*	*	*	*	*
Test	Holm-Sidak Method	Holm-Sidak Method	Holm-Sidak Method	Tukey-Kramer	Holm-Sidak Method	Holm-Sidak Method

Vertically, LS-means with the same letter are not significantly different, different letters indicate a significant difference based on the mentioned test.
level of significance: * indicates P<0.05

Table 4. ^{15}N enrichment of soil inorganic N species. Values are treatment means (n = 4) ± standard deviation.

Treatment	Day 42			Day 51		
	NH_4^+ [atm% ^{15}N]	NO_2^- [atm% ^{15}N]	NO_3^- [atm% ^{15}N]	NH_4^+ [atm% ^{15}N]	NO_2^- [atm% ^{15}N]	NO_3^- [atm% ^{15}N]
Control-	---	---	---	---	---	---
Control+	41.0 ± 0.9^{ab}	48.3 ± 0.4^{a}	21.6 ± 1.6^{a}	40.5 ± 0.2^{a}	48.1 ± 1.4^{a}	21.7 ± 3.9^{a}
Antibacterial	41.1 ± 0.3^{a}	42.6 ± 4.3^{a}	20.1 ± 1.3^{a}	41.0 ± 0.3^{a}	48.5 ± 0.3^{a}	24.2 ± 0.4^{a}
Antifungal	37.3 ± 0.3^{ab}	42.5 ± 2.9^{a}	19.5 ± 0.8^{a}	36.7 ± 0.4^{b}	49.3 ± 0.6^{a}	24.2 ± 1.7^{a}
Antibacterial + Antifungal	36.5 ± 0.7^{b}	42.5 ± 2.0^{a}	19.5 ± 1.6^{a}	36.7 ± 1.4^{b}	48.0 ± 1.1^{a}	23.1± 1.9^{a}
Level of significance Test	* Tukey	n.s.	n.s.	* Holm-Sidak Method	n.s.	n.s.

Vertically, LS-means with the letter are not significantly different, different letters indicate a significant difference based on the mentioned test.
level of significance: * indicates P<0.05, --- indicates no available data

4.3.2 N_2O and N_2 emissions

There was a short initial peak in N_2O emissions observed during the first 48 h period following treatment application (< 20 µg N_2O-N m^2 h^{-1}). However, after this time there were no increases in N_2O emissions until day 26. In the positive control, emissions of N_2O peaked at 1080 ± 378 µg N_2O-N m^{-2} h^{-1} on Day 42 (Fig. 30 b), and at 229 ± 171 µg N_2O-N m^{-2} h^{-1} on day 51 (Fig. 30 c).
After microbial inhibition on Day 42 the negative control had N_2O emissions <10 µg N_2O-N m^2 h^{-1} (Fig. 30 b). Before microbial inhibition at Day 42, N_2O emissions from the positive control were 133 ± 29 µg N_2O-N m^2 h^{-1}. Twenty four hours after applying microbial inhibition treatments the N_2O emissions from the positive control (where the incubated soil had been stirred to simulate the mixing occurring in the soil treated with) had increased to 1080 ± 378 µg N_2O-N m^2 h^{-1}. Relative to the positive control at this time the application of the antifungal treatment reduced N_2O emissions by ca.76 %, while application of the combined 'antifungal + antibacterial' treatment reduced N_2O emissions by ca. 86% (Table 5). Application of solely the antibacterial treatment resulted in no change in the N_2O emissions relative to the positive control (Table 5).
Microbial inhibition at Day 51 did not elevate N_2O emissions in the negative control (where only soil mixing occurred). Before microbial inhibition at Day 51 the positive control emitted 229 ± 102 µg

N_2O-N m^{-2} h^{-1}. Twenty four hours after inhibition at Day 51, N_2O emissions from the positive control remained unchanged (209 ± 171 µg N_2O-N m^2 h^{-1}), but higher compared to the negative control, while antifungal and 'antifungal + antibacterial' treatments reduced N_2O emissions by > 66% (p < 0.068; Table 6).

Calculated N_2O_{co} emissions for the positive control on Day 42 prior to application of the inhibition treatments were 103 ± 24 µg N_2O_{co}-N m^{-2} h^{-1}. Twenty four hours after applying the microbial inhibition treatments the positive control emissions (where only soil mixing occurred) increased to 362 ± 121 µg N_2O_{co}-N m^{-2} h^{-1} (33% of total N_2O emissions) while in the antifungal and 'antifungal + antibacterial' treatments N_2O_{co} emissions were reduced by > 76 % relative to the positive control (Table 5). The antibacterial treatment did not alter emissions relative to the positive control.

At Day 51 N_2O_{co} emissions from the positive control were 100 ± 45 µg N_2O_{co}-N m^{-2} h^{-1} before microbial inhibition. Twenty four hours after the inhibition treatments were applied, N_2O_{co} emissions from the positive control were 88 ± 71 µg N_2O_{co}-N m^2 h^{-1} (42 % of total N_2O emissions). The N_2O_{co} emissions from the antibacterial and antibacterial + antifungal treatments did not differ from the positive control (Table 6).

For the positive control the N_2 emissions at Day 42 were 2.9 µg N_2-N m^{-2} h^{-1} before inhibition. Twenty four hours after microbial inhibition the antibacterial treatments had not affected the N_2 emission rates which averaged 2.8 µg N_2-N m^{-2} h^{-1} (Table 5). At this time emissions of N_{2co} were 0.9 µg N_2-N m^{-2} h^{-1} before microbial inhibition, and this increased 24 hours after inhibition to 1.6 µg N_2-N m^{-2} h^{-1} (53% of total N_2 emissions). No treatment effects on N_{2co} were detected before and after the microbial inhibition (Table 5).

Dinitrogen emissions at Day 51 were 1.4 µg N_2-N m^{-2} h^{-1}, prior to inhibition, and increased significantly 24 hours after applying microbial inhibition, reaching 39.9 µg N_2-N m^{-2} h^{-1} in the positive control. Application of the antifungal and 'antifungal + antibacterial' treatments resulted in N_2 emissions being > 88 % higher than in the positive control (Table 6).

The N_{2co} flux in the positive control before microbial inhibition equated to 0.9 µg N_2-N m^{-2} h^{-1}. Twenty four hours after inhibition was applied, the flux in the positive control had increased to 1.4 µg N_2-N m^2 h^{-1} (3.5% of total N_2 emissions), while all inhibitory treatments induced a 32% reduction in N_{2co} emissions compared to the positive control (Table 6).

Table 5. Gaseous emission rates from Day 42 samples, 24 h after inhibition. Values are treatment means ± standard deviation.

treatment	N_2O total [µg N m^{-2} h^{-1}]	N_2O_{co} [µg N m^{-2} h^{-1}]	N_2 total [µg N m^{-2} h^{-1}]	N_{2co} [µg N m^{-2} h^{-1}]
Control-	64.5 ± 76.7^{b}	---	---	---
Control+	1080.4 ± 378.3^{a}	362.5 ± 121.2^{a}	2.9 ± 0.08^{a}	1.6 ± 0.03^{a}
Antibacterial	981.1 ± 479.8^{a}	320.7 ± 162.2^{a}	2.8 ± 0.04^{a}	1.6 ± 0.02^{a}
Antifungal	261.7 ± 173.4^{b}	85.9 ± 56.8^{b}	2.9 ± 0.02^{a}	1.6 ± 0.01^{a}
Antibacterial + Antifungal	156.1 ± 74.2^{b}	50.8 ± 23.3^{b}	3.0 ± 0.08^{a}	1.6 ± 0.00^{a}
Level of significance test	* Holm-Sidak Method	* Holm-Sidak Method	n.s.	n.s.

Vertically, LS-means with the letter are not significantly different, different letters indicate a significant difference based on the mentioned test.
level of significance: * indicates P<0.05, --- marks no available data

Table 6. Gaseous emission rates from Day 51 samples, 24 h after inhibition. Values are treatment means ± standard deviation.

Treatment	N_2O total [µg N m^{-2} h^{-1}]	N_2O_{co} [µg N m^{-2} h^{-1}]	N_2 total [µg N m^{-2} h^{1}]	N_{2co} [µg N m^{-2} h^{-1}]
Control-	0.4 ± 0.4^{b}	---	---	---
Control+	209.6 ± 171.4^{a}	87.8 ± 71.4^{a}	39.9 ± 0.52^{b}	1.4 ± 0.01^{a}
Antibacterial	151.9 ± 67.4^{a}	128.5 ± 56.2^{a}	65.1 ± 11.38^{ab}	0.9 ± 0.03^{b}
Antifungal	71.3 ± 21.5^{ab}	56.0 ± 20.2^{a}	77.4 ± 0.89^{a}	1.0 ± 0.01^{b}
Antibacterial + Antifungal	56.2 ± 7.2^{ab}	45.3 ± 6.4^{a}	75.0 ± 3.15^{a}	1.0 ± 0.00^{b}
Level of significance test	* Tukey	n.s.	* Tukey	* Tukey

LS-means with the letter are not significantly different, different letters indicate a significant difference based on the mentioned test.
level of significance: * indicates P<0.05, --- marks no available data

4.4 Discussion

4.4.1 Soil inorganic-N pools and ^{15}N enrichments

The application and subsequent hydrolysis of the applied urea explains the elevation in soil NH_4^+ concentrations. Urea hydrolysis results in an increase of OH^- ions, which caused the observed increase in soil pH (Avnimelech and Laher 1977). Elevation of soil pH (> 7.0) also shifts the equilibrium between NH_4^+ and NH_3, favouring NH_3. Free NH_3 inhibits the organisms responsible for oxidation of both NH_4^+ and NO_2^- (Venterea et al. 2015; Zhu et al. 2013b). The prolonged period of relatively high NH_4^+ concentrations and the lack of any significant increase in either NO_2^- or NO_3^- during the period (Days 0 – 33) of high soil pH (> 7.0) can be explained by free NH_3 being present at inhibiting concentrations, as evident from the theoretical NH_3 concentrations calculated, which were higher than previously reported values that were observed to inhibit nitrification (Monaghan and Barraclough 1992). It was only when the soil pH began to decline at Day 33, an initial consequence of H^+ release during NH_3 volatilisation (Avnimelech and Laher 1977), that levels of free NH_3 decreased sufficiently for NH_4^+ and NO_2^- oxidation to occur. Nitrification also results in a net source of H^+ ions (Wrage et al. 2001) further contributing to the observed decline in soil pH. Periods of NH_3 toxicity *in situ*, as evidenced by soil pH dynamics and the appearance of increasing soil NO_2^- concentrations, are typically much shorter. For example, Clough et al. (2009) observed *in situ* NO_2^- concentrations peaking 7 to 10 days after ruminant urine application. These NH_3 toxicity periods are shorter in the field, than in the laboratory, due to wind removing NH_3 away from the soil surface, thus enhancing the diffusion gradient for NH_3 loss, or plant uptake of NH_4^+, rainfall and/or irrigation, all of which remove substrate for NH_3 production. Nitrification of NH_4^+, in the urea-affected soil, was responsible for the observed elevation of the NO_2^- and NO_3^- concentrations on Days 42 and 51 (Fig. 30 a; Table 3). The observed increase in soil NH_4^+ concentrations in the inhibitory treatments, on average ca. 92 μg NH_4^+-N g^{-1} soil (Day 42, Table 3), implied either a reduction in the consumption of NH_4^+ or an increase in the supply of NH_4^+ as a result of the antibiotic applications or lysis of inhibited microbial cells. A decrease in consumption would indicate slower nitrification or immobilization of NH_4^+-N. Streptomycin has been previously shown to inhibit nitrification by 79 % relative to a control in a neutral mineral soil of pH 7.0 (Koijman et al. 2016). A similar effect would explain the elevated NH_4^+-N concentration observed in the current study for the antibacterial treatment (streptomycin + penicillin). However, Koijman et al. (2016) found nitrification activity remained high when cycloheximide was applied to the same soil at pH 7.0, while nitrification was reduced by cycloheximide in an acidic soil of pH 3.7, possibly because of the inhibition of heterotrophic nitrification. Alternatively, cycloheximide may have inhibited the contribution of archaea to nitrification as discussed below.

A less ^{15}N-enriched NH_4^+ pool, compared with the positive control as observed in the antifungal treatment (Table 4), either by itself or in combination with the antibacterial treatment, demonstrates that a dilution of the $^{14/15}NH_4^+$ pool occurred, with the ^{14}N derived from an external (e.g. inhibitor decomposition) or organic source(s). However, this was not observed in the antibacterial treatment, were the ^{15}N enrichment of the NH_4^+ pool was not different from the positive control. Considering this and the constant decrease of NH_4^+ concentration over time due to ongoing nitrification, the observed high NH_4^+ concentration in the antibacterial treatment is more likely the result of inhibited NH_4^+ oxidation.

On Day 42 the trend for NO_2^- concentrations to decline under either the antifungal, or the antibacterial treatment, a trend which became statistically significant when both antimicrobial inhibitors were applied concurrently, is likely the result of a decline in nitrification rates as evidenced by the accompanying decline in soil NO_3^- concentrations (Table 3). This implies that fungi were contributing to heterotrophic nitrification as previously reported (Hirsch et al. 1961; Stroo et al. 1986; Yokoyama et al. 2012; Zhu et al. 2015). Alternatively, the significant contribution of archaea to nitrification in cropping soils has recently been reported (Bottomley et al. 2012; Giguere et al. 2015), thus a decline in nitrification rates as a consequence of cycloheximide inhibiting ammonia oxidizing archaea (Taylor et al. 2010) cannot be ruled out. It was also assumed that, based on the study of Weisburg and Tanner (1982) that streptomycin had no inhibitory effect on archaea but such an effect cannot be ruled out.

In the positive control on Day 42 the similarity of the ^{15}N enrichment of the NH_4^+ and NO_2^- pools after inhibition (Table 4) indicates the NO_2^- was derived from the NH_4^+ pool, while the ca. 50% reduction observed in the NO_3^- pool ^{15}N enrichment can be attributed to the antecedent soil NO_3^-, present in the soil at the start of the experiment, diluting the ^{15}N enriched NO_3^- pool formed during nitrification. Where the fungal inhibitor was applied the lower ^{15}N enrichments observed in the NH_4^+ pool (ca. 4 atm%) did not occur in the NO_2^- pool possibly because the period of inhibition was too short for the diluted NH_4^+-^{15}N pool to be transformed and/or that the nitrification of the NH_4^+ was inhibited as discussed above (Barraclough et al. 1992; Taylor et al. 2010).

On Day 51 the reason for the lack of any effects of the inhibited treatments, on the soil NH_4^+, NO_2^- and NO_3^- concentrations, relative to the positive control, is not immediately obvious. It is possible that after a further nine days the rate of nitrification varied on Day 51 relative to Day 42. For example, the rate of increase in NO_2^- was slower between Days 42 and 51 when compared to Days 33 to 42 (Fig. 30 a). Hence, the influence and outcome of the inhibited treatments, in terms of inorganic-N concentrations were less pronounced. However, the decrease in the NH_4^+-^{15}N enrichment mirrored that observed on Day 42, when a fungal inhibitor was applied for reasons discussed above.

4.4.2 N_2O and N_2 emissions

Venterea et al. (2015) found N_2O fluxes were strongly linked to the presence of NO_2^-. Thus given that N_2O fluxes began to increase substantially between Days 33 and 42, and NO_2^- had increased by Day 42, it can be concluded that the NO_2^- pool was contributing to N_2O formation.

The increased N_2O emissions observed after stirring of the soil, performed to mix in the inhibitors but also performed in the negative and positive control treatments, resulted from the release of N_2O contained in soil pore spaces (Clough et al. 2003).

The > 76 % reduction in total N_2O production observed on Day 42 in the treatments containing cycloheximide (Table 5) demonstrates fungi, possibly in addition with archaea made a significant contribution to N_2O production with a similar albeit not statistical effect on Day 51 (Table 6).

Fungi and archaea lack the ability to produce N_2O reductase which leads to a release of N_2O when fungi and archaea utilize NO_2^- (Maeda et al. 2015; Philippot 2002; Spott et al. 2011). However, the activity of archaea with respect to N_2O emissions is low following NH_4^+ amendment of soils (Hink et al. 2017) and archaea are not capable of nitrifier-denitrification in terrestrial ecosystems as oxygen becomes limiting (Stieglmeier et al. 2014). Thus it is likely fungi played a larger role than archaea in N_2O production. During fungal denitrification NO_2^- is reduced by metal containing enzymes e.g. Cu containing NIR, (Averill 1996) to form nitric oxide (NO) which is further reduced by nitric oxide reductase (P450nor) in the presence of nicotinamide adenine dinucleotide (NADH), a co-enzyme, to form N_2O. The NADH can be replaced by a nucleophilic co-substrate (e.g. NH_4^+) acting as an electron and N donator to form hybrid N_2O (Shoun 2005; Su et al. 2004). Shoun et al. (2005) also noted the possibility of hybrid N_2O formation by way of P450nor facilitating the combining of two NO molecules derived from separate N pools. Thus inhibiting fungi and archaea, active in processing NO_2^-, will reduce N_2O emissions as observed in the current study.

N_2O data from Day 42 clearly show that N_2O emissions were derived predominately via fungal mechanisms, assuming any response by archaea was minor in nature as noted above, since N_2O total fluxes decreased when applying cycloheximide (Table 5). Furthermore, the fungal contribution to N_2O_{co} was evident from the application of cycloheximide where a reduction of > 76 % in N_2O_{co} occurred, relative to the positive control (Table 5). Interestingly, when the combined anti fungal+anti bacterial treatment was applied an N_2O flux still occurred, both total and N_2O_{co} (Table 5), indicating either incomplete inhibition of microbes or the presence of an abiotic mechanism(s). Pertinent to the current study are the results of Phillips et al. (2016) who demonstrated, *in vitro,* the abiotic formation of N_2O when fungal necromass was also present, using a NO_2^- enriched medium (0.2 mmol NO_2^--N L^{-1} and 0.2 mmol glutamine-N L^{-1}). Cycloheximide inhibits eukaryote protein synthesis and ultimately leads to fungal cell death over a period of 24 – 48 h (Badalucco et al. 1994). However, the time period of inhibition in the current study may have limited the potential effect of fungal necromass, given the results of Castaldi et al. (1998), who found the biocidal effect was negligible in

the first 48 h after application of cycloheximide at ≤ 2 mg g^{-1} soil. Still, cycloheximide concentrations of > 2 mg g^{-1} soil may have caused fungal cell death, including cell lysis, (Badalucco et al. 1994) which may have affected the N_2O and N_2 fluxes as described by Phillips et al. (2016). Likewise, other abiotic mechanism cannot be excluded (Chalk and Smith 1983; Heil et al. 2016).

On Day 51 the total N_2O fluxes of each treatment were lower relative to the same treatment on Day 42. But the fact that the positive control of Day 51 had higher total N_2O fluxes than the negative control of the same day demonstrated that the observed inorganic-N pools were providing substrate for N_2O production pathways. Furthermore, the fact that the application of cycloheximide, with or without the antibacterial inhibitor, resulted in N_2O emissions being reduced to a level where they were not significantly different from the negative control (Table 6) showed that fungi and possibly archaea, were again playing a significant role in N_2O production at this time. The N_2O_{co} fluxes were also observed to decline on Day 51 with cycloheximide application, although this was not significant ($p < 0.103$).

Lower total N_2O fluxes on Day 51, relative to Day 42, coincided with higher total N_2 fluxes, although there were no differences in the antifungal or antifungal + antibacterial treatments with respect to N_2 emissions at this time. It is possible that, in the antifungal treatment where bacteria were still active, N_2O reductase activity may have increased over time as N_2O substrate became more available (Morales et al. 2015). Recently, microbes have been identified as carrying type I or type II N_2O reductase genes (nosZ type I and II) that have different physiology and affinity for N_2O (Hallin et al. 2017). The chemical and physical conditions of Day 42 and 51 samples might have enhanced either nosZ type I or type II with the result that rates of N_2O and N_2 production varied due to differing microbial function.

Alternatively, increased total N_2 fluxes may have occurred because of fungal necromass production influencing abiotic N_2 emissions as discussed above. The reason for the large shift in the contribution of N_{2co} to total N_2 production, from > 50% on Day 42 to < 1.4% on Day 51, and the lower N_{2co} emission rates observed on Day 51, remains unclear and may be a function of the differences in the rate of NO_2^- formation as noted above. This contrasted with the results of (Selbie et al. 2015b) who observed sustained emissions of co-denitrified N_2, which comprised 95% of total N flux, in a field study where ruminant urine was applied. The differences may have been due to the presence of plants and associated root exudation providing codenitrification substrates, and regular rainfall events producing oscillating soil moisture conditions which in turn could have created cycles of substrate supply through mineralization (e.g. inorganic-N) which in turn promoted codenitrification upon soil wetting. It is also likely that the presence of plants and plant root exudates resulted in a significantly higher number of active soil bacteria in the field. This may have caused a higher microbial reduction capacity of N_2O, produced by fungi, and or affected N_2O: N_2 ratios.

4.4.3 Conclusions

Following the application of either antibacterial or antifungal inhibitors to urea-amended soil, an increase in soil NH_4^+ concentrations was observed. This is thought to result from antibacterial treatment inhibiting autotrophic nitrification and in the case of the antifungal treatment, it may result from degradation of the inhibitor or inhibition of other nitrification pathways. The apparent inhibition of nitrification when the fungal inhibitor was applied requires further study. Concurrent reductions in NO_2^--N and NO_3^--N provided further evidence for nitrification inhibition under both antibacterial and antifungal treatments. Codenitrification was also observed to contribute to both total emissions of both N_2O and N_2 in urine amended grassland soils. Inhibition of fungi decreased the NH_4^+-^{15}N enrichments and reduced total N_2O fluxes by $\geq$ 66% and N_2O_{co} by $\geq$ 42%. This study clearly shows that fungi play a significant role in the production of N_2O when soils are affected by high rates of urea, as happens in ruminant urine patches.

Chapter 5
Impact of N compounds on fungal and bacterial contributions to codenitrification in a pasture soil

A manuscript from this study has been submitted to Scientific Reports and is currently under revision: Rex D, Clough TJ, Richards KG, Condron LM, de Klein CAM, Morales SE, Lanigan GJ 2018. Impact of nitrogen compounds on fungal and bacterial contributions to codenitrification in a pasture soil. Scientific Reports.

5.1 Introduction

The nitrous oxide (N_2O) molecule is a potent greenhouse gas, with a global warming potential 298 times that of carbon dioxide over a 100 year time period (WMO 2013). It is also a precursor to reactions involved in the depletion of stratospheric ozone (Ravishankara et al. 2009). A major source of anthropogenic N_2O emissions is the intensive grazing of grasslands and the resulting ruminant urine deposition that occurs (Flessa et al. 1996; Oenema et al. 1997). Thus, in order to achieve mitigation of N_2O emissions from intensively managed pasture soils it is important to identify and understand the processes that lead to N_2O formation and consumption within ruminant urine-affected soil.

Typically, ruminant urine-N deposited onto pasture soil is comprised of > 70% urea-N. Upon contact with the soil the urea begins to hydrolyse, forming ammonium (NH_4^+) and bicarbonate ions (HCO_3^-), with the latter hydrolysed to form carbonate (CO_3^{2-}) and hydroxyl (OH^-) ions, resulting in a rapid elevation of soil pH to 8.0 or higher (Avnimelech and Laher 1977). The equilibrium between NH_4^+ and ammonia (NH_3) is pH driven (Körner et al. 2001; Sherlock and Goh 1985). Soil pH > 7.0 leads to elevated NH_3 concentrations in the soil, that not only result in NH_3 volatilization (Laubach et al. 2015) but which can also inhibit the microbial oxidation of nitrite (NO_2^-) by *Nitrobacter sp.* (Breuillin-Sessoms et al. 2017; Venterea et al. 2015). Over time, both NH_3 volatilization and nitrification result in the net release of H^+ ions causing the soil pH to be restored to its initial value, or lower. As the pH decreases to ca. < 7.0, the equilibrium between NH_4^+ and NH_3 shifts in favour of NH_4^+, which may undergo clay mineral fixation, plant uptake, immobilization or nitrification (Sebilo et al. 2013). Production of N_2O may occur via the microbial pathways of nitrification, denitrification, and nitrifier-denitrification (Wrage et al. 2001). However, under ruminant urine-affected soil it is bacteria, not archaea, that respond to the high concentration of NH_4^+ substrate that forms in the soil following ruminant urine deposition (Di et al. 2009; Samad et al. 2017), since bacterial nitrifiers operate under conditions of high inorganic NH_4^+ inputs (Hink et al. 2017; Prosser and Nicol 2012; Samad et al. 2017). During the conventional nitrification process bacteria produce N_2O as a by-product of NH_2OH oxidation (Otte et al. 1999) or during nitrifier-denitrification following nitric oxide (NO) reduction

(Hink et al. 2017). However, the major source of N_2O emissions from ruminant urine-affected soil occurs as a result of the NO_3^- formed, as a consequence of nitrification, being denitrified: under anaerobic conditions microbes denitrify NO_3^- to sequentially form NO_2^-, NO, N_2O and dinitrogen (N_2), which are all obligate intermediaries of the denitrification pathway (Butterbach-Bahl et al. 2013; Cameron et al. 2013; Spott et al. 2011; Wrage et al. 2001). In order to conserve both energy and oxygen, nitrifier-denitrification may occur in response to limited soil oxygen conditions (Kool et al. 2011), whereupon nitrifiers convert NO_2^- to NO, N_2O and N_2 (Wrage et al. 2001) although the significance of this process may have been overestimated in some studies (Bakken and Frostegård 2017). In addition to these N_2O production pathways, N_2O may also be produced as 'hybrid' N_2O via codenitrification, a process involving two different N pools (Iwasaki et al. 1956; Spott et al. 2011). Spott et al. (2011) reviewed possible biotic and abiotic reactions that may be included under the term 'codenitrification'. For example, abiotic reactions involving reduced iron (Fe^{2+}) and NO_2^-, may occur at the interface between an aerobic zone overlying an anaerobic zone when NO_2^- diffusing downwards meets Fe^{2+} (Sørensen and Thorling 1991; van Cleemput and Baert 1983). However, this process is unlikely to contribute significantly to N_2O emissions due to insufficient Fe^{2+} ion concentrations in most soils (Cleemput and Samater 1996; Nelson and Bremner 1970). A more common abiotic reaction that occurs in acid soil (pH < 5.0) is that of chemodenitrification (abiotic-nitrosation), whereby NO_2^- and H^+ react to form nitrous acid (HNO_2), which can then react with amino compounds, NH_2OH, NH_4^+ or other organic N compounds resulting in the formation of N_2O (Chalk and Smith 1983; Heil et al. 2016). However, under alkaline conditions when oxygen is depleted codenitrification may occur via biologically mediated nitrosation (Selbie et al. 2015b; Spott et al. 2011). Under such conditions the hydrogen atom in an organic compound is replaced with a nitroso group (-N=O). Enzymatic nitrosyl compounds attract nucleophile compounds (e.g. NH_2OH, NH_4^+, hydrazine (N_2H_2), amino compounds and NH_3) resulting in hybrid N_2O or N_2 species, containing one N atom derived from the nucleophile and one N atom derived from the nitrosyl compound (Spott et al. 2011). Recent studies have revealed the significant contribution of codenitrification to gaseous N losses from grassland soils (Clough et al. 2017; Laughlin and Stevens 2002; Selbie et al. 2015b). Using a ^{15}N tracer approach, Laughlin and Stevens (2002) found evidence for fungal dominated $^{15}NO_3^-$ depletion leading to hybrid N_2 emissions where 92% of the N_2 evolved was derived from codenitrification. Selbie et al. (2015b) confirmed, in-situ, the dominance of codenitrification derived N_2 under urine patch conditions when 56% of applied urine was codenitrified. Recently, studies have found further evidence for N_2O production via codenitrification under simulated ruminant urine patch conditions (Clough et al. 2017; Rex et al. 2018). However, knowledge about the nucleophile species that potentially partake in codenitrification under ruminant urine patch conditions is still lacking. Nucleophiles such as amino acids, NH_4^+ and NH_2OH have previously been proven to be capable of generating hybrid N_2O/N_2 in vitro when utilized by one microbial species in combination

with either NO_3^- or NO_2^- (Garber and Hollocher 1982; Immoos et al. 2004; Kumon et al. 2002; Shoun and Tanimoto 1991). Amino acids have been reported to be freely available within the soil solution, for example, phenylalanine (8 – 50 µg N g^{-1} soil) and glycine (35 – 193 µg N g^{-1} soil) were measured in long-term agricultural land on a Stagni-Haplic Luvisol (Friedel and Scheller 2002) and in different cattle manure treated crop fields on a sandy Orthic Luvisol (Scheller and Raupp 2005). Reported concentrations of NH_2OH are orders of magnitude lower, for example, Liu et al. (2014) reported concentrations of <0.0348 µg N g^{-1} in a forest soil, while NH_4^+ and NH_3 are routinely reported following ruminant urine deposition events (Selbie et al. 2015a). The aim of this study was to assess and quantify the relative contribution of different N-compounds to codenitrification, and determine the relative roles of bacteria and fungi to the process under simulated ruminant urine soil conditions.

5.2 Materials and Methods

5.2.1 Experimental design

A bulked soil sample was taken from a sandy loam pasture soil on the Lincoln University dairy farm (0 - 10 cm), New Zealand (43°38'25.23"S, 172°27'24.71"E, Typic Immature Pallic Soil). The pasture consisted of perennial rye grass (*Lolium perenne L.*) and white clover (*Trifolium repens L.*). Field moist soil was sieved (4 mm) to remove stones and plants and then placed into jars (250 mL, Ø 8.1 cm), corresponding to 100 g dry weight (ca. 82 cm^3), and moistened to 50% of water-holding capacity (Rex et al. 2018) (ca. 83% water-filled pore space).

Treatments consisted of ^{15}N enriched nucleophile species (glycine (98), L-phenylalanine (98), NH_4^+ (99) and NH_2OH (98); atom% ^{15}N enrichment in bracket) with each nucleophile treatment further split into five microbial inhibition treatments (no inhibition, fungal inhibition, bacterial inhibition, fungal and bacterial inhibition ('combined inhibition') and soil total microbial inhibition (heat sterilised soil)). Treatments were replicated thrice. The amino acid nucleophile treatment concentrations were based on the findings of Scheller and Raupp (2005), and in order to apply a realistic concentration, these were applied at a rate of 20 µg nucleophile-N g dry $soil^{-1}$. Hydroxylamine and NH_4^+ were applied at equal rates for comparative purposes.

Initially the jars, with soil, were placed in an incubator, in the dark, at 23ºC and wetted-up daily to preincubation weight. After four days, any germinated weed seedlings were removed and the experimental period of 14 days commenced (Day -2 to Day 11). An aqueous urea solution (500 µg urea-N g dry $soil^{-1}$) was applied on Day 0 in order to simulate a bovine urine deposition event (Clough et al. 2017; Haynes and Williams 1993). On Day 8, microbial inhibition treatments were applied with the nucleophile treatments applied immediately after this in an aqueous solution (4 mL) as noted below.

According to Anderson and Domsch (1974) cycloheximide, a fungal inhibitor, was applied at a rate of 8 mg g^{-1} soil and streptomycin, a bacterial inhibitor, at a rate of 5 mg g^{-1} soil. Both chemicals were applied as a dry powder on to the soil surface and subsequently mixed into the soil with a spatula for 1 min. The combined inhibition included the simultaneous application of cycloheximide and streptomycin and was designed to inhibit both bacteria and fungi. Sterilizing (as complete microbial inhibition) was performed by heating the soil. This was achieved by microwaving the soil in the jars for 4 minutes, remoistening the dry soil, and then microwaving the jars for another 3 minutes, as microwave heating is a proven method to stop microbial activities (Islam and Weil 1998; Wang et al. 2001). Thereafter, the microwaved soils were readjusted to 50% water-holding-capacity and also mixed for 1 minute. The control treatment contained urea, but no inhibitors were applied, and the soil was mixed to replicate the physical disturbance of the other treatments. Immediately after application of the inhibitor treatments the nucleophile treatments were applied according to treatment at a rate of 20 µg nucleophile-N g^{-1} dry soil.

In addition, three further control treatments were set up; a positive control (soil with urea but no nucleophile or inhibitor addition (n = 3), also physically mixed on Day 8; a negative control (n = 3) consisting of soil without urea , inhibitors, or nucleophiles, also physically mixed on Day 8; and a NO_2^- control (soil with urea but no nucleophile addition, physically mixed on Day 8) for soil NO_2^--N sampling at 4 different times over the duration of the experiment.

5.2.2 Gas sampling and analysis

On Day -2, -1, 0, 1, 2, 4, 6, 7, 8 (before inhibitor application), 9, 10 and 11, the jars were sealed with lids equipped with rubber septa. Jar headspace gas samples were taken with a plastic syringe, fitted with a three-way-stop cock and a 25G hypodermic needle, and injected into a previously evacuated Exetainer® vials (Labco Ltd., High Wycombe, UK). The first gas sample (12 mL) was taken immediately after sealing the jar headspace. The second gas sample was taken after 1 h, only from the positive control to verify the linearity of the increase in the headspace gas concentration, and the third gas sample was taken after a 2 h incubation time (12 mL, all jars). On Days 8, 9, 10 and 11, the third gas sample (30 mL), was split between a 6 mL Exetainer® that received 12 mL, and an evacuated and helium flushed 12 mL Exetainer® that received 18 mL for ^{15}N-N_2O determination.
Nitrous oxide concentrations were determined using a gas chromatograph (SRI-8610, SRI Instruments, Torrance, CA) coupled to an auto sampler (Gilson 222XL; Gilson, Middleton, WI) equipped with a ^{63}Ni electron capture detector (Clough et al. 2006b). PeakSimple 4.44 software (SRI Instruments, Torrance, CA) and several N_2O standards (range 0 – 100 µL L^{-1}, BOC, New Zealand) were used to determine the N_2O concentrations. The N_2O fluxes (µg N_2O-N m^{-2} h^{-1}) were determined according to equation (10). The ^{15}N enrichment of the N_2O evolved was determined by analysing the

gas samples with a continuous-flow-isotope ratio mass spectrometry CFIRMS (Sercon 20/20; Sercon, Chesire, UK) inter-faced with a TGII cryofocusing unit (Sercon, Chesire, UK). If required, gas samples were diluted by injecting 4 mL of sample gas into a helium-filled 12 mL Exetainer® (1:4 dilution). Codenitrification fluxes were calculated as described in chaper 3.

The measured ^{15}N concentration of the headspace N_2 was close to natural abundance thus a determination of the N_2 flux was not possible, hence, the N_2 emissions were not considered further.

5.2.3 Surface pH and inorganic-N measurement

Surface pH was measured on Days -2, 0, 1, 3, 5, 7, 9 and 11, by adding one drop of deionised water to the soil surface and then placing a flat surface pH probe (Broadley James Corp., Irvine, California) onto the soil surface.

The NO_2^- concentration in the unmixed NO_2^- control (soil + urea solution) was determined by subsampling soil with a corer (diameter 1.6 cm, depth 1.5 cm). The soil was then blended with 2M potassium chloride (KCl), adjusted to pH 8 with potassium hydroxide (Stevens and Laughlin 1995) at a 1:6 ratio. This procedure was performed on Days 1, 4, 6 and 10.

Subsamples of moist soil (4 g dry weight) were taken after Day 11, from the positive and negative controls, and extracted with 2M KCl in order to determine the NH_4^+ and NO_3^- concentrations at the end of the experiment (Blakemore et al. 1987; Clough et al. 2001b). Inorganic-N concentrations in the extracts were determined using Flow Injection Analysis (Blakemore et al. 1987).

5.2.4 Statistics

The single jars were defined as experimental units by the independent applications of treatments. The experiment focussed on achieving the most sensitive test of treatment differences and inference is not claimed for a population wider than the paddock, used for sampling. All statistical analyses were performed using SigmaPlot 13.0 (Systat Software Inc., Chicago). For each variable of interest a general linear model (ANOVA equivalent) was fitted with nucleophile treatment or a factorial combination of nucleophile treatment and inhibition method as explanatory variables. Tests for normality and variance were used to evaluate the residuals and define the most powerful test for each comparison of means. Hence, means comparisons were adjusted for multiplicity using Tukey, Holm-Sidak or Student's t-test adjustments to *p* values.

5.3 Results

5.3.1 Soil pH, and mineral N

Within 6 h of applying the urea solution soil surface pH values increased uniformly in all treatments from an average of 5.6 ± 0.2 on Day -2 to >7.6 on Day 0. The surface soil pH peaked 30 h after the urea application, at 7.9, followed by a steady decline to 4.8 ± 0.1 on Day 9 (Fig. 31). The surface pH in the negative control ranged from 5.4 ± 0.05 to 5.6 ± 0.06 over the course of the experiment (Fig. 31). Soil NO_2^- concentrations were significantly elevated within the first 4 days following urea application ($p < 0.05$). Soil NO_2^- concentrations peaked at 1.5 ± 0.2 µg NO_2^--N g^{-1} soil on Day 9, subsequent to the physical mixing and then decreased to 0.6 ± 0.1 µg NO_2^--N g^{-1} soil on Day 11 (Fig. 31 b).
Both the soil NO_3^- and NH_4^+ concentrations were higher ($p < 0.01$) in the positive control at Day 12 compared with the negative control. The NO_3^- concentrations in the positive control were in the range of 366 ± 122 µg NO_3^--N g^{-1} soil while NH_4^+ concentrations were 174 ± 7 µg NH_4^+-N g^{-1} soil. The soil NO_3^- and NH_4^+ concentrations in the negative control were 64 ± 23 µg NO_3^--N g^{-1} soil and 22 ± 1 µg NH_4^+-N g^{-1} soil, respectively.

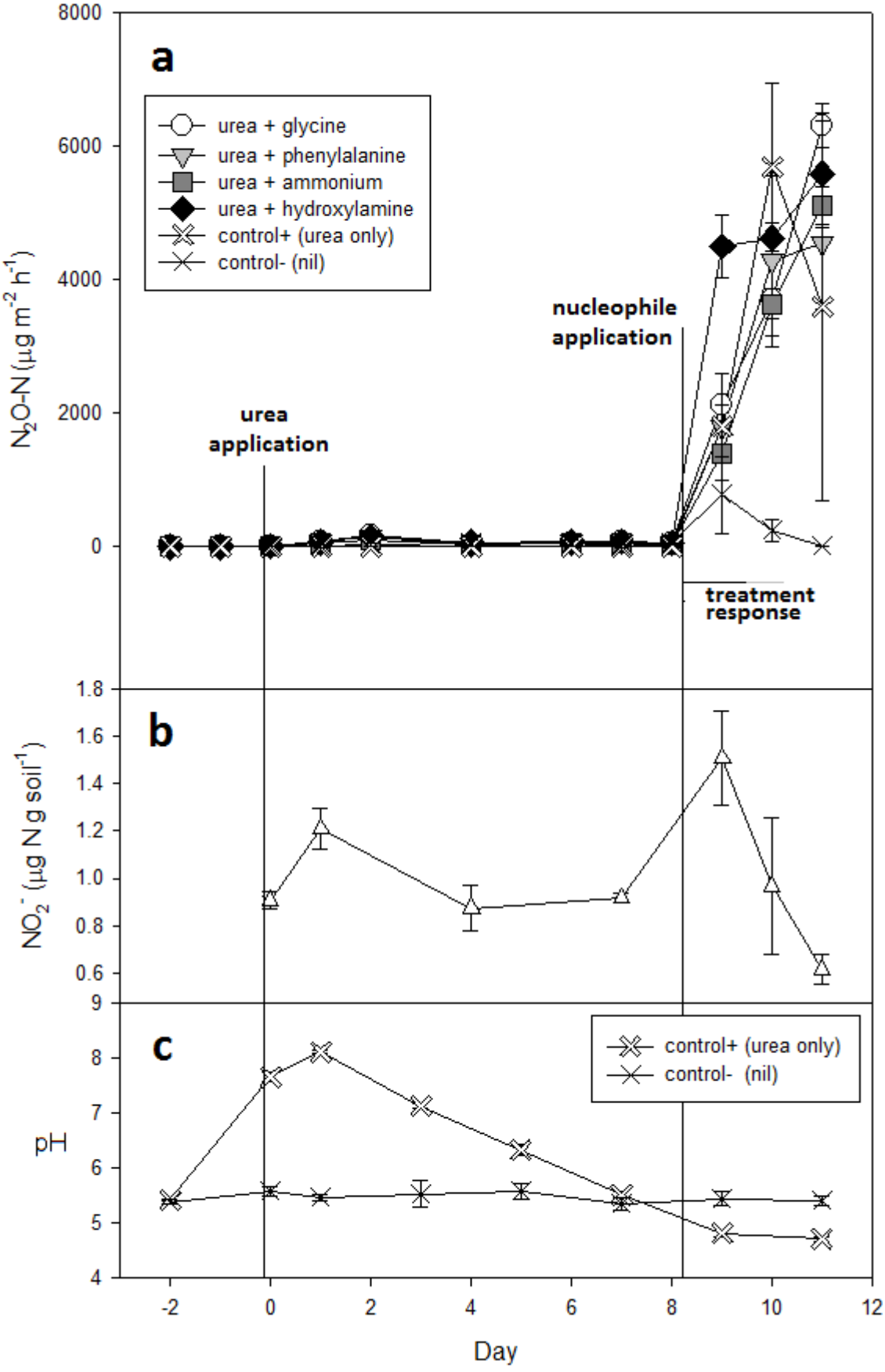

Figure 31. Soil response to urea and treatment application. The N_2O fluxes over time (a) of the no inhibition treatments. Below the NO_2^- concentration in the soils as measured in the NO_2^- control (b) and the soil surface pH of the positive and negative control (c). Each symbol represents mean (n = 3) and standard deviation.

5.3.2 N_2O fluxes

Initially N_2O fluxes increased within the first 48 h following urea application, with treatments and positive controls emitting 100 – 200 µg N_2O-N m^{-2} h^{-1}. From Day 4 to Day 8, the N_2O fluxes from the urea-treated soil were <100 µg N_2O-N m^{-2} h^{-1} across all treatments. Following N_2O flux measurement on Day 8, the process of mixing the soil and/or the addition of nucleophiles increased N_2O fluxes at Day 9 (Figure 31). In the absence of microbial inhibition, the addition of the NH_2OH nucleophile resulted in higher N_2O fluxes (4496 µg N_2O-N m^{-2} h^{-1}) when compared to the amino acid (1796 to 2130 µg N_2O-N m^{-2} h^{-1}) and NH_4^+ (1405 µg N_2O-N m^{-2} h^{-1}) treatments on Day 9 ($p < 0.001$), 24 h after nucleophile addition.

The magnitude of the decrease in the N_2O fluxes, following inhibition treatment, varied due to inhibitor type and nucleophile applied (Table 7). The N_2O fluxes of both amino acid treatments (1796 – 2130 µg N_2O-N m^{-2} h^{-1}), and the NH_2OH treatment (4496 µg N_2O-N m^{-2} h^{-1}) in the no inhibition treatments, decreased when fungi were inhibited by 46, 34 and 21% in the glycine, phenylalanine, and NH_2OH treatments, respectively, while fungal inhibition did not affect fluxes from the NH_4^+ treatment. Bacterial inhibition reduced N_2O fluxes by 14, and 26% in the glycine and NH_2OH treatments, respectively, while fluxes from the phenylalanine and NH_4^+ treatments were unaffected by bacterial inhibition (Table 7). Applying both inhibitors simultaneously (combined inhibition) resulted in N_2O flux reductions of 29-41% in all nucleophile treatments (Table 7). In the glycine nucleophile treatment fungal inhibition reduced N_2O fluxes more than bacterial inhibition, but this reduction was not enhanced in combined inhibitor treatment (Table 7). While bacterial inhibition did not significantly reduce N_2O fluxes in the phenylalanine nucleophile treatment, the fungal inhibition either alone or within the combined inhibition did reduce N_2O fluxes (Table 7). Sterilizing effectively eliminated N_2O fluxes in both the amino acid treatments, and the NH_4^+ treatment (Table 7). However, this was not the case when NH_2OH was applied where emissions decreased by 72% (Table 7).

Table 7. Emission rates of total N_2O (µg N_2O-N m^{-2} h^{-1}) of the inhibitor × nucleophile treatments on Day 9, 24 h after the treatment application.

nucleophile	no inhibition	fungal inhibition	bacterial inhibition	combined inhibition	sterilized soil	test & significance
Glycine	2130 **a** ± 134	1144 **c** ± 177	1830 **b** ± 163	1331 **c** ± 114	2 **d** ± 0	Holm-Sidak*
Phenyl.	1796 **a** ± 333	1182 **b** ± 66	1705 **a** ± 36	1267 **b** ± 93	1 **c** ± 1	t-tests*
Ammonium	1405 **a** ± 49	1142 **ab** ± 301	1010 **ab** ± 873	904 **b** ± 111	3 **c** ± 0	Tukey**
Hydroxy.	4496 **a** ± 467	3563 **b** ± 358	3324 **bc** ± 240	2671 **c** ± 253	1246 **d** ± 21	Holm-Sidak*

Values are means (n = 3) with standard deviation, different letters indicate the level of significance based on the mentioned test, where all inhibition treatments for each nucleophile are tested against each other. Level of significance: *p < 0.05, **p = 0.001.

5.3.3 N_2O-^{15}N enrichment

The positive control (urea only at natural abundance) had a N_2O-^{15}N enrichment of 0.363 ± 0.004 (SEM) on Day 9. At the same time, the addition of a nucleophile resulted in small increases in the N_2O-^{15}N enrichments in all treatments with the following exceptions (Table 8): the phenylalanine treatment, with either no inhibition or bacterial inhibition, and the NH_4^+ treatment with bacterial inhibition had no increase in N_2O-^{15}N enrichments (Table 8). Within a nucleophile treatment, when comparing the N_2O-^{15}N enrichment of the no inhibition treatment and a specific inhibitor treatment, few treatments differences occurred. Under glycine only the sterilized soil treatment varied, with a higher N_2O-^{15}N enrichment relative to the no inhibition treatment (Table 8). Applying phenylalanine resulted in the highest N_2O-^{15}N enrichment in the sterilized soil treatment but this was not statistically different from the no inhibition treatment (Table 8). With NH_4^+ as the nucleophile the N_2O-^{15}N enrichment was again highest in the sterilized soil treatment, but none of the inhibitor treatments caused N_2O-^{15}N enrichment to differ from the no inhibitor treatment (Table 8). The biggest shifts in N_2O-^{15}N enrichment with inhibition treatments occurred in the NH_2OH treatment where applying bacterial inhibition, either alone or within the combined inhibition, caused significant decreases in N_2O-^{15}N enrichment relative to the no inhibition treatment (Table 8).

Table 8. N_2O ^{15}N enrichment (atm%) of the inhibitor × nucleophile treatments on Day 9, 24 h after the treatment application.

nucleophile	no inhibition	fungal inhibition	bacterial inhibition	combined inhibition	sterilized soil	test & significance
Glycine	0.370 **b** ± 0.001	0.380 **ab** ± 0.001	0.373 **ab** ± 0.002	0.375 **ab** ± 0.006	1.211 **a** ± 0.104	Tukey*
Phenyl.	*0.363* **ab** *± 0.003*	0.377 **ab** ± 0.003	*0.360* **b** *± 0.003*	0.378 **ab** ± 0.011	0.900 **a** ± 0.170	Dunn's Method*
Ammonium	0.481 **ab** ± 0.034	0.374 **b** ± 0.003	*0.475* **ab** *± 0.026*	0.384 **ab** ± 0.003	0.896 **a** ± 0.088	Tukey*
Hydroxy.	41.587 **a** ± 1.414	43.147 **a** ± 4.055	27.165 **b** ± 1.555	30.384 **b** ± 3.499	44.219 **a** ± 4.625	Dunn's Method*

Values are means (n = 3) with standard deviation, different letters indicate the level of significance based on the mentioned test where all inhibition treatments for each nucleophile are tested against each other. Italic font indicates no significant difference if compared to the positive control (+ urea, nil nucleophile) on the same day (0.363 ± 0.004). Level of significance: *p < 0.05

5.3.4 Codenitrification N_2O

Increased ^{15}N enrichment of the N_2O fluxes revealed the formation of hybrid N_2O. Amino acid and NH_4^+ treatments emitted 13 – 17 µg N_2O_{co}-N m^{-2} h^{-1} in case of no inhibition, while bacterial inhibition and/or fungal inhibition reduced these fluxes by > 30% (Table 9). With sterilized soil under these nucleophile treatments codenitrification fluxes ceased (Table 8). The N_2O codenitrification fluxes from the NH_2OH treatment decreased significantly in the presence of the combined inhibition (> 46%, Table 9) but not when applied individually. Under NH_2OH, sterilized soil significantly reduced codenitrification fluxes to 617 µg N_2O_{co}-N m^{-2} h^{-1} (> 83%, compared to the no inhibition treatment; > 71%, compared to the combined inhibitor treatment; Table 9).

Table 9. Codenitrification fluxes (N_2Oco, µg N_2O-N m^{-2} h^{-1}) of the inhibitor × nucleophile treatments on Day 9, 24 h after the treatment application.

nucleophile	no inhibition		fungal inhibition		bacterial inhibition		combined inhibition		sterilized soil		test & significance
Glycine	16 ± 0	**a**	9 ± 0	**b**	14 ± 0	**a**	10 ± 0	**b**	0 ± 0	**c**	Holm-Sidak*
Phenyl.	13 ± 0	**a**	9 ± 0	**b**	12 ± 0	**ab**	10 ± 0	**ab**	0 ± 0	**c**	Holm-Sidak*
Ammonium	17 ± 0	**a**	9 ± 0	**ab**	12 ± 4	**ab**	7 ± 0	**ab**	0 ± 0	**b**	Tukey*
Hydroxy.	3851 ± 365	**a**	3432 ± 717	**ab**	3034 ± 190	**ab**	2198 ± 853	**b**	617 ± 138	**c**	Holm-Sidak*

Values are means (n = 3) with standard deviation, different letters indicate the level of significance based on the mentioned test where all inhibition treatments for each nucleophile are tested against each other. Level of significance: *p < 0.05.

5.4 Discussion

5.4.1 Soil pH, and mineral N

The hydrolysis of urea and its resulting products increased NH_4^+ and OH^- concentrations in the soil (Avnimelech and Laher 1977) with the latter responsible for the elevated soil surface pH observed in treatments containing urea. Urea application elevated soil NH_4^+-N concentrations, as evidenced by the higher concentrations in the positive control when compared with the negative control. Elevated soil pH will have resulted in the NH_4^+-N forming an equilibrium with NH_3 (Avnimelech and Laher 1977). However, by Day 8 the concentration of NH_3 will have been relatively low based on soil pH values at this time (Avnimelech and Laher 1977). While NH_3 can inhibit NO_2^- oxidisers under urea-affected soil (Breuillin-Sessoms et al. 2017; Venterea et al. 2015) the elevated soil NO_3^--N concentrations at the end of the experiment and the decline in NO_2^- from Day 1 to 7 demonstrates NO_2^- oxidisers were functioning. The soil NO_3^--N concentration on Day 9 was higher when compared to a previous study by Rex et al. (2018), at a similar time following urea application, which indicates a more rapid rate of nitrification most likely due to the lower initial urea-N loading rate in the current study. Considering the soil pH and inorganic-N dynamics it can be concluded that the application of urea was representative of conditions under a typical urine patch, and that the nucleophile treatments were applied during a period of relatively rapid inorganic-N transformation.

5.4.2 N_2O emissions

The rapid increase in N_2O fluxes following inhibitor application was partially the result of physically mixing the soil in order to distribute the inhibitors, which resulted in entrapped N_2O, in the soil, being released (Clough et al. 2001a). Furthermore, soil, not previously exposed to oxygen, would have become exposed and thus there is also the possibility that inhibition of N_2O reductase occurred, preventing complete denitrification (Davidson et al. 1990). However, the nucleophile-N also contributed to the N_2O flux as demonstrated by the increased N_2O-^{15}N enrichments, particularly in the case of the NH_2OH treatment (Fig. 31, a), and the substances applied as nucleophiles have all previously been shown to be readily transformed within the soil matrix (Tzanakakis and Paranychianakis 2017).

Soil N_2O emissions are strongly driven by the presence and turn-over of NO_2^- which is the 'gate-way molecule' for N_2O production (Maharjan and Venterea 2013; Venterea et al. 2015). In the current study soil NO_2^- concentrations were elevated on Day 9 but at concentrations lower than previously observed (e.g. Clough et al. (2017)) due to the lower urea application rate in the current study preventing NH_3 inhibition of NO_2^- oxidation (Maharjan and Venterea 2013). Hence, the ensuing N_2O emissions most likely result from the net effects of microbial or abiotic processes utilising NO_2^- and/or the nucleophiles added.

The effects of the microbial inhibitors, cycloheximide, streptomycin and heat sterilization on N_2O production were assessed 12 h after inhibitor application since maximum efficacy is reported within 24 h of application (Badalucco et al. 1994). The reduction in the N_2O fluxes following fungal inhibition within the amino acid and NH_2OH nucleophile treatments demonstrates fungal mechanisms were responsible for a portion of the N_2O produced (21 – 46%). Previous studies have shown fungi are able to produce N_2O (Laughlin and Stevens 2002; Rex et al. 2018; Shoun et al. 2012; Su et al. 2004). Nitric oxide reductase (P450nor), possessed by fungi, is a key feature of fungal denitrification and has been observed to require hypoxia and either NO_3^- or NO_2^- substrate to generate N_2O (Ma et al. 2008; Shoun et al. 2012): these conditions occurred within the current study. Similarly, NH_2OH has been shown to stimulate biotic N_2O emissions from non-autoclaved soil suspensions when both NH_2OH and NO_3^- are present (Spott et al. 2011) as was the case in the current study following NH_2OH application. Thus, the decline in N_2O emissions in the NH_2OH treatment, with fungal inhibition, implies a fungal mechanism was partially responsible for the N_2O flux, via NH_2OH utilisation.

With bacterial inhibition, the decline in the N_2O flux under the NH_2OH treatment likely occurred due to the bacterial inhibitor preventing the function of the ammonia oxidising bacteria which have, previously, also been shown to respond to NH_2OH application. Increased mRNA transcription levels of the functional genes present in AOB that encode for NH_2OH oxidoreductase (*haoA*), and the

reductases for NO_2^- and NO, which are *nirK* and *norB*, respectively, were shown to be elevated following NH_2OH application (Terada et al. 2017). A similar result and explanation might have been expected following bacterial inhibition in the NH_4^+ treatment, given that NH_2OH is an intermediate in the nitrification pathway, and while mean fluxes did decrease considerably, most likely due to AOB inhibition, variability in the data meant this was not statistically significant (Table 31). Lower N_2O fluxes from the glycine treatment under bacterial inhibition may also have resulted from mineralized glycine-N undergoing reduced nitrification of the resulting NH_4^+, and thus delivering less NO_2^- to the soil pool. However, this did not occur under the phenylalanine treatment possibly because it is a more complex molecule and potentially slower to be mineralized, and thus potentially bacteria played less of a role in the N_2O fluxes derived from phenylalanine. Again, with glycine the combined inhibition treatment demonstrated the role of fungi in generating N_2O. This was also the case with phenylalanine where the combined inhibition reduced N_2O emissions to a level comparable to fungal inhibition alone.

The near complete suppression of N_2O emissions in the amino acid and NH_4^+ treatments, under the combined inhibition treatment, demonstrates that the observed N_2O fluxes were almost entirely from biologically driven processes. As previously shown, from the $\delta^{13}C$ signatures of respired amino acid–CO_2-C, amino acids are readily mineralized, forming NH_4^+ (McLain and Martens 2005). Consequently, amino acids will contribute to N_2O fluxes if this NH_4^+ is nitrified, or via the denitrification of the nitrification products (McLain and Martens 2005). The residence time of amino acids in soils is generally reported in hours and depends on soil type (Jones 1999; Jones and Shannon 1999; McLain and Martens 2005). However, the lack of a significant N_2O flux response to amino acid and NH_4^+ nucleophile additions at Day 9, relative to the positive control (Fig. 31), is most likely due to the large background NH_4^+ pool present at the time of nucleophile addition, derived from the urea addition. Hence, the NH_4^+ formed from either amino acid mineralization or direct NH_4^+ addition will have been diluted by at least 10-fold, assuming all nucleophile-N was immediately available. Furthermore, it is likely other amino acids were also present to further dilute the amino acid additions. For example, after extracting three soils McLain and Martens et al. (2005) found the sum of 18 amino acids to range from 9 to 20 g kg^{-1} of soil.

With the exception of NH_2OH, the near-zero N_2O emissions after applying the nucleophiles to the sterilized soils showed that the N_2O fluxes from soil that was non-inhibited, or had biology partially inhibited, were dominated by biotic processes. This was not the case for NH_2OH where the N_2O flux from the sterilized soil was ~ 28% that of the no inhibition treatment. It has previously been shown that the NH_2OH molecule may decompose abiotically to produce N_2O (Bremner et al. 1980; Heil et al. 2015; Nelson 1982; Terada et al. 2017).

Ignoring the potential dilution effects of other amino acids being present, the lack of any corresponding shifts in the relatively low ^{15}N enrichments of the N_2O evolved from the amino acid treatments, under the various inhibition treatments, suggests fungi were not directly utilising the amino acids for N_2O production. The codenitrification product depends on the redox state of the N-donor, and prior studies have shown amines (-R-NH_2) to be codenitrified to N_2 (Shoun et al. 2012). Thus, the lack of any corresponding shifts in the relatively low ^{15}N enrichments of the N_2O evolved from the amino acid treatments may have also been the result of N_2 being produced. Despite this fungal inhibition reduced amino acid derived codenitrified N_2O (Table 9) indicating that products derived from the amino acid mineralization are involved in fungal codenitrification. The lack of any bacterial inhibition effect on the codenitrification flux demonstrates the dominant role of fungi in codenitrification (Rex et al. 2018).

Increasing ^{15}N enrichment of the N_2O molecule demonstrates that the N_2O-N partially derives from a ^{15}N enriched source. In the case of the NH_2OH, applied with an enrichment of 98 atom% ^{15}N, the highly ^{15}N enriched N_2O emissions demonstrate the applied NH_2OH contributed strongly to the evolved N_2O flux.

Using soil suspensions Spott and Stange (2011) concluded N_2O production from NH_2OH in soil was complex due to the interaction of production pathways involving both abiotic formation and biogenic formation, resulting from both codenitrification and denitrification. Adding the NH_2OH nucleophile to the sterilized soil (abiotic conditions) the ^{15}N enrichment of the N_2O (~ 44 atom%) aligned closely with calculated ^{15}N enrichment of 49 atom% that indicates hybrid N_2O production via abiotic N-nitrosation. The formation of N_2O via NH_2OH reacting with NO_2^- occurs due to abiotic nitrosation processes (Liu et al. 2017a), and has been previously observed in sterilized soils (Heil et al. 2015). NH_2OH has also been reported to decay abiotically to form N_2O with the process slowed down in the presence of NO_2^- (Liu et al. 2017a). However, had this been the main process for N_2O formation the ^{15}N enrichment of the N_2O evolved would have aligned more with the applied NH_2OH ^{15}N enrichment. The combined inhibition treatment significantly reduced the N_2O codenitrification flux by 50% (Table 9) compared to the no inhibition treatment (Table 8) indicating abiotic reactions were also contributing substantially to the observed N_2O flux.

Fungi contributed to N_2O production when NH_2OH was applied, as indicated by the flux reduction under the fungal inhibition treatment, however, the lack of any change in the N_2O-^{15}N enrichment indicates fungal inhibition was not affecting the process generating ^{15}N enriched N_2O. Conversely, the further reduction in both the N_2O flux and N_2O-^{15}N enrichment in the bacterial inhibition and the combined inhibition treatments, showed that the N_2O production process was both inhibited and

that less ^{15}N enriched NH_2OH contributed to the N_2O flux produced. In addition, the codenitrification flux also tended to decline in the presence of the bacterial inhibitor. Bacterial inhibition reduces, amongst others, the activity of AOB and thus (i) reduces the consumption of NH_2OH via bacterial nitrification, (ii) reduces the enrichment of the nitrification products derived from ^{15}N enriched NH_2OH, and thus (iii) reduces the formation of ^{15}N enriched nitrification intermediaries NO_2^- and NO, which have been shown be involved in codenitrification, and which in turn would also have been reduced in concentration leading to lower N_2O fluxes with lower ^{15}N enrichment. Furthermore, had ^{15}N enriched NH_2OH progressed to NO_2^- then any denitrification of this NO_2^- that contributed to the ^{15}N enriched N_2O pool, would also have been reduced or prevented with inhibition of bacterial denitrifiers.

5.4.3 Conclusions

Codenitrification occurs when N-donors, such as those studied here (NH_4^+, glycine, phenylalanine and NH_2OH) react with a nitrosyl compound, to form hybrid N_2O. Using selective microbial inhibition treatments, and simulating a ruminant urine patch environment, we demonstrated that ^{15}N-labelled nucleophiles contribute to codenitrification. Hydroxylamine was the most important nucleophile with respect to increasing the N_2O flux and contributing to codenitrification. The codenitrification N_2O fluxes following amino acid-^{15}N addition were orders of magnitude lower, potentially due to dilution from antecedent amino acids or their break down products. Fungal inhibition significantly reduced amino acid derived codenitrification fluxes. Given the results of this study the in situ dynamics of potential N-donors warrant further detailed investigation, in conjunction with N_2O fluxes, under ruminant urine patches.

Chapter 6
Modelling the influence of soil moisture on N transformation rates from a urea-affected pasture soil

6.1 Introduction

The ability to manufacture synthetic nitrogen (N) fertilizers via the Haber-Bosch process has increased the application of N to grasslands and crops, resulting in the leakage of reactive N from agroecosystems into the atmosphere, and both terrestrial and aquatic ecosystems (Galloway et al. 2003). Nitrous oxide (N_2O), a form of reactive N, is a greenhouse gas and tropospheric concentrations of N_2O continue to increase (Hua et al. 2015; Moss et al. 2010; Pachauri 2016). Furthermore, the N_2O molecule contributes to stratospheric ozone depletion and it is forecast to be the dominant ozone-depleting substance emitted in the 21st century (Ravishankara et al. 2009). Anthropogenic N_2O emissions result predominately from agricultural ecosystems, via animal manures and N fertiliser use (Davidson 2009; IPCC AR5), due to microbial processes predominately utilising ammonium (NH_4^+) and/or nitrate (NO_3^-).

As a consequence, in an effort to find potential mitigation strategies, N_2O has been the focus of intensive research in order to better understand the production and consumption of this gas in agroecosystems (Ball 2013; Smith 2017). Within agricultural grazed pasture ecosystems there occur 'urine patches': as a consequence of ruminant livestock urine deposition the urine-affected pasture soil contains inorganic-N far in excess of the pasture's immediate demands. Over 70% of ruminant urine-N is typically deposited as urea (Dijkstra et al. 2013), which is hydrolysed by the enzyme urease to form ammonium (NH_4^+) and bicarbonate (HCO_3^-) ions (Avnimelech and Laher 1977). Further hydrolysis of the HCO_3^- ions results in the soil pH becoming elevated to values of 8 to 9. If not removed from the soil inorganic-N pool by plant or microbial uptake, ammonia (NH_3) volatilisation, or fixation, the NH_4^+ is subsequently nitrified to form NO_3^-. Under suitable conditions the NO_3^- molecule may be denitrified forming N_2O and/or dinitrogen (N_2). Soil moisture plays a dominant role in determining the oxygen (O_2) status of the soil which in turn regulates the potential rates of the various nitrification and denitrification processes (Wrage-Mönnig et al. 2018).

While many ^{15}N tracing studies have examined NH_4^+ and NO_3^- dynamics within soil most of these have been over a relatively short time period (ca. < 300 hours) and there is a dearth of studies where urea has been the initial substrate, especially at the rates found within ruminant urine patches. In contrast to NH_4^+-based fertilisers, or organic manures, urea has the potential to induce relatively extreme changes in soil chemistry. The rapid and relatively high increase in soil pH following urea deposition has the potential to influence soil inorganic-N dynamics via solubilisation of soil organic matter, the NH_4^+-NH_3 equilibrium, and microbial community structure and function. For

example, Anderson et al. (2018) found that mobilized dissolved organic matter, as consequence of soil pH increase, resulted in increased microbial metabolism: a 25-fold increase of denitrification enzyme activity and increased dissimilatory nitrate reduction were observed, increasing the soil NH_4^+ concentration up to 10 times the initial value. The elevated soil pH (> pH ~7.0) results in the NH_4^+-NH_3 equilibrium favouring NH_3 which, in turn, can affect NO_2^- dynamics and associated N_2O emissions (Breuillin-Sessoms et al. 2017; Venterea et al. 2015).

Thus the objective of this chapter was to examine, by way of modelling, how a urea simulated urine patch (deposition) event at two different moisture levels influenced inorganic-N dynamics and urea-N fate with respect to soil organic-N pools, in order to assess the implications for codenitrification in urea affected pasture soil.

6.2 Materials and Methods

The raw data used for this modelling experiment were derived from a previously published incubation experiment (Clough et al. 2017)[1*], performed at two levels of soil moisture with urea-^{15}N applied to simulate a ruminant urine deposition event. In brief: a Haplic Cambisol soil (54% sand, 31% silt, 15% clay) from the Teagasc Moorepark Research Centre, County Cork, Ireland, was collected (sample depth 5 – 20 cm). This was sieved (≤ 2 mm) and shipped to New Zealand where the soil was repacked in stainless steel rings (7.3 cm inner diameter) to a depth of 4.1 cm in depth and a bulk density of 1.1 Mg m^{-3}. A factorial experiment consisted of two factors: N rate was adjusted to represent a control and a urine patch event (0 and 1000 kg N ha^{-1}, as urea) while soil moisture was adjusted to simulate near saturated and field capacity conditions (-1 kPa and -10 kPa, permanently adjusted using tension tables, corresponding to 53% and 30% volumetric water content, or 91% and 52% water-filled pore space (WFPS), n = 4). On experimental Day 0, 10 mL of a urea solution (42 g urea-N L^{-1}; 50 atm%, Cambridge Isotope Laboratories Inc., USA) was applied to the soil surface of those mesocosms receiving N, controls received equivalent volumes of water. The experiment was performed at 20°C. Following the treatment application, destructive soil chemical analyses for NH_4^+ and NO_3^-, on Day 0, 3, 7, 14, 21, 35 and 63, were performed in order to determine the soil mineral N concentration dynamics as well as the ^{15}N enrichment of each N pool ($^{15}NH_4^+$ and $^{15}NO_3^-$).

6.2.1 Model development

The initial version of the ^{15}N tracing model used in this study was introduced by Müller et al. (2004). This basic model included 4 mineral and 2 organic soil N pools and 9 possible N transformations

[1*] The full publication of Clough et al. (2017) can be found in the appendix, p. 143

(model B). This model was later on extended (Inselsbacher et al. 2013) to a total of 7 N pools (now including plant uptake) and 14 transformations. Since the study of Clough et al. (2017) did not include any plants, the 'plant uptake' pool was excluded and instead the model was extended by adding N pools for urea and NH_3. These pool were connected via 16 possible N transformations, following either zero, first order or Michaelis-Menten kinetics.

Finally, this further extended version, included eight pools: urea, NH_3, NH_4^+, NO_3^-, labile (N_{lab}) and recalcitrant organic nitrogen (N_{rec}) as well as adsorbed/stored NH_4^+ and NO_3^-. Nitrogen losses from the NO_3^- and N_{rec} pool via N_2O and N_2 fluxes were not modelled with the N that would potentially be lost via these fluxes retained in the N_{rec} pool (Fig. 32).

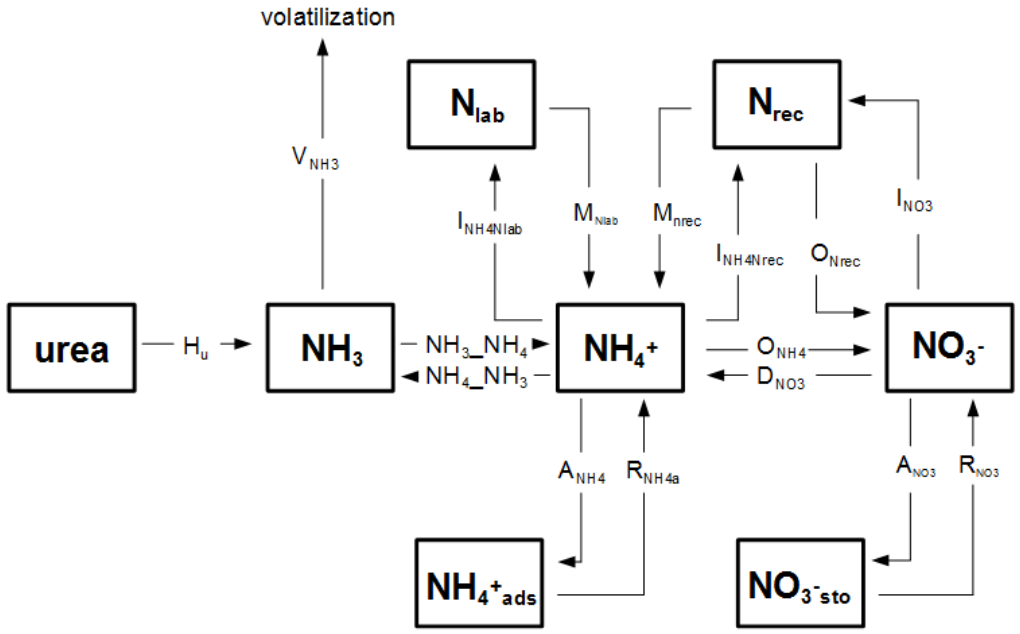

Figure 32. Conceptual model of the urea ^{15}N tracing used in this study to analyse gross N transformation rates. The different N-pools are; N_{lab} = labile soil organic N, N_{rec} = recalcitrant soil organic N, NH_3 = ammonia, NH_4^+ = ammonium, $NH_4^+_{ads}$ = sorbed NH_4^+, NO_3^- = nitrate, $NO_3^-_{sto}$ = stored NO_3^-. The transformation rates are; A = sorption, D = dissimilatory nitrate reduction, H = hydrolysis, I = immobilisation, M = mineralisation, R = release, O = oxidation, V = volatilisation.

6.2.2 Performing model simulations

MatLab (Version 8.6, The MathWorks Inc.) was used for programming. The model was programmed to repeat many runs with slightly changed (= step number) flux rates according to a Monte Carlo (MC) sampling, in order to find the minimum misfit function (= optimal flux adjustment) via trial and error. To restrict the number of misfit calculations, a random walk technique was used here where every step depends on the previous one, illustrating a Markov chain (Metropolis and Ulam 1949). This Markov chain Monte Carlo (MCMC) routine was performed in MatLab with 500-50,000 iterations in order to find the global minimum misfit function without becoming trapped in a local minimum

(Müller et al. 2007). Each iteration creates a new parameter set, governed by a random step width and direction, which is subsequently tested and compared with the previous one. After each model run a misfit-function was calculated in the form of a quadratic error for the calculated and measured values and compared with the previous one. If the misfit was reduced, the new parameter was accepted, if the misfit increased, new values were generated based on a likelihood function (Müller et al. 2007; Rütting and Müller 2008). The algorithm itself was called 'N trace Urea' and was set up in Simulink (Version 6.3, The MathWorks Inc.), a companion software to MatLab. Furthermore, the solver *ode5* was used, one of Simulink's solvers for ordinary differential equations that is based on the Runge-Kutta formula, a formula describing an algorithm procedure for a numerical approximation, according to Müller et al. (2007). The N fluxes within this model were initially set to transformation rates with units of µmol N g^{-1} soil h^{-1}, before being converted to µg N g^{-1} soil d^{-1} for better comparison with the measured values.

Initially, all measured N pool concentrations over time, according to the measured values of Clough et al. (2017), were fitted in the operating spreadsheets. Initially, model test runs with the data of the -1 kPa treatment were performed with relatively few iterations (c.500) and large step numbers (with the difference from one flux rate in a model run to the next automatically adjusted, e.g. ± 0.2 µmol N g^{-1} soil d^{-1}), to identify suitable initial parameters. These initial parameters were used as a preliminary approximation to the global minimum misfit function. The following runs were typically adjusted to 5,000 iterations, 3 sequences and smaller step numbers (e.g. 0.01 µmol N g^{-1} soil d^{-1}) in order to gain the next better approximation for the N flux parameters. For the final runs, which were then were adjusted to 50,000 iterations and step numbers of also 0.01 µmol N g^{-1} soil d^{-1}, these preliminary approximated data were used and the set up repeated with the new best fit parameters. A reduction factor was used describe the difference between the output of all three sequences. This factor compares the within and between variance of the optimization sequences (Rütting and Müller 2008). The optimization procedure was stopped after the adjusted number of iterations were completed and accepted if the reduction factor between the three sequences was below 1.1 for each parameter (meaning that the variance between the sequences almost equals the variance within a sequence for each parameter). Otherwise, another model run with 50,000 iterations was started. Suitable data for the -1 kPa treatment were gained after a total of 18 model runs. These parameters were then used as initial starting parameters for the -10 kPa treatment and the procedure was repeated to estimate transformation rates, leading to suitable result after 10 model runs.

6.2.3 Statistics

Since the optimization procedure used in this study is identical with the one used by Rütting and Müller (2008), it results in a normally distributed probability density function (PDF) for each parameter. Thus, these functions are used for the parameter average calculation in addition to standard deviation and correlation coefficient (Müller et al. 2007). The correlation coefficients of the parameters are only available for N pools with measured data, and were calculated individually for each pool before an average correlation coefficient was used to express the general model fit to all the measured data, resulting in one (average) r^2 value per treatment.
The average and standard deviation of each modelled transformation rate's PDF were used for a direct treatment comparison. Simple student t-tests were then performed in order to determine significant differences. Statistical calculations were performed with Sigma Plot (Version 13.0, Statistical Graphs Inc.).

6.3 Results

6.3.1 NH_4^+ and NO_3^- concentrations and ^{15}N enrichment

Within the -1 kPa treatment, the measured data showed a rapid increase in soil NH_4^+ subsequent to the urea application, up to 1757 ± 457 µg NH_4^+-N g^{-1} soil, after 78 h, followed by a swift decrease, to 1354 ± 206 µg NH_4^+-N g^{-1} after 174 h and thereafter a slow almost linear decrease, reaching 349 ± 114 µg NH_4^+-N g^{-1} after 1518 h (Fig. 33, a). The NO_3^- concentration increased more slowly within the first 174 h, to reach 67.7 ± 22.9 µg NO_3^--N g^{-1} before peaking at 429.2 ± 76.5 µg NO_3^--N g^{-1} after 846 h and subsequently decreasing to 219.8 ± 73.2 µg NO_3^--N g^{-1} after 1518 h (Fig. 33, e).
The NH_4^+-^{15}N enrichment increased almost immediately following urea deposition to equal 43.5 ± 0.7 atm% within the first 6 h, where after it declined to be ca. 39.6 ± 0.6 atm% at the conclusion of the experiment (Fig. 33, c). Increases in the NO_3^--^{15}N enrichment occurred more slowly reaching a maximum of 39.7 ± 1.8 atm% after 342 h and remaining relatively constant until the end of the experiment.

Following the urea application at -10 kPa, the pattern of increasing NH_4^+ concentration followed that observed in the -1 kPa treatment, increasing to 1730 ± 168 µg NH_4^+-N g^{-1} after 174 h before decreasing at 342 h prior to a slow, linear decrease towards 809 ± 22 µg NH_4^+-N g^{-1} by the end of the experiment at 1518 h (Fig. 33, b). The concentration of the NO_3^- increased from a background level of 44.8 ± 7.7 µg NO_3^--N g^{-1} to only 74.9 ± 29.4 µg NO_3^--N g^{-1} within the first 510 h, followed by a rapid increase to 335.0 ± 18.3 µg NO_3^--N g^{-1} after 846 h to finally reach 377.8 ± 21.8 µg NO_3^--N g^{-1} after 1518 h (Fig. 33, f). The NH_4^+-^{15}N enrichment increased in a similar manner to that observed in the -1

kPa treatment, rapidly to 44.5 ± 0.3 atm% after only 6 h to finally be 37.4 ± 0.9 atm% after 1518 h (Fig. 33, d). Unlike the -1 kPa treatment, the NO_3^--^{15}N enrichment constantly increased. However, the rate of increase in the ^{15}N enrichment slowed down with time reaching a final enrichment of 34.2 ± 1.3 atm% after 1518 h (Fig. 33, h).

Running the N trace model described above resulted in a set of interdependent gross N transformation rates for each treatment. Calculating the N concentrations for each N pool (Fig. 32) based on these gross rates over time resulted in a modelled N pool development over time. In the case of NH_4^+-N, NO_3^--N, NH_4^+-^{15}N and NO_3^--^{15}N this modelled concentration was compared with the measured data at the end of each model run iteration, the regression coefficient of the final run was used to estimate the model fit. Comparing the measured and modelled NH_4^+ and NO_3^- concentrations and their respective enrichments a final regression coefficient of $r^2 = 0.999$ was found for the -1 kPa treatment and $r^2 = 0.998$ for the -10 kPa treatment, indicating a good model fit for both treatments.

At -1 kPa the model tracked well the NH_4^+ concentration throughout the experiment but this was not the case for the soil NO_3^- concentration. The NO_3^- concentration was modelled as linearly increasing over time and over the first 510 hours the model tracked the soil NO_3^- concentration well but overestimated the value at 846 h and then underestimated the value at 1519 h (Fig. 33, e). However, the modelled ^{15}N enrichments of NH_4^+ and NO_3^- were in good agreement with the measured values (Fig. 33, c, g).

For the -10 kPa treatment, the modelled concentration of NH_4^+-N over time and the NH_4^+ ^{15}N enrichment were again in good agreement with the measured data (Fig. 33, b, d), however, the modelled rates for the NO_3^- concentration and NO_3^- ^{15}N enrichment lead to a less precise output (Fig. 33, f, h). Again the model showed NO_3^--N concentrations increasing in a linear manner resulting in an overestimate from 510-846 h and an underestimate from 846 h onwards (Fig. 33, f). The modelled NO_3^- ^{15}N enrichment followed the measured trend in NO_3^- ^{15}N enrichment well, but as time progressed the model increasingly underestimated the NO_3^- ^{15}N enrichment (Fig. 33, h).

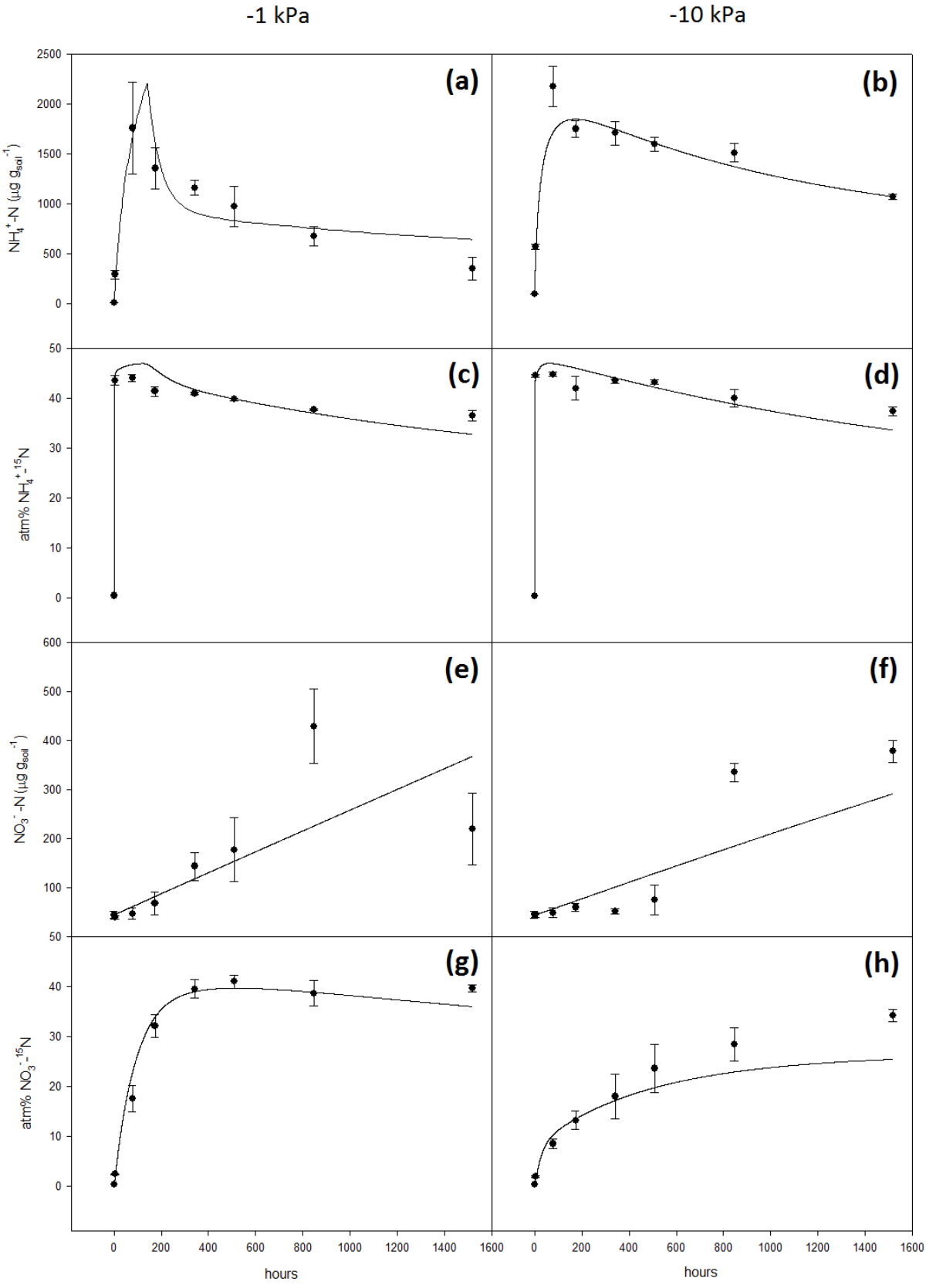

Figure 33. Measured concentrations and ^{15}N enrichments of the soil NH_4^+ and NO_3^- pools over time. Symbols represent the mean measured values ((n = 4) ± standard deviation, and the solid lines represent the modelled values (both treatments; $r^2 > 0.99$).

6.3.2 Modelled N transformation rates

The modelled urea hydrolysis rate (H_u) averaged 75 µg N g^{-1} d^{-1} for both soil moisture treatments (Table 10). However, this rate was initially much higher during the first 200 h and significantly different between the treatments ($p < 0.001$), starting at 4672 µg N g^{-1} d^{-1} and 1579 µg N g^{-1} d^{-1} for the -1 kPa and -10 kPa treatments, respectively, followed by a rapid decrease to almost 0 after 220 h at -1 kPa, but taking more than twice this time (591 h) to decrease to 0 at -10 kPa. (Fig. 34, a, b).

Following urea hydrolysis NH_4^+ is formed and the ensuing high soil pH creates a chemical equilibrium between the NH_4^+ and NH_3 pools. While the daily gross N transformation rates for NH_3-NH_4^+ (NH3_NH4) and NH_4^+-NH_3 (NH4_NH3) were not statistically significant due to soil moisture treatment (Table 10) the trend was for these rates to be higher under the -10 kPa treatment (Fig. 34, a, b). An equilibrium between NH_3-NH_4^+ and NH_4^+-NH_3 occurred at ca. 200 h (150 µg N g^{-1} d^{-1}) at -1 kPa with the rate decreasing thereafter to 110 µg N g^{-1} d^{-1} at 1519 h. In the -10 kPa treatment, this equilibrium was reached after 536 h at a higher exchange rate of 340 µg N g^{-1} d^{-1} before this also slowly decreased to 281 µg N g^{-1} d^{-1} at the end of the experiment (Fig. 34, a, b).

The average modelled volatilisation rates (V_{NH3}) did not differ with soil moisture (Table 10) but were higher under the -1 kPa treatment over the first 100 h (Fig. 34, e, f).

In both treatments, the best model fit was obtained when the sorption and release rates for stored NO_3^- were set to 0, a possible $NO_{3\,sto}^-$ pool (Fig. 32) was therefore not considered further.

Modelling NH_4^+ sorption (A_{NH4}) and NH_4^+ release (R_{NH4}) showed higher rates of A_{NH4}, over the first 200 h in the -1 kPa treatment compared with the R_{NH4}, peaking at 651 µg N g^{-1} d^{-1} at 141 h before decreasing, while R_{NH4} increased slowly over this time, reaching an equilibrium with A_{NH4} after 312 h at 280 µg N g^{-1} d^{-1} (Fig. 34, a). The modelled values of A_{NH4} and R_{NH4} were much higher in the -10 kPa treatment throughout the experimental period, with the A_{NH4} peaking after 170 h at 1168 µg N g^{-1} d^{-1} and R_{NH4} reaching the same level 100 h later (Fig. 34, b). The average A_{NH4} rate over time was observed to be 258.67 ± 65.20 µg N g^{-1} d^{-1} for the -1 kPa treatment and significantly higher within the -10 kPa treatment with 889.83 ± 316.78 µg N g^{-1} d^{-1}. A similar significant different output was modelled for the average R_{NH4} rates, 225.70 ± 48.25 µg N g^{-1} d^{-1} for the -1 kPa treatment and 867.74 ± 278.68 µg N g^{-1} d^{-1} for -10 kPa (Tab. 10).
A similar pattern was given by the model for the immobilization of NH_4^+ into the labile N pool ($I_{NH4Nlab}$) and mineralisation of N from the labile N pool (M_{Nlab}). These fluxes were closely linked but were constantly higher in the -10 kPa treatment (> 400 µg N g^{-1} d^{-1}) than in the -1 kPa treatment (< 80 µg N g^{-1} d^{-1}) (Table 10; Fig. 34, c, d).

The mineralization of recalcitrant N (M_{Nrec}) was constant, and significantly higher ($p < 0.001$) in the -1 kPa treatment at 40.5 µg N g^{-1} d^{-1} compared with a constant rate of 13.8 µg N g^{-1} d^{-1} in the -10 kPa treatment (Table 10, Fig. 34, d). The reverse flux, the immobilization of NH_4^+ into the recalcitrant N pool ($I_{NH4Nrec}$) N_{rec} pool was slightly higher than M_{Nrec} but not significantly different with mean rates of 67.7 and 72.2 µg N g^{-1} d^{-1}, in the -1 kPa and -10 kPa treatments, respectively (Table 10). At -1 kPa, in contrast to the M_{Nrec} rate, the rate of $I_{NH4Nrec}$ peaked after a rapid increase, at 141 h to be 170 µg N g^{-1} d^{-1} before decreasing to a stable rate of 65 µg N g^{-1} d^{-1} after 400 h (Fig. 34, c). At -10 kPa treatment the $I_{NH4Nrec}$ rate only peaked at 95 µg N g^{-1} d^{-1} after 170 h, and decreased at a slower rate to equal 53 µg N g^{-1} d^{-1} by the end of the study (Fig. 34, d).

The modelled rates for oxidation of recalcitrant N (O_{Nrec}), immobilisation of NO_3^- (I_{NO3}), oxidation of NH_4^+ (O_{NH4}) and dissimilatory reduction of NO_3^- (D_{NO3}) were all constant over the experimental period and were always higher (Table 10) in the -10 kPa treatment (34, 10, 9 and 28 µg N g^{-1} d^{-1}, respectively) when compared with the -1 kPa treatment (0.03, 0.5, 11 and 6 µg N g^{-1} d^{-1}, respectively). However, the NH_4^+ oxidation rate (O_{NH4}) although constant, did not differ due to soil moisture treatments (Table 10).

Within the -1 kPa treatment, a combined average gross transformation rate of 114.93 (± 43.43) µg N g^{-1} d^{-1} was determined for NH_4^+ being removed from the NH_4^+ pool ($I_{NH4Nrec}$, $I_{NH4Nlab}$ and O_{NH4}), while the combined gains from mineralisation and DNRA (M_{Nlab}, M_{Nrec} and D_{NO3}) equalled 82.79 (± 21.19) µg N g^{-1} d^{-1}. This resulted in a net flux out of the NH_4^+ pool of 32.14 µg N g^{-1} d^{-1}.

At -10 kPa the respective combined fluxes were 654.05 (± 314.25) µg N g^{-1} d^{-1} for NH_4^+ removal and 613.6 (± 124.95) µg N g^{-1} d^{-1} for gains of NH_4^+, resulting in a net flux rate out of the NH_4^+ pool of 40.45 µg N g^{-1} d^{-1}.

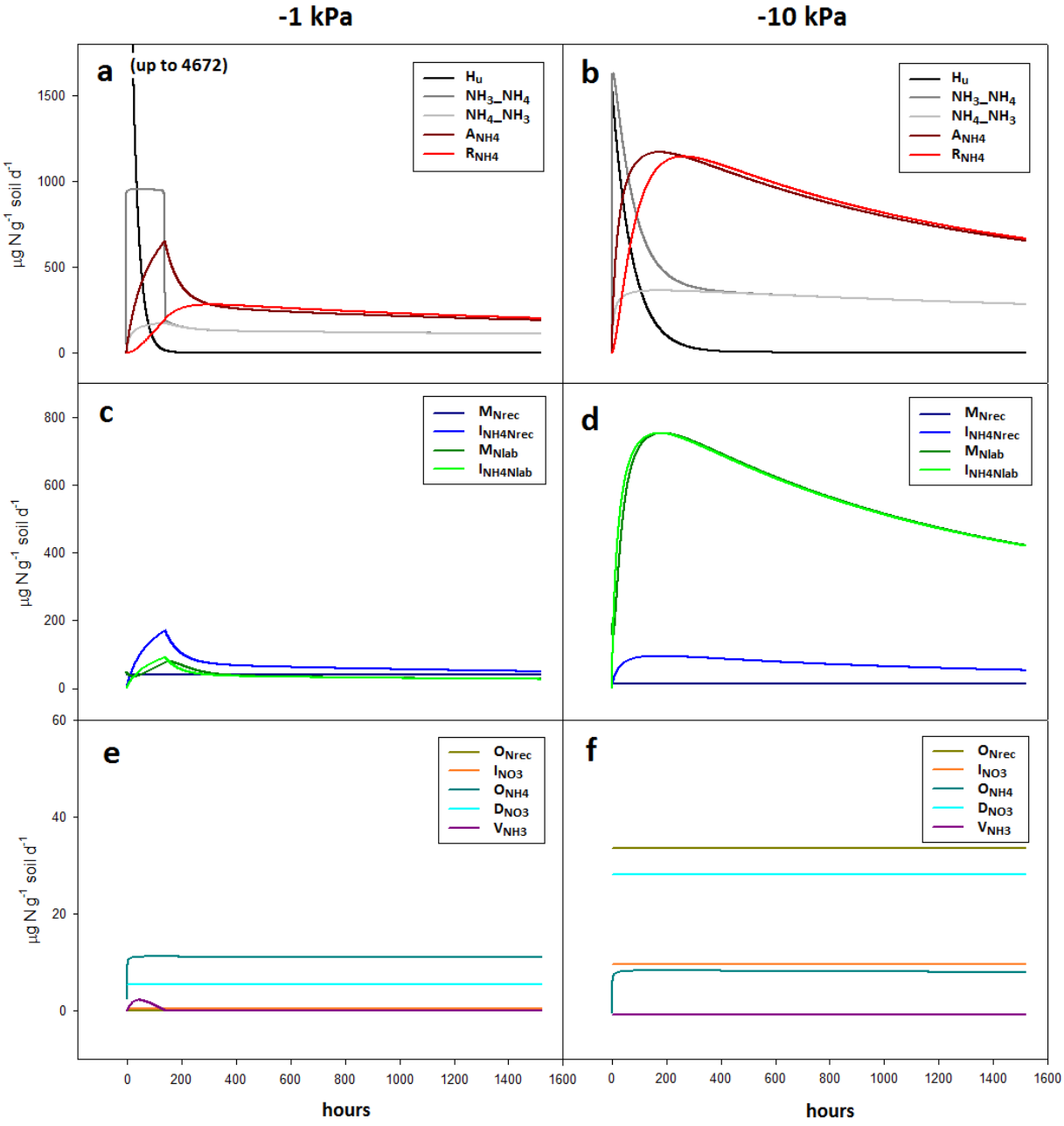

Figure 34. Modelled N transformation rate dynamics over the experimental duration. The transformation rates are; H_u = urea hydrolysis, $NH_3\_NH_4$ = conversion of NH_3 to NH_4^+, $NH_4\_NH_3$ = conversion of NH_4^+ to NH_3, A_{NH4} = mineral sorption of NH_4^+, R_{NH4} = release of adsorbed NH_4^+, M_{Nrec} = mineralization of recalcitrant N, $I_{NH4Nrec}$ = immobilisation of NH_4^+ into recalcitrant N, M_{Nlab} = mineralisation of labile N, $I_{NH4Nlab}$ = immobilisation of NH_4^+ into labile N, O_{Nrec} = oxidation of recalcitrant N, I_{NO3} = immobilization of NO_3^- into recalcitrant N, O_{NH4} = oxidation of NH_4^+ to NO_3^-, D_{NO3} = dissimilatory NO_3^- reduction (DNRA), V_{NH3} = volatilization of NH_3.

Table 10. Average modelled N transformation rates for the two soil moisture treatments (n = 3)

N transformation	final kinetics	Treatment -1 kPa rate in µg N g^{-1} d^{-1}	-10 kPa rate in µg N g^{-1} d^{-1}	difference (t-test)	P
M_{Nrec}	0	40.50 ± 2.07	13.83 ± 8.72	**	0.001
$I_{NH4Nrec}$	1	67.69 ± 13.23	72.16 ± 3.27	n.s.	
M_{Nlab}	1	36.74 ± 18.09	571.36 ± 105.86	***	< 0.001
$I_{NH4Nlab}$	1	36.15 ± 29.02	572.97 ± 309.42	*	0.014
O_{Nrec}	0	0.03 ± 0.02	33.70 ± 9.66	***	< 0.001
I_{NO3}	0	0.46 ± 0.35	10.31 ± 2.56	***	< 0.001
O_{NH4}	2	11.09 ± 1.18	8.92 ± 1.56	n.s.	
D_{NO3}	0	5.55 ± 1.03	28.41 ± 10.37	**	0.005
A_{NH4}	1	258.67 ± 65.20	889.83 ± 316.78	**	0.008
R_{NH4a}	1	225.70 ± 48.25	867.74 ± 278.68	**	0.004
A_{NO3}	1	0	0	n.s.	
R_{NO3}	1	0	0	n.s.	
H_u	1	75.33 ± 82.15	75.33 ± 6.06	n.s.	
V_{NH3}	1	0.13 ± 0.08	0.01 ± 0.00	n.s.	
NH_3_NH_4	2	198.96 ± 66.76	396.51 ± 169.82	n.s.	
NH_4_NH_3	2	123.76 ± 76.86	321.19 ± 354.62	n.s.	
NH_4^+ removal ($I_{NH4Nrec}$, $I_{NH4Nlab}$ and O_{NH4})		114.93 ± 43.43	654.05 ± 314.25	n.a.	
NH_4^+ gains (M_{Nlab}, M_{Nrec} and D_{NO3})		82.79 ± 21.19	613.60 ± 124.95	n.a.	
Net NH_4^+ removal		32.14	40.45	n.a.	

Level of significance: n.s. = not significant, n.a. = not applicable, * <0.05, **<0.01, ***<0.001

6.3.3 N pool dynamics

The gross modelled rates (Fig. 34, Table 10) were used to plot the development and dynamics of the N-pools (excluding the $NO_3^-{}_{sto}$ pool) as depicted in Figure 35.

After 200 h the urea applied (4768 µg N g^{-1} at 0 h) was almost completely hydrolysed with most of the urea-N present as either freely available (NH_4^+) or adsorbed ($NH_4^+{}_{ads}$, Fig. 35, a, b). At -1 kPa the concentration of the free NH_4^+-N pool reached its maximum of 2203 µg N g^{-1} between 100 - 150 h (1458 µg N g^{-1}, for the -10 kPa treatment) with the peak in $NH_4^+{}_{ads}$ following 150 h later; 2908 µg N g^{-1} in the -1 kPa treatment and 2411 µg N g^{-1} in the -10 kPa treatment. At the same time, the modelled NH_3 pool remained at < 8.5 µg N g^{-1} and < 0.5 µg N g^{-1} for the -1 kPa and the -10 kPa treatments,

respectively (Fig. 35, a, b). At -1 kPa, despite the constant decrease of free NH_4^+-N, 43.8% of the applied N remained in this pool after 1519 h (29.3% for the -10 kPa) with a ^{15}N enrichment of 34.4 atm% and 29.3 atm% for the -1 kPa and -10 kPa treatments, respectively (Fig. 36).

Modelling showed the N_{lab} pool to be consistently< 150 µg N g^{-1} in the -1 kPa treatment and < 350 in the -10 kPa treatment, despite the high immobilization and mineralization rates (Fig. 35, c, d, Table 10). The N_{lab} pool in the -1 kPa treatment peaked prior to 200 h and then continued to decline over time, while in the -10 kPa treatment 2.1% of the applied N was retained in this pool, with a ^{15}N enrichment of 33.7 atm% (Fig. 36), due to a higher initial pool, that again peaked at 200 h even though it declined at a faster rate (Fig. 35, c, d).

The size of the N_{rec} pool was initially set at 4116 µg N g^{-1} (background) and this increased to 5084 µg N g^{-1} (-1 kPa) and 4934 µg N g^{-1} (-10 kPa) within the first 400 h before the rate of increase slowed in both soil moisture treatments. By the end of the experiment (1519 h), the N_{rec} pool had reached 5864 µg N g^{-1} in the -1 kPa treatment and 6326 µg N g^{-1} in the -10 kPa treatment (Fig. 35, a, b), representing 36.7% (22.2 atm%) and 46.4% (23.7atm%) of the applied N, for the -1 and -10 kPa treatments, respectively (Fig. 36).

The model estimated that the soil NO_3^- concentration increased in a linear manner as described above (Fig. 33, e, f) and this resulted in the NO_3^- N pool at 1519 h equating to 6.8% of the N applied being transformed at -1 kPa and 5.1% at -10 kPa treatment, respectively, with respective ^{15}N enrichments of 36.0 atm% and 25.4 atm%. The model predominately assigned the applied N to the NH_4^+, $NH_4^+{}_{ads}$ and N_{rec} pools, despite the latter already having a high initial concentration (Fig. 36).

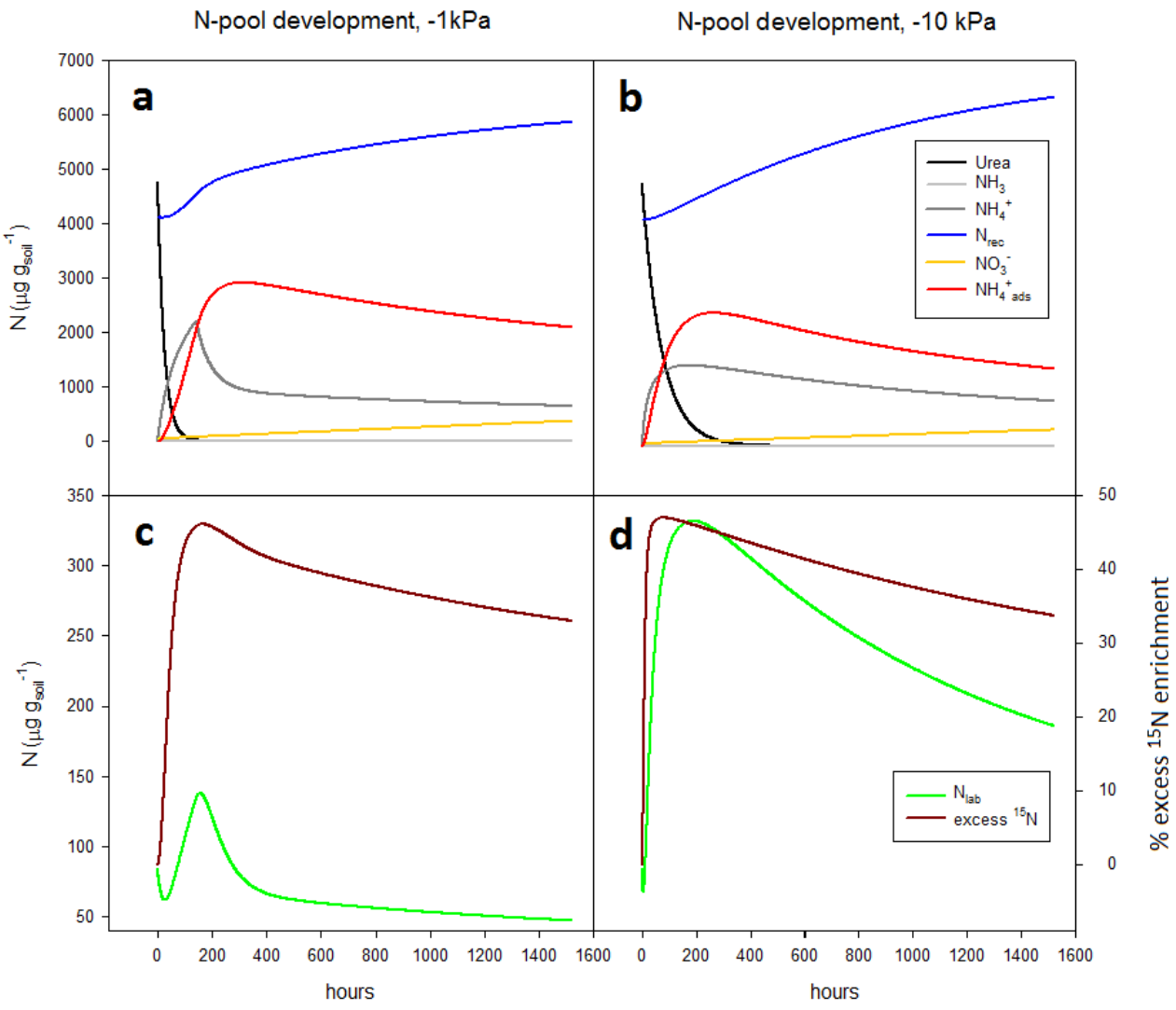

Figure 35. The modelled development of different N pools over time for the (a, c) -1 kPa treatment and (b, d) -10 kPa treatment. The concentrations of urea-N, NH_3-N, NH_4^+-N, N_{rec}-N, NO_3^--N and $NH_4^+{}_{ads}$-N (a, b), the labile N (N_{lab}) pool in combination with its ^{15}N enrichment (c, d) is shown on a separate axis due to its smaller magnitude.

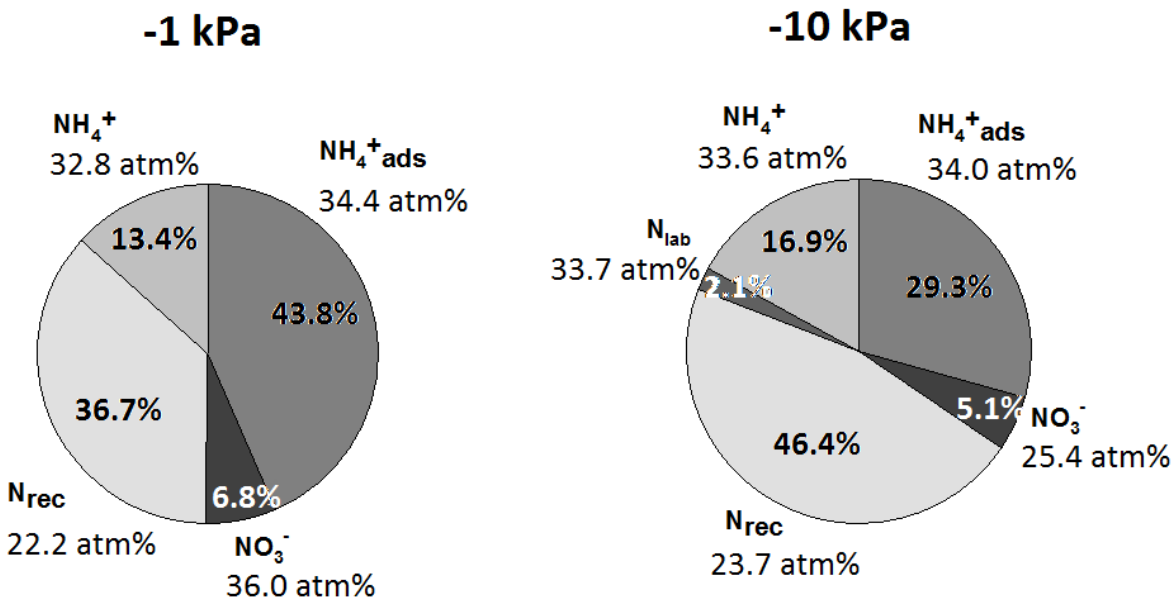

Figure 36. The modelled final distribution of the applied urea-N in % of N remaining in the soil and atm% of 15N enrichment, after the 1519 h incubation.

6.4 Discussion

6.4.1 Model evaluation

As depicted in Figure 33, the modelled values were generally closely aligned with the measured data values. This was especially true for soil NH_4^+ concentrations. The discrepancies between modelled and fitted values were greater, after 500 h, for the soil NO_3^- concentrations and the ^{15}N enrichment of the NO_3^- at -10 kPa. At 846 h, for both -1 and -10 kPa, and at 1519 h under the -10 kPa treatment the model tended to underestimate the soil NO_3^- concentration indicating that either the N transformations resulting in the modelled removal of NO_3^- were over estimated at these times, or that the N transformations resulting in soil NO_3^- increases were under estimated. Under estimates of the soil NO_3^- concentration at -10 kPa were possibly due to underestimating contributions from ^{15}N enriched sources as indicated by the model's increasing tendency to under estimate the measured ^{15}N enrichment of the NO_3^- pool over time (Fig. 33).

A critical N pool partaking in soil N transformations, not included in the current ^{15}N tracing model, is the nitrite (NO_2^-) pool through which NH_4^+-N must pass to form NO_3^- via nitrification. Clough et al. (2017) measured the presence of NO_2^- between 300 – 700 h with peak NO_2^--N concentrations of ~40 µg NO_2^--N g^{-1} and ~80 µg NO_2^--N g^{-1} in the -1 kPa and -10 kPa treatments, respectively, at 504 h. Soil NO_2^- had declined to background values by 850 h. Given that the model predicted very well the NH_4^+ pool size and its ^{15}N enrichment under both soil moisture treatments it indicates the flux parameter

values, for fluxes into and out of the NH_4^+ pool were well optimised, and that perhaps the flux parameters for D_{NO3}, O_{Nrec} and I_{NO3} require further optimisation to improve the modelled NO_3^--^{15}N enrichment.

Given that the model underestimates NO_3^- after the observed appearance of NO_2^- (Clough et al. 2017) it would be interesting to further compartmentalise the model to include the NO_2^- pool, a compound known to be highly reactive and transient. In situ soil NO_2^- concentrations following ruminant urine deposition have been reported to peak shortly before the NO_3^- concentrations increase (Clough et al. 2017; Clough et al. 2009). In practice oxidation of NH_4^+ to NO_3^- is generally acknowledged to be facilitated by two sequential enzymatic steps and so rather than assuming a constant oxidation rate of NH_4^+ (O_{NH4}) an improvement between the measured and modelled NO_3^- concentrations (-1 and -10 kPa) and the NO_3^--^{15}N enrichment (-10 kPa) might occur if O_{NH4} was further developed to also reflect NO_2^- oxidation, and it is recommended that further study is performed to link the current model with the ^{15}N trace model of Rütting and Müller (2008) who have previously modelled NO_2^- dynamics.

Conversely, at 1519 h under the -1 kPa treatment the model overestimated the soil NO_3^- concentration. It is most likely the modelled N transformations, at -1 kPa at 1519 h, underestimated soil NO_3^- removal via denitrification reactions, since these were not separately modelled. The moisture content would have favoured denitrification and the measured soil NO_3^- concentration had actually declined since 846 h. Clough et al. (2017) stated the N_2 losses from the soils in this experiment via codenitrification and denitrification as being 10 and 2% of N applied for the -1 kPa and -10 kPa treatment, respectively.

Apart from the discrepancies with NO_3^- and its ^{15}N enrichment the modelled output fitted the data well ($r^2 > 0.99$) and provides useful information on N pool dynamics and their potential roles in codenitrification.

6.4.2 Effect of soil moisture on N transformations following urea deposition

While the gross average hydrolysis rate did not differ with soil moisture (Table 10) there were differences in the daily rate with a higher initial rate at -1 kPa which resulted in a shorter duration for urea hydrolysis at this moisture content (Fig. 34). Urea hydrolysis generally proceeds rapidly following urea deposition to soils unless the environment is too dry (Ernst and Massey 1960), which was not the case in this study. Exactly why a greater rate of urea hydrolysis occurred under the wetter soil conditions is not immediately apparent, given both soil moisture treatments are equal to

or in excess of field capacity. It may have occurred as a result of differences in the spatial distribution of the urea solution applied and the ensuing hydrolysis kinetics that resulted.

Gross average rates of NH_3_NH_4 and NH_4_NH_3 were again similar but the daily transformation rates revealed a different story with the soil with greater air-filled porosity, at -10 kPa, taking longer to reach equilibrium between NH_4^+ and NH_3. In the pH data reported for this study (Clough et al. 2017) it was observed that the soil pH was higher for longer at -10 kPa and it was speculated upon that this indicated that nitrification, a N transformation process resulting in enhanced soil acidity, was potentially delayed due to NH_3 toxicity affecting NO_2^- oxidisers. The daily transformation results modelled here for NH_3_NH_4 and NH_4_NH_3, with a longer period required for equilibrium and a higher rate of NH_4_NH_3 lend support to this theory.

Interesting was the effect of soil moisture on the rates of NH_4^+ adsorption and release, A_{NH4} and R_{NH4}, respectively, both of which were higher under the drier -10 kPa treatment. Murphy et al. (1997) showed that when injecting ^{15}N labelled NH_3 into soil that ^{15}N labelled NH_4^+ was readily formed. Water-filled pore space at -1 and -10 kPa were 91 and 52%, respectively (Clough et al. 2017). Thus any NH_3 gas formed would have had a greater opportunity to diffuse through the soil and form NH_4^+, prior to NH_4^+ adsorption, in the -10 kPa treatment. Consistent with this idea is the modelled adsorption of NH_4^+ preceding the commencement of NH_4^+ release in the model which is consistent with NH_3 first being distributed within the soil and adsorbed as NH_4^+ prior to its release.

The NH_3 molecule may also be fixed by soil organic matter (Nommik and Vahtras 1982). A key feature of ruminant urine deposition, simulated here by urea, is the elevated pH that ensues and which results, not only in NH_3 production, but which also leads to enhanced dissolution of organic matter. The dissolved organic carbon (DOC) concentrations in the study were three orders of magnitude higher under the applied urea and generally more than twice as high under the -10 kPa treatment (Clough et al. 2017). Elevated DOC concentrations in the -10 kPa treatment were thought to be a consequence of the urea solution applied contacting a larger volume of soil as it infiltrated further into the drier soil at -10 kPa (Clough et al. 2017).

The dissolution of soil organic matter and the subsequent formation of the DOC pool and its dynamics may also assist in interpreting the observed dynamics of the labile and recalcitrant N pools. For example, the higher and more prolonged rates of A_{NH4} and R_{NH4}, may have been a function of the interaction between NH_3 and DOC. Also conducive to a higher NH_3 fixation rate at -10 kPa by DOC was the elevated O_2 supply. The fixation of NH_3 under alkaline conditions requires the uptake of O_2 (Broadbent et al. 1960; Nommik and Vahtras 1982; Nommik and Nilsson 1963) and so at -10 kPa the

greater air-filled pore space and relative gas diffusivity would have facilitated O_2 diffusion and this may have further assisted NH_3 fixation by DOC or other forms of organic matter in the soil.

It has been reported that not all the NH_3 that may be fixed onto soil organic matter is readily returned, chemically or biologically, to the soil solution (Flaig 1960; Mortland and Wolcott 1965; Nommik and Vahtras 1982). Thus if NH_3 fixation occurred then it is also possible that ^{15}N entered the recalcitrant N pool. This might have happened due to polymerization of aromatic compounds reacting with NH_3 (Broadbent and Stevenson 1966) or due to substitution reactions leading to the formation of secondary and tertiary amines or N heterocyclic (Fig. 37).

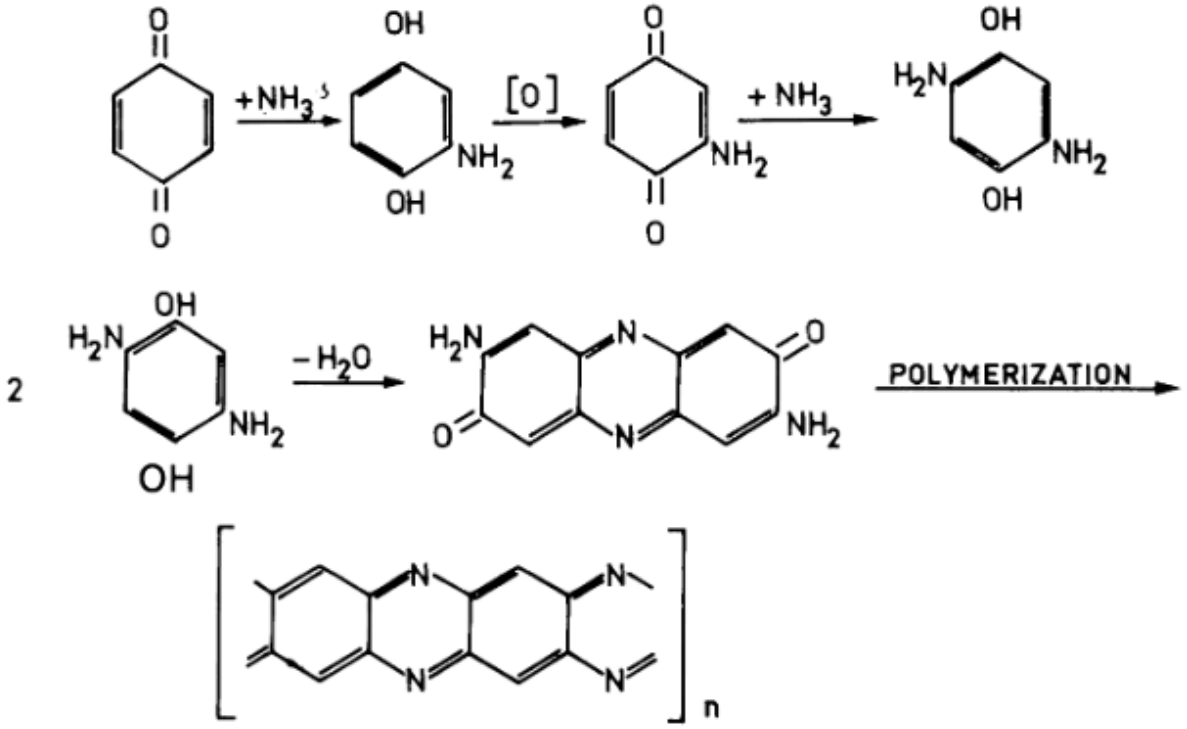

Figure 37. An example of an NH_3 fixation mechanism involving *p*-quinone (Broadbent and Stevenson 1966)

Thus, the model's immediate increase in the N_{rec} pool and the resulting high fraction of ^{15}N residing in the N_{rec} pool at the end of the experiment may be a consequence of NH_3 fixation occurring within the first 200 h. Future studies, under urine patch events should examine this potential interaction.

Previous studies using ^{15}N labelled urea and intact soil have reported significant amounts of ^{15}N to be retained in the soil organic matter pool after many months, where subsequently a slow depletion rate might be assumed as reported for humic compounds. Using the same rate of applied N (1000 kg N ha^{-1} as urine, containing ^{15}N labelled urea), in a lysimeter study containing the identical soil as used in the current modelling study, Selbie et al. (2015) recovered 23-33% of the applied ^{15}N in the soil after one year. The higher recovery occurred in a treatment containing dicyandiamide (DCD), a nitrification inhibitor. It has been postulated that DCD may enhance NH_3 presence, and or losses. But use of DCD could potentially also enhance fixation of NH_3 as postulated above, and this may explain the higher recovery found by Selbie et al. (2015). Clough et al. (1998) found that after 406 days 21-24% of ^{15}N labelled urea was recovered under urine patches with variation due to different soil textures. While Fraser et al. (1998) found that even after a year 20% of the initially applied N (^{15}N labelled urea in urine at 500 kg N/ha) remained in the soil organic matter pool. Given these previous results showing significant ^{15}N recoveries in the soil organic matter pool after considerable periods of time, and the modelled increase in the Nrec pool following urea application future consideration must be given to the role that NH_3 plays in developing this long term pool of urea derived-N.

Dissolved organic matter may also contain labile nitrogen (N_{lab}) which may consist of amino acids, amino sugars, DNA/RNA fragments, and compounds with microbially accessible N. Such products may occur as the result of cell lysis. Following urea application, in the same incubation experiment, Samad et al. (2017)[2*] observed an increasing DNA abundance for some bacterial groups (e.g. *Bacteriodetes, Firmicutes*) but there was also, simultaneously, a decrease in the DNA abundance of other microbial groups (e.g. the Phyla Thaumarchaeota and Verrucomicrobia) could contribute to the labile biomass (N_{lab}) via cell lysis.

Thus, besides the potential NH_3 reactions with DOC increasing the N_{rec} pool it is also possible that NH_3 reacted with DOC to form constituents of the N_{lab} pool as indicated by the rapid ^{15}N enrichment increase. This might happen due to physical or chemical sorption. Physical sorption, such as the formation of H-bounds with O or OH group containing molecules [Eq. 21,22] (James and Harward 1964) or the replacement of water molecules in complex molecule structures around metal ions (M) [Eq. 23] (Mortland 1966) might form microbially accessible N compounds. Chemical sorption, such as the reaction of NH_3 with protons provided from OH groups, associated with silicon on the edges of clay minerals [Eq. 24] (Mortland 1966), might also be seen as labile N, although a clear distinction between fixation and adsorption processes cannot be considered with the current N trace model.

[2*] The full publication of Samad et al. (2017) can be found in the appendix, p. 156

$$NH_3 + OX \leftrightarrow NH_3 \cdots OX \quad [21]$$

$$NH_3 + HOX \leftrightarrow NH_3 \cdots HOX \quad [22]$$

$$M(H_2O)_nX + n\,NH_3 \leftrightarrow M(NH_3)_nX + n\,H_2O \quad [23]$$

$$\equiv Si - OH + NH_3 \leftrightarrow \equiv Si - O - NH_4 \quad [24]$$

Ammonia may also react with quinones as mentioned above, and this may be considered as labile N until polymerisation occurs. A wide range of humus compounds may contribute to the formation of labile N, since they contain required OH groups. Still many of those compounds have not been sufficiently characterized and exact reaction pathways remain unclear (Kalbitz et al. 2000).

Thus, the sudden decrease in the N_{lab} pool in the -1 kPa treatment, and its rapid ^{15}N enrichment (Fig. 35, c), within the first 100 h may have been the result of NH_3 and/or NH_4^+ reacting with constituents of the N_{lab} pool. The subsequent increase in the N_{lab} pool, at -1 kPa, and which peaked at ca. 200 h, may have occurred as the result of NH_3 reacting with DOC, as was also observed in the -10 kPa treatment over this period. After ca. 200 h the N_{lab} pool stoped increasing in the - 1 kPa treatment and declined in a similar manner to the NH_4^+ pool, which was thought to happen earlier in the -1 kPa treatment due to nitrification commencing sooner than in the -10 kPa treatment. As a consequence less NH_3 forms, likely resulting in a decline in the build-up of the N_{lab} pool as a consequence of less NH_3 being available to react with DOC. Conversely, at -10 kPa where the NH_3 was more freely able to diffuse through the soil there will have been greater opportunity for N_{lab} pool creation via possible reactions with DOC [Eq. 21 - 24] and this may explain the larger N_{lab} pool at -10 kPa.

In addition, soil conditions at -1 kPa favour denitrification processes and the reduction in the N_{lab} pool at -1 kPa that commenced at ca. 200 h also coincides with the observed increase in soil NO_2^- (Clough et al. 2017) and so it is perhaps possible that the N_{lab} pool also diminished as a result of the N_{lab} pool constituents acting as nucleophiles in codenitrification processes, especially if NO_2^- was further transformed to produce NO (see Fig. 6). While NO_2^- was also present at -10 kPa there would have been less opportunity for NO formation via denitrification due to the better aerated soil.

More study of the potential interactions between NH_3 and DOC constituents is clearly required to better interpret trends observed in the N_{lab} and N_{rec} pools.

The DNRA flux was modelled to be both constant and higher within the more aerobic moisture treatment (-10 kPa). This initially appears to be inconsistent with the literature given that DNRA has been reported to occur under anaerobic conditions (Tiedje 1988). However, Fazzolari et al. (1998)

demonstrated that DNRA activity was less sensitive than denitrification to the inhibitory effect of O_2 and concluded that carbon was the main driving factor regulating NO_3^- distribution between denitrification and DNRA. Alternatively, Friedl et al. (2018) reported that a change in redox potential, the result of perennial pastures containing high labile C and wetting events reducing soil redox, to be the driver of shifting patterns of NO_3^- consumption between denitrification and DNRA. Anderson et al. (2018) found that increasing the soil pH to simulate the soil pH under ruminant urine conditions with KOH, in the absence of additional N substrate, under anaerobic conditions, also resulted in increases in DOC and changes in the microbial community: there was a large increase in Firmicutes (including *Bacillus*, *Paenibacillus*, *Clostridium* and *Alkaliphilus* spp.) that also corresponded with an increase in potential denitrification enzyme activity potential. Anderson et al. (2018) also reported that cultured representatives of selected Firmicutes were able to produce NH_4^+, and inferred through the use of culture studies their ability to perform DNRA. Microbial data from Samad et al. (2017) also revealed a sustained increase in Firmicutes immediately following the deposition of the urea, with higher numbers of Firmicutes initially observed under the -10 kPa treatment: there were observed maximum-fold changes of 10.8 and 16.2 under the -1 and -10 kPa treatments, respectively. O'Callaghan et al. (2010) also found increased numbers of Firmicutes following ruminant urine application (600 kg N ha^{-1}) to a pasture soil. Thus the modelled rates of DNRA are consistent with the recent results and trends reported by Anderson et al. (2018), and the higher abundance of Firmicutes observed in the current study Samad et al. (2017) may explain the higher DNRA rates at -10 kPa.

Harty et al. (2015) used a ^{15}N-tracing model to examine the effects of nitrification inhibitors on N transformation rates. In the current modelling study, with the exception of DNRA, the gross average transformation rates were 1-3 orders of magnitude higher than those reported in the laboratory study of Harty et al. (2015). This is most likely a consequence of the higher initial urea-N loading rate used by Clough et al. (2017), since other parameters like soil moisture, temperature and soil mesocosm set up were comparable.

6.4.3 Implications for codenitrification

In this experiment the reported codenitrification rates (Clough et al. 2017) were highest under the -1 kPa treatment and occurred predominately when NO_2^- was present, between day 7 to 35 (168-245 h) leading Clough et al. (2017) to conclude that codenitrification occurred when NO_2^- or its downstream denitrification product (NO) was readily available. For codenitrification to occur there must be a suitable nucleophile to generate the hybrid N_2O or N_2. By the end of the experiment significant amounts of urea-^{15}N had entered all of the three N pools that have previously been identified to contribute to denitrification and codenitrification; NH_4^+, NO_3^- and N_{rec} (Rütting and Müller 2008),

significantly enriching potential sources of N_2O and N_2 (Fig. 34, b, d). Based on the studies above (chapter 4 and 5) we know that hydroxylamine, amines and NH_4^+ are capable of contributing to codenitrification fluxes. In the -1 kPa treatment the labile N pool was consistently smaller and this may have been the source of nucleophiles. However, the rapid ^{15}N increase in the N_{lab} pool indicated a change from nucleophiles like amino acids and amides to NH_3-DOC components over time. Based on the current knowledge of labile N compounds and as a consequence of the possible reactions of NH_3 with DOC (Nommik and Vahtras 1982), a wide range of possible organic compounds with physically and/or chemically sorped NH_3 may be assumed to act as nucleophiles 100 h after the urea application.

Previously, a key codenitrification publication (Selbie et al. 2015) measured, in situ, codenitrification fluxes over a 123 d period. The modelling here suggests that the N_{lab} pool will have diminished to low levels, although in situ there will be potentially more inputs than in the currently modelled laboratory study. The current modelling shows the elevated and long term nature of the N_{rec} pool and this aligns well with the relatively long period of codenitrification observed by Selbie et al. (2015). The exact process by which codenitrification occurs remains to be elucidated with respect to specific compounds within N_{lab} and N_{rec} pools. Thus, four N pools, NH_4^+, NO_3^-, N_{rec} and N_{lab}, should be further considered and researched with respect to codenitrification reactions.

6.4.4 Conclusions

Applied urea-^{15}N distribution has been successfully modelled under conditions representative of a ruminant urine deposition event under two moisture treatments. The modelled N transformation rates provided by the N trace model show daily N turnover in the treated soils and dynamics of the related N pools over time.

Changes in the modelled N pools were dramatic and rapid within the first 200 h following urea deposition. The mineralisation and immobilisation rate of NH4+ to and from the Nlab pool were significantly higher within the -10 kPa treatment simultaneously with significant higher NH4+ clay mineral sorbtion and release rates. This difference with soil moisture conditionswas most likely because of the way WFPS (gas diffusivity) affected NH_3 distribution in the soil.

The modelled data reveal potentially significant roles for the Nl_{ab} and N_{rec} pools in the soil N cycle under ruminant urine deposition and their formation may be linked to NH_3 dynamics and this requires further evaluation.

In terms of codenitrification the modelled N pools demonstrate the capacity for codenitrification substrates to be present, and under conditions where codenitrification dominated (-1 kPa) there were observed reductions in N_{lab} possibly due to N_{lab} consumption during codenitrification. Further work should investigate the role of labile dissolved organic matter in codenitrification.

The data demonstrate the considerable time period that is needed for soils to re-establish equilibrium, and which was not achieved in this current study, following the initial conditions after a bovine urine event, especially in case of a high N loading rate.

Note: The full publications related to the same study, Clough et al. (2017) and Samad et al. (2017) can be found in the appendix.

Chapter 7
General discussion and conclusions

Literature was reviewed in order to identify present and missing knowledge about codenitrification and to find appropriate methods for a systematic characterisation of these hybrid N-gas forming reactions under urine patch conditions. Pilot studies were performed to optimize the experimental design for the investigation of codenitrification in soil mesocosms and thereafter, two major experiments were conducted. Additionally, soil N flux rates have been modelled in order to identify the related N transformation rates and elucidate the conditions favouring codenitrification. The main findings of both experiments and the model run are summarized and discussed within this section.

7.1 Summary of results

7.1.1 Chapter 4:

The effects of bacterial (streptomycin), fungal (cycloheximide), and combined inhibitor treatments were measured in a laboratory mesocosm experiment, on soil that had received ^{15}N labelled urea. Soil inorganic-N concentrations, N_2O and N_2 gas fluxes were measured over 51 days. On Days 42 and 51, when nitrification was actively proceeding in the positive control, the inhibitor treatments inhibited nitrification as evidenced by increased soil NH_4^+-N concentrations and decreased soil NO_2^--N and NO_3^--N concentrations. Codenitrification was observed to contribute to total fluxes of both N_2O ($\geq$ 33%) and N_2 ($\geq$ 3%) in urine-amended grassland soils. Cycloheximide inhibition decreased NH_4^+-^{15}N enrichment and reduced N_2O fluxes while reducing the contribution of codenitrification to total N_2O fluxes by $\geq$ 66% and $\geq$ 42%, respectively. Thus, given archaea do not respond to significant to urea deposition, it is proposed that fungi, not bacteria, dominated total N_2O fluxes, and the codenitrification N_2O fluxes, from a simulated urine amended pasture soil.

7.1.2 Chapter 5

The objective of this study was to assess the relative significance of different nucleophiles to codenitrification and to determine the contributions of fungi and bacteria to codenitrification. ^{15}N-labelled ammonium, hydroxylamine (NH_2OH) and two amino acids (phenylalanine or glycine) were applied, separately, to sieved soil mesocosms eight days after a simulated urine event, in the absence or presence of bacterial and fungal inhibitors. Soil chemical variables and N_2O fluxes were monitored and the codenitrified N_2O fluxes determined. Fungal inhibition decreased N_2O fluxes by ca. 40% for both amino acid treatments, while bacterial inhibition only reduced the N_2O flux of the glycine treatment by 14%. Hydroxylamine (NH_2OH) generated the highest N_2O fluxes which declined

with either fungal or bacterial inhibition alone, while combined inhibition resulted in a 60% reduction in the N_2O flux. Trends for codenitrification under the NH_2OH nucleophile treatment followed those of gross N_2O fluxes. Codenitrification fluxes under non-NH_2OH nucleophile treatments were two orders of magnitude lower, and significant reductions in these only occurred with fungal inhibition in the amino acid nucleophile treatments. All the nucleophiles examined contributed to some extent in codenitrification, with fungal inhibition reducing this pathway of N_2O formation when amino acids were involved. These results demonstrate that in situ studies are required to better understand the dynamics of codenitrification nucleophiles in grazed pasture soils and the associated role that fungi have with respect to codenitrification.

7.1.3 Chapter 6

The data set of a previous experiment with measured codenitrification products was used to model the N transformation rates and N pools in the soil, under two moisture regimes. The use of ^{15}N labelled urea permitted a ^{15}N tracing model to be applied, designed to model the N fluxes between different N pools within the soil matrix and the distribution of the applied N between these pools over time. The modelled N transformation rates provided by the ^{15}N trace model matched the measured data well (NH_4^+, NO_3^- concentrations and their respective ^{15}N enrichments over time) and gave insight to (i) inorganic concentration and ^{15}N enrichment over time, (ii) unmeasured in N pools and fluxes, which could not readily be measured.

The model revealed rapid changes in labile and recalcitrant N pools, depending on the soil moisture conditions, and associated fluxes, immediately after urea hydrolysis occurred, which were thought to be the result of NH_3 dynamics within the soil. Soil moisture is postulated to regulate the magnitude of NH_3 dynamics due to constrains on gas diffusion under extremely wet soil conditions, while at field capacity a greater volume of soil was affected by NH_3 dynamics. Previously associated measurements of dissolved organic carbon, an indicator of dissolved organic matter may explain the NH_3 dynamics further as they related to changes in the labile and recalcitrant N pools.

Codenitrification rates, previously measured, were higher under the wet soil conditions and it was here that the labile N pool declined rapidly during the period of codenitrification suggesting that the labile pool is involved in codenitrification reactions.

Having other measured variables such as the molecular microbial data (Samad et al. 2017) provided valuable synergies and insights to the modelling study, e.g. the role of Firmicutes.

Finally, the modelling study demonstrates the relatively long time period required for soils to re-establish initial equilibrium conditions between soil N pools after a bovine urine event which is consistent with observed ^{15}N dynamics observed in long-term field studies.

7.2 General conclusions

7.2.1 Pathways of codenitrification

Codenitrification forms hybrid N_2O via nitrogen-nitrosation that co-metabolizes mineral and organic N compounds. Since urine patches are characterized by a high urea N loading rate, which alters dissolved organic matter concentrations and soil pH, codenitrification must be performed with N compounds originating and subsequently being made available under these conditions. However, one long term study (Selbie et al. 2015) indicates that N sources for codenitrification may also become available over the long-term (> 100 days).

Previous studies have reported the lysis of microbial cells might enrich the soil with easy degradable organic material such as amino acids, amino sugars, DNA and RNA fragments. The results of chapter 5 suggest that these compounds might be used for codenitrification reactions. However, the results of chapter 6 suggests, that labile N may also include NH_3 and NH_4^+ being loosely bound at organic C compounds (Nommik and Vahtras 1982). Once oxygen becomes limited, it might be assumed that these easy degradable N compounds are the first source of N used for the formation of hybrid N_2O and N_2 (Fig 38, codenitrification I).
After initial N_2O and N_2 formation (possibly leading to N_{lab} pool depletion), the applied N swiftly enriches all other soil N pools (chapter 6). For later codenitrification fluxes, however, according to the model output of chapter 6, this seems to be a different type of codenitrification, were more recalcitrant organic N compounds were utilized. Typical for this reaction pathway would be the N_{rec} pool as nucleophile source and the simultaneous occurrence with conventional denitrification (Fig. 38, codenitrification II).

In general, it can be concluded that at least three different reaction pathways lead to the formation of hybrid N_2O and N_2 and might therefore be considered as codenitrification pathways under urine patch conditions (i) abiotic codenitrification might occur via NH_2OH, leaking out of NH_4^+ oxidizing microbial cells (Liu et al. 2017b), reacting with NO_2^- from degraded labile or recalcitrant soil organic N (Fig. 38, abiotic codenitrification). The two other codenitrification pathways most likely to occur are codenitrification, where and enzymatic reaction merges urea-N derived NO_2^- with NO_2^- from oxidized labile N (codenitrification I) or recalcitrant N (codenitrification II). This would explain the results of chapter 4 and 5 as well as the findings from Selbie et al. (2015b) and Clough et al. (2017).

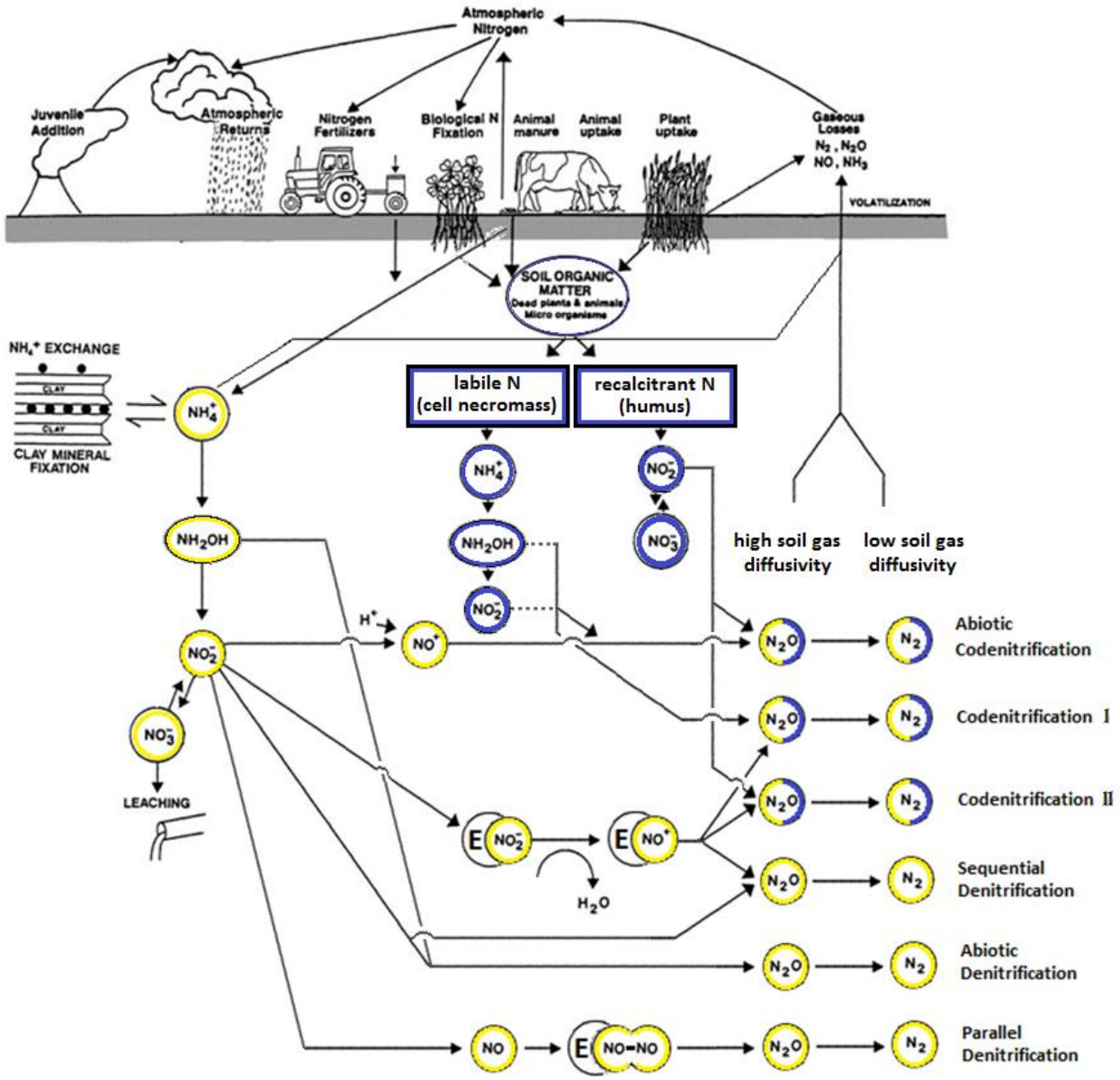

Figure 38. Main N_2O and N_2 generating N transformations in grasslands under urine patch conditions.

7.2.2 Microbiology of codenitrification

Several microbial species have been reported of being capable of codenitrification reactions (Spott et al. 2011), but it was unknown if these function under urine patch conditions within soil. Initial results from a soil matrix indicated fungi as being the most important microbial group (Laughlin and Stevens 2002). Based on the indications given by the present literature (chapter 2) and the findings of chapter 4, 5 and the consideration of the chemical pathways as discussed above (Fig. 38) soil saprophytic fungi are likely to be the dominant microbial group performing codenitrification under urine patch conditions in grassland soils.

The role of mycorrhizal fungi might be negligible, considering the presence of codenitrification in the study of Clough et al. (2017) as well as the experiments of chapter 4 and 5, where there was an absence of plants. It still remains unclear what fungal species dominate the codenitrification process, however, this might strongly vary between different pasture soils due to their unique microbial community.

Despite the importance of fungi for codenitrification, it can be assumed that bacteria perform a critical role in providing precursor substrates (NO_2^- and/or NO). Therefore, although fungi might be predominately responsible for hybrid N_2O and N_2 formation, the structure and fungal:bacterial biomass ratio might also be important for the determination of the final gaseous product.

7.2.3 Characterisation of codenitrification

Given the results of the previous chapters in context of the present literature, the following can be stated as characterisations of codenitrification under urine patch conditions:

- Codenitrification can contribute significantly to N_2O emissions across different pasture soils.
- Codenitrification occurs under low oxygen conditions and may possibly be promoted by frequent soil drying-rewetting cycles due to drying encouraging mineralization and subsequent wetting creates anaerobic conditions.
- Although different microbial groups are capable of performing codenitrification, soil saprophytic fungi are most likely the main contributing microorganisms in pasture soils.
- Labile organic N compounds, e.g. amino acids, and their breakdown products, e.g. NH_2OH and NH_4^+, may represent the major fraction of available nucleophiles for codenitrification in grassland soils.
- Modelling of N transformation rates and N pools under high rates of urea, typical of urine patches, show rapid, significant, and long lasting changes in soil N pools following NH_3 formation. Indicating that perhaps NH_3 fixation reactions generate compounds within labile and/or recalcitrant N pools capable of partaking or providing nucleophiles that partake in codenitrification.

7.3 Recommendations for future research

These studies were performed to better characterize codenitrification under urine patch conditions in pasture soils. Possible future research ideas, in order of preference, and by no means exhaustive, include:

1. To examine the concentration of the recognized nucleophiles in situ and factors affecting these. For example, hydroxylamine.

2. Given the role of fungi in codenitrification, examine the dynamics of fungi in pasture soils with respect to biomass and fungal community composition and determine if these factors vary with environmental conditions (e.g. soil moisture).

3. Expand the ^{15}N trace urea model to include NO_2^- and N_2O, N_2 fluxes, with available data to date from Clough et al. (2017).

4. Investigate how soil organic matter concentrations affect codenitrification.

5. Determine how wetting-drying events, especially the frequency of these, might affect codenitrification from various N pools, in particular the N_{rec} pool.

6. Determine the role of plant uptake and mycorrhizal fungi on codenitrification reactions.

References

Aerssens E, Tiedje JM, Averill BA (1986) Isotope labeling studies on the mechanisms of N-N bond formation in denitrification J Biol Chem 261:9652-9656

Ambus P, Christensen S (1995) Spatial and seasonal nitrous oxide and methane fluxes in danish forest-, grassland-, and agroecosystems J Environ Qual 24:993-1001

Anderson CR, Peterson ME, Frampton RA, Bulman SR, Keenan S, Curtin D (2018) Rapid increase in soil pH solubilises organic matter, dramatically increases denitrification potential and strongly stimulates microorganisms from the Firmicutes phylum PeerJ Preprints 6:e26903v26901

Anderson IC, Levine JS (1986) Relative rates of nitric oxide and nitrous oxide production by nitrifiers, denitrifiers, and nitrate respirers Appl Environ Microbiol 51:938-945

Anderson J, Domsch KH (1973) Quantification of bacterial and fungal contributions to soil respiration Arch Microbiol 93:113-127

Anderson JPE, Domsch KH (1974) Measurement of bacterial and fungal contributions to respiration of selected agricultural and forest soils Can J Microbio 21:314-322

Anderson JPE, Domsch KH (1978) A physiological method for the quantitative measurement of microbial biomass in soils Soil Biol Biochem 10:215-221

Arah JRM (1997) Apportioning nitrous oxide fluxes between nitrification and denitrification using gas-phase mass spectrometry Soil Biol Biochem 29:1295-1299

Averill BA (1996) Dissimilatory nitrite and nitric oxide reductases. Chem Rev 96:2951 - 2964

Avnimelech Y, Laher M (1977) Ammonia Volatilization From Soils: Equilibrium Considerations Soil Sci Soc Am J 41:1080-1084

Badalucco L, Pomarè F, Grego S, Landi L, Nannipieri P (1994) Activity and degradation of streptomycin and cycloheximide in soil Biol Fertil Soils 18:334-340

Bailey VL, Smith JL, Bolton H, Jr (2002) Fungal-to-bacteria ratios in soils investigated for enhanced C sequestration Soil Biol Biochem 34:997-1007

Bakken LR, Frostegård Å (2017) Sources and sinks for N2O, can microbiologist help to mitigate N2O emissions? Environ Microbiol 19:4801-4805 doi:doi:10.1111/1462-2920.13978

Balaine N, Clough TJ, Beare MH, Thomas SM, Meenken ED (2016) Soil gas diffusivity controls N_2O and N_2 emissions and their ratio Soil Sci Soc Am J 80:529-540

Ball B (2013) Soil structure and greenhouse gas emissions: a synthesis of 20 years of experimentation Europ J Soil Sci 64:357-373

Barnabe G (1990) Agriculture. Ellis Harwood, London

Barraclough D (1991) The use of mean pool abundances to interpret ^{15}N tracer experiments I. Theory Plant Soil 131:89-96

Barraclough D, Jarvis SC, Davies GP, Williams J (1992) The relationship between fertilizer nitrogen applications and nitrate leaching from grazed grassland Soil Use Manag 8:51-56

Bender SF et al. (2014) Symbiotic relationships between soil fungi and plants reduce N2O emissions from soil. ISME Journal 8:1336-1345

Betteridge K, Andrewes W, Sedcole J (1986) Intake and excretion of nitrogen, potassium and phosporus by grazing steers J Agri Sci 106:393-404

Bjarnason S (1988) Calculation of gross nitrogen immobilization and mineralization in soil J Soil Sci 39:393-406

Blakemore LC, Searle PL, Daly BK (1987) Methods for Chemical Analysis of Soils vol 80. NZ Soil Bureau, Dep Sci Ind Res,

Boast CW, Mulvaney RL, Baveye P (1988) Evaluation of nitrogen -15 tracer techniques for direct measurement of denitrification in soil: I. theory Soil Sci Soc Am J 52:1317-1322

Bothner-By A, Friedman L (1952) The reaction of nitrous acid with hydroxylamine J Chem Phys 20:459-462

Bottomley F (1978) Electrophilic behavior of coordinated nitric oxide Acc Chem Res 11:158-163

Bottomley PJ, Taylor AE, Myrold DD (2012) A consideration of the relative contributions of different microbial subpopulations to the soil N cycle Front Terr Microbiol 3:Article 373

Bremner JM, Blackmer AM, Waring SA (1980) Formation of nitrous oxide and dinitrogen by chemical decomposition of hydroxylamine in soils Soil Biol Biochem 12:263-269

Bremner JM, Edwards AP (1965) Determination and isotope-ratio analysis of different forms of nitrogen in soils: I. apparatus and procedure for distillation and determination of ammonium Soil Sci Soc Am Proc 29:504-507

Breuillin-Sessoms F, Venterea RT, Sadowsky MJ, Coulter JA, Clough TJ, Wang P (2017) Nitrification gene ratio and free ammonia explain nitrite and nitrous oxide production in urea-amended soils Soil Bio Biochem 111:143-153 doi:https://doi.org/10.1016/j.soilbio.2017.04.007

Broadbent F, Burge W, Nakashima T (1960) Factors influencing the reaction between ammonia and soil organic matter Transactions 7th int Congr Soil Sci 2:509-516

Broadbent F, Stevenson F (1966) Organic matter interactions. In: McVickar H (ed) Agricultural Anhydrous Ammonia. Technology and Use. Am Soc Agron, Memphis, pp 169-187

Brooks PD, Stark JM, McInteer BB, Preston T (1989) Diffusion Method To Prepare Soil Extracts For Automated Nitrogen-15 Analysis Soil Sci Soc Am J 53:1707-1711 doi:10.2136/sssaj1989.03615995005300060016x

Butterbach-Bahl K, Baggs EM, Dannenmann M, Kiese R, Zechmeister-Boltenstern S (2013) Nitrous oxide emissions from soils, how well do we understand the processes and their controls Phil Trans R Soc Lond B368:16-21 doi:10.1098/rstb.2013.0122

Cameron K, Di H, Moir J (2013) Nitrogen losses from the soil/plant system: a review Ann Appl Biol 162:145-173

Cameron KC, Di HJ, Moir JL (2014) Dicyandiamide (DCD) effect on nitrous oxide emissions, nitrate leaching and pasture yield in Canterbury, New Zealand. NZ J Agri Res 57:251-270

Cameron KC, Haynes RJ (1986) Retention and movements of nitrogen in soils. In: Haynes RJ, Cameron KC, Goh KM, Sherlock RR (eds) Mineral nitrogen in the plant/soil system. Acad Press, New York, pp 166-241

Castaldi S, Smith KA (1998) Effect of cycloheximide on N_2O and NO_3^- production in a forest and an agricultural soil Biol Fertil Soils 27:27-34

Castignetti D, Hollocher TC (1984) Heterotrophic nitrification among denitrifiers Appl Environ Microbiol 47:620-623

Chalk PM, Smith CJ (1983) Chemodenitrification. In: Freney JR, Simpson JR (eds) Gaseous loss of nitrogen from plant soil systems. Martinus Nijhoff and Dr W Junk, Dordrecht, pp 65-89

Chen D, Suter HC, Islam A, Edis R (2010) Influence of nitrification inhibitors on nitrification and nitrous oxide (N_2O) emissio from a clay loam soil fertilized with urea Soil Biol Biochem 42:660-664

Chen DL, Chalk PM, Freney JR (1995) Distribution of reduced products of ^{15}N-labelled nitrate in anaerobic soils Soil Biol Biochem 27:1539-1545

Cleemput OV, Baert L (1983) Nitrite stability influenced by iron compounds Soil Biol Biochem 15:137-140 doi:10.1016/0038-0717(83)90093-7

Cleemput OV, Samater AH (1996) Nitrite in soils: accumulation and role in the formaion of gaseous N compounds Fertil Res 45:81-89

Clegg CJ, Mackean DG (2006). In: Advanced Biology: Principles and Applications, Second Edition. Hodder Education,

Clough TJ, Bertram JE, Sherlock RR, Leonard RL, Nowicki BL (2006a) Comparison of measured and EF5-r-derived N_2O fluxes from a spring-fed river. Glob Change Biol 12:352-363 doi:10.1111/j.1365-2486.2005.01089.x

Clough TJ, Kelliher FM, Wang YP, Sherlock RR (2006b) Diffusion of $^{15}N_2$-labelled N_2O into soil columns: a promising method to examine the fate of N_2O in subsoils Soil Biol Biochem 38:1462-1468

Clough TJ et al. (2017) Influence of soil moisture on codenitrification fluxes from a urea-affected pasture soil Sci Rep -17-02278 doi:10.1038/S41598-017-02278-y

Clough TJ et al. (2009) The mitigation potential of hippuric acide on N_20 emissions from urine patches: An *in situ* determination of its effect Soil Biol Biochem 41:2222-2229

Clough TJ, Rolston DE, Stevens RJ, Laughlin RJ (2003) N_2O and N_2 gas fluxes, soil gas pressures, and ebullition events following irrigation of $^{15}NO_3^-$-labelled subsoils Aust J Soil Res 41:401-420

Clough TJ, Sherlock RR, Cameron KC, Ledgard SF (1996) Fate of urine nitrogen on mineral and peat soils in NZ Plant Soil 178:141-152

Clough TJ, Sherlock RR, Cameron KC, Stevens RJ, Laughlin RJ, Müller C (2001a) Resolution of the ^{15}N balance enigma? Aust J Soil Res 39:1419-1431

Clough TJ, Stevens RJ, Laughlin RJ, Sherlock RR, Cameron KC (2001b) Transformations of inorganic-N in soil leachate under differing storage conditions Soil Biol Biochem 33:1473-1480

Costa E, Pérez J, Kreft J-U (2006) Why is metabolic labour divided in nitrification? Trends Microbiol 14:213-219

Czygan F-C (1971) Der Stickstoff-Kreislauf in der Natur Biol Zeit 1:101-110

Daims H et al. (2015) Complete nitrification by *Nitrospira* bacteria Nature 528:504-509

Davidson EA (2009) The contribution of manure and fertilizer nitrogen to atmospheric nitrous oxide since 1860 Nat Geosci 2:659-662

Davidson EA, Stark JM, Firestone MK (1990) Microbial production and consumption of nitrate in an annual grassland Ecology 71:1968-1975

de Klein CAM, Barton L, Sherlock RR, Li Z, Littlejohn RP (2003) Estimating a nitrous oxide emission factor for animal urine from some New Zealand pastoral soils Aust J Soil Res 41:381-399

de Vries FT, Bloem J, van Eekeren N, Brusaard L, Hoffland E (2007) Fungal biomass in pastures increases with age and reduced N input Soil Biol Biochem 39:1620-1630

Demmers T, Burgess L, Short J, Phillips V, Clark J, Wathes C (1999) Ammonia emissions from two mechanically ventilated UK livestock buildings Atmos Environ 33:217-227

Di HJ, Cameron KC (2002) Nitrate leaching in temperate agroecosystems: sources, factors and mitigation strategies. Nut Cyc Agroecosys 64:237-256

Di HJ, Cameron KC, Podolyan A, Robinson A (2014) Effect of soil moisture status and a nitrification inhibitor, dicyandiamide, on ammonia oxidizer and denitrifier growth and nitrous oxide emissions in a grassland soil Soil Biol Biochem 73:59-68

Di HJ, Cameron KC, Shen JP, Winefield CS, Callaghan M, Bowatte S, He JZ (2009) Nitrification driven by bacteria and not archaea in nitrogen-rich grassland soils Nat Geosci 2:621-624

Dijkstra J, Oenema O, Groeningen JWv, Spek JW, Vuuren AMv, Bannink A (2013) Diet effects on urine composition of cattle and N2O emissions Animal: an international journal of animal bioscience 7:292-302

Duan YF, Kong XW, Schramm A, Labouriau R, Eriksen J, Petersen SO (2016) Microbial N Transformations and N2O Emission after Simulated Grassland Cultivation: Effects of the Nitrification Inhibitor 3,4-Dimethylpyrazole Phosphate (DMPP). Appl Environ Microbiol 82:5236-5248

Ehrlich HL, Oremland RS, Zehr JP (2000) Biogeochemical cycles. London: Nature Publishing Group

Environment Mft (2015) New Zealand's greenhouse gas emissions reduction targets Climate Change Information New Zealand https://www.climatechange.govt.nz/reducing-our-emissions/targets.html

Eriksson T, Rustas B-O (2014) Effects on milk urea concentration, urine output, and drinking water intake from incremental doses of potassium bicarbonate fed to mid-lactation dairy cows J Dairy Sci 97:4471-4484

Ermel M et al. (2018) Hydroxylamine released by nitrifying microorganisms is a precursor for HONO emission from drying soils Sci Rep 8:1877

Ernst J, Massey H (1960) The Effects of Several Factors on Volatilization of Ammonia Formed from Urea in the Soil 1 Soil Sci Soc Am J 24:87-90

Eurostat (2012) Agricultural census in Ireland https://eceuropaeu/eurostat/statistics-explained/indexphp/Agricultural_census_in_Ireland#Further_Eurostat_information

Fazzolari É, Nicolardot B, Germon JC (1998) Simultaneous effects of increasing levels of glucose and oxygen partial pressures on denitrification and dissimlatory reduction to ammonium in repacked soil cores Eur J Soil Biol 34:47-52

Firestone MK, Davidson EA (1989) Microbiological basis of NO and N_2O production and consumption in soil. In: Andreae MO, Schimel DS (eds) Exchange of trace gases between terrestrial ecosystems and the atmosphere. John Wiley & Sons, New York, pp 7-21

Flaig W Comparative chemical investigations on natural humic compounds and their model substances. In: Scientific Proceedings of the Royal Dublin Society, Series A, 1960. pp 149-162

Flessa H, Dörsch P, Beese F, König H, Bouwman AF (1996) Influence of Cattle Wastes on Nitrous Oxide and Methane Fluxes in Pasture Land J Environ Qual 25:1366-1370

Focht DD, Verstraete E (1977) Biochemical ecology of nitrification and denitrification. In: Alexander M (ed) Advances in Microbial Ecology, vol 1. Plenum Press, New York, pp 135-214

Freeman JP (1973) Less familiar reactions of oximes Chem Rev 73:283-292

Friedel JK, Scheller E (2002) Composition of hydrolysable amino acids in soil organic matter and soil microbial biomass Soil Biol Biochem 34:315-325

Friedl J, De Rosa D, Rowlings DW, Grace PR, Müller C, Scheer C (2018) Dissimilatory nitrate reduction to ammonium (DNRA), not denitrification dominates nitrate reduction in subtropical pasture soils upon rewetting Soil Biol Biochem 125:340-349

Frostegård A, Bååth E (1996) The use of phospholipid fatty acid analysis to estimate bacterial and fungal biomass in soil Biol Fertil Soils 22:59-65

Galloway JN, Aber JD, Erisman JW, Seitzinger SP, Howarth RW, Cowling EB, Cosby BJ (2003) The nitrogen cascade AIBS Bulletin 53:341-356

Garber EAE, Hollocher TC (1981) ^{15}N tracer studies on the role of NO in denitrification J Biol Chem 256:5459

Garber EAE, Hollocher TC (1982) N-15, O-18 tracer studies on the activation of nitrite by denitrifying bacteria – nitrite water-oxygen exchange and nitrosation reactions as indicators of electrophilic catalysis J Biol Chem 257:8091-8097

Giguere AT, Taylor AE, Myrold DD, Bottomley PJ (2015) Nitrification responses of soil ammonia-oxidizing archaea and bacteria to ammonium concentrations Soil Sci Soc Am J 79:1366-1374

Giguere AT, Taylor AE, Suwa Y, Myrold DD, Bottomley PJ (2017) Uncoupling of ammonia oxidation from nitrite oxidation: Impact upon nitrous oxide production in non-cropped Oregon soils Soil Biol Biochem 104:30-38

Goh KM, Haynes RJ (1986) Nitrogen and Agronomic Practice. In: Haynes RJ (ed) Mineral Nitrogen in the Plant-Soil System. Academic Press, Orlando, Florida, pp 379-442

Goretski J, Hollocher TC (1991) Catalysis of nitrosyl transfer by denitrifying bacteria is facilitated by nitric oxide Biochem Biophys Res Commun 175:901-905

Grimbert L (1899) Action du Bacillus coli et du Bacillus d'Eberth sur les nitrates. Annales de L'Institut Pasteur 13:67-76

Hallin S, Philippot L, Löffler FE, Sanford RA, Jones CM (2017) Genomics and Ecology of Novel N2O-Reducing Microorganisms. Trends Microbiol S0966-842X:30173-30177

Hamonts K et al. (2013) Influence of soil bulk density and matric potential on microbial dynamics, inorganic N transformations, N_2O and N_2 fluxes following urea deposition Soil Biol Biochem 65:1-11

Hart H (1989) Organische Chemie. VHC Verlagsgesellschaft, Weinheim,

Harty M et al. (2015) The effect of urea fertiliser formulations on gross nitrogen transformations in a permanent grassland soil. Paper presented at the EGU General Assembly 2015 Vienna, 12-17 April 2015

Hauck RD, Melsted SW, Yankwich PE (1958) Use of N-isotope distribution in nitrogen gas in the study of denitrification Soil Sci 86:287-291

Haynes RJ, Williams PH (1992) Changes in soil solution composition and pH in urine-affected areas of pasture J Soil Sci 43:323-334

Haynes RJ, Williams PH (1993) Nutrient cycling and soil fertility in the grazed pasture ecosystem Adv Agron 49:119-199

He J-Z, Hu H-W, Zhang L-M (2012a) Current insights into the autotrophic thaumarchaeal ammonia oxidation in acidic soils Soil Biol Biochem 55:146-154

He J-Z, Shen J-P, Zhang L-M, Di HJ (2012b) A review of ammonia-oxidizing bacteria and archaea in Chinese soils Front Microbiol 3:296

Heil J, Liu S, Vereecken H, Brüggemann N (2015) Abiotic nitrous oxide production from hydroxylamine in soils and their dependence on soil properties Soil Biol Biochem 84:107-115

Heil J, Vereecken H, Brüggemann N (2016) A review of chemical reactions of nitrification intermediates and their role in nitrogen cycling and nitrogen trace gas formation in soil Eur J Soil Sci 67:23-39

Higgins SA et al. (2016) Detection and diversity of fungal nitric oxide reductase genes (p450nor) in agricultural soils Appl Environ Microbiol:AEM. 00243-00216

Hillel D (1998) Flow of water in unsaturated soil. In: Hillel D (ed) Environmental soil physics. Academic Press, San Diego, pp 203-242

Hink L, Nicol GW, Prosser JI (2017) Archaea produce lower yields of N2O than bacteria during aerobic ammonia oxidation in soil Environ Microbiol 19:4829-4837

Hirsch P, Overrein L, Alexander M (1961) Formation of nitrite and nitrate by actinomycetes and fungi J Bact 82:442-448

Hodge A, Fitter AH (2010) Substantial nitrogen acquisition by arbuscular mycorrhizal fungi from organic material has implications for N cycling Proceed Nat Acad Sci 107:13754

Hoogendoorn C, Betteridge K, Costall D, Ledgard S (2010) Nitrogen concentration in the urine of cattle, sheep and deer grazing a common ryegrass/cocksfoot/white clover pasture NZ J Agri Res 53:235-243

Hua W, Chen H, Sun S, Zhou L (2015) Assessing climatic impacts of future land use and land cover change projected with the CanESM2 model International J Climat 35:3661-3675

Hüser R, Habfast K, von Bradke M (1960) Die Bestimmung der Stickstoff-Isotopenhäufigkeit im Ammoniakstickstoff Z Anal Chem 176:429-436

Immoos CE, Chou J, Bayachou M, Blair E, Greaves J, Farmer PJ (2004) Electrocatalytic Reductions of Nitrite, Nitric Oxide, and Nitrous Oxide by Thermophilic Cytochrome P450 CYP119 in Film-Modified Electrodes and an Analytical Comparison of Its Catalytic Activities with Myoglobin J Am Chem Soc 126:4934-4942 doi:10.1021/ja038925c

Inselsbacher E et al. (2010) Short-term competition between crop plants and soil microbes for inorganic N fertilizer Soil Biol Biochem 42:360-372

Inselsbacher E, Wanek W, Strauss J, Zechmeister-Boltenstern S, Müller C (2013) A novel ^{15}N tracer model reveals: Plant nitrate uptake governs nitrogen transformation rates in agricultural soils Soil Biol Biochem 57:301-310

IPCC (AR5) www.ipccch/report/ar5/

Islam KR, Weil RR (1998) Microwave irradiation of soil for routine measurement of microbial biomass carbon Biol Fertil Soils 27:408-416

Iwasaki H, Matsubayashi R, Mori T (1956) Studies on denitrification. 2. Production of nitric oxide and its utilization in the N-N-linkage formation by denitrifying bacteria J Biochem 43:295-305

James D, Harward M (1964) Competition of NH3 and H2O for Adsorption Sites on Clay Minerals 1 Soil Sci Soc Am J 28:636-640

Jansson SL (1955) Orientierende Studien uber den Stickstoff kreislauf im Boden mit Hilfe von^{15}N als Leitisotop Z Pflanzenern Bodenk 69:190-198

Jarvis S, Pain B Ammonia volatilization from agricultural land. In: Proceed-Fertil Soc, 1990. vol 298.

Jarvis SC, Scholefield D, Pain B (1995) Nitrogen cycling in grazing systems. In: Bacon PE (ed) Nitrogen fertilization in the environment. Marcel Dekker, New York, pp 381-419

Jones DL (1999) Amino acid biodegradation and its potential effects on organic nitrogen capture by plants Soil Biol Biochem 31:613-622

Jones DL, Shannon D (1999) Mineralization of amino acids applied to soils: impact of soil sieving, storage, and inorganic nitrogen additions Soil Sci Soc Am J 63:1199-1206

Justice JK, Smith RL (1962) Nitrification of ammonium sulfate in a calcareous soil as influenced by combinations of moisture, temperature, and levels of added nitrogen Soil Sci Soc Am Proc 26:246-250

Kalbitz K, Solinger S, Park J-H, Michalzik B, Matzner E (2000) Controls of the dynamics of dissolved organic mater in soils: a review Soil Sci 165:277-304

Kamble PN, Bååth E (2016) Comparison of fungal and bacterial growth after alleviating induced N-limitation in soil Soil Biol Biochem 103:97-105

Keeney DR, Nelson DW (1982) Nitrogen - inorganic forms. In: Part 2 Chemical and microbiological properties, vol Monograph No. 9. Methods of soil analysis, 2nd edn. ASA-SSSA, Madison, USA,

Kelley KR, Ditsch DC, Alley MM (1991) Diffusion and Automated Nitrogen-15 Analysis of Low-Mass Ammonium Samples Soil Sci Soc Am J 55:1016-1020 doi:10.2136/sssaj1991.03615995005500040021x

Kirkham D, Bartholomew WV (1954) Equations for following nutrient transformations in soil, utilizing tracer data Soil Sci Soc Am Proc 18:33-34

Kirkham D, Bartholomew WV (1955) Equations for following nutrient transformations in soil, utilizing tracer data: II. Soil Sci Soc Am Proc 19:189-192

Klemedtsson L, Svensson BH, Rosswall T (1988) A method of selective inhibition to distinquish between nitrification and denitrification as sources of nitrous oxide in soil Biol Fertil Soils 6:112-119

Knowles R (1982) Denitrification Microbiol Rev 46:43-70

Koijman AM, Bloem J, Dalen BRv, Kalbitz K (2016) Differences in activity and N demand between bacteria and fungi in a microcosm incubation experiment with selective inhibition Appl Soil Ecol 99:29-39

Kool DM, Dolfing J, Wrage N, van Groenigen JW (2011) Nitrifier denitrification as a distinct and significant source of nitrous oxide from soil Soil Biol Biochem 43:174-178

Körner S, Das SK, Veenstra S, Vermaat JE (2001) The effect of pH variation at the ammonium/ammonia equilibrium in wastewater and its toxicity to Lemna gibba Aquat Bot 71:71-78 doi:https://doi.org/10.1016/S0304-3770(01)00158-9

Kreutzer W (1963) Selective toxicity of chemicals to soil microorganisms Annu Rev Phytopathol 1:101-126

Kumon Y, Sasaki Y, Kato I, Takaya N, Shoun H, Beppu T (2002) Codenitrification and denitrification are dual metabolic pathways through which dinitrogen evolves from nitrate in *Streptomyces antibioticus* J Bact 184:2963-2968

Kuypers MMM (2015) A division of labour combined Nature 528:487-488

Kuypers MMM, Marchant HK, Kartal B (2018) The microbial nitrogen-cycling network Nature Reviews Microbiology 16:263 doi:10.1038/nrmicro.2018.9

Lantinga EA, Keuning JA, Groenwold J, Deenen PJAG (1987) Distribution of excreted nitrogen by grazing cattle and its effects on sward quality, herbage production and utilization. Develop Plant Soil Sci 30:103-117

Laubach J et al. (2015) Review of greenhouse gas emissions from the storage and land application of farm dairy effluent NZ J Agri Res 58:203-233 doi:10.1080/00288233.2015.1011284

Laubach J, Taghizadeh-Toosi A, Gibbs SJ, Sherlock RR, Kelliher FM, Grover SPP (2013) Ammonia emissions from cattle urine and dung excreted on pasture Biogeosci 10:327-338

Laughlin RJ, Stevens RJ (2002) Evidence for Fungal Dominance of Denitrification and Codenitrification in a Grassland Soil Soil Sci Soc Am J 66:1540-1548 doi:10.2136/sssaj2002.1540

Leathwick J, Stephens R (1998) Climate surfaces for New Zealand Landcare Research Contract Report LC9798 126:1-19

Lebinay C, Rigaud T, Salon C, Lemanceau P, Mougel C (2012) Interaction between *Medicago truncatula* and *Pseudomonas fluorescens*: Evaluation of costs and benefits across an elevated atmospheric CO_2 PLOS One 7:e45740

Leininger S et al. (2006) Archaea predominate among ammonia-oxidizing prokaryotes in soils Nature 442:806-809

Lin Q, Brookes PC (1999) Comparison of substrate induced respiration, selective inhibition and biovolume measurements of microbial biomass and its communitiy structure in unamended, ryegrass-amended, fumigated and pesticide-treated soils Soil Biol Biochem 31:1999-2014

Liu S, Berns AE, Vereecken H, Wu D, Brüggemann N (2017a) Interactive effects of MnO_2, organic matter and pH on abiotic formation of N_2O from hydroxylamine in artificial soil mixtures Sci Rep 7:39590 doi:10.1038/srep39590

Liu S, Han P, Hink L, Prosser JI, Wagner M, Bruggemann N (2017b) Abiotic conversion of extracellular NH2OH contributes to N2O emission during ammonia oxidation Environ Sci Tech 51:13122-13132

Liu S, Vereecken H, Brüggemann N (2014) A highly sensitive method for the determination of hydroxylamine in soils Geoderma 232-234:117-122

Liu YP, Mulvaney RL (1992) Use of diffusion for automated nitrogen-15 analysis of soil extracts Commun Soil Sci Plant Anal 23:613-629

Löhnis F (1926) Der Kreislauf des Stickstoffs: Nitrat-Reduktion. Amid-, Ammon- und Nitrat-Assimilation. Verluste und Gewinne an gebundenem Stickstoff. In: Löhnis F (ed) Vorlesungen über landwirtschaftliche Bakteriologie. 2. edn. Verlag von Gebrüder Bornträger, Berlin, pp 157-172

Long A, Heitman J, Tobias C, Philips R, Song B (2013) Co-Occurring anammox, denitrification, and codenitrification in Agricultural Soils Appl Environ Microbiol 79:168-176

Lundquist EJ, Jackson LE, Scow KM (1999) Wet-dry cycles affect dissolved organic carbon in two California agricultural soils Soil Biol Biochem 31:1031-1038

Luo J et al. (2013) Nitrous oxide emissions from grazed hill land in New Zealand Agric Ecosys Environ 181:58-68

Luo J, Tillman RW, Ball PR (2000) Nitrogen loss through denitrification in a soil under pasture in New Zealand Soil Biol Biochem 32:497-509

Luo J, Tillman RW, White RE, Ball PR (1998) Variation in denitrification activity with soil depth under pasture Soil Biol Biochem 30:897-903

Luzzatto L, Apirion D, Schlessinger D (1968) Mechanism of action of streptomycin in E. coli: interruption of the ribosome cycle at the initiation of protein synthesis Proceed Nat Acad Sci USA 60:873

Ma WK, Farrell RE, Siciliano SD (2008) Soil formate regulates the fungal nitrous oxide emission pathway Appl Environ Microbiol 74:6690-6696

Maeda K et al. (2015) N_2O production, a widespread trait in fungi Sci Rep 5:9697

Maharjan B, Venterea RT (2013) Nitrite intensity explains N management effects on N_2O emissions in maize Soil Biol Biochem 66:229-238

Mary B, Recous S, Robin D (1998) A model for calculating nitrogen fluxes in soil using ^{15}N tracing Soil Biol Biochem 30:1963-1979

McLain JET, Martens DA (2005) Nitrous oxide flux from soil amino acid mineralization Soil Biol Biochem 37:289-299

McLaren RG, Cameron KC (1996) Soil science sustainable production and environmental protection. 2nd edn. Oxford University Press, Auckland

Meinhardt KA, Stopnisek N, Pannu MW, Strand SE, Fransen SC, Casciotti KL, Stahl DA (2018) Ammonia-oxidizing bacteria are the primary N2O producers in an ammonia-oxidizing archaea dominated alkaline agricultural soil Environ Microbiol

Metropolis N, Rosenbluth AW, Rosenbluth MN, Teller AH (1953) Equation of state calculations by fast computing machines J Chem Phys 21:1087-1092

Metropolis N, Ulam S (1949) The Monte Carlo method J Am Stat Ass 55:335-341

Ministry for the Environment (2016) New Zealand's Greenhouse Gas Inventory 1990-2014. Fulfilling reporting requirements under the United Nations Framework Convention on Climate Change. Wellington, New Zealand. ISSN: 1179-223X (electronic), Publication number: ME 1239 vol ISSN: 1179-223X (electronic) Publication number: ME 1239. Wellington, New Zealand.

Moir J, Cameron K, Di H (2007) Effects of the nitrification inhibitor dicyandiamide on soil mineral N, pasture yield, nutrient uptake and pasture quality in a grazed pasture system Soil Use Manag 23:111-120

Moir JL, Cameron C, Di H, Fertsak U (2011) The spatial coverage of dairy cattle urine patches in an intensively grazed pasture system J Agri Sci 149:473-485

Monaghan RM, Barraclough D (1992) Some chemical and physical factors affecting the rate and dynamics of nitrification in urine-affected soil Plant Soil 143:11-18

Monaghan RM, Barraclough D (1993) Nitrous oxide and dinitrogen emissions from urine-affected soil under controlled conditions Plant Soil 151:127-138

Monaghan RM, Carey P, Metherell AK, Singleton PL, Drewry J, Addison B (1999) Depth distribution of simulated urine in a rangge of soils soon after deposition. NZ J Agri Res 42:501-511

Morales SE, Jha N, Saggar S (2015) Biogeography and biophysicochemical traits link N_2O emissions, N_2O emission potential and microbial communities across New Zealand pasture soils Soil Biol Biochem 82:87-98

Mortland M (1966) Ammonia interactions with soil materials. In: al. Me (ed) Agricultural Anhydrous Ammonia. Technology and Use. Ammerica Society of Agronnomy and Soil Soc Am, St. Louis,

Mortland M, Wolcott A (1965) Sorption of inorganic nitrogen compounds by soil materials Soil Nitrogen: 150-197

Moss RH et al. (2010) The next generation of scenarios for climate change research and assessment Nature 463:747-756

Mothapo N, Chen H, Cubeta MA, Grossman JM, Fuller F, Shi W (2015) Phylogenetic, taxonomic and functional diversity of fungal denitrifiers and associated N2O production efficacy Soil Biol Biochem 83:160-175 doi:https://doi.org/10.1016/j.soilbio.2015.02.001

Müller C Understanding the nitrogen cycle in a changing world. In: XIV Congress of the Italian Federation of Life Sciences (FISV), Rome, 20-23 September 2016 2016.

Müller C, Laughlin RJ, Spott O, Rütting T (2014) Quantification of N_2O emission pathways via a ^{15}N tracing model Soil Biol Biochem 72:44-54 doi:10.1016/j.soilbio.2014.01.013

Müller C, Rütting T, Kattge J, Laughlin RJ, Stevens RJ (2007) Estimation of parameters in complex ^{15}N tracing models by Monte Carlo sampling Soil Biol Biochem 39:715-726

Müller C, Stevens RJ, Laughlin RJ (2004) A ^{15}N tracing model to analyse N transformations in old grassland soil Soil Biol Biochem 36:619-632

Müller C, Stevens RJ, Laughlin RJ (2006) Sources of nitrite in a permanent grassland soil Europ J Soil Sci 57:337-343

Munkvold L, Kjøller R, Vestberg M, Rosendahl S, Jakobsen I (2004) High functional diversity within species of arbuscular mycorrhizal fungi New Phytol 164:357-364

Munroe JW, McCormick I, Deen W, Dunfield KE (2016) Effects of 30 years of crop rotation and tillage on bacterial and archaeal ammonia oxidizers J Environ Qual 45:940-948

Murphy D, Fillery IRP, Sparling GP (1997) Method to label soil cores with $^{15}NH_3$ gas as a prerequisite for ^{15}N isotopic dilution and measurement of gross N mineralization Soil Biol Biochem 29:1731-1741

Myers RJK (1975) Temperature effects on ammonification and nitrification in a tropical soil Soil Biol Biochem 7:83-86

Myrold DD, Tiedje JM (1986) Simultaneous estimation of several nitrogen cycle rates using ^{15}N: theory and application Soil Biol Biochem 18:559-568

Naudé SM (1929) The isotopes of nitrogen, mass 15, and oxygen mass 18 and 17, and their abundance Phys Rev 36:333-346

Nelson DW (1982) Gaseous losses of nitrogen other than through denitrification. In: Stevenson FJ (ed) Nitrogen in agricultural soils, vol Agronomy Monograph 22. ASA-CSSA-SSSA, Madison, pp 327-363

Nelson DW, Bremner JM (1970) Gaseous products of nitrite decomposition in soils Soil Biol Biochem 2:203-204 doi:10.1016/0038-0717(70)90008-8

Nishio T (1994) Estimating nitrogen transformation rates in surface aerobic soil of a paddy field Soil Biol Biochem 26:1273-1280

Nishio T, Kanamori T, Fujimoto T (1985) Nitrogen transformations in an aerobic soil as determined by a $^{15}NH_4^+$ dilution technique Soil Biol Biochem 17:149-154

Noggle GR, Wynd FL (1941) The Determination of Selected Chemical Characteristics of Soil Which Affect the Growth and Composition of Plants Plant Physiol 16:39-60

Nommik H, Vahtras K (1982) Retention and fixation of ammonium and ammonia in soils. In: Stevenson FJ (ed) Nitrogen in agricultural soils, vol Agronomy Monograph 22. ASA-CSSA-SSSA, Madison, pp 123-171

Nommik HH, Nilsson K-O (1963) Fixation of ammonia by the organic fraction of the soil Acta Agriculturae Scandinavica 13:371-390

O'Callaghan M et al. (2010) Effect of the nitrification inhibitor dicyandiamide (DCD) on microbial communities in a pasture soil amended with bovine urine Soil Biol Biochem 42:1425-1436

Oenema O, Velthof GL, Yamulki S, Jarvis SC (1997) Nitrous oxide emissions from grazed grasslands Soil Use Manag 13:288-295

Okada N, Nomura N, Nakajima-Kambe T, Uchiyama H (2005) Characterization of the Aerobic Denitrification in Mesorhizobium sp. Strain NH-14 in Comparison with that in Related Rhizobia Microbes Environ 20:208-215

Olsson P, Francis R, Read D, Söderström B (1998) Growth of arbuscular mycorrhizal mycelium in calcareous dune sand and its interaction with other soil microorganisms as estimated by measurement of specific fatty acids Plant Soil 201:9-16

Olsson PA (1999) Signature fatty acids provide tools for determination of the distribution and interactions of mycorrhizal fungi in soil FEMS Microbiology Ecology 29:303-310 doi:10.1111/j.1574-6941.1999.tb00621.x

Olsson PA, Bååth E, Jakobsen I, Söderström B (1995) The use of phospholipid and neutral lipid fatty acids to estimate biomass of arbuscular mycorrhizal fungi in soil Mycol Res 99:623-629 doi:https://doi.org/10.1016/S0953-7562(09)80723-5

Oremland RS, Capone DG (1988) Use of "specific" inhibitors in biogeochemistry and microbial ecology. In: Advances in microbial ecology. Springer, pp 285-383

Otte S, Schalk J, Kuenen JG, Jetten MSM (1999) Hydroxylamine oxidation and subsequent nitrous oxide production by the heterotrophic ammonia oxidizer *Alcaligens faecalis* App Microbiol Biotech 51:255-261

Overrein L, Moe P (1967) Factors Affecting Urea Hydrolysis and Ammonia Volatilization in Soil 1 Soil Sci Soc Am J 31:57-61

Pachauri R (2016) The Intergovernmental Panel on Climate Change (IPCC) Fifth Assessment Report and Its Implications for Human Health and Urban Areas. In: Climate Health Risks in Megacities. CRC Press, pp 47-52

Peterson BJ (1999) Stable isotopes as tracers of organic matter input and transfer in benthic food webs: a review Acta Oecol 20:479-487

Peterson BJ, Fry B (1987) Stable isotopes in ecosystem studies Ann Rev Ecol Syst 18:293-320

Philippot L (2002) Denitrifying genes in bacterial and Archael genomes Biochim Biophys Acta 1577:355-376

Phillips RL, Song B, McMillan AMS, Grelet G, Weir BS, Palmada T, Tobias C (2016) Chemical formation of hybrid di-nitrogen calls fungal codenitrification into question Sci Rep 6 doi:10.1038/srep39077

Prosser JI, Nicol GW (2008) Relative contributions of archaea and bacteria to aerobic ammonia oxidation in the environment Environ Microbiol 10:2931-2941

Prosser JI, Nicol GW (2012) Archaeal and bacterial ammonia oxidisers in soil: the quest for niche specialisation and differentiation Trends Microbiol 20:523-532

Rabot E, Cousin I, Hénault C (2015) A modeling approach of the relationship between nitrous oxide fluxes from soils and the water-filled pore space Biogeochem 122:395-408

Ravishankara AR, Daniel JS, Portmann RW (2009) Nitrous Oxide (N_2O): The Dominant Ozone-Depleting Substance Emitted in the 21st Century Science 326:123-125 doi:10.1126/science.1176985

Renner ED, Becker GE (1970) Production of nitric oxide and nitrous oxide during denitrification by *Corynebacterium nephridii* J Bacteriol 101:821-826

Rex D, Clough TJ, Richards KG, de Klein C, Morales SE, Samad Md S, Grant J, Lanigan GJ (2018) Fungal and bacterial contributions to codenitrification emissions of N_2O and N_2 following urea deposition to soil Nut Cyc Agroecosys 110:135-149 doi:https://doi.org/10.1007/s10705-017-9901-7

Rex D, Schimmelpfennig S, Jansen-Willems A, Moser G, Kammann C, Müller C (2015) Microbial community shifts 2.6 years after top dressing of Miscanthus biochar, hydrochar and feedstock on a temperate grassland site Plant Soil 397:261-271 doi:10.1007/s11104-015-2618-y

Rhoades MB et al. (2010) Continuous ammonia emission measurements from a commercial beef feedyard in Texas Transact Am Soc Agric Biol Engin 53:1823-1831

Richards I, Wolton K (1975) A note on urine scorch caused by gracing animals Grass Forage Sci 30:187-188

Rillig MC, Wright SF, Nichols KA, Schmidt WF, Torn MS (2001) Large contribution of arbuscular mycorrhiza fungi to soil carbon pools in tropical forest soils Plant Soil 233:167-177

Rittenberg D (1948) The preparation of gas samples for mass spectrographic isotope analysis. In: Wilson DW, Nier AOC, Reimann SP (eds) Preparation and measurement of isotopic tracers., vol Ann Arbor. Edwards, J. W., Mich., pp 31-42

Robertson LA, Cornelisse R, de Vos P, Hadioetomo R, Kuenen JG (1989) Aerobic denitrification in various heterotorophic nitrifiers Antonie Leeuwenhoek 56:289-299

Rodens B (2014) Ireland: 50% mehr Milch bis 2020 Top Agrar Online 7

Römpp H (1999) Römpp-chemie Lexikon. In. Thieme-Verlag, Stuttgart,

Rütting T, Müller C (2008) Process-specific analysis of nitrite dynamics in a permanent grassland soil by using a Monte Carlo sampling technique Eur J Soil Sci 59:208-215

Sabey BR, Bartholomew WV, Shaw R, Pesek J (1956) Influence of temperature on nitrification in soils Soil Sci Soc Am Proc 20:357-360

Saggar S, Bolan N, Bhandral R, Hedley C, Luo J (2004) A review of emissions of methane, ammonia, and nitrous oxide from animal excreta deposition and farm effluent application in grazed pastures NZ J Agri Res 47:513-544

Sahrawat K (2008) Factors affecting nitrification in soils Commun Soil Sci Plant Anal 39:1436-1446

Samad MS, Johns C, Richards KG, Lanigan GJ, Klein CAMd, Clough TJ, Morales SE (2017) Response to nitrogen addition reveals metabolic and ecological strategies of soil bacteria Molecular Ecology 26:5500-5514 doi:10.1111/mec.14275

Sameshima-Saito R, Chiba K, Minamisawa K (2004) New Method of Denitrification Analysis of Bradyrhizobium Field Isolates by Gas Chromatographic Determination of ^{15}N-Labeled N_2 Appl Environ Microbiol 70:2886-2891 doi:10.1128/AEM.70.5.2886-2891.2004

Santoro AE (2016) The do-it-all nitrifier Science 351:342-343

Scheller E, Raupp J (2005) Amino Acid and Soil Organic Matter Content of Topsoil in a Long Term Trial with Farmyard Manure and Mineral Fertilizers Biol Agric Hortic 22:379-397 doi:10.1080/01448765.2005.9755299

Schimel JP, Jackson LE, Firestone MK (1989) Spatial and temporal effects on plant-microbial competition for inorganic nitrogen in a california annual grassland Soil Biol Biochem 21:1059-1066

Schneider-Poetsch T et al. (2010) Inhibition of eukaryotic translation elongation by cycloheximide and lactimidomycin Nat Chem Biol 6:209

Schreiber F, Wunderlin P, Udert KM, Wells GF (2012) Nitric oxide and nitrous oxide turnover in natural and engineered microbial communities:biological pathways, chemical reactions, and novel technologies Front Terr Microbiol 3:Article272

Sebilo M, Mayer B, Nicolardot B, Pinay G, Mariotti A (2013) Long-term fate of nitrate fertilizer in agricultural soils PNAS 110:18185-18189

Selbie DR, Buckthought LE, Shepherd MA (2015a) The challenge of the urine patch for managing nitrogen in grazed pasture systems Adv Agron 129:229-292

Selbie DR et al. (2015b) Confirmation of co-denitrification in grazed grassland Sci Rep 5:17361

Setälä H, McLean MA (2004) Decomposition rate of organic substrates in relation to the species diversity of soil saprophytic fungi Oecologia 139:98-107

Sherlock RR, Goh KM (1985) Dynamics of ammonia volatilization from simulated urine patches and aqueous urea applied to pasture. II. Theoretical derivation of a simplified model Fert Res 6:3-22

Sherlock RR, Jewell P, Clough TJ (2009) Review of New Zealand specific FRACGASM and FRACGASF emissions factors. Lincoln University, Christchurch,

Shi X-Z, Hu H-W, Müller C, He J-Z, Chen D, Suter H (2016) Effects of the nitrification inhibitor 3,4-dimethylpyrazole phosphate (DMPP) on nitrification and nitrifiers in two contrasting agricultural soils Appl Environ Microbiol 62:5236-5248 doi:10.1128/AEM.01031-16

Shoun H (2005) Basic studies on fungal unique P450s for industrial applications. Report on the Noda Institute for Sci Res 48:112-114

Shoun H, Fushinobu S, Jiang L, Kim S-W, Wakagi T (2012) Fungal denitrification and nitric oxide reductase cytochrome P450nor Phil Trans R Soc B 367:1186-1194

Shoun H, Kim D-H, Uchiyama H, Sugiyama J (1992) Denitrification by fungi FEMS Microb Lett 94:277-282

Shoun H, Suyama W, Kim D-h (1991) Unique nitrate/nitrite-inducible cytochrome P-450 in *Fusarium oxysporum* and related fungal species Agric Biol Chem 55:593-596

Shoun H, Tanimoto T (1991) Denitrification by the fungus *Fusarium oxysporum* and involvement of cytochrome P-450 in the respiratory nitrite reduction J Biol Chem 266:11078-11082

Smith CJ, Chalk PM, Crawford DM, Wood JT (1994) Estimating gross nitrogen mineralization and immobilization rates in anaerobic and aerobic soil suspensions Soil Sci Soc Am J 58:1652-1660

Smith K (2017) Changing views of nitrous oxide emissions from agricultural soil: key controlling processes and assessment at different spatial scales Europ J Soil Sci 68:137-155

Sorensen DL, Fresquez PR (1991) Nitrification potential in reclaimed coal mine spoils and soils in the semiarid southwest J Environ Qual 20:279-285

Sørensen J, Thorling L (1991) Stimulation by lepidocrocite (7-FeOOH) of Fe(II)-dependent nitrite reduction Geochimica et Cosmochimica Acta 55:1289-1294 doi:10.1016/0016-7037(91)90307-Q

Spek J, Dijkstra J, van Duinkerken G, Hendriks WH, Bannink A (2013) Prediction of urinary nitrogen and urinary urea nitrogen excretion by lactating dairy cattle in northwestern Europe and North America: A meta-analysis J Dairy Sci 96:4310-4322

Spott O, Russow R, Stange CF (2011) Formation of hybrid N_2O and hybrid N_2 due to codenitrification: First review of a barely considered process of microbially mediated N-nitrosation Soil Biol Biochem 43:1995-2011

Spott O, Stange CF (2011) Formation of hybrid N_2O in a suspended soil due to co-denitrification of NH_2OH J Plant Nutr Soil Sci 174:554-567

St John RT, Hollocher TC (1977) Nitrogen 15 tracer studies on the pathway of denitrification in *Pseudomonas aeruginosa* J Biol Chem 252:212-218

Stevens RJ, Laughlin RJ (1994) Determining nitrogen-15 nitrite or nitrate by producing nitrous oxide Soil Sci Soc Am J 58:1108-1116

Stevens RJ, Laughlin RJ (1995) Nitrate Transformations during Soil Extraction with Potassium Chloride. Soil Sci Soc Am J 59:933-938

Stieglmeier M, Mooshammer M, Kitzler B, Wanek W, Zechmeister-Boltenstern S, Richter A, Schleper C (2014) Aerobic nitrous oxide production through N-nitrosating hybrid formation in ammonia-oxidizing archaea Internat Soc Microb Ecol J 8:1135-1146 doi:10.1038/ismej.2013.220

Stout W (2003) Effect of urine volume on nitrate leaching in the northeast USA Nut Cyc Agroecosys 67:197-203

Stroo HF, Klein TM, Alexander M (1986) Heterotrophic nitrification in an acid forest soil and by an acid-tolerant fungus Appl Environ Microbiol 52:1107-1111

Su F, Takaya N, Shoun H (2004) Nitrous oxide-forming codenitrification catalyzed by cytochrome P450nor Biosci Biotech Biochem 68:473-475

Tanimoto T, Hatano K, Kim D, Uchiyama H, Shoun H (1992) Co-denitrification by the denitrifying system of the fungus *Fusarium oxysporum* FEMS Microb Lett 93:177-180

Tarnawski S, Hamelin J, Jossi M, Aragno M, Fromin N (2006) Phenotypic structure of *Pseudomonas* populations is altered under elevated CO_2 in the rhizosphere of perennial grasses Soil Biol Biochem 38:1193-1201

Taylor AE, Zeglin LH, Dooley S, Myrold DD, Bottomley PJ (2010) Evidence for Different Contributions of Archaea and Bacteria to the Ammonia-Oxidizing Potential of Diverse Oregon Soils Appl Environ Microbiol 76:7691-7698

Terada A et al. (2017) Hybrid Nitrous Oxide Production from a Partial Nitrifying Bioreactor: Hydroxylamine Interactions with Nitrite Environ Sci Technol 51:2748-2756 doi:10.1021/acs.est.6b05521

Thomas RQ, Canham CD, Weathers KC, Goodale CL (2010) Increased tree carbon storage in response to nitrogen deposition in the US Nature Geoscience 3:13 doi:10.1038/ngeo721 https://www.nature.com/articles/ngeo721#supplementary-information

Tiedje JM (1988) Ecology of denitrification and dissimilatory nitrate reduction to ammonium. In: Zehnder AJB (ed) Biology of anaerobic microorganisms. John Wiley & Sons, New York, pp 179-244

Tietema A, Wessel WW (1992) Gross nitrogen transformations in the organic layer of acid forest ecosystems subjected to increased atmospheric nitrogen input Soil Biol Biochem 24:943-950

Treseder KK, Allen EB, Egerton-Warburton LM, Hart MM, Klironomos JN, Maherali H, Tedersoo L (2018) Arbuscular mycorrhizal fungi as mediators of ecosystem responses to nitrogen deposition: A trait-based predictive framework J Ecol 106:480-489

Treseder KK, Turner KM (2007) Glomalin in ecosystems Soil Sci Soc Am J 71:1257-1266

Tsao PH (1970) Selective media for isolation of pathogenic fungi Annu Rev Phytopathol 8:157-186

Turner DA et al. (2008) Spatial variability of nitrous oxide emissions from an Australian irrigated dairy pasture Plant Soil 309:77-88

Turtschin FB, Bersenjewa SN, Koritzkaja IA, Shidkick GG, Lobowikowa GA Die Stickstoffumwandlung im Boden nach den Angaben der Untersuchungen unter des Isotops N^{15}. In: 7th International Congress of Soil Science, Madison, Wisconsin, 15 August 1960. Elsevier, pp 236-245

Tzanakakis VA, Paranychianakis NV (2017) Divergent response of ammonia oxidizers to various amino acids Appl Soil Ecol 114:45-51 doi:https://doi.org/10.1016/j.apsoil.2017.02.019

Vajrala N, Bottomley PJ, Stahl DA, Arp DJ, Sayavedra-Soto LA (2014) Cycloheximide prevents the de novo polypeptide synthesis required to recover from acetylene inhibition in Nitrosopumilus maritimus FEMS Microbiol Ecol 88:495-502

van Cleemput O, Baert L (1983) Nitrite stability influenced by iron compounds Soil Biol Biochem 15:137-140

Van der Heijden MGA, Martin FM, Selosse M-A, Sanders IR (2015) Mycorrhizal ecology and evolution: the past, the present, and the future New Phytol 205:1406-1423

Van Groenigen JW, Huygens D, Boeckx P, Kuyper TW, Lubbers IM, Rütting T, Groffman PM (2016) The soil N cycle: new insights and key challenges Soil 1:235-256 doi:10.5194/soil-1-235-2015

Van Kessel MAHJ et al. (2015) Complete nitrification by a single microorganism Nature 528:555-559

van Vuuren AM, Smits MCJ (1997) Effect of nitrogen and sodium chloride intake on production and composition of urine in dairy cows. In: Jarvis SC, Pain BF (eds) Gaseous nitrogen emissions from grasslands. CAB International, New York, pp 95-99

Venterea RT, Clough TJ, Coulter JA, Breuillin-Sessoms F, Wang P, Sadowsky MJ (2015) Ammonium sorption and ammonia inhibition of nitrite-oxidizing bacteria explain contrasting soil N_2O production Sci Rep 5:12153 doi:10.1038/srep12153

Vermoesen A, Demeyer P, Hofman G, van Cleemput O Ammonia volatilization from mineral N-fertilizers, influenced by pH, temperature and soil moisture content. In: Diekkrüger B, Heinemeyer O, Nieder R (eds) 9th nitrogen workshop, Braunschweig, Germany, 9 - 12 September 1996 1996. Technische Universität Braunschweig, Forschungsanstalt für Landwirtschaft (FAL), pp 573-576

Viebrock A, Zumft WG (1988) Molecular cloning, heterologous expression, and primary structure of the structural gene for the copper enzyme nitrous oxide reductase from denitrifying *Pseudomonas stutzeri* J Bacteriol 170:4658

Wakelin SA, Gregg AL, Simpson RJ, Li GD, Riley IT, McKay AC (2009) Pasture management clearly affects soil microbial community structure and N-cycling bacteria Pedobiologia 52:237-251

Wang W, Dalal RC, Moody PW (2001) Evaluation of the microwave irradiation method for measuring soil microbial biomass Soil Sci Soc Am J 65:1696-1703

Wang Y, Averill BA (1996) Direct Observation by FTIR Spectroscopy of the Ferrous Heme− NO+ Intermediate in Reduction of Nitrite by a Dissimilatory Heme cd 1 Nitrite Reductase J Am Chem Soc 118:3972-3973

Wankel SD et al. (2017) Evidence for fungal and chemodenitrification based N 2 O flux from nitrogen impacted coastal sediments Nature Communications 8:15595

Weier KL, Doran JW, Power JF, Walters DT (1993) Denitrification and the dinitrogen/nitrous oxide ratio as affected by soil water, available carbon, and nitrate Soil Sci Soc Am J 57:66-72

Weisburg WG, Tanner RS (1982) Aminoglycoside sensitivity of archaebacteria Federation of European Microbiological Societies - Microbiology Letters 14:307-310

Wessel WW, Tietema A (1992) Calculating gross N transformation rates of ^{15}N pool dilution experiments with acid forest litter: analytical and numerical approaches Soil Biol Biochem 24:931-942

Whitehead DC (1995) Grassland nitrogen. CAB International, Wallingford

Williams DLH (2004) Nitrosation reactions and the chemistry of nitric oxide. Elsevier,

Williams P, Gregg P, Hedley M (1990) Use of potassium bromide solutions to simulate dairy cow urine flow and retention in pasture soils NZ J Agri Res 33:489-495

Williams PH, Haynes RJ (1993) Forms of sulphur in sheep excreta and their fate after application on to pasture soil J Sci Food Agric 62:323-329

Williams PH, Haynes RJ (1994) Comparison of initial wetting pattern,nutrient concentrations in soil solution and the fate of ^{15}N-labelled urine in sheep and cattle urine patch areas of pasture soil Plant Soil 162:49-59

Winogradsky S (1890) Recherches sur les Organismes de la Nitrification Compt Rend Acad Sci (Paris) 110:1013-1016

WMO (2013) The state of greenhouse gases in the atmosphere based on global observations through 2012 WMO Greenhouse Gas Bulletin 9:1-4

Wrage-Mönnig N, Horn MA, Well R, Müller C, Velthof G, Oenema O (2018) The role of nitrifier denitrification in the production of nitrous oxide revisited Soil Biol Biochem 123:A3-A16

Wrage N, Velthof GL, van Beusichem ML, Oenema O (2001) Role of nitrifier denitrification in the production of nitrous oxide Soil Biol Biochem 33:1723-1732

Yan T, Frost JP, Keady TWJ, Agnew RE, Mayne CS (2007) Prediction of nitrogen excretion in feces and urine of beef cattle offered diets containing grass silage. Soil Biol Biochem 30:491-500

Yang X-R et al. (2015) Potential Contribution of Anammox to Nitrogen Loss from Paddy Soils in Southern China Appl Environ Microbiol 81:938-947 doi:10.1128/AEM.02664-14

Ye RW, Torosuarez I, Tiedje JM, Averill BA (1991) (H2O)-O-18 isotope exchange studies on the mechanism of reduction of nitric-oxide and nitrite to nitrous oxide by denitrifying bacteria – evidence for an electronic nitrosyl during reduction of nitric oxide J Biol Chem 266:12848-12851

Yokoyama K, Jinnai K, Sakiyama Y, Touma M (2012) Contribution of fungi to acetylene-tolerant and high ammonia aviability-dependent nitrification potential in tea field soils with relatively neutral pH Appl Soil Ecol 62:37-41

Global New Zealand-international trade, investment, and travel profile: year ended December 2013. (2013).

Zhang J, Müller C, Cai Z (2015a) Heterotrophic nitrification of organic N and its contribution to nitrous oxide emissions in soils Soil Biol Biochem 84:199-209 doi:10.1016/j.soilbio.2015.02.028

Zhang J, Wang J, Zhong W, Cai Z (2015b) Organic nitrogen stimulates the heterotrophic nitrification rate in an acidic forest soil Soil Biol Biochem 80:293-295

Zhu T, Meng T, Zhang J, Yin Y, Cai Z, Yang W, Zhong W (2013a) Nitrogen mineralization, immobilization turnover, heterotrophic nitrification, and microbial groups in acid forest soils of subtropical China Biol Fertil Soils 49:323-331

Zhu T, Meng T, Zhang J, Zhong W, Müller C, Cai Z (2015) Fungi-dominant heterotrophic nitrification in a subtropical forest soil of China J Soils Sedim 15:705-709 doi:10.1007/s11368-014-1048-4

Zhu X, Burger M, Doane TA, Horwath WR (2013b) Ammonia oxidation pathways and nitrifer denitrification are significant sources of N_2O and NO under low oxygen availability PNAS 110:6328-6333

Zollinger H (1988) Diazotisations in Highly Concentrated Mineral Acids: The nitrosation mechanism of anilinium and hydroxylammonium ions through proton loss from the ammonio group Helvetica Chimica Acta 71:1661-1664

Zollinger H (1995) Diazo Chemistry II: Aliphatic, Inorganic and Organometallic Compounds. In. VCH Verlagsgesellschaft mbH, Weinheim,

Appendix

7.4 Clough et al. 2017

www.nature.com/scientificreports

SCIENTIFIC REPORTS

Correction: Author Correction

OPEN

Influence of soil moisture on codenitrification fluxes from a urea-affected pasture soil

Received: 16 December 2016
Accepted: 10 April 2017
Published online: 19 May 2017

Timothy J. Clough[1], Gary J. Lanigan[2], Cecile A. M. de Klein[3], Md. Sainur Samad[4], Sergio E. Morales[4], David Rex[1,2], Lars R. Bakken[5], Charlotte Johns[1,2], Leo M. Condron[1], Jim Grant[6] & Karl G. Richards[2]

Intensively managed agricultural pastures contribute to N_2O and N_2 fluxes resulting in detrimental environmental outcomes and poor N use efficiency, respectively. Besides nitrification, nitrifier-denitrification and heterotrophic denitrification, alternative pathways such as codenitrification also contribute to emissions under ruminant urine-affected soil. However, information on codenitrification is sparse. The objectives of this experiment were to assess the effects of soil moisture and soil inorganic-N dynamics on the relative contributions of codenitrification and denitrification (heterotrophic denitrification) to the N_2O and N_2 fluxes under a simulated ruminant urine event. Repacked soil cores were treated with ^{15}N enriched urea and maintained at near saturation (−1 kPa) or field capacity (−10 kPa). Soil inorganic-N, pH, dissolved organic carbon, N_2O and N_2 fluxes were measured over 63 days. Fluxes of N_2, attributable to codenitrification, were at a maximum when soil nitrite (NO_2^-) concentrations were elevated. Cumulative codenitrification was higher ($P = 0.043$) at −1 kPa. However, the ratio of codenitrification to denitrification did not differ significantly with soil moisture, 25.5 ± 15.8 and 12.9 ± 4.8% (stdev) at −1 and −10 kPa, respectively. Elevated soil NO_2^- concentrations are shown to contribute to codenitrification, particularly at −1 kPa.

The concentration of nitrous oxide (N_2O) in the atmosphere has increased since 1750 due to human activity with values surpassing the highest concentrations recorded in ice cores during the past 800,000 years, and exceeding the pre-industrial level by 20%[1]. Reductions in the anthropogenic forcing of Earth's climate system and the recovery of the ozone layer would be enhanced if anthropogenic emissions of N_2O were reduced[1,2]. However, the atmospheric N_2O concentration continues to increase, predominately due to agricultural intensification, with 80% of the increase resulting from increased fertilizer use and manure applications for the purpose of food production[3]. Nitrous oxide emissions from grazed grasslands make a significant contribution to anthropogenic N_2O emissions[4,5] as a consequence of ruminant urine patches supplying nitrogen (N) substrate that is in excess of the pasture sward's N requirement[6,7]. Emissions of N_2O from pastures result from microbial transformations of N substrates applied via nitrification, nitrifier-denitrification, heterotrophic denitrification (hereafter referred to as denitrification unless otherwise stated), and codenitrification[8–10]. A further significant consequence of denitrifying mechanisms is the production and loss of dinitrogen (N_2). Although environmentally benign, N_2 losses lead to poor N use efficiency and reduced production, resulting in economic losses through the need to add further inorganic N. While reactive N (Nr) losses, such as nitrate (NO_3^-) leaching and ammonia (NH_3) volatilization, are well researched, the loss of N_2 from pasture systems is poorly studied and often only identified by default via the application of N balance methods[11]. For example, of the N applied to grasslands some 20–40% is typically unaccounted for and assumed to be lost as N_2[11–13]. Therefore, methods to reduce emissions of both N_2O and N_2 require a better understanding of the emission pathways.

Shoun *et al.*[14] and Tanimoto *et al.*[15] first described codenitrification after demonstrating, with ^{15}N tracer, that N_2O and N_2 production occurred in a different manner to the routinely accepted pathways of nitrification and

[1]Department of Soil and Physical Sciences, Lincoln University, Lincoln, New Zealand. [2]Teagasc, Environmental Research Centre, Johnstown Castle, Wexford, Ireland. [3]AgResearch Invermay, Mosgiel, New Zealand. [4]Department of Microbiology and Immunology, Otago School of Medical Sciences, University of Otago, Dunedin, New Zealand. [5]Department of Environmental Sciences, Norwegian University of Life Sciences, Ås, Norway. [6]Statistics and Applied Physics, Teagasc, Ashtown, Dublin 15, Ireland. Correspondence and requests for materials should be addressed to T.J.C. (email: Timothy.Clough@lincoln.ac.nz)

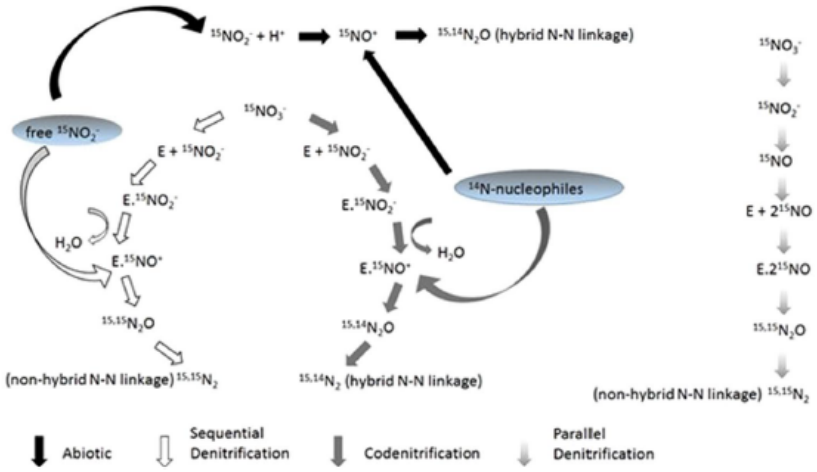

Figure 1. Simplified diagram (adapted from Spott *et al.*[16], Weeg-Aerssens *et al.*[18], Schmidt *et al.*[55]) showing abiotic denitrification, parallel denitrification, sequential denitrification and codenitrification pathways. During abiotic production an electrophile (e.g. the nitrosonium cation NO^+ which is formed under acidic soil conditions) replaces the hydrogen atom of a nucleophile with a hybrid N-N bond formed following deprotonation. The parallel pathway results in a non-hybrid N-N bond as the result of two NO_2^- or two NO molecules being bound, simultaneously to one enzyme (E), which theoretically excludes the possibility of a nitrosation reaction occurring and the formation of a hybrid N-N bond[55,56]. However, a two-step process occurs in the sequential pathway when NO_2^- or NO molecules initially bind to an enzyme (E) followed by a free NO_2^-, or NO molecule, (originating from the original NO_3^- pool) reacting with the enzyme complexed N species to form a non-hybrid N-N bond. The two-step sequence also permits the enzyme complexed N species to function as an electrophile which is able to be to be attacked by nucleophiles producing a hybrid N-N bond. Nucleophiles able to partake in codenitrification reactions include amines, ammonium, hydrazine, and ammonia.

denitrification. It has been suggested that codenitrification results from microbially mediated N-nitrosation reactions[14–16]. Codenitrification is one of the least studied N loss pathways and its contribution to agricultural N_2O and N_2 emissions remains unclear[17].

Codenitrification is a process that co-metabolises organic N compounds, such as amines, to produce N_2O and/or N_2, and is also referred to as biotic N-nitrosation[16]. Codenitrification involves the replacement of a hydrogen atom in an organic compound with a nitroso group (—N=O). Under near neutral to alkaline soil pH conditions, common to pasture soils, codenitrification may occur via enzymatic catalysis (Fig. 1), with enzymatic nitrosyl compounds (E-NO^+ or E-NO) attracting nucleophilic compounds[16,18]. Nucleophiles involved in codenitrification include hydroxylamine, ammonium (NH_4^+), hydrazine, amino compounds, and ammonia (NH_3). The resulting gas products formed, N_2O or N_2, contain one N atom originating from the inorganic-N (e.g. NO_2^-), and a second atom from the co-metabolised organic compound[16,18]. Significant rates of both partial and complete codenitrification are only likely to occur if nucleophile concentrations are at least one or two orders of magnitude greater than that of NO_2^- and NO[16].

Heterotrophic denitrification results in the reduction of NO_3^- to N_2 with nitrite (NO_2^-), nitric oxide (NO), and N_2O obligate intermediaries[19] (Fig. 1). Formation of the N_2O molecule is recognized as occurring via parallel or sequential pathways[16] and references therein. In the parallel pathway simultaneous bonding of two NO_2^- or two NO molecules to an enzyme, where both NO_2^- and NO are derived from the same NO_3^- source, creates a non-hybrid N-N bond, thus precluding the occurrence of codenitrification[16]. However, a two-step reaction, the sequential pathway, results in either NO_2^- or NO initially bonding with an enzyme, which in turn may react with either free NO_2^- or NO to form a non-hybrid N-N bond, or alternatively, this enzyme bound N can act as an electrophile and react with nucleophiles (e.g. amines) to form a hybrid N-N bond (Fig. 1). Consequently, hybrid N-N gas production, codenitrification, can occur simultaneously as a result of conventional denitrification (Fig. 1)[16]. Formation of hybrid N_2 has also been reported to occur when NH_3, hydrazine (N_2H_4) or amines are co-metabolised during codenitrification[20].

Abiotic nitrosation is also a well-recognized phenomena[21,22]. In abiotic reactions, free NO_2^- derived from nitrification or denitrification processes is chemically transformed to produce the nitrosonium cation (NO^+) under acidic conditions. The NO^+ cation reacts with a nucleophile (e.g. amine) to produce a hybrid N-N linkage (Fig. 1)[16] and references therein. This process differs from codenitrification since the formation of the NO^+ electrophile is chemically dependent on the soil pH and involves free NO_2^- in the soil solution as the precursor. Nucleophiles involved in abiotic reactions include hydroxylamine, NH_4^+, hydrazine, amines, and NH_3. However, relatively high soil pH values under grazed pasture conditions mean that the equilibrium concentrations of free nitrosating agents are generally inadequate for abiotic nitrosation to be significant[16].

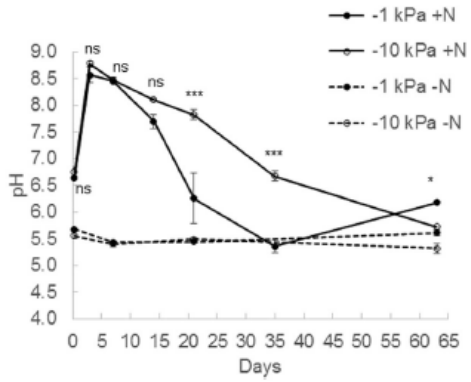

Figure 2. Changes in soil pH over time. Soil pH under near saturated (−1 kPa) or field capacity (−10 kPa) soil moisture conditions, following urea application (+N) or nil urea application (−N). Symbols are means (n = 4) with vertical error bars the standard error of the mean. Asterisks *,**,***indicate significant differences between moisture treatments under urea treatments at $P < 0.05$, $P < 0.01$, and $P < 0.001$, respectively.

In grazed pastures ruminant urine deposition onto pasture soil temporarily elevates soil pH following urea hydrolysis, creating a urinary-N cascade that produces potential nucleophiles (e.g. NH_4^+ and NH_3) at high concentrations. Simultaneously, enzyme bound nitrosating agents (E-NO^+ or E-NO), may be formed during denitrification of nitrate (NO_3^-) or as supplied by NO_2^- or NO during processes such as nitrification of nitrifier-denitrification[19]. Thus urine patches are potentially conducive to codenitrification occurring. In the only *in vivo* study to date to focus on codenitrification, Selbie *et al.*[23] confirmed the occurrence of codenitrification within ruminant urine-affected pasture soil with 95% of the N_2 emitted over 123 days resulting from codenitrification, with N_2 the dominant product, and where the codenitrified N_2 was equivalent to 56% of the N applied. This experiment by Selbie *et al.*[23] received regular rainfall and it may be that the dominance of codenitrified N_2 over codenitrified N_2O may have been the result of, as the authors suggest, hybrid N_2O being converted to hybrid N_2 via heterotrophic denitrification (Fig. 1). Conceptually, the recognized environmental constraints on denitrification should also apply to codenitrification[16], since codenitrification depends on enzyme bound nitrosyl compounds, formed during denitrification, being present (Fig. 1). A key driver of denitrification is the soil's oxygen status, and wetter soils result in higher levels of anaerobiosis since oxygen diffuses 1×10^4 times slower through water when compared to air[24]. Thus wetter soils should have higher rates of codenitrification. In order to test this hypothesis, and better understand the constraints and importance of codenitrification in pasture soils, we performed an experiment using either saturated soil or soil at field capacity to determine relative rates of codenitrification. The objective of the study was to investigate the effect of soil moisture on the rate of codenitrification from simulated urine applied to a free draining permanent grassland soil.

Results

Soil moisture, pH, DOC and inorganic-N. The −1 kPa and −10 kPa moisture treatments imposed resulted in average WFPS values (%±s.e.m) of 88.9 ± 1.1 and 48.5 ± 0.4, respectively. The relative gas diffusivity values at −1 and −10 kPa were 0.0028 and 0.2079, respectively. There was a significant interaction of soil moisture and sampling date ($p < 0.001$) on soil pH, DOC and inorganic N contents (Figs 2–4). Soil pH in the non-urea treatment was generally constant over time (Fig. 2) regardless of soil moisture treatment, averaging 5.49 ± 0.11 (Stdev). However, soil pH ($p < 0.001$) increased within 6 hours of urea application, and increased further, peaking at 8.57 ± 0.29 and 8.78 ± 0.09 in the −1 kPa and −10 kPa treatments, respectively, on day 3 before declining over time (Fig. 2). On days 21 and 35 the soil pH was lower in the −1 kPa treatment than in the −10 kPa treatment ($p < 0.001$) with the reverse occurring on day 63 ($p < 0.05$).

Soil DOC was higher ($P < 0.001$) under the urea treatment throughout the experiment (Fig. 3) and within the urea treatment soil DOC concentrations were significantly lower at −1 kPa than at −10 kPa from day 3 to day 62 (Fig. 3). In the urea treatment soil DOC correlated strongly with soil pH at both −1 kPa ($r = 0.79$; $p < 0.001$) and −10 kPa ($r = 0.89$; $p < 0.001$).

Soil NH_4^+-N concentrations increased following urea application (Fig. 4), peaking at day 3 and then declining over time with a faster rate of decline in the −1 kPa treatment from day 14 ($p < 0.05$) such that soil NH_4^+-N concentrations were lower at −1 kPa on days 35 and 63 (Fig. 4). The ^{15}N enrichment of the NH_4^+-N in the urea treatment declined from 44 to 37 atom% over the experiment with higher ^{15}N enrichment on days 14, 21 and 35 in the −10 kPa treatment (Fig. 5). Concentrations of NO_2^--N increased from day 7 under the urea treatment and peaked at day 21, with more NO_2^--N present in the −1 kPa treatment, prior to returning to background levels at day 35 (Fig. 4). Concentrations of NO_2^--N, extracted from the urea treatment, were only sufficient for ^{15}N enrichment determinations on days 14 and 21, where the ^{15}N enrichment was higher ($p < 0.05$) at −1 kPa than at −10 kPa on day 14, with no differences on day 21 (Fig. 5). Soil NO_3^--N concentrations also began to increase at day 7 under the urea treatment and were consistently higher ($p < 0.001$) in the −1 kPa treatment on days 14 and 21. Soil NO_3^--N concentrations peaked on day 35, before they declined to be less than those observed in the

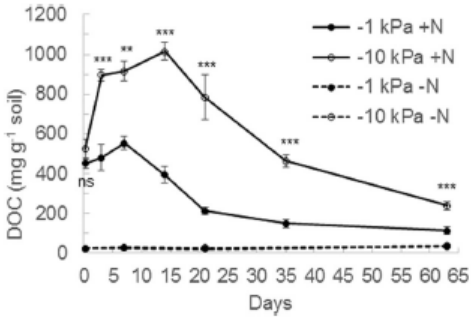

Figure 3. Changes in soil cold water extractable organic carbon (DOC) over time. Concentrations of soil DOC under near saturated (−1 kPa) or field capacity (−10 kPa) soil moisture conditions, following urea application (+N) or nil urea application (−N). Symbols are means (n = 4) with vertical error bars the standard error of the mean. Asterisks *,**,***indicate significant differences between moisture treatments under urea treatments at $P < 0.05$, $P < 0.01$, and $P < 0.001$, respectively.

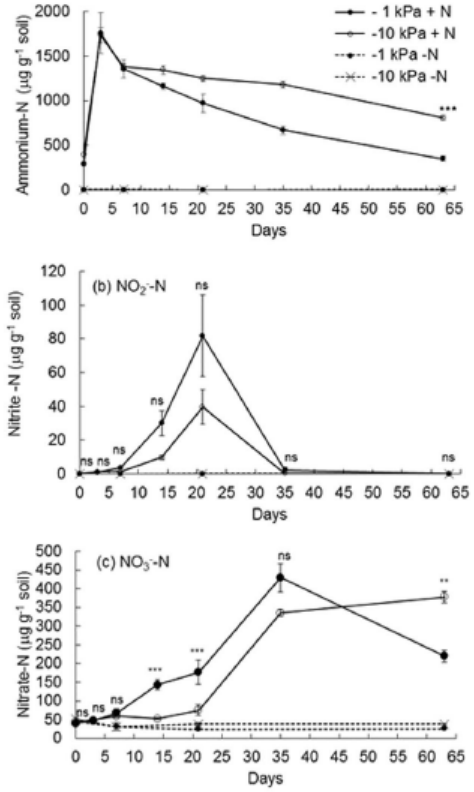

Figure 4. Changes in soil inorganic-N over time. Concentrations of extractable (**a**) ammonium-N (**b**) nitrite-N and (**c**) nitrate-N under near saturated (−1 kPa) or field capacity (−10 kPa) soil moisture conditions, following urea application (+N) or nil urea application (−N). Symbols are means (n = 4) with vertical error bars the standard error of the mean. Asterisks *,**,***indicate significant differences between moisture treatments under urea treatments at $P < 0.05$, $P < 0.01$, and $P < 0.001$, respectively.

−10 kPa treatment ($p < 0.01$) at day 63 (Fig. 4). Changes in soil NO_3^--^{15}N enrichment reflected the concentration dynamics with ^{15}N enrichment increasing faster at −1 kPa to 41 atom% ^{15}N at day 21 while at −10 kPa the NO_3^--^{15}N enrichment was only 34 atom% ^{15}N by day 63 (Fig. 5).

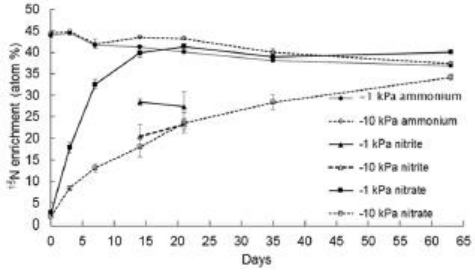

Figure 5. Inorganic-N ^{15}N enrichment over time. The ^{15}N enrichment of the ammonium-N (NH_4^+-N), nitrite-N (NO_2^--N) and nitrate-N (NO_3^--N) are shown over time following ^{15}N urea application at near saturated (−1 kPa) or field capacity (−10 kPa) soil moisture conditions. Symbols are means (n = 4) with vertical error bars the standard error of the mean.

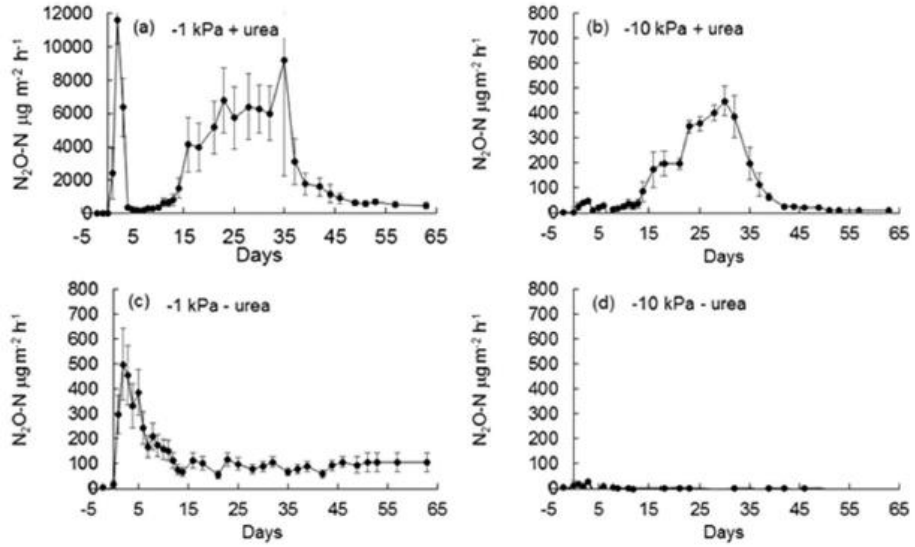

Figure 6. Nitrous oxide fluxes over time. Fluxes of N_2O under near saturated (−1 kPa) or field capacity (−10 kPa) soil moisture conditions, following urea application (+N) or nil urea application (−N) where (**a**) −1 kPa +N (**b**) −10 kPa +N (**c**) −1 kPa –N and (**d**) −10 kPa –N show N_2O fluxes over time. Note differing y-axis scales. Symbols are means (n = 4) with vertical error bars the standard error of the mean.

N_2O-N fluxes and ^{15}N enrichment. Trends in daily N_2O fluxes differed with treatment (Fig. 6). At −10 kPa in the absence of urea N_2O-N fluxes were generally $<5\,\mu g\ m^{-2}\ h^{-1}$, with fluxes only greater than this ($\leq 29\,\mu g\ m^{-2}\ h^{-1}$) between day 0 and day 10 following treatment application (Fig. 6). Under the −1 kPa treatment, in the absence of urea, N_2O-N fluxes also peaked after water application on day 2 at $498\,\mu g\ m^{-2}\ h^{-1}$, before declining to ca $100\,\mu g\ m^{-2}\ h^{-1}$ on day 12, where after N_2O-N fluxes were constant until day 63, averaging $92\,\mu g\ N_2O\text{-}N\ m^{-2}\ h^{-1}$ between days 12 to 63 (Fig. 6). Adding urea at −10 kPa caused N_2O-N fluxes to increase steadily from day 12 until they peaked at day 30 ($449\,\mu g\ m^{-2}\ h^{-1}$) where after they steadily declined to $<10\,\mu g\ m^{-2}\ h^{-1}$ by day 51 (Fig. 6). The highest N_2O-N fluxes were observed at −1 kPa with urea addition, where a rapid increase in the flux occurred peaking at $11{,}603\,\mu g\ m^{-2}\ h^{-1}$ on day 2, followed by a rapid decrease to $163\,\mu g\ m^{-2}\ h^{-1}$ by day 7. Then the flux gradually increased until day 35 ($9220\,\mu g\ m^{-2}\ h^{-1}$) whereupon it too decreased to be $476\,\mu g\ m^{-2}\ h^{-1}$by day 61 (Fig. 6).

Soil moisture treatment influenced cumulative N_2O-N fluxes ($p < 0.001$) with total emissions of 0.08 and 2.26 g N_2O-N m^{-2} at −10 and −1 kPa, respectively, when averaged over plus and minus urea treatments. Similarly, application of urea increased cumulative N_2O-N fluxes ($p < 0.001$) from 0.10 to 2.25 g N_2O-N m^{-2} when averaged over soil moisture treatments. An interaction between soil moisture and N application ($p < 0.002$) resulted in higher cumulative N_2O-N fluxes at −1 kPa when urea was applied equal to 3.99 g m^{-2} (Table 1). The N_2O-N emission factors for the urea-N applied, allowing for non-N fluxes equated to 4.14% and 0.18% of N applied at −1 kPa and −10 kPa, respectively.

Urea-N	Moisture (kPa)	N_2O		N_{2DN}		N_2co	
+N	−1	3.99	A	8.61	A	1.92	A
+N	−10	0.18	B	1.98	A	0.26	B
−N	−1	0.16	B	na		na	
−N	−10	−0.0003	C	na		na	
P value		0.0321		0.0554		0.0437	

Table 1. Mean cumulative N_2O, N_{2DN} and N_2co emissions (g N m^{-2}). P values are for the interaction between treatments. Tukey-Kramer grouping: LS-means with the same letter are not significantly different, na not applicable. N_{2DN} and N_2co represent heterotrophic denitrification and codenitrification, respectively.

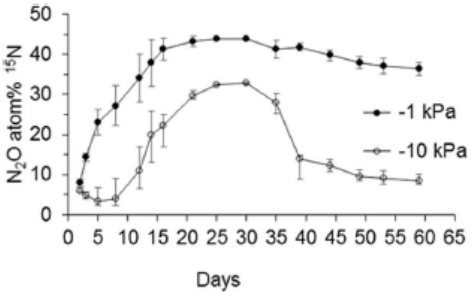

Figure 7. Nitrous oxide ^{15}N enrichment over time. The ^{15}N enrichment of the N_2O molecule, over time, is shown for N_2O evolved from soil under near saturated (−1 kPa) or field capacity (−10 kPa) conditions, following ^{15}N urea application. Symbols are means (n = 4) with vertical error bars the standard error of the mean.

Upon urea application, the atom % ^{15}N enrichment of the N_2O emitted at −1 kPa increased steadily to reach a maximum value of 43.9 atom % ^{15}N on day 25 before declining at a relatively slow rate to a value of 36.3 atom % ^{15}N by day 59 (Fig. 7). With the exception of day 2, the atom % ^{15}N enrichment of the N_2O emitted at −1 kPa was higher than that emitted at −10 kPa ($P < 0.05$) on any given day. At −10 kPa the atom % ^{15}N enrichment of the N_2O flux was observed to increase abruptly at day 12, reaching a maximum of 32.8 on day 30 and thereafter declining relatively abruptly to remain at ca 10 atom % ^{15}N (Fig. 7). Fluxes of N_2O associated with codenitrification were low and only measurable on days 2, 5, 8 and 12 for the −1 kPa treatment and days 3, 5, 8, 12 and 16 for the −10 kPa treatment (Fig. 8). Highest fluxes were observed for the −1 kPa treatment (3637 μg N_2O-N m^{-2} hr^{-1}) comprising 20% of total N_2O flux with emissions of codenitrified N_2O subsequently reducing rapidly. Codenitrified N_2O fluxes in the −10 kPa treatment were extremely low and never rose above 70 μg N_2O-N m^{-2} hr^{-1}).

N_2 fluxes and codenitrification after urea addition. The average daily denitrification fluxes were 1.48 (0.34) g N m^{-2} d^{-1} and 0.53 (0.07) g m^{-2} d^{-1} (s.e.m in brackets) at −1 and −10 kPa, respectively. At −1 kPa denitrification fluxes initially peaked at day 5 and then were higher after day 30, peaking on day 49 (Fig. 8). The decline in soil NO_3^- concentration after day 35 coincided with higher denitrification fluxes. At −10 kPa denitrification fluxes were highest after the initial wetting up following treatment application where after they generally declined (Fig. 8). Consequently, cumulative denitrification as N_2 was higher ($p = 0.055$) at −1 kPa, totaling 8.61 g N m^{-2}, than at −10 kPa where observed fluxes were 1.98 g N m^{-2} (Fig. 8).

The average daily codenitrification fluxes under urea treatments at −1 and −10 kPa were 0.38 (0.15) g N m^{-2} d^{-1} and −10 kPa 0.07 (0.01) g N m^{-2} d^{-1}, respectively. Codenitrification fluxes peaked on day 12 regardless of soil kPa value, but were higher on day 10 at −1 kPa (Fig. 8). Average daily codenitrification fluxes were ca 5-fold higher at −1 kPa after day 30 than at −10 kPa. Consequently, cumulative codenitrification rates of N_2 were also higher ($p = 0.043$) at −1 kPa (1.91 g N m^{-2}) than at −10 kPa (0.26 g N m^{-2}). Cumulative codenitrification, as a proportion of denitrification, did not vary as a result of soil matric potential equaling 25.5 ± 15.8% and 12.9 ± 4.8% (±stdev) at −1 and −10 kPa, respectively. The contribution of codenitrification as a proportion of total denitrification (codenitrification plus denitrification) also did not vary with soil matric potential, being 19.3 ± 10.4% and 11.3 ± 3.8% (±stdev) at −1 and −10 kPa, respectively.

Discussion

Inorganic-N pools and ^{15}N enrichment. Following urea application to the soil the ensuing hydrolysis produces NH_4^+ and bicarbonate (HCO_3^-) ions. The HCO_3^- ions are further hydrolysed to produce hydroxide ions (OH^-) and carbon dioxide[25] and it is this second hydrolysis reaction that generated the observed increase in soil pH under the urea treatments (Fig. 2). Elevated soil pH also influences the equilibrium between NH_4^+ and ammonia (NH_3): as soil pH becomes elevated (>7.0) concentrations of NH_3 increase[25]. Urea-N not volatilized as NH_3 may be transferred along the inorganic-N cascade via NH_4^+, NO_2^- and NO_3^-.

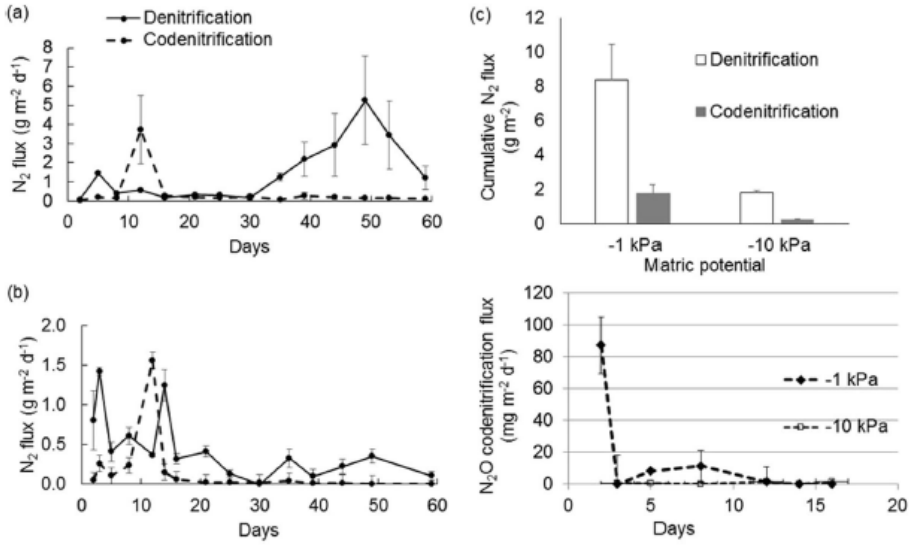

Figure 8. Denitrification and codenitrification fluxes over time. The codenitrification and denitrification fluxes, over time since ^{15}N urea addition, are shown as daily N_2 fluxes for (**a**) soil at −1 kPa (**b**) soil at −10 kPa and (**c**) as cumulative codenitrification and denitrification N_2 fluxes, while (**d**) is the N_2O codenitrification flux, over time since ^{15}N urea addition, as daily N_2O fluxes. Symbols are means (n = 4) with vertical error bars the standard error of the mean.

During nitrification microbes utilise NH_4^+ and oxidise it to NO_2^-. Elevated NH_3 concentrations may inhibit NH_4^+ oxidation[26,27]. Thus the slower decline in the NH_4^+ concentration observed in the −10 kPa treatment, under urea, may have been due to NH_3 inhibition of nitrification. In favour of this were both the relative gas diffusivity of the soil being 2 orders of magnitude higher at −10 kPa, which would have facilitated NH_3 diffusion through the soil, and the soil pH remaining higher for longer (Fig. 2). The latter would have promoted the presence of NH_3 for longer. A slower rate of decline in soil pH at −10 kPa also demonstrates nitrification was slower, since nitrification results in the net release of H^+ ions[19]. Further evidence to support a slower rate of NH_4^+ oxidation can be found in the slower rate of increase in ammonium oxidizing bacteria (*AOB*) gene and transcript abundance[28].

Elevated soil NO_2^- concentrations resulted from nitrification of NH_4^+ and their increase, from day 5 until day 20, occurred over a period when soil pH was sufficiently high to result in NH_3 generation. Ammonia toxicity acts more strongly on nitrifier NO_2^- oxidation than nitrifier NH_4^+ oxidation[29]. It has been shown that solution-phase NH_3 (*sl*NH_3) inhibits NO_2^- oxidation, as evidenced by strong relationships between cumulative *sl*NH_3 and cumulative NO_2^- and static copy numbers of the *nxr*A gene, which is associated with nitrite oxidoreductase, and as a consequence soil NO_2^- is strongly correlated with N_2O production[29]. The high N_2O fluxes that occurred, between ca. days 7 to 35, at both −1 and −10 kPa under urea, where the soil NO_2^- concentrations were elevated strongly demonstrates this, and it can be assumed *sl*NH_3 induced NO_2^- toxicity lead to the ensuing N_2O emissions.

The higher NO_3^- concentrations observed under urea on days 14 and 21 at −1 kPa were a consequence of the more rapid nitrification rates in this treatment, while the lower NO_3^- concentration in this treatment observed at day 63 resulted from higher denitrification induced losses of NO_3^-, which is further supported by the increase in soil pH under this treatment, since denitrification results in a net release of OH^- ions[19].

The ^{15}N enrichment of the NH_4^+ pool, under urea, shows that it was predominantly derived from the urea applied, regardless of soil moisture treatment. The fact the NH_4^+ pool ^{15}N enrichment was initially ca. 5 atom% lower than the urea solution applied was likely due to the release of NH_4^+ as a consequence of the high soil pH solubilising soil organic matter, as demonstrated by the elevated DOC concentrations under the urea treatment. Solubilisation of soil organic matter is routinely observed following urine or urea application to soil[30]. The reason for the NO_2^- pool ^{15}N enrichment being ca. half that observed in the NH_4^+ pool on days 14 and 21 at −1 kPa, shows antecedent soil N was also contributing to this pool which could have come from mineralization and subsequent oxidation of NH_4^+, despite the presence of NH_3, since relatively low quantities of NH_4^+ would be needed to dilute the NO_2^- pool, or alternatively there may have been some denitrification of antecedent NO_3^- generating NO_2^-. The fact that the NO_3^- pool ^{15}N enrichment aligned closely with that of the NO_2^- pool ^{15}N enrichment at −10 kPa demonstrates NO_2^- was the dominant precursor to NO_3^- pool at −10 kPa. Furthermore, the slower rate of increase in the NO_3^- pool ^{15}N enrichment at −10 kPa, when compared to −1 kPa, further supports the fact there was a slower rate of nitrification at −10 kPa. The increase in the NO_3^- pool ^{15}N enrichment over time, in both the −1 and −10 kPa treatments, demonstrates the NO_3^- pool was initially dominated by antecedent soil NO_3^- as in fact occurred (Fig. 4c).

N_2O fluxes and ^{15}N enrichment. While simply wetting of the soil, as occurred under the non-urea treatment, induced N_2O fluxes at −1 kPa, this wetting effect was not sufficient to generate the high N_2O fluxes observed under urea from days 0 to 4. These high initial N_2O fluxes under urea, as previously observed[31], are due to the chemically induced anoxia that results from the hydrolysis reactions generating both NH_3 and CO_2, as demonstrated *in situ*[32]. Such high fluxes were not observed at −10 kPa during this period because the higher relative gas diffusivity of the soil at −10 kPa ensured the soil was not as anaerobic.

As noted above periods of high N_2O flux between days 14 and 37 aligned with the presence of elevated NO_2^- concentrations. The atom % ^{15}N enrichment of the N_2O at −10 kPa was comparable with that of the NO_2^- pool at this time, further demonstrating that the N_2O flux predominately originated from the NO_2^- pool, and because the ^{15}N enrichment of the N_2O declined as NO_2^- concentrations declined. Despite both the NO_3^- concentration and NO_3^- ^{15}N enrichment both increasing after this time, this was not reflected in any increased N_2O fluxes or its ^{15}N enrichment because the higher relative gas diffusivity at −10 kPa made conditions unsuitable for the denitrification of NO_3^-[24].

However, at −1 kPa the N_2O evolved predominately via denitrification of the NO_3^- pool up until ca. day 15 as demonstrated by the alignment of the N_2O ^{15}N enrichment with the NO_3^- pool ^{15}N values. The higher N_2O fluxes at −1 kPa between days 15 to 35 were ca. 15-fold higher due to the more anaerobic conditions and, as inferred above, are presumed to have occurred as a result of the relatively high NO_2^- concentrations over this period. However, the N_2O ^{15}N enrichment did not reflect that of the KCl extracted NO_2^- pool measured on days 14 and 21 at −1 kPa, but did reflect that of the NH_4^+ and NO_3^- pools on these days. Differences in the ^{15}N enrichment of the KCl extracted NO_2^- and actual *in situ* ^{15}N enrichment of the NO_2^- pool may possibly have arisen due to the method of treatment application where, in the −10 kPa treatment the urea solution infiltrated further and contacted a greater soil volume than at −1 kPa, as evidenced by the greater release of DOC at −10 kPa (Fig. 3), and which would have resulted in a more uniform NO_2^- pool. It is likely that, at −1 kPa, denitrification of antecedent NO_3^- occurred and that this generated sufficient NO_2^- to isotopically dilute the relatively small ^{15}N enriched NO_2^- pool, derived from NH_4^+ and/or NO_3^-, when the soil was extracted. After day 35, the N_2O ^{15}N enrichment reflected that of the NO_3^- pool, and given the compatible conditions for denitrification, it can be assumed that denitrification of the NO_3^- pool dominated N_2O production after day 30, and this assumption is supported by the elevated denitrification flux occurring after this time (Fig. 8).

N_2 denitrification and codenitrification of N_2 and N_2O. As expected denitrification occurred at higher rates under the more anaerobic moisture treatment as a result of the lower *Dp/Do* conditions promoting denitrification in the presence of NO_3^- substrate.

The N transformations that ensued following urea hydrolysis, and hydrolysis itself, generated previously recognized codenitrification nucleophiles that include NH_4^+, NH_3, and possibly organic-N compounds such as amines[16]. The latter might occur as a result of the dissolution of soil organic matter. While the enzymatically utilized NO_2^- and NO compounds, that form electrophiles, are generated during nitrification and denitrification[19].

Codenitrification N_2O fluxes were generally low for both treatments, with measurable values mainly associated with the initial soil wetting. Conversely, codenitrification to N_2 was observed to peak on day 12, regardless of soil moisture, when NH_3, NH_4^+ and NO_2^- were all present at an elevated soil pH (≥7.70), and at relatively high concentrations. Thus it is possible that either NH_3 or NH_4^+ were undertaking the role of the nucleophile at this time, since the elevated pH (>5.5) would have prevented any significant abiotic nitrosation occurring via NO^+ formation[16]. Recently, however, the formation of both N_2O and N_2, under both oxic and anoxic conditions, was reported in an *in vitro* experiment maintained at pH 6.2–6.9 where either live fungi or fungal necromass were incubated with glutamine and NO_2^-[33]. A subsequent isotope experiment with glutamine and $^{15}NO_2^-$ demonstrated the hybrid formation of N_2 after an incubation period of >7 days, again under either oxic or anoxic conditions[33]. Hence, based on this recent study, even though the soil in the current study was at a pH (≥7.70) sufficient to prevent acidic pathways of abiotic hybrid N-N bonds forming, we cannot rule out the possibility that abiotic reactions, under alkaline conditions, contributed to the codenitrification flux measured in the current experiment.

Production of N_2O or N_2 via biotic codenitrification may result from the actions of archaea, bacteria or fungi. While archaea have been found to generate N_2O through N-nitrosating hybrid formation[34] they are unlikely to have been the dominant mechanism in the current study since archaea are thought to prefer low N conditions[35,36] and urea addition resulted in lower ammonia oxidizing archaea gene copy numbers[28]. The codenitrification observed is most likely to be the result of fungi or bacterial activity. Delineation of the relative contributions made by fungi or bacteria to codenitrification is beyond the scope of the present study, however, future studies should aim to examine relative fungal and bacterial contributions.

Spott *et al.*[16] conceptualized that the recognized constraints on denitrification might also apply to codenitrification, and thus higher codenitrification fluxes might be expected under more anaerobic conditions. The current results support this concept: after day 30 the higher daily codenitrification fluxes under the more anaerobic (−1 kPa) soil moisture conditions, when at the same time denitrification fluxes were higher, resulted in higher cumulative codenitrification fluxes. This reinforces the fact that NO_2^- and or NO play a key role in the codenitrification process. The NO molecule has been observed to readily diffuse within the soil profile[37], at relatively high concentrations, during denitrification and this would result in reactions with nucleophiles.

Unlike the results of Selbie *et al.*[23] codenitrification did not dominate the N_2 fluxes observed in the current study. This could be the result of the experimental system used in the current study differing to that used by Selbie *et al.*[23]. Differences include the lack of a pasture turf and associated microbiology and root exudation, the use of sieved repacked soil that may also have altered the fungal-bacterial community structure or activity as a result of sieving, constant soil moisture contents as opposed to wetting and drying events, and the lack of other climatic variables such as wind and rainfall.

Depth	Bulk density (Mg m^{-3})	Porosity (%)	Texture	Sand (%)	Silt (%)	Clay (%)
0–10	1.19	0.55	Sandy loam	53	31	16
10–20	1.28	0.52	Sandy loam	55	31	14

Table 2. Physical and textural characteristics of soil sampled.

In particular, fungal populations may have been reduced on sieving, and given that fungal P450 NOR is implicated in supplying enzyme bound nitrosating agents this could have had a significant influence on the results[38]. Given that enzyme bound nitrosating agents produced during denitrification may also consist of metal-nitrosyl complexes[16] any differences in soil Fe and Cu levels between studies may also explain the observed differences in codenitrification. Likewise, differences in the kinetic properties of different nucleophiles, combined with the ratio of NO or NO_2^- availability to nucleophile concentration, have also been shown to significantly impact on codenitrification/denitrification: lower K_m and high nitrosyl donor/nucleophile ratios have been shown to reduce the level of codenitrification[15,20].

This study confirms the role of anaerobic soil conditions in enhancing codenitrification fluxes under ruminant urine/urea deposition. It also demonstrates for the first time that high levels of NO_2^-, or other transitional N compounds ensuing from NO_2^-, that may occur during nitrification, are also able to contribute to codenitrification processes. To progress knowledge of codenitrification in grazed pastures more detailed studies are now required to both identify the microbial pathways operating and the relative importance of the possible nucleophiles and nitrosating agents that occur in grazed pastures.

Materials and Methods

Soil collection and experimental design. Soil was collected in early spring (March) from a permanently grazed dairy pasture at the Teagasc Moorepark Research Centre, County Cork, Ireland (8°15′W, 52°9′N). The top 5 cm of soil was removed and the A-horizon was sampled, 5–20 cm depth. Soil physical and textural characteristics are shown in Table 2. Cows had not grazed the pasture for over one month so recent urine deposition sites were avoided. The soil is classified as a Typical Brown earth from the Clashmore Series[39], or as a Haplic Cambisol in the World Reference Database[40]. Field moist soil was then bagged and shipped to Lincoln University, New Zealand, following appropriate biosecurity protocols. It was then sieved (≤2 mm) to remove any stones, plant roots or earthworms. Sieved soil, with a gravimetric water content (θg) of 0.24 g water g^{-1} soil, was then packed into stainless steel rings (7.3 cm internal diameter, 7.4 cm deep) to a depth of 4.1 cm at a bulk density of 1.1 Mg m^{-3}, the latter simulating the *in situ* soil bulk density. This resulted in a total porosity of 0.58 cm^3 pores cm^{-3} soil. Packed soil cores were then arranged in a factorial experiment replicated four times.

Treatments consisted of two levels of soil moisture, −1 kPa and −10 kPa simulating 'near-saturation' and 'field-capacity', respectively, and two levels of urea, (0 and 1000 kg N ha^{-1}), replicated 4 times, with 7 destructive sampling times (112 cores in total). Preliminary tests showed that −1 and −10 kPa corresponded to 53% and 30% volumetric water content, or 91% and 52% water-filled pore space (WFPS). Soil cores were maintained at these water contents using tension tables[41]. Soil relative gas diffusivity values were calculated using the values for air-filled pore space and total porosity and the generalized-density corrected equation of Chamindu Deepagoda *et al.*[42]; Equation 9b. It is recognized that artificial urine simulation does not generate identical effects to ruminant urine[43], that urea contributes >70% of the total urine-N pool[6,44], and that this N source is predominately responsible for the subsequent dynamics and transformations of organic and inorganic N in the soil under ruminant urine patches. Thus, in order to apply the N treatments, soil cores were wetted up on the tension tables to a point where there remained the capacity to add a further 10 mL of liquid, without inducing drainage. Subsequently, in the plus N treatment, 10 mL of a urea solution (42 g urea-N L^{-1}; 50 atom%, Cambridge Isotope Laboratories Inc., USA) was slowly applied to the soil surface, to avoid drainage, to mimic an extreme bovine urine deposition event with a potentially high N_2 flux. Real urine could not be used since there was a need to have the urea-N highly enriched with ^{15}N to detect N_2 fluxes. In the nil N treatment 10 mL of deionized water was applied instead of a urea solution. Tension tables were maintained in a room with a mean temperature of 20 °C.

Soil chemical analyses. After treatment application and throughout the experiment, on days 0, 3, 7, 14, 21, 35, and 63, soil inorganic N concentrations were determined by destructively sampling 16 soil cores (2 levels of urea × two levels of soil moisture × 4 replicates). Soil cores were fully extracted, homogenized, and a subsample was taken to determine θg: by drying the soil at 105 °C for 24 hours. A flat surface pH electrode was used to determine soil pH (Broadley James Corp., Irvine, California). Then further soil subsamples were extracted (equivalent of 10 g dry soil: 100 mL 2 M KCl shaken for 1 hour) and filtered (Whatman 42) to determine soil inorganic-N. The NH_4^+-N, NO_2^--N, and NO_3^--N concentrations were analysed using flow injection analysis[45]. The ^{15}N enrichment of NH_4^+-N was determined according to Stark and Hart[46] while NO_2^--^{15}N and NO_3^--^{15}N enrichments were determined according to the methods of Stevens and Laughlin[47]. Concentrations of dissolved organic carbon (DOC) in the soil were measured according to Ghani *et al.*[48] with analyses performed on a Shimadzu TOC analyzer (Shimadzu Oceania Ltd., Sydney, Australia).

Gas flux determinations. Nitrous oxide and N_2 fluxes were regularly determined, from two days before until 63 days after treatment application using only the last batch of soil cores to be destructively analysed. This was performed by placing a soil core into a 1-L stainless steel tin fitted with a gas-tight lid and rubber septa. Samples for N_2O flux determinations were taken upon lid closure and then after 15 and 30 minutes. A further sample

was taken for N_2O-^{15}N enrichment and N_2 flux determination after 3 hours, after which cores were returned to the tension tables. Gas samples were taken using a 20-mL glass syringe fitted with a 3-way tap and a 0.5 mm by 16 mm needle and placed in either 6 mL vials for the N_2O flux determinations or 12 mL vials for the N_2O-^{15}N enrichment and N_2 flux samples (Exetainer; Labco Ltd., Lampeter, UK). An automated gas chromatograph (8610; SRI Instruments, Torrance, CA), coupled to an autosampler (Gilson 222XL; Gilson, Middleton, WI), was used to determine N_2O gas concentrations in the samples, as previously described[49]. A continuous-flow-isotope mass spectrometer (Sercon 20/20; Sercon, Chesire, UK) inter-faced with a TGII cryofocusing unit (Sercon, Chesire, UK), was used to determine the ^{15}N enrichment of the N_2O-N and N_2-N gas samples[50].

The ion currents (I) at mass to charge ratios (m/z) of 44, 45, and 46 facilitated the calculation of the N_2O molecular mass ratios ^{45}R ($^{45}I/^{44}I$) and ^{46}R ($^{46}I/^{44}I$). The N_2O sources were subsequently allocated to either the fraction derived from the denitrifying pool (d'_D) of enrichment aD or the fraction derived from the pool or pools at natural abundance $d'_N = (1\text{-}d'_D)$ using the method of Arah (1997). The ion currents at m/z 28, 29, and 30 permitted the N_2 molecular ratios ^{29}R ($^{29}I/^{28}I$) and ^{30}R ($^{30}I/^{28}I$) to be quantified. Differences between the N_2 molecular ratios of the enriched and ambient atmospheres were expressed as $\Delta^{29}R$ and $\Delta^{30}R$ The N_2 flux was subsequently calculated using three methods:

(i) The enrichment of the denitrifying pool ($^{15}X_N$) was calculated using $\Delta^{29}R$ and $\Delta^{30}R$, and then the N_2 flux[51],
(ii) Using only the $\Delta^{30}R$ data with the assumption that the enrichment of the denitrifying pool was aD[52] and the equation of Mulvaney[53]
(iii) Using $\Delta^{29}R$ and $\Delta^{30}R$ to calculate the relative contributions of denitrification (N_{2DN}), according to method (ii), and codenitrification (N_{2CO}).

Increases in $\Delta^{29}R$ and $\Delta^{30}R$ may occur from denitrification but codenitrification contributes most to $\Delta^{29}R$ where the ratio of $\Delta^{29}R$ to $\Delta^{30}R$ is always 272[54]. By assuming all $\Delta^{30}R$ was the result of denitrification, method (ii), N_{2DN} was calculated. Then using the 'backsolver' facility in Microsoft Excel™, the contribution of $\Delta^{29}R$ to N_{2DN} was determined. The difference between the total measured value of $\Delta^{29}R$ and $\Delta^{29}R$ determined for N_{2DN} was assigned to codenitrification. Thus the fraction of the total number of moles of N_2 in the headspace, resulting from codenitrification (d_{CD}) were calculated as:

$$d_{CD} = -\Delta^{29}Rp_1^2/(-\Delta^{29}Rp_1^2 + \Delta^{29}Rp_1p_2 + q_1p_2 - q_2p_1) \quad (1)$$

where p_1 (0.9963) and q_1 (0.0037) represent the atom fractions of ^{14}N and ^{15}N in the natural abundance pool, respectively, and p_2 and q_2 are the atom fractions of ^{14}N and ^{15}N in the enriched NO_3^- pool, respectively, from which codenitrification is assumed to occur. Using the headspace volume of the sample chamber, corrected for standard temperature and pressure, the mass of N_2-N in the headspace was determined with the amount derived from denitrification or codenitrification ascertained by multiplying by d_D or d_{CD}, respectively.

Data analyses. Data were analysed using the Glimmix procedure within the SAS® software version 9.4 (SAS, 2014). Cumulative results were analysed for the +N treatment only. For all other variables, analyses was as N treatment × moisture × day or moisture × day factorials. Any repeated measurements over time were modelled using correlation structures and spatial covariance was used to model the unequally-spaced time measurements. Residual checks were made and, where required, log transformation was used to correct for skew and non-constant variance. Multiplicity adjustments were made for simple effects within interactions, as interest was primarily in comparisons within time points.

References

1. IPCC, Summary for Policymakers. In Climate Change 2013: The Physical Science Basis. Contribution of Working Group I to the Fifth Assessment Report of the Intergovernmental Panel on Climate Change, edited by Stocker, T. F. *et al.*, pp. 1535 (Cambridge University Press, 2013).
2. Ravishankara, A. R., Daniel, J. S. & Portmann, R. W. Nitrous Oxide (N_2O): The Dominant Ozone-Depleting Substance Emitted in the 21st Century. *Science* **326**, 123–125, doi:10.1126/science.1176985 (2009).
3. Ciais, P. *et al.* Carbon and Other Biogeochemical Cycles. In: Climate Change 2013: The Physical Science Basis. Contribution of Working Group I to the Fifth Assessment Report of the Intergovernmental Panel on Climate Change. (Cambridge University Press, Cambridge, United Kingdom, 2013).
4. Hargreaves, P. R., Rees, R. M., Horgan, G. W. & Ball, B. C. Size and Persistence of Nitrous Oxide Hot-Spots in Grazed and Ungrazed Grassland. *Environ. Nat. Resor. Res.* **5**(4), 1, doi:10.5539/enrr.v5n4p1 (2015).
5. Oenema, O. *et al.* Trends in global nitrous oxide emissions from animal production systems. *Nutr. Cycl. Agroecosyst.* **72**(1), 51–65, doi:10.1007/s10705-004-7354-2 (2005).
6. Haynes, R. J. & Williams, P. H. Nutrient cycling and soil fertility in the grazed pasture ecosystem. *Adv. Agron.* **49**, 119–199, doi:10.1016/S0065-2113(08)60794-4 (1993).
7. Selbie, D. R., Buckthought, L. E. & Shepherd, M. A. The Challenge of the Urine Patch for Managing Nitrogen in Grazed Pasture Systems. *Adv. Agron.* **129**, 229–292, doi:10.1016/bs.agron.2014.09.004 (2015).
8. Zhu, X., Burger, M., Doaneb, T. A. & Howarth, W. R. Ammonia oxidation pathways and nitrifier denitrification are significant sources of N_2O and NO under low oxygen availability. *P Natl. Acad. Sci. USA* **110**(16), 6328–6333, doi:10.1073/pnas.1219993110 (2013).
9. Laughlin, R. J. & Stevens, R. J. Evidence for fungal dominance of denitrification and codenitrification in a grassland soil. *Soil Sci. Soc. Am. J.* **66**(5), 1540–1548, doi:10.2136/sssaj2002.1540 (2002).
10. Firestone, M. K. & Davidson, E. A. Microbiological Basis of NO and N_2O Production and Consumption in Soil In *Exchange of Trace Gases between Terrestrial Ecosystems and the Atmosphere*, edited by Andreae, M. O. & Schimel, D. S., pp. 7–21(John Wiley & Sons Ltd, New York, 1989).
11. Allison, F. E. The enigma of soil nitrogen balance sheets. *Adv. Agron.* **7**, 213–250, doi:10.1016/S0065-2113(08)60339-9 (1955).
12. Clough, T. J. *et al.* Resolution of the N-15 balance enigma? *Aust. J. Soil Res.* **39**(6), 1419–1431, doi:10.1071/SR00092 (2001).

13. Ball, R., Keeney, D. R., Theobald, P. W. & Nes, P. Nitrogen balance in urine-affected areas of a New Zealand pasture. *Agron. J* **71**, 309–314, doi:10.2134/agronj1979.00021962007100020022x (1979).
14. Shoun, H., Kim, D. H., Uchiyama, H. & Sugiyama, J. Denitrification by fungi. *FEMS Microbiol. Lett.* **94**, 277–281, doi:10.1111/fml.1992.94.issue-3 (1992).
15. Tanimoto, T., Hatano, K., Kim, D. H., Uchiyama, H. & Shoun, H. Co-denitrification by the denitrifying system of the fungus Fusarium oxysporum. *FEMS Microbiol. Lett.* **93**, 177–180, doi:10.1111/fml.1992.93.issue-2 (1992).
16. Spott, O., Russow, R. & Stange, C. F. Formation of hybrid N_2O and hybrid N_2 due to codenitrification: First review of a barely considered process of microbially mediated N-nitrosation. *Soil Biol. Biochem.* **43**, 1995–2011, doi:10.1016/j.soilbio.2011.06.014 (2011).
17. Baggs, E. M. & Philippot, L. Microbial terrestrial pathways to nitrous oxide. In *Nitrous Oxide and Climate Change* (Earthscan, 2010).
18. Weeg-Aerssens, E., Tiedje, J. M. & Averill, B. A. Evidence from isotope labeling studies for a sequential mechanism for dissimilatory nitrite reduction. *J Am. Chem. Soc.* **110**, 6851–6856 (1988).
19. Wrage, N., Velthof, G. L., van Beusichem, M. L. & Oenema, O. Role of nitrifier denitrification in the production of nitrous oxide. *Soil Biol. Biochem.* **33**, 1723–1732, doi:10.1016/S0038-0717(01)00096-7 (2001).
20. Kim, C. H. & Hollocher, T. C. Catalysis of nitrosyl transfer-reactions by a dissimilatory nitrite reductase (cytochrome-cd1). *J. Biol. Chem.* **259**, 2092–2099 (1984).
21. Van Cleemput, O. & Samater, A. H. Nitrite in soils: accumulation and role in the formation of gaseous N compounds. *Fert. Res.* **45**, 81–89, doi:10.1007/BF00749884 (1996).
22. Sen, S. & Chalk, P. M. Chemical interactions between soil N and alkaline-hydrolysing N fertilizers. *Fert. Res.* **36**, 239–248, doi:10.1007/BF00748702 (1993).
23. Selbie, D. R. *et al.* Confirmation of co-denitrification in grazed grassland. *Scientific Reports* 5, Article number: 17361 (2015).
24. Balaine, N., Clough, T. J., Beare, M. H., Thomas, S. M. & Meenken, E. D. Soil Gas Diffusivity Controls N_2O and N_2 Emissions and their Ratio. *Soil Sci. Soc. Am. J* (2016).
25. Avnimelech, Y. & Laher, M. Ammonia volatilization from soils: Equilibrium considerations. *Soil Sci. Soc. Am. J.* **41**, 1080–1084, doi:10.2136/sssaj1977.03615995004100060013x (1977).
26. Anthonisen, A. C., Loehr, R. C., Prakasam, T. B. S. & Srinath, E. G. Inhibition of nitrification by ammonia and nitrous acid. *J. Water Pollut. Control Fed.* **48**, 835–852 (1976).
27. Park, S. & Bae, W. Modeling kinetics of ammonium oxidation and nitrite oxidation under simultaneous inhibition by free ammonia and free nitrous acid. *Proc. Biochem.* **44**, 631–640, doi:10.1016/j.procbio.2009.02.002 (2009).
28. Samad, M. S. *et al.* Response to nitrogen addition reveals metabolic and ecological strategies of soil bacteria. *bioRxiv* (107961) (2017).
29. Venterea, R., Clough, T. J., Coulter, J. A. & Breuillin-Sessoms, F. Ammonium sorption and ammonia inhibition of nitrite-oxidizing bacteria explain contrasting soil N_2O production. *Science Reports* **5**, 12153, doi:10.1038/srep12153 (2015).
30. Clough, T. J. *et al.* The mitigation potential of hippuric acid on N_2O emissions from urine patches: An *in situ* determination of its effect. *Soil Biol. Biochem.* **41**, 2222–2229, doi:10.1016/j.soilbio.2009.07.032 (2009).
31. Krol, D. J., Forrestal, P. J., Lanigan, G. J. & Richards, K. G. *In situ* N_2O emissions are not mitigated by hippuric and benzoic acids under denitrifying conditions. *Sci. Total Environ* **511**, 362–368, doi:10.1016/j.scitotenv.2014.12.074 (2015).
32. Owens, J. *et al.* Nitrous Oxide Fluxes, Soil Oxygen, and Denitrification Potential of Urine- and Non-Urine-Treated Soil under Different Irrigation Frequencies. *J. Environ. Qual.* **45**(4), 1169–1177, doi:10.2134/jeq2015.10.0516 (2016).
33. Phillips, R. L. *et al.* Chemical formation of hybrid di-nitrogen calls fungal codenitrification into question. *Scientific Reports* **6**, 39077, doi:10.1038/srep39077 (2016).
34. Stieglmeier, M. *et al.* Aerobic nitrous oxide production through N-nitrosating hybrid formation in ammonia-oxidizing archea. *ISME J.* **8**, 1135–1146, doi:10.1038/ismej.2013.220 (2014).
35. Di, H. J. *et al.* Nitrification driven by bacteria and not archaea in nitrogen-rich grassland soils. *Nat. Geosci.* **2**, 621–624, doi:10.1038/ngeo613 (2009).
36. Sterngren, A. E., Hallin, S. & Bengtson, P., Archaeal Ammonia Oxidizers Dominate in Numbers, but Bacteria Drive Gross Nitrification in N-amended Grassland Soil *Front. Microbiol.* **6**, doi:10.3389/fmicb.2015.01350, Article Number 1350 (2015).
37. Clough, T. J., Rolston, D. E., Stevens, R. J. & Laughlin, R. J. N_2O and N_2 gas fluxes, soil gas pressures, and ebullition events following irrigation of $^{15}NO_3^-$-labelled subsoils. *Aust. J. Soil Res.* **41**(3), 401–420, doi:10.1071/SR02104 (2003).
38. Wasser, I. M., de Vries, S., Moenne-Loccoz, P., Schroder, I. & Karlin, K. D. Nitric oxide in biological denitrification: Fe/Cu metalloenzyme and metal complex NOx redox chemistry. *Chem. Rev.* **102**, 1201–1234, doi:10.1021/cr0006627 (2002).
39. Gardiner, M. J. & Radford, T. Soil Associations of Ireland and Their Land Use Potential – Explanatory Bulletin to Soil Map of Ireland 1980 (The Agricultural Institute, Dublin, 1980).
40. WRB, IUSS Working Group WRB. 2006. World reference base for soil resources 2006. (Rome, 2006).
41. Romano, N., Hopmans, J. W. & Dane, G. H. Water retention and storage. In *Methods of Soil Analysis, Part 4, Physical Methods*, edited by G. C. Topp & G. H. Dane, pp. 692–698 (Soil Science Society of America, Madison, WI, 2002).
42. Chamindu Deepagoda, T. K. K. *et al.* Generalized Density-Corrected Model for Gas Diffusivity in Variably Saturated Soils. *Soil Sci. Soc. Am. J.* **75**(4), 1315–1329, doi:10.2136/sssaj2010.0405 (2011).
43. Kool, D. M., Hoffland, E., Abrahamse, S. P. A. & van Groenigen, J. W. What artificial urine composition is adequate for simulating soil N_2O fluxes and mineral N dynamics? *Soil Biol. Biochem.* **38**(7), 1757–1763, doi:10.1016/j.soilbio.2005.11.030 (2006).
44. Bathhurst, N. O. The amino acids of sheep and cow urine. *J. Agr. Sci.* **42**, 476–478, doi:10.1017/S0021859600057385 (1952).
45. Blakemore, L. C., Searle, P. L. & Daly, B. K. *Methods for chemical analysis of soils*. (Manaaki-Whenua Press, Lincoln, New Zealand, 1987).
46. Stark, J. M. & Hart, R. H. Diffusion technique for preparing salt solutions, Kjeldahl digests, and persulfate digests for nitrogen-15 analysis. *Soil Sci. Soc. Am. J.* **60**, 1846–1855, doi:10.2136/sssaj1996.03615995006000060033x (1996).
47. Stevens, R. J. & Laughlin, R. J. Determining nitrogen−15 in nitrite or nitrate by producing nitrous oxide. *Soil Sci. Soc. Am. J.* **58**, 1108–1116, doi:10.2136/sssaj1994.03615995005800040015x (1994).
48. Ghani, A., Dexter, M. & Perrott, K. W. Hot-water extractable carbon in soils: a sensitive measurement for determining impacts of fertilisation, grazing and cultivation. *Soil Biol. Biochem.* **35**, 1231–1243, doi:10.1016/S0038-0717(03)00186-X (2003).
49. Clough, T. J., Kelliher, F. M., Wang, Y. P. & Sherlock, R. R. Diffusion of N-15-labelled N_2O into soil columns: a promising method to examine the fate of N_2O in subsoils. *Soil Biol. Biochem.* **38**(6), 1462–1468, doi:10.1016/j.soilbio.2005.11.002 (2006).
50. Stevens, R. J., Laughlin, R. J., Atkins, G. J. & Prosser, S. J. Automated determination of nitrogen-15 labelled dinitrogen and nitrous oxide by mass spectrometry. *Soil Sci. Soc. Am. J.* **57**, 981–988, doi:10.2136/sssaj1993.03615995005700040017x (1993).
51. Mulvaney, R. L. & Boast, C. W. Equations for determination of nitrogen-15 labelled dinitrogen and nitrous oxide by mass spectrometry. *Soil Sci. Soc. Am. J.* **50**, 360–363, doi:10.2136/sssaj1986.03615995005000020021x (1986).
52. Stevens, R. J. & Laughlin, R. J. Lowering the detection limit for dinitrogen using the enrichment of nitrous oxide. *Soil Biol. Biochem.* **33**, 1287–1289, doi:10.1016/S0038-0717(01)00036-0 (2001).
53. Mulvaney, R. L. Determination of ^{15}N-labeled dinitrogen and nitrous oxide with triple-collector mass spectrometers. *Soil Sci. Soc. Am. J.* **48**, 690–692, doi:10.2136/sssaj1984.03615995004800030045x (1984).
54. Clough, T. J., Stevens, R. J., Laughlin, R. J., Sherlock, R. R. & Cameron, K. C. Transformations of inorganic-N in soil leachate under differing storage conditions. *Soil Biol. Biochem.* **33**(11), 1473–1480, doi:10.1016/S0038-0717(01)00056-6 (2001).

55. Schmidt, H. L., Werner, R. A., Yoshida, N. & Well, R. Is the isotopic composition of nitrous oxide an indicator for its origin from nitrification or denitrification?A theoretical approach from referred data and microbiological and enzyme kinetic aspects. *Rapid Commun. Mass Spectrom.* **18**, 2036–2040, doi:10.1002/rcm.1586 (2004).
56. Ye, R. W., Torosuarez, I., Tiedje, J. M. & Averill, B. A. (H2O)-O-18 isotope exchange studies on the mechanism of reduction of nitric-oxide and nitrite to nitrous oxide by denitrifying bacteria - evidence for an electrophilic nitrosyl during reduction of nitric oxide. *J. Biol. Chem.* **266**, 12848–12851 (1991).

Acknowledgements

The authors gratefully acknowledge the assistance of Manjula Premaratne and Roger Cresswell in assisting with gas chromatography analyses and mass spectrometer analyses. This work was funded by the New Zealand Government through the New Zealand Fund for. Global Partnerships in Livestock Emissions Research to support the objectives of the Livestock Research Group of the Global Research Alliance on Agricultural Greenhouse Gases (Agreement number: 16084) awarded to SEM and the University of Otago. Charlotte Johns gratefully acknowledges funding received from the Teagasc Walsh Fellowship Scheme.

Author Contributions

C.d.K., K.R. and G.L. were the principal investigators for the project funding. T.C., K.R., G.L. and L.C. designed the experiment. C.J. conducted the measurements. T.C., K.R. and G.L. drafted the manuscript with C.d.K., S.E.M., DR, M.S.S., and L.B. providing assistance with data interpretation and manuscript preparation, while J.G. assisted with statistical interpretation.

Additional Information

Competing Interests: The authors declare that they have no competing interests.

Publisher's note: Springer Nature remains neutral with regard to jurisdictional claims in published maps and institutional affiliations.

Author Correction: Influence of soil moisture on codenitrification fluxes from a urea-affected pasture soil

Timothy J. Clough, Gary J. Lanigan, Cecile A. M. de Klein, Md. Sainur Samad, Sergio E. Morales, David Rex, Lars R. Bakken, Charlotte Johns, Leo M. Condron, Jim Grant & Karl G. Richards

Scientific Reports **8**, Article number: 4363 (2018) | Download Citation

The original article was published on 19 May 2017

Correction to: *Scientific Reports* https://doi.org/10.1038/s41598-017-02278-y, published online 19 May 2017

This Article contains an error in Figure 3, where the y-axis 'DOC (µg g^{-1} soil)' is incorrectly labelled as 'DOC (mg g^{-1} soil)'. The correct Figure 3 appears below as Figure 1.

Figure 1

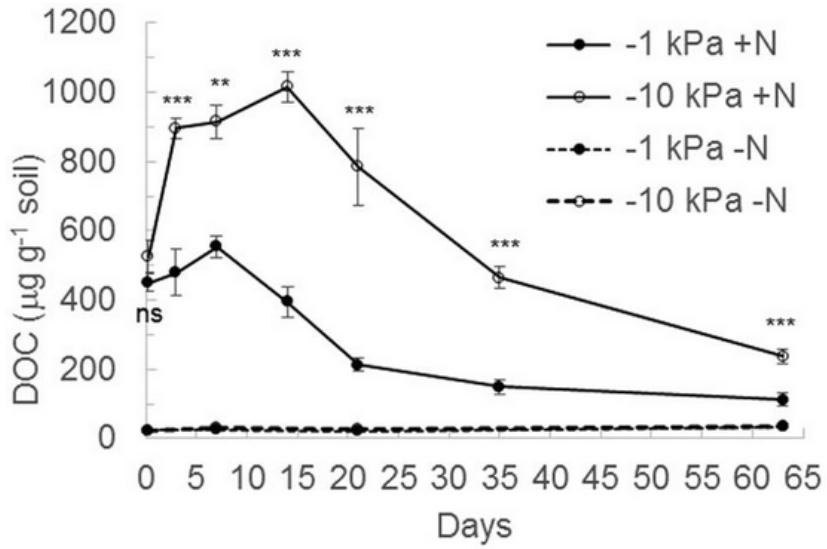

Changes in soil cold water extractable organic carbon (DOC) over time. Concentrations of soil DOC under near saturated (−1 kPa) or field capacity (−10 kPa) soil moisture conditions, following urea application (+N) or nil urea application (−N). Symbols are means (n = 4) with vertical error bars the standard error of the mean. Asterisks *'**'***indicate significant differences between moisture treatments under urea treatments at $P < 0.05$, $P < 0.01$, and $P < 0.001$, respectively.

Full size image »

7.5 Samad et al. 2017

(This publication was removed due to copyright restrictions. As stated in the reference list, the full publication can be found at Wiley Online Library, Molecular Ecology (2017) 26:5500-5514; "Response to nitrogen addition reveals metabolic and ecological strategies of soil bacteria", by Samad MS, Johns C, Richards KG, Lanigan GJ, Klein CAMd, Clough TJ, Morales SE, doi:10.1111/mec.14275)

7.6 Paparua sandy loam – soil analysis report

Hill Laboratories
TRIED, TESTED AND TRUSTED
R J Hill Laboratories Limited
28 Duke Street Frankton 3204
Private Bag 3205
Hamilton 3240 New Zealand
T 0508 HILL LAB (44 555 22)
T +64 7 858 2000
E mail@hill-labs.co.nz
W www.hill-laboratories.com

ANALYSIS REPORT

Client:	Lincoln University	**Lab No:**	1869339
Address:	PO Box 85084 Lincoln Christchurch 7647	**Date Received:**	01-Nov-2017
		Date Reported:	06-Nov-2017
		Quote No:	88615
		Order No:	LU452993
		Client Reference:	
Phone:	03 325 2811 ext 8386	**Submitted By:**	J Breitmeyer

Sample Name: 2 Exp PSL54 **Lab Number:** 1869339.1
Sample Type: SOIL Mixed Pasture (S1)

Analysis		Level Found	Medium Range
pH	pH Units	5.9	5.8 - 6.2
Olsen Phosphorus	mg/L	11	20 - 30
Potassium	me/100g	0.83	0.40 - 0.60
Calcium	me/100g	6.4	4.0 - 10.0
Magnesium	me/100g	0.70	1.00 - 1.60
Sodium	me/100g	0.18	0.20 - 0.50
CEC	me/100g	12	12 - 25
Total Base Saturation	%	65	50 - 85
Volume Weight	g/mL	1.09	0.60 - 1.00
Potentially Available Nitrogen (15cm Depth)*	kg/ha	86	150 - 250
Anaerobically Mineralisable N*	µg/g	52	
Organic Matter*	%	3.9	7.0 - 17.0
Total Carbon*	%	2.3	
Total Nitrogen*	%	0.24	0.30 - 0.60
C/N Ratio*		9.5	
Anaerobically Mineralisable N/Total N Ratio*	%	2.2	3.0 - 5.0
'Total' Phosphorus	mg/kg	601	700 - 1600
'Total' Sulphur	mg/kg	300	600 - 1000
'Total' Calcium*	mg/kg	2,830	
'Total' Zinc*	mg/kg	43	
'Total' Copper*	mg/kg	7	
'Total' Molybdenum*	mg/kg	0.2	
'Total' Cobalt*	mg/kg	3.8	
'Total' Selenium	mg/kg	0.2	0.5 - 1.0
'Total' Chromium*	mg/kg	11.3	
'Total' Arsenic*	mg/kg	2.6	
'Total' Lead*	mg/kg	12.2	
'Total' Nickel*	mg/kg	8.3	
'Total' Mercury*	mg/kg	< 0.10	
'Total' Cadmium*	mg/kg	0.17	

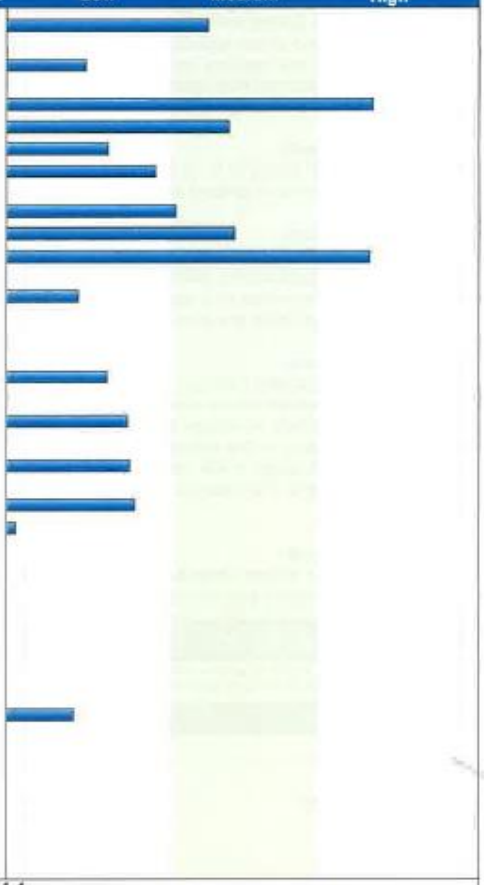

Base Saturation %	K 6.7	Ca 52	Mg 5.6	Na 1.4
MAF Units	K 19	Ca 9	Mg 17	Na 9

The above nutrient graph compares the levels found with reference interpretation levels. NOTE: It is important that the correct sample type be assigned, and that the recommended sampling procedure has been followed. R J Hill Laboratories Limited does not accept any responsibility for the resulting use of this information. IANZ Accreditation does not apply to comments and interpretations, i.e. the 'Range Levels' and subsequent graphs.

Hill Laboratories
TRIED, TESTED AND TRUSTED
R J Hill Laboratories Limited
28 Duke Street Frankton 3204
Private Bag 3205
Hamilton 3240 New Zealand
T 0508 HILL LAB (44 555 22)
T +64 7 858 2000
E mail@hill-labs.co.nz
W www.hill-laboratories.com

ANALYSIS REPORT

Client:	Lincoln University	**Lab No:**	1869339 v1
Address:	PO Box 85084 Lincoln Christchurch 7647	**Date Received:**	01-Nov-2017
		Date Reported:	06-Nov-2017
		Quote No:	88615
		Order No:	LU452993
		Client Reference:	
Phone:	03 325 2811 ext 8386	**Submitted By:**	J Breitmeyer

Analyst's Comments

Sample 1 Comment:
The medium or optimum range guidelines shown in the histogram report relate to sampling protocols as per Hill Laboratories' crop guides and are based on reference values where these are published. Results for samples collected to different depths than those described in the crop guide should be interpreted with caution.
For pastoral soils, the medium ranges are specific for a 75mm sample depth, but if a 150mm sampling depth is used the nutrient levels measured may appear low against these ranges, as nutrients are typically more concentrated in the top of the soil profile. These soil profile differences are altered upon cultivation or contouring.

Sample 1 Comment:
While soil Mg MAF levels of 8-10 (0.4 - 0.6 me/100g) are sufficient for pasture production, soil levels of 25-30 (1 - 1.6 me/100g) are required to ensure adequate Mg content in pasture for animal health (greater than 0.22% in the herbage).

Sample 1 Comment:
For interpretation of 'Total' Sulphur results in pastoral soils, the following guidelines are suggested: 0-600 mg/kg Low (responsive to S application), 600-1000 mg/kg Medium (moderately responsive to S application), greater than 1000 mg/kg High (poor or no response to S application). Soils located closer to coastal areas can expect 5-10 kg S inputs through sea showers. Raw peat soils are excluded from these guidelines.

Sample 1 Comment:
The Potentially Available Nitrogen (kg/ha) test above assumes the sample is taken to a 15 cm depth. If the depth is 7.5 cm, then the result reported above should be divided by two.
To calculate Potentially Available Nitrogen (as kgN/ha) for other sample depths use the reported Anaerobic Mineralisable Nitrogen (AMN) result in the following equation:
AN (kg/ha) = AMN (µg/g) x VW (g/ml) x sample depth (cm) x 0.1
Note that the AN and AMN results reported include the readily available Mineral N (NH4-N and NO3-N) fraction, which is typically quite low.

Sample 1 Comment:
The medium range shown describes typical 'Total' Phosphorus levels for mineral soils in New Zealand. The 'Total' P test has not been correlated against pasture growth response rates so should be interpreted along with other observations.

SUMMARY OF METHODS

The following table(s) gives a brief description of the methods used to conduct the analyses for this job. The detection limits given below are those attainable in a relatively clean matrix. Detection limits may be higher for individual samples should insufficient sample be available, or if the matrix requires that dilutions be performed during analysis.

Sample Type: Soil

Test	Method Description	Default Detection Limit	Sample No
Sample Registration*	Samples were registered according to instructions received.	-	1
Soil Prep (Dry & Grind)*	Air dried at 35 - 40°C overnight (residual moisture typically 4%) and crushed to pass through a 2mm screen. Analysed at 25 Te Aroha Street, Hamilton.	-	1
pH	1:2 (v/v) soil:water slurry followed by potentiometric determination of pH. Analysed at 1 Clyde Street, Hamilton.	0.1 pH Units	1
Olsen Phosphorus	Olsen extraction followed by Molybdenum Blue colorimetry. . Analysed at 1 Clyde Street, Hamilton.	1 mg/L	1
Potentially Available Nitrogen*	Determined by NIR, calibration based on Available N by Anaerobic incubation followed by extraction using 2M KCl followed by Berthelot colorimetry. (Calculation based on 15cm depth sample). Note that any Mineral N present is included in the AN/AMN result reported. Analysed at 1 Clyde Street, Hamilton.	1 mg/L	1
Anaerobically Mineralisable N*	As for Potentially Available Nitrogen but reported as µg/g. Analysed at 1 Clyde Street, Hamilton.	5 µg/g	1

Hill Laboratories
TRIED, TESTED AND TRUSTED
R J Hill Laboratories Limited
28 Duke Street Frankton 3204
Private Bag 3205
Hamilton 3240 New Zealand
T 0508 HILL LAB (44 555 22)
T +64 7 858 2000
E mail@hill-labs.co.nz
W www.hill-laboratories.com

ANALYSIS REPORT

Client:	Lincoln University	**Lab No:**	1869339
Address:	PO Box 85084 Lincoln Christchurch 7647	**Date Received:**	01-Nov-2017
		Date Reported:	06-Nov-2017
		Quote No:	88615
		Order No:	LU452993
		Client Reference:	
Phone:	03 325 2811 ext 8386	**Submitted By:**	J Breitmeyer

Sample Type: Soil

Test	Method Description	Default Detection Limit	Sample No
'Total' Sulphur	Nitric/hydrochloric digestion (based on US EPA 200.2) followed by ICP-OES. (Total recoverable nutrients reported on a dry weight basis) The levels from this method are referred to as 'Totals' in quotation marks, as they will be a slight under-estimation of the true Totals for some elements. Analysed at 1 Clyde Street, Hamilton.	45 mg/kg	1
Organic Matter*	Organic Matter is 1.72 x Total Carbon. Analysed at 1 Clyde Street, Hamilton.	0.2 %	1
Total Carbon*	Determined by NIR, calibration based on Total Carbon by Dumas combustion. Analysed at 1 Clyde Street, Hamilton.	0.1 %	1
Total Nitrogen*	Determined by NIR, calibration based on Total N by Dumas combustion. Analysed at 1 Clyde Street, Hamilton.	0.04 %	1
'Total' Phosphorus	Nitric/hydrochloric digestion (based on US EPA 200.2) followed by ICP-OES. (Total recoverable nutrients reported on a dry weight basis) The levels from this method are referred to as 'Totals' in quotation marks, as they will be a slight under-estimation of the true Totals for some elements. Analysed at 1 Clyde Street, Hamilton.	65 mg/kg	1
'Total' Calcium*	Nitric/hydrochloric digestion (based on US EPA 200.2) followed by ICP-OES. (Total recoverable nutrients reported on a dry weight basis) The levels from this method are referred to as 'Totals' in quotation marks, as they will be a slight under-estimation of the true Totals for some elements. Analysed at 1 Clyde Street, Hamilton.	100 mg/kg	1
'Total' Zinc*	Nitric/hydrochloric digestion (based on US EPA 200.2) followed by ICP-OES. (Total recoverable nutrients reported on a dry weight basis) The levels from this method are referred to as 'Totals' in quotation marks, as they will be a slight under-estimation of the true Totals for some elements. Analysed at 1 Clyde Street, Hamilton.	4 mg/kg	1
'Total' Copper*	Nitric/hydrochloric digestion (based on US EPA 200.2) followed by ICP-OES. (Total recoverable nutrients reported on a dry weight basis) The levels from this method are referred to as 'Totals' in quotation marks, as they will be a slight under-estimation of the true Totals for some elements. Analysed at 1 Clyde Street, Hamilton.	4 mg/kg	1
'Total' Molybdenum*	Nitric/hydrochloric digestion (based on US EPA 200.2) followed by ICP-MS. (Total recoverable nutrients reported on a dry weight basis) The levels from this method are referred to as 'Totals' in quotation marks, as they will be a slight under-estimation of the true Totals for some elements.	0.2 mg/kg	1
'Total' Cobalt*	Nitric/hydrochloric digestion (based on US EPA 200.2) followed by ICP-MS. (Total recoverable nutrients reported on a dry weight basis) The levels from this method are referred to as 'Totals' in quotation marks, as they will be a slight under-estimation of the true Totals for some elements.	0.02 mg/kg	1

Hill Laboratories
TRIED, TESTED AND TRUSTED
R J Hill Laboratories Limited
28 Duke Street Frankton 3204
Private Bag 3205
Hamilton 3240 New Zealand
T 0508 HILL LAB (44 555 22)
T +64 7 858 2000
E mail@hill-labs.co.nz
W www.hill-laboratories.com

ANALYSIS REPORT

Client:	Lincoln University	**Lab No:**	1869339
Address:	PO Box 85084	**Date Received:**	01-Nov-2017
	Lincoln	**Date Reported:**	06-Nov-2017
	Christchurch 7647	**Quote No:**	88615
		Order No:	LU452993
		Client Reference:	
Phone:	03 325 2811 ext 8386	**Submitted By:**	J Breitmeyer

Sample Type: Soil

Test	Method Description	Default Detection Limit	Sample No
'Total' Selenium	Nitric/hydrochloric digestion (based on US EPA 200.2) followed by ICP-MS. (Total recoverable nutrients reported on a dry weight basis) The levels from this method are referred to as 'Totals' in quotation marks, as they will be a slight under-estimation of the true Totals for some elements.	0.2 mg/kg	1
'Total' Chromium*	Nitric/hydrochloric digestion (based on US EPA 200.2) followed by ICP-MS. (Total recoverable nutrients reported on a dry weight basis) The levels from this method are referred to as 'Totals' in quotation marks, as they will be a slight under-estimation of the true Totals for some elements.	0.2 mg/kg	1
'Total' Arsenic*	Nitric/hydrochloric digestion (based on US EPA 200.2) followed by ICP-MS. (Total recoverable nutrients reported on a dry weight basis) The levels from this method are referred to as 'Totals' in quotation marks, as they will be a slight under-estimation of the true Totals for some elements.	0.2 mg/kg	1
'Total' Lead*	Nitric/hydrochloric digestion (based on US EPA 200.2) followed by ICP-MS. (Total recoverable nutrients reported on a dry weight basis) The levels from this method are referred to as 'Totals' in quotation marks, as they will be a slight under-estimation of the true Totals for some elements.	0.04 mg/kg	1
'Total' Nickel*	Nitric/hydrochloric digestion (based on US EPA 200.2) followed by ICP-MS. (Total recoverable nutrients reported on a dry weight basis) The levels from this method are referred to as 'Totals' in quotation marks, as they will be a slight under-estimation of the true Totals for some elements.	0.2 mg/kg	1
'Total' Mercury*	Nitric/hydrochloric digestion (based on US EPA 200.2) followed by ICP-MS. (Total recoverable nutrients reported on a dry weight basis) The levels from this method are referred to as 'Totals' in quotation marks, as they will be a slight under-estimation of the true Totals for some elements.	0.10 mg/kg	1
'Total' Cadmium*	Nitric/hydrochloric digestion (based on US EPA 200.2) followed by ICP-MS. (Total recoverable nutrients reported on a dry weight basis) The levels from this method are referred to as 'Totals' in quotation marks, as they will be a slight under-estimation of the true Totals for some elements.	0.02 mg/kg	1
Potassium	1M Neutral ammonium acetate extraction followed by ICP-OES. Analysed at 1 Clyde Street, Hamilton.	0.01 me/100g	1
Calcium	1M Neutral ammonium acetate extraction followed by ICP-OES. Analysed at 1 Clyde Street, Hamilton.	0.5 me/100g	1
Magnesium	1M Neutral ammonium acetate extraction followed by ICP-OES. Analysed at 1 Clyde Street, Hamilton.	0.04 me/100g	1
Sodium	1M Neutral ammonium acetate extraction followed by ICP-OES. Analysed at 1 Clyde Street, Hamilton.	0.05 me/100g	1
CEC	Summation of extractable cations (K, Ca, Mg, Na) and extractable acidity. May be overestimated if soil contains high levels of soluble salts or carbonates. Analysed at 1 Clyde Street, Hamilton.	2 me/100g	1

Hill Laboratories
TRIED, TESTED AND TRUSTED
R J Hill Laboratories Limited
28 Duke Street Frankton 3204
Private Bag 3205
Hamilton 3240 New Zealand
T 0508 HILL LAB (44 555 22)
T +64 7 858 2000
E mail@hill-labs.co.nz
W www.hill-laboratories.com

ANALYSIS REPORT

Client:	Lincoln University	**Lab No:**	1869339
Address:	PO Box 85084	**Date Received:**	01-Nov-2017
	Lincoln	**Date Reported:**	06-Nov-2017
	Christchurch 7647	**Quote No:**	88615
		Order No:	LU452993
		Client Reference:	
Phone:	03 325 2811 ext 8386	**Submitted By:**	J Breitmeyer

Sample Type: Soil

Test	Method Description	Default Detection Limit	Sample No
Total Base Saturation	Calculated from Extractable Cations and Cation Exchange Capacity. Analysed at 1 Clyde Street, Hamilton.	5 %	1
Volume Weight	The weight/volume ratio of dried, ground soil. Analysed at 1 Clyde Street, Hamilton.	0.01 g/mL	1

These samples were collected by yourselves (or your agent) and analysed as received at the laboratory.

Samples are held at the laboratory after reporting for a length of time depending on the preservation used and the stability of the analytes being tested. Once the storage period is completed the samples are discarded unless otherwise advised by the client.

Andrew Whitmore BSc (Tech)
Client Services Manager - Agriculture

Department of Soil and Physical Sciences
Faculty of Agriculture and Life Sciences

T 64 3 423 0768
PO Box 85084, Lincoln University
Lincoln 7647, Christchurch, New Zealand

www.lincoln.ac.nz

30th October 2017

Annette Rodgers
Department of Earth and Ocean Sciences
c/o Science Store, Gate 8 Hillcrest Road
University of Waikato
Hamilton 3240

Dear Annette

Please find enclosed 1 soil sample for particle size analysis labelled David Rex, 2EXPPSLS4. We require the results in the following formats for the soils:- USDA system (please report the % totals of each of these three fractions).

% sand >63µm % silt 2-63µm % clay <2µm

ISSS system (please report the % totals of each of these three fractions).

% sand >20µm % silt 2-20µm % clay <2µm

The order number for this job is LU452994.

Please email and post the results through when completed. My email address is jason.breitmeyer@lincoln.ac.nz.

Yours sincerely

Jason Breitmeyer
Technical Officer
Department of Soil & Physical Sciences